

PDR UNRESTRICTED DISTRIBUTION  
DATE \_\_\_\_\_ WEC



Westinghouse Energy Systems



9109050260 910829  
PDR ADOCK 05000425  
P PDR

FOR UNRESTRICTED DISTRIBUTION  
DATE \_\_\_\_\_ WEC



REPRODUCTION OF THIS  
DOCUMENT IS PROHIBITED  
WITHOUT THE WRITTEN  
PERMISSION OF THE  
WESTERN ELECTRIC COMPANY

WCAP-13007

ANALYSIS OF CAPSULE U FROM THE  
GEORGIA POWER COMPANY  
VOGTLE ELECTRIC GENERATING PLANT UNIT 2  
REACTOR VESSEL  
RADIATION SURVEILLANCE PROGRAM

E. Terek  
S. L. Anderson  
L. Albertin

August 1991

Work Performed Under Shop Order GURP-106

Prepared by Westinghouse Electric Corporation  
for the Georgia Power Company

Approved by:

T. A. Meyer  
T. A. Meyer, Manager  
Structural Reliability and  
Plant Life Optimization

WESTINGHOUSE ELECTRIC CORPORATION  
Nuclear and Advanced Technology Division  
P.O. Box 355  
Pittsburgh, Pennsylvania 15230-0355

PREFACE

This report has been technically reviewed and verified.

Reviewer:

Sections 1 through 5, 7, 8 and  
Appendix A

J. M. Chicots

*J. M. Chicots*

Section 6

E. P. Lippincott

*E. P. Lippincott*

Appendix B

N. K. Ray

*N. K. Ray*

## TABLE OF CONTENTS

<u>Section</u>	<u>Title</u>	<u>Page</u>
1.0	SUMMARY OF RESULTS	1-1
2.0	INTRODUCTION	2-1
3.0	BACKGROUND	3-1
4.0	DESCRIPTION OF PROGRAM	4-1
5.0	TESTING OF SPECIMENS FROM CAPSULE U	5-1
	5.1 Overview	5-1
	5.2 Charpy V-Notch Impact Test Results	5-4
	5.3 Tension Test Results	5-6
	5.4 Compact Tension Tests	5-7
6.0	RADIATION ANALYSIS AND NEUTRON DOSIMETRY	6-1
	6.1 Introduction	6-1
	6.2 Discrete Ordinates Analysis	6-2
	6.3 Neutron Dosimetry	6-7
7.0	SURVEILLANCE CAPSULE REMOVAL SCHEDULE	7-1
8.0	REFERENCES	8-1
APPENDIX A -	LOAD-TIME RECORDS FOR CHARPY SPECIMEN TESTS	
APPENDIX B -	EVALUATION OF PRESSURIZED THERMAL SHOCK FOR VOGTLE ELECTRIC GENERATING PLANT UNIT 2	

## LIST OF TABLES

<u>Table</u>	<u>Title</u>	<u>Page</u>
4-1	Chemical Composition of the Vogtle Electric Generating Plant Unit 2 Reactor Vessel Surveillance Material	4-3
4-2	Heat Treatment History of the Vogtle Electric Generating Plant Unit 2 Reactor Vessel Core Region Shell Plates and Weld Seams	4-4
4-3	Chemical Composition of Two Vogtle Electric Generating Plant Unit 2 Charpy Specimens Removed from Surveillance Capsule U	4-5
4-4	Chemistry Results from the NBS Certified Reference Standards	4-6
5-1	Charpy V-Notch Impact Data for the Vogtle Electric Generating Plant Unit 2 Lower Shell Plate B8628-1 Irradiated at 550°F, Fluence $4.44 \times 10^{18}$ n/cm <sup>2</sup> (E > 1.0 MeV)	5-8
5-2	Charpy V-Notch Impact Data for the Vogtle Electric Generating Plant Unit 2 Reactor Vessel Weld Metal and HAZ Metal Irradiated at 550°F, Fluence $4.44 \times 10^{18}$ n/cm <sup>2</sup> (E > 1.0 MeV)	5-9
5-3	Instrumented Charpy Impact Test Results for the Vogtle Electric Generating Plant Unit 2 Lower Shell Plate B8628-1 Irradiated at 550°F, Fluence $4.44 \times 10^{18}$ n/cm <sup>2</sup> (E > 1.0 MeV)	5-10
5-4	Instrumented Charpy Impact Test Results for the Vogtle Electric Generating Plant Unit 2 Weld Metal and Heat-Affected-Zone (HAZ) Metal, Irradiated at 550°F, Fluence $4.44 \times 10^{18}$ n/cm <sup>2</sup> (E > 1.0 MeV)	5-11

## LIST OF TABLES

<u>Table</u>	<u>Title</u>	<u>Page</u>
5-5	Effect of 550°F Irradiation to $4.44 \times 10^{18}$ n/cm <sup>2</sup> (E > 1.0 MeV) on the Notch Toughness Properties of the Vogtle Electric Generating Plant Unit 2 Reactor Vessel Surveillance Materials	5-12
5-6	Comparison of the Vogtle Electric Generating Plant Unit 2 Surveillance Material 30 ft-lb Transition Temperature Shifts and Upper Shelf Energy Decreases with Regulatory Guide 1.99 Revision 2 Predictions	5-13
5-7	Tensile Properties for the Vogtle Electric Generating Plant Unit 2 Reactor Vessel Surveillance Materials Irradiated at 550°F to $4.44 \times 10^{18}$ n/cm <sup>2</sup> (E > 1.0 MeV)	5-14
6-1	Calculated Fast Neutron Exposure Parameters at the Surveillance Capsule Center	6-14
6-2	Calculated Fast Neutron Exposure Rates at the Pressure Vessel Clad/Base Metal Interface	6-15
6-3	Relative Radial Distributions of Neutron Flux (E > 1.0 MeV) within the Pressure Vessel Wall	6-16
6-4	Relative Radial Distributions of Neutron Flux (E > 0.1 MeV) within the Pressure Vessel Wall	6-17
6-5	Relative Radial Distributions of Iron Displacement Rate (dpa) within the Pressure Vessel Wall	6-18
6-6	Nuclear Parameters for Neutron Flux Monitors	6-19

## LIST OF TABLES

<u>Table</u>	<u>Title</u>	<u>Page</u>
6-7	Monthly Thermal Generation During the First Fuel Cycle of the Vogtle Electric Generating Plant Unit 2 Reactor	6-20
6-8	Measured Sensor Activities and Reactions Rates	6-21
6-9	Summary of Neutron Dosimetry Results	6-23
6-10	Comparison of Measured and FERRET Calculated Reaction Rates at the Surveillance Capsule Center	6-24
6-11	Adjusted Neutron Energy Spectrum at the Surveillance Capsule Center	6-25
6-12	Comparison of Calculated and Measured Exposure Levels for Capsule U	6-26
6-13	Neutron Exposure Projections at Key Locations on the Pressure Vessel Clad/Base Metal Interface	6-27
6-14	Neutron Exposure Values for use in the Generation of Heatup/Cooldown Curves	6-28
6-15	Updated Lead Factors for Vogtle Electric Generating Plant Unit 2 Surveillance Capsules	6-29

## LIST OF ILLUSTRATIONS

<u>Figure</u>	<u>Title</u>	<u>Page</u>
4-1	Arrangement of Surveillance Capsules in the Vogtle Electric Generating Plant Unit 2 Reactor Vessel	4-7
4-2	Capsule U Diagram Showing Location of Specimens, Thermal Monitors and Dosimeters	4-8
5-1	Charpy V-Notch Impact Properties for Vogtle Electric Generating Plant Unit 2 Reactor Vessel Lower Shell Plate B8628-1 (Longitudinal Orientation)	5-15
5-2	Charpy V-Notch Impact Properties for Vogtle Electric Generating Plant Unit 2 Reactor Vessel Lower Shell Plate B8628-1 (Transverse Orientation)	5-16
5-3	Charpy V-Notch Impact Properties for Vogtle Electric Generating Plant Unit 2 Reactor Vessel Surveillance Weld Metal	5-17
5-4	Charpy V-Notch Impact Properties for Vogtle Electric Generating Plant Unit 2 Reactor Vessel Weld Heat-Affected-Zone Metal	5-18
5-5	Charpy Impact Specimen Fracture Surfaces for Vogtle Electric Generating Plant Unit 2 Reactor Vessel Lower Shell Plate B8628-1 (Longitudinal Orientation)	5-19
5-6	Charpy Impact Specimen Fracture Surfaces for Vogtle Electric Generating Plant Unit 2 Reactor Vessel Lower Shell Plate B8628-1 (Transverse Orientation)	5-20

LIST OF ILLUSTRATIONS (Cont)

<u>Figure</u>	<u>Title</u>	<u>Page</u>
5-7	Charpy Impact Specimen Fracture Surfaces for Vogtle Electric Generating Plant Unit 2 Reactor Vessel Surveillance Weld Metal	5-21
5-8	Charpy Impact Specimen Fracture Surfaces for Vogtle Electric Generating Plant Unit 2 Reactor Vessel Weld Heat-Affected-Zone Metal	5-22
5-9	Tensile Properties for Vogtle Electric Generating Plant Unit 2 Reactor Vessel Lower Shell Plate B8628-1 (Longitudinal Orientation)	5-23
5-10	Tensile Properties for Vogtle Electric Generating Plant Unit 2 Reactor Vessel Lower Shell Plate B8628-1 (Transverse Orientation)	5-24
5-11	Tensile Properties for Vogtle Electric Generating Plant Unit 2 Reactor Vessel Surveillance Weld Metal	5-25
5-12	Fractured Tensile Specimens from Vogtle Electric Generating Plant Unit 2 Reactor Vessel Lower Shell Plate B8628-1 (Longitudinal Orientation)	5-26
5-13	Fractured Tensile Specimens from Vogtle Electric Generating Plant Unit 2 Reactor Vessel Lower Shell Plate B8628-1 (Transverse Orientation)	5-27
5-14	Fractured Tensile Specimens from Vogtle Electric Generating Plant Unit 2 Reactor Vessel Surveillance Weld Metal	5-28

LIST OF ILLUSTRATIONS (Cont)

<u>Figure</u>	<u>Title</u>	<u>Page</u>
5-15	Engineering Stress-Strain Curves for Plate B8628-1 Tensile Specimens BL1 and BL2 (Longitudinal Orientation)	5-29
5-16	Engineering Stress-Strain Curves for Plate B8628-1 Tensile Specimens BL3 (Longitudinal Orientation) and BT1 (Transverse Orientation)	5-30
5-17	Engineering Stress-Strain Curves for Plate B8628-1 Tensile Specimens BT2 and BT3 (Transverse Orientation)	5-31
5-18	Engineering Stress-Strain Curves for Weld Metal Tensile Specimens BW1 and BW2	5-32
5-19	Engineering Stress-Strain Curve for Weld Metal Tensile Specimen BW3	5-33
6-1	Plan View of a Dual Reactor Vessel Surveillance Capsule	6-13

SECTION 1.0  
SUMMARY OF RESULTS

The analysis of the reactor vessel materials contained in surveillance Capsule U, the first capsule to be removed from the Georgia Power Company Vogtle Electric Generating Plant Unit 2 reactor pressure vessel, led to the following conclusions:

- o The capsule received an average fast neutron fluence ( $E > 1.0$  MeV) of  $4.44 \times 10^{18}$  n/cm<sup>2</sup> after 1.18 EFPY of plant operation.
- c Irradiation of the reactor vessel lower shell plate B8628-1 Charpy specimens, oriented with the longitudinal axis of the specimen parallel to the major rolling direction (longitudinal orientation), to  $4.44 \times 10^{18}$  n/cm<sup>2</sup> ( $E > 1.0$  MeV) resulted in no 30 ft-lb transition temperature increase and in a 50 ft-lb transition temperature increase of 5°F. This results in a 30 ft-lb transition temperature of -10°F and a 50 ft-lb transition temperature of 50°F for longitudinally oriented specimens.
- o Irradiation of the reactor vessel lower shell plate B8628-1 Charpy specimens, oriented with the longitudinal axis of the specimen normal to the major rolling direction (transverse orientation), to  $4.44 \times 10^{18}$  n/cm<sup>2</sup> ( $E > 1.0$  MeV) resulted in no 30 ft-lb transition temperature increase and in a 50 ft-lb transition temperature increase of 5°F. This results in a 30 ft-lb transition temperature of 30°F and a 50 ft-lb transition temperature of 80°F for transversely oriented specimens.
- o The weld metal Charpy specimens irradiated to  $4.44 \times 10^{18}$  n/cm<sup>2</sup> ( $E > 1.0$  MeV) resulted in no 30 and 50 ft-lb transition temperature increases. This results in a 30 ft-lb transition temperature of -15°F and a 50 ft-lb transition temperature of 5°F for the weld metal.

- o Irradiation of the reactor vessel weld Heat-Affected-Zone (HAZ) metal Charpy specimens to  $4.44 \times 10^{18}$  n/cm<sup>2</sup> (E > 1.0 MeV) resulted in no 30 and no 50 ft-lb transition temperature increases. This results in a 30 ft-lb transition temperature of -80°F and a 50 ft-lb transition temperature of -45°F for the weld HAZ metal.
- o The average upper shelf energy of lower shell plate B8628-1 (longitudinal orientation) resulted in a energy increase of 10 ft-lb after irradiation to  $4.44 \times 10^{18}$  n/cm<sup>2</sup> (E > 1.0 MeV). This results in an upper shelf energy of 99 ft-lb for longitudinally oriented specimens.
- o The average upper shelf energy of lower shell plate B8628-1 (transverse orientation) resulted in a energy increase of 9 ft-lb after irradiation to  $4.44 \times 10^{18}$  n/cm<sup>2</sup> (E > 1.0 MeV). This results in an upper shelf energy of 79 ft-lb for transversely oriented specimens.
- o The average upper shelf energy of the weld metal increased 6 ft-lb after irradiation to  $4.44 \times 10^{18}$  n/cm<sup>2</sup> (E > 1.0 MeV). This results in an upper shelf energy of 98 ft-lb for the weld metal.
- o The average upper shelf energy of the weld HAZ metal increased 16 ft-lb after irradiation to  $4.44 \times 10^{18}$  n/cm<sup>2</sup> (E > 1.0 MeV). This results in an upper shelf energy of 122 ft-lb for the weld HAZ metal.
- o The surveillance capsule U test results indicate that the surveillance material 30 ft-lb transition temperature changes and upper shelf energy decreases are less than the Regulatory Guide 1.99 Revision 2 predictions.

- o The surveillance capsule materials exhibit a more than adequate upper shelf energy level for continued safe plant operation and are expected to maintain an upper shelf energy of no less than 50 ft-lb throughout the life (32 EFPY) of the vessel as required by 10CFR50, Appendix G.
- o The calculated end-of-life (32 EFPY) maximum neutron fluence ( $E > 1.0$  MeV) for the Vogtle Electric Generating Plant Unit 2 reactor vessel is as follows:

Vessel inner radius \* -  $3.04 \times 10^{19}$  n/cm<sup>2</sup>  
Vessel 1/4 thickness -  $1.66 \times 10^{19}$  n/cm<sup>2</sup>  
Vessel 3/4 thickness -  $3.59 \times 10^{18}$  n/cm<sup>2</sup>

\* Clad/base metal interface

- o All  $RT_{PTS}$  values remain below the NRC screening values for PTS. The PTS values for the limiting beltline region lower shell plate B8628-1 for 32 EFPY and 48 EFPY are 124°F and 127°F, respectively.

## SECTION 2.0 INTRODUCTION

This report presents the results of the examination of Capsule U, the first capsule to be removed from the reactor in the continuing surveillance program which monitors the effects of neutron irradiation on the Georgia Power Company Vogtle Electric Generating Plant Unit 2 reactor pressure vessel materials under actual operating conditions.

The surveillance program for the Georgia Power Company Vogtle Electric Generating Plant Unit 2 reactor pressure vessel materials was designed and recommended by the Westinghouse Electric Corporation. A description of the surveillance program and the preirradiation mechanical properties of the reactor vessel materials is presented in WCAP-11381 entitled "Georgia Power Company Vogtle Electric Generating Plant Unit 2 Reactor Vessel Radiation Surveillance Program" by L. R. Singer [1]. The surveillance program was planned to cover the 40-year design life of the reactor pressure vessel and was based on ASTM E185-82, "Standard Practice for Conducting Surveillance Tests for Light-Water Cooled Nuclear Power Reactor Vessels". Westinghouse Power Systems personnel were contracted to aid in the preparation of procedures for removing capsule "U" from the reactor and its shipment to the Westinghouse Science and Technology Center Hot Cell Facility, where, the postirradiation mechanical testing of the Charpy V-notch impact and tensile surveillance specimens was performed.

This report summarizes the testing of and the postirradiation data obtained from surveillance capsule "U" removed from the Georgia Power Company Vogtle Electric Generating Plant Unit 2 reactor vessel and discusses the analysis of the data.

## SECTION 3.0 BACKGROUND

The ability of the large steel pressure vessel containing the reactor core and its primary coolant to resist fracture constitutes an important factor in ensuring safety in the nuclear industry. The beltline region of the reactor pressure vessel is the most critical region of the vessel because it is subjected to significant fast neutron bombardment. The overall effects of fast neutron irradiation on the mechanical properties of low alloy, ferritic pressure vessel steels such as A533 Grade B Class 1 (base material of the Georgia Power Company Vogtle Electric Generating Plant Unit 2 reactor pressure vessel lower shell plate B8628-1) are well documented in the literature. Generally, low alloy ferritic materials show an increase in hardness and tensile properties and a decrease in ductility and toughness under certain conditions of irradiation.

A method for performing analyses to guard against fast fracture in reactor pressure vessels has been presented in "Protection Against Nonductile Failure," Appendix G to Section III of the ASME Boiler and Pressure Vessel Code<sup>[4]</sup>. The method uses fracture mechanics concepts and is based on the reference nil-ductility temperature ( $RT_{NDT}$ ).

$RT_{NDT}$  is defined as the greater of either the drop weight nil-ductility transition temperature (NDTT per ASTM E-208) or the temperature 60°F less than the 50 ft-lb (and 35-mil lateral expansion) temperature as determined from Charpy specimens oriented normal (transverse) to the major working direction of the plate. The  $RT_{NDT}$  of a given material is used to index that material to a reference stress intensity factor curve ( $K_{IR}$  curve) which appears in Appendix G to the ASME Code. The  $K_{IR}$  curve is a lower bound of dynamic, crack arrest, and static fracture toughness results obtained from several heats of pressure vessel steel. When a given material is indexed to the  $K_{IR}$  curve, allowable stress intensity factors can be obtained for this material as a function of temperature. Allowable operating limits can then be determined using these allowable stress intensity factors.

$RT_{NDT}$  and, in turn, the operating limits of nuclear power plants can be adjusted to account for the effects of radiation on the reactor vessel material properties. The radiation embrittlement changes in mechanical properties of a given reactor pressure vessel steel can be monitored by a reactor surveillance program, such as the Vogtle Electric Generating Plant Unit 2 Reactor Vessel Radiation Surveillance Program<sup>[1]</sup>, in which a surveillance capsule is periodically removed from the operating nuclear reactor and the encapsulated specimens are tested. The increase in the average Charpy V-notch 30 ft-lb temperature ( $\Delta RT_{NDT}$ ) due to irradiation is added to the original  $RT_{NDT}$  to adjust the  $RT_{NDT}$  for radiation embrittlement. This adjusted  $RT_{NDT}$  ( $RT_{NDT}$  initial +  $\Delta RT_{NDT}$ ) is used to index the material to the  $K_{IR}$  curve and, in turn, to set operating limits for the nuclear power plant which take into account the effects of irradiation on the reactor vessel materials.

SECTION 4.0  
DESCRIPTION OF PROGRAM

Six surveillance capsules for monitoring the effects of neutron exposure on the Vogtle Electric Generating Plant Unit 2 reactor pressure vessel core region material were inserted in the reactor vessel prior to initial plant start-up. The six capsules were positioned in the reactor vessel between the neutron pads and the vessel wall as shown in Figure 4-1. The vertical center of the capsules is opposite the vertical center of the core.

Capsule U was removed after 1.18 Effective Full Power Years (EFPY) of plant operation. This capsule contained Charpy V-notch, tensile, and 1/2 T compact tension (CT) specimens (Figure 4-2) from the lower shell plate B8628-1 and submerged arc weld metal identical to the weldment used in the girth seam between the intermediate and lower shell plates and Charpy V-notch specimens from weld HAZ material.

Test material obtained from the lower shell plate (after the thermal heat treatment and forming of the plate) was taken at least one plate thickness from the quenched ends of the plate. All test specimens were machined from the 1/4 thickness [a] location of the plate after performing a simulated postweld, stress-relieving treatment on the test material and also from weld and heat-affected-zone (HAZ) metal of a stress-relieved weldment joining lower shell plate B8628-1 and adjacent lower shell plate B8825-1. All HAZ test specimens were taken from weld and weld HAZ of lower shell plate B8628-1.

Base metal Charpy V-notch impact and tension specimens were oriented with the longitudinal axis of the specimen parallel to the major rolling direction of the plate (longitudinal orientation) and also normal to the major rolling direction (transverse orientation). Charpy V-notch and tensile specimens from the weld metal were oriented such that the long dimension of the specimen was normal to the welding direction.

- a. The compact test specimens were obtained from the 3/4 T-thickness location of the plate.

Capsule U, also, contained 1/2T CT test specimens from the lower shell plate B8628-1 and were machined in both the longitudinal and transverse orientations. The 1/2T CT Test specimens from the weld metal were machined with the notch oriented in the direction of welding. All CT specimens were fatigue precracked according to ASTM E399.

The chemical composition and heat treatment of the surveillance material is presented in Tables 4-1 through 4-4. The chemical analysis reported in Table 4-1 was obtained from unirradiated material used in the surveillance program<sup>[1]</sup>. In addition, a chemical analysis using Inductively Coupled Plasma Spectrometry (ICPS) was performed on irradiated Charpy specimens BL-1 (plate material) and BW-2 (weld metal). The chemistry results from the NBS certified reference standards are reported in Table 4-4.

Capsule U contained dosimeter wires of pure copper, iron, nickel, and aluminum-0.15 weight percent cobalt wire (cadmium-shielded and unshielded). In addition, cadmium shielded dosimeters of neptunium ( $Np^{237}$ ) and uranium ( $U^{238}$ ) were placed in the capsule to measure the integrated flux at specific neutron energy levels.

Thermal monitors made from the two low-melting eutectic alloys and sealed in Pyrex tubes were included in the capsule. These thermal monitors were used to define the maximum temperature attained by the test specimens during irradiation. The composition of the two alloys and their melting points are as follows:

2.5% Ag, 97.5% Pb	Melting Point: 579°F (304°C)
1.5% Ag, 1.0% Sn, 97.5% Pb	Melting Point: 590°F (310°C)

The arrangement of the various mechanical specimens, dosimeters and thermal monitors contained in capsule U are shown in Figure 4-2.

TABLE 4-1

CHEMICAL COMPOSITION OF THE VOGTLE ELECTRIC GENERATING  
PLANT UNIT 2 REACTOR VESSEL SURVEILLANCE MATERIAL

Element	Chemical Composition (wt%)			
	Lower Shell Plate B8628-1		Weld Metal (d)	
C	0.24	0.23	0.075	0.099
Mn	1.34	1.30	1.27	1.25
P	0.007	0.007	0.007	0.008
S	0.016	0.014	0.010	0.013
Si	0.25	0.23	0.50	0.43
Ni	0.59	0.59	0.12	0.17
Mo	0.59	0.50	0.52	0.47
Cr	0.02 (a)	0.07 (b)	0.07 (a)	0.061 (b)
Cu	0.05	0.05	0.06	0.040
Al	0.029	0.034	--	0.015
Co	0.004	0.008	--	0.002
Pb	(c)	<0.07	--	<0.01
W	<0.01	<0.05	--	<0.01
Ti	<0.01	0.005	--	<0.001
Zr	<0.001	0.03	--	<0.01
V	0.004	<0.005	0.004	<0.004
Sn	0.017	0.007	--	<0.001
As	0.007	0.008	--	0.003
Cb	<0.01	<0.05	--	<0.002
N	0.008	0.007	--	0.002
B	<0.001	0.008	--	0.009

a. Chemical Analysis by Combustion Engineering, Inc.<sup>[1]</sup>

b. Chemical Analysis by Westinghouse<sup>[1]</sup>

c. Not detected

d. Representative of the closing girth seam. Weld wire Heat No. 87005, Linde 124 Flux Lot No. 1061.

TABLE 4-2

HEAT TREATMENT HISTORY OF THE VOGTLE ELECTRIC GENERATING PLANT UNIT 2  
REACTOR VESSEL CORE REGION SHELL PLATES AND WELD SEAMS<sup>[1]</sup>

Material	Temperature (°F)	Time (hr)	Cooling
Intermediate Shell Plates R-4-1 R-4-2 R-4-3	Austenitizing: 1600 ± 25 (871°C)	4 <sup>[a]</sup>	Water-quenched
	Tempered: 1225 ± 25 (663°C)	4 <sup>[a]</sup>	Air-cooled
	Stress Relief: 1150 ± 50 (621°C)	16.5 <sup>[b]</sup>	Furnace-cooled
Lower Shell Plates B8825-1 R-8-1 B8628-1	Austenitizing: 1600 ± 25 (871°C)	4 <sup>[a]</sup>	Water-quenched
	Tempered: 1225 ± 25 (663°C)	4 <sup>[a]</sup>	Air-cooled
	Stress Relief: 1150 ± 50 (621°C)	12.0 <sup>[b]</sup>	Furnace-cooled
Intermediate Shell Longitudinal Seam Welds	Stress Relief: 1150 ± 50 (621°C)	16.5 <sup>[b]</sup>	Furnace-cooled
Lower Shell Longitudinal Seam Welds		12.0 <sup>[b]</sup>	Furnace-cooled
Intermediate to Lower Shell Girth Seam Weld	Local Stress Relief: 1150 ± 50 (621°C)	5.0	Furnace-cooled
<b>Surveillance Program Test Material</b>			
Surveillance Program Weldment Test Plate "D" (Representative of Closing Girth Seam)	Post Weld Stress Relief: 1150 ± 50 (621°C)	6.0 <sup>[c]</sup>	Furnace-cooled

a. Lukens Steel Company, Combustion Engineering, Inc. Certification Reports.

b. Stress Relief includes the Intermediate to Lower Shell Closing Girth Seam Post Weld Heat Treatment.

c. The Stress Relief Heat Treatment received by the Surveillance Test Weldment has been simulated.

TABLE 4-3

Chemical Composition of Two Vogtle Electric Generating Plant  
Unit 2 Charpy Specimens Removed from Surveillance Capsule U

Specimen No. Material	Concentration in Weight Percent	
	BL-1 PLATE	BW-2 WELD
Fe	MATRIX ELEMENT: Remainder by Difference	
Mn	1.199	1.111
Cr	0.061	0.061
Ni	0.598	0.091
Mo	0.546	0.529
Co	0.020	0.025
Cu	0.053	0.045
P	0.0084	0.0124
V	<0.010	<0.010
C	0.181	0.074
S	0.0098	0.0106
Si	0.201	0.484

Analyses	Method of Analysis
Metals	ICPS, Inductively Coupled Plasma Spectrometry
Carbon	EC-12, LECO Carbon Analyzer
Sulfur	Combustion/titration
Silicon	Dissolution/gravimetric

TABLE 4-4  
Chemistry Results from the NBS  
Certified Reference Standards

Material ID	Low Alloy Steel: NBS Certified Reference Standards			
	NBS 361		NBS 362	
	Certified	Measured	Certified	Measured
-----				
<u>Metals</u>	<u>Concentration in Weight Percent</u>			
Fe *	95.60	(matrix)	95.30	(matrix)
Mn	0.66	0.632	1.04	1.036
Cr	0.694	0.690	0.30	0.314
Ni	2.00	above cal	0.59	0.601
Mo	0.19	0.212	0.068	0.069
Co	0.032	0.040	0.30	0.336
Cu	0.042	0.042	0.50	0.495
P	0.014	0.0184	0.041	0.0384
V	0.011	0.011	0.040	0.039
C	0.383	0.378	0.160	0.162
S	0.014	N.A.	0.036	0.0364
Si	0.222	0.203	0.39	N.A.
-----				

Material ID	Low Alloy Steel: NBS Certified Reference Standards			
	NBS 363		NBS 364	
	Certified	Measured	Certified	Measured
-----				
<u>Metals</u>	<u>Concentration in Weight Percent</u>			
Fe *	94.4	(matrix)	96.7	(matrix)
Mn	1.50	1.500	0.255	0.242
Cr	1.31	1.358	0.063	0.063
Ni	0.30	0.275	0.144	0.101
Mo	0.028	0.028	0.49	0.490
Co	0.048	0.025	0.15	0.157
Cu	0.10	0.100	0.249	0.243
P	0.029	0.0361	0.01	0.0104
V	0.31	0.310	0.105	0.111
C	0.62	N.A.	0.87	N.A.
S	0.0068	N.A.	0.0250	0.0197
Si	0.74	0.724	0.065	N.A.
-----				

\* Matrix element calculated as difference for material balance. ( )  
N.A. - Not analyzed

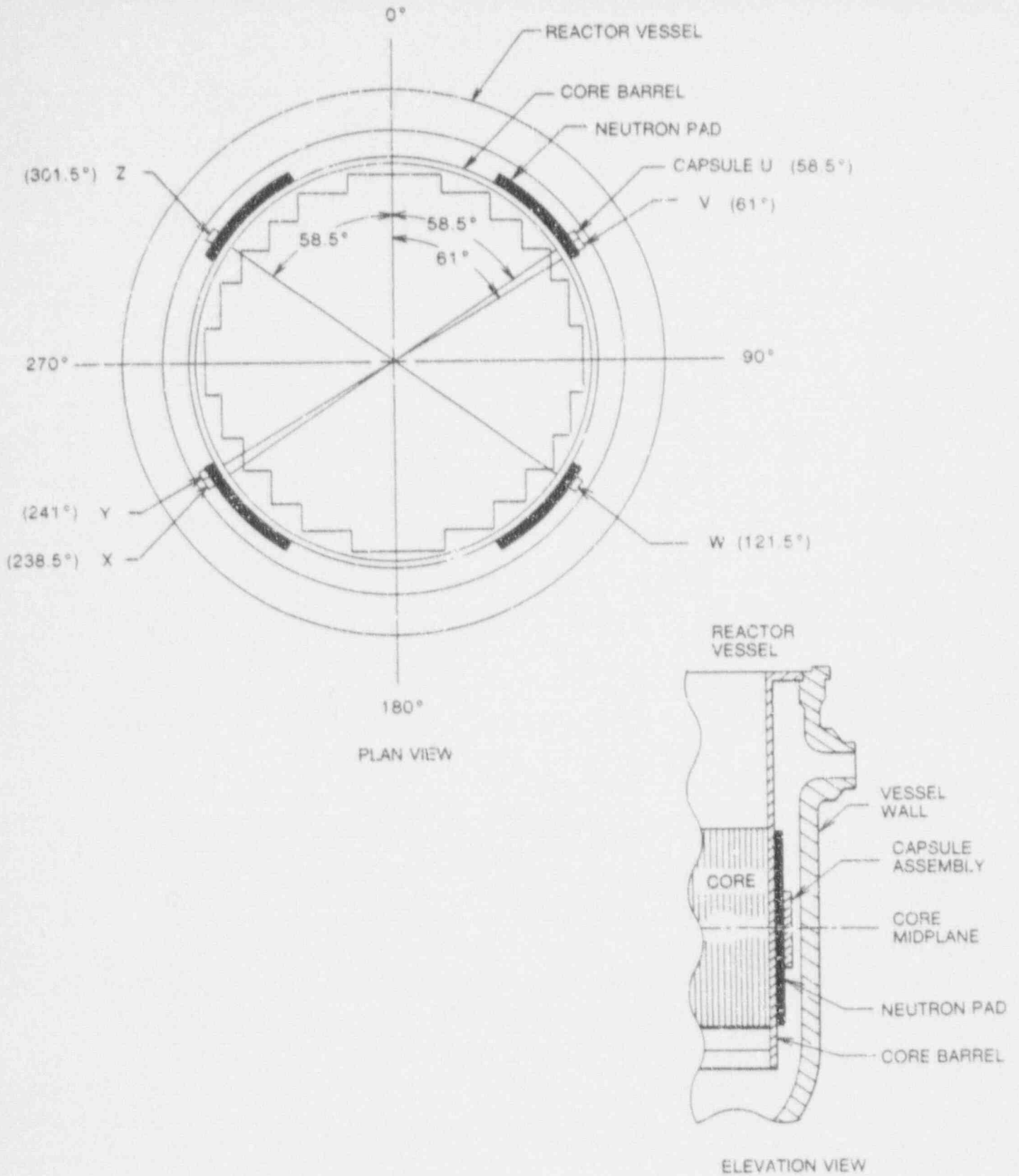
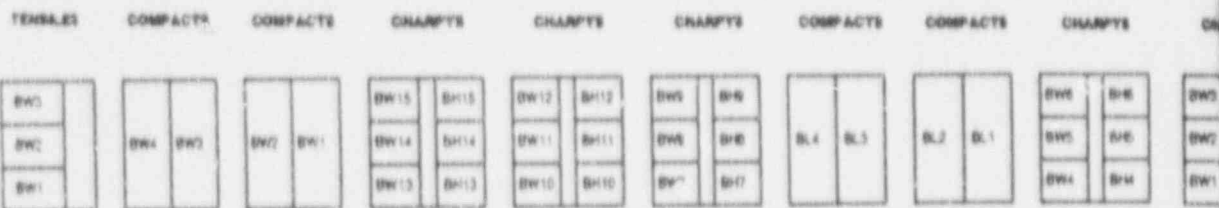
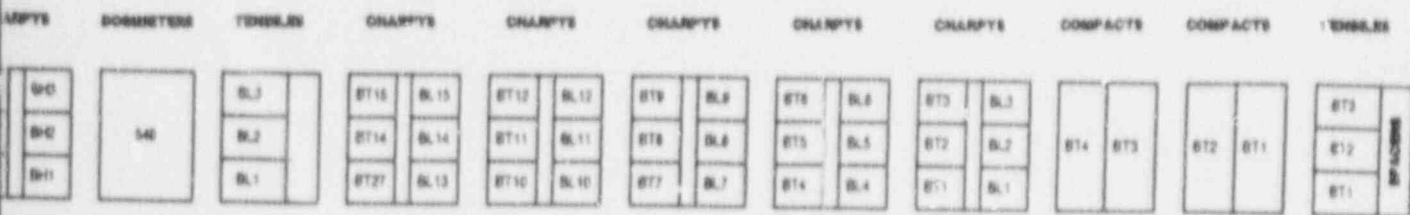


Figure 4-1. Arrangement of Surveillance Capsules in the Vogtle Electric Generating Plant Unit 2 Reactor Vessel



LEGEND: BL - LOWER SHELL PLATE B8628-1 (LONGITUDINAL)  
 BT - LOWER SHELL PLATE B8628-1 (TRANSVERSE)  
 BW - WELD METAL  
 BH - HEAT-AFFECTED-ZONE MATERIAL



## SI APERTURE CARD

Also Available On  
Aperture Card

Figure 4-2 Capsule U Diagram Showing Location of Specimens, Thermal Monitors and Dosimeters

9109050260-01

SECTION 5.0  
TESTING OF SPECIMENS FROM CAPSULE U

5.1 Overview

The post-irradiation mechanical testing of the Charpy V-notch and tensile specimens was performed at the Westinghouse Science and Technology Center hot cell with consultation by Westinghouse Power Systems personnel. Testing was performed in accordance with 10CFR50, Appendices G and H<sup>[2]</sup>, ASTM Specification E185-82<sup>[6]</sup>, and Westinghouse Remote Metallographic Facility (RMF) Procedure 8402, Revision 1 as modified by RMF Procedures 8102, Revision 1 and 8103, Revision 1.

Upon receipt of the capsule at the hot cell laboratory, the specimens and spacer blocks were carefully removed, inspected for identification number, and checked against the master list in WCAP-11381<sup>[1]</sup>. No discrepancies were found.

Examination of the two low-melting point 579°F (304°C) and 590°F (310°C) eutectic alloys indicated no melting of either type of thermal monitor. Based on this examination, the maximum temperature to which the test specimens were exposed was less than 579°F (304°C).

The Charpy impact tests were performed per ASTM Specification E23-88<sup>[7]</sup> and RMF Procedure 8103, Revision 1 on a Tinius-Olsen Model 74, 358J machine. The tup (striker) of the Charpy machine is instrumented with an Effects Technology Model 500 instrumentation system. With this system, load-time and energy-time signals can be recorded in addition to the standard measurement of Charpy energy ( $E_D$ ). From the load-time curve (Appendix A), the load of general yielding ( $P_{GY}$ ), the time to general yielding ( $t_{GY}$ ), the maximum load ( $P_M$ ), and the time to maximum load ( $t_M$ ) can be determined. Under some test conditions, a sharp drop in load indicative of fast fracture was observed. The load at which fast fracture was initiated is identified as the fast fracture load ( $P_F$ ), and the load at which fast fracture terminated is identified as the arrest load ( $P_A$ ).

The energy at maximum load ( $E_M$ ) was determined by comparing the energy-time record and the load-time record. The energy at maximum load is roughly equivalent to the energy required to initiate a crack in the specimen. Therefore, the propagation energy for the crack ( $E_p$ ) is the difference between the total energy to fracture ( $E_D$ ) and the energy at maximum load.

The yield stress ( $\sigma_Y$ ) was calculated from the three-point bend formula having the following expression:

$$\sigma_Y = P_{GY} * \{L/[B*(W-a)^2*C]\} \quad (1)$$

where L = distance between the specimen supports in the impact testing machine; B = the width of the specimen measured parallel to the notch; W = height of the specimen, measured perpendicularly to the notch; a = notch depth. The constant C is dependent on the notch flank angle ( $\phi$ ), notch root radius ( $\rho$ ), and the type of loading (i.e., pure bending or three-point bending).

In three-point bending a Charpy specimen in which  $\phi = 45^\circ$  and  $\rho = 0.010$ ", Equation 1 is valid with C = 1.21. Therefore (for L = 4W),

$$\sigma_Y = P_{GY} * \{L/[B*(W-a)^2*1.21]\} = [3.3P_{GY}W]/[B(W-a)^2] \quad (2)$$

For the Charpy specimens, B = 0.394 in., W = 0.394 in., and a = 0.070 in. Equation 2 then reduces to:

$$\sigma_Y = 33.3 * P_{GY} \quad (3)$$

where  $\sigma_Y$  is in units of psi and  $P_{GY}$  is in units of lbs. The flow stress was calculated from the average of the yield and maximum loads, also using the three-point bend formula.

Percent shear was determined from post-fracture photographs using the ratio-of-areas methods in compliance with ASTM Specification A370-89<sup>[8]</sup>. The lateral expansion was measured using a dial gage rig similar to that shown in the same specification.

Tension tests were performed on a 20,000-pound Instron Model 1115, split-console test machine, per ASTM Specification E8-89b<sup>[9]</sup> and E21-79 (1988)<sup>[10]</sup>, and RMF Procedure 8102, Revision 1. All pull rods, grips, and pins were made of Inconel 718 hardened to HRC45. The upper pull rod was connected through a universal joint to improve axially of loading. The tests were conducted at a constant crosshead speed of 0.05 inches per minute throughout the test.

Deflection measurements were made with a linear variable displacement transducer (LVDT) extensometer. The extensometer knife edges were spring-loaded to the specimen and operated through specimen failure. The extensometer gage length is 1.00 inch. The extensometer is rated as Class B-2 per ASTM E83-85<sup>[11]</sup>.

Elevated test temperatures were obtained with a three-zone electric resistance split-tube furnace with a 9-inch hot zone. All tests were conducted in air.

Because of the difficulty in remotely attaching a thermocouple directly to the specimen, the following procedure was used to monitor specimen temperature. Chromel-alumel thermocouples were inserted in shallow holes in the center and each end of the gage section of a dummy specimen and in each grip. In the test configuration, with a slight load on the specimen, a plot of specimen temperature versus upper and lower grip and controller temperatures was developed over the range of room temperature to 550°F (288°C). The upper grip was used to control the furnace temperature. During the actual testing the grip temperatures were used to obtain desired specimen temperatures. Experiments indicated that this method is accurate to  $\pm 2^\circ\text{F}$ .

The yield load, ultimate load, fracture load, total elongation, and uniform elongation were determined directly from the load-extension curve. The yield strength, ultimate strength, and fracture strength were calculated using the original cross-sectional area. The final diameter and final gage length were determined from post-fracture photographs. The fracture area used to calculate the fracture stress (true stress at fracture) and percent reduction in area was computed using the final diameter measurement.

## 5.2 Charpy V-Notch Impact Test Results

The results of the Charpy V-notch impact tests performed on the various materials contained in Capsule U, which was irradiated to  $4.44 \times 10^{18}$  n/cm<sup>2</sup> ( $E > 1.0$  MeV), are presented in Tables 5-1 through 5-4 and are compared with unirradiated results<sup>[1]</sup> as shown in Figures 5-1 through 5-4. The transition temperature increases and upper shelf energy decreases for the Capsule U materials are summarized in Table 5-5.

Irradiation of the reactor vessel lower shell plate B8628-1 Charpy specimens oriented with the longitudinal axis of the specimen parallel to the major rolling direction of the plate (longitudinal orientation) to  $4.44 \times 10^{18}$  n/cm<sup>2</sup> ( $E > 1.0$  MeV) at 550°F (Figure 5-1) resulted in no 30 ft-lb transition temperature increase and in a 50 ft-lb transition temperature increase of 5°F. This resulted in the 30 ft-lb transition temperature remaining at 10°F and a 50 ft-lb transition temperature of 50°F (longitudinal orientation).

The average upper shelf energy (USE) of the lower shell plate B8628-1 Charpy specimens (longitudinal orientation) resulted in a energy increase of 10 ft-lb after irradiation to  $4.44 \times 10^{18}$  n/cm<sup>2</sup> ( $E > 1.0$  MeV) at 550°F. This results in an average USE of 99 ft-lb (Figure 5-1).

Irradiation of the reactor vessel lower shell plate B8628-1 Charpy specimens oriented with the longitudinal axis of the specimen normal to the major rolling direction of the plate (transverse orientation) to  $4.44 \times 10^{18}$  n/cm<sup>2</sup> ( $E > 1.0$  MeV) at 550°F (Figure 5-2) resulted in no 30 ft-lb transition temperature increase and in a 50 ft-lb transition temperature increase of 5°F. This resulted in the 30 ft-lb transition temperature remaining at 30°F and a 50 ft-lb transition temperature of 80°F (transverse orientation).

The average upper shelf energy (USE) of the lower shell plate B8628-1 Charpy specimens (transverse orientation) resulted in an energy increase of 9 ft-lb after irradiation to  $4.44 \times 10^{18}$  n/cm<sup>2</sup> (E > 1.0 MeV) at 550°F. This resulted in an average USE of 79 ft-lb (Figure 5-2).

Irradiation of the reactor vessel core region weld metal Charpy specimens to  $4.44 \times 10^{18}$  n/cm<sup>2</sup> (E > 1.0 MeV) at 550°F (Figure 5-3) resulted in no 30 and 50 ft-lb transition temperature increases. The 30 ft-lb transition temperature remained at -15°F and the 50 ft-lb transition temperature remained at 5°F.

The average upper shelf energy (USE) of the reactor vessel core region weld metal resulted in an energy increase of 6 ft-lb after irradiation to  $4.44 \times 10^{18}$  n/cm<sup>2</sup> (E > 1.0 MeV) at 550°F. This resulted in an average USE of 98 ft-lb (Figure 5-3).

Irradiation of the reactor vessel weld Heat-Affected-Zone (HAZ) metal specimens to  $4.44 \times 10^{18}$  n/cm<sup>2</sup> (E > 1.0 MeV) at 550°F (Figure 5-4) resulted in no 30 and 50 ft-lb transition temperature increases. The 30 ft-lb transition temperature remained at -80°F and the 50 ft-lb transition temperature remained at -45°F.

The average upper shelf energy (USE) of the reactor vessel weld HAZ metal experienced an energy increase of 16 ft-lb after irradiation to  $4.44 \times 10^{18}$  n/cm<sup>2</sup> (E > 1.0 MeV) at 550°F. This resulted in an average USE of 122 ft-lb (Figure 5-4).

The fracture appearance of each irradiated Charpy specimen from the various materials is shown in Figures 5-5 through 5-8 and show an increasingly ductile or tougher appearance with increasing test temperature.

A comparison of the 30 ft-lb transition temperature increases and upper shelf energy decreases for the various Vogtle Electric Generating Plant Unit 2 surveillance materials with predicted values using the methods of NRC Regulatory Guide 1.99, Revision 2<sup>[3]</sup> is presented in Table 5-6. This comparison indicates that the transition temperature increases and the USE decreases resulting from irradiation to  $4.44 \times 10^{18}$  n/cm<sup>2</sup> (E > 1.0 MeV) are less than the Regulatory Guide predictions.

The load-time records for the individual instrumented Charpy specimen tests are shown in Appendix A.

### 5.3 Tension Test Results

The results of the tension tests performed on the various materials contained in capsule U irradiated to  $4.44 \times 10^{18}$  n/cm<sup>2</sup> (E > 1.0 MeV) are presented in Table 5-7 and are compared with unirradiated results<sup>[1]</sup> as shown in Figures 5-9 through 5-11.

The results of the tension tests performed on the lower shell plate B8628-1 (longitudinal orientation) indicated that irradiation to  $4.44 \times 10^{18}$  n/cm<sup>2</sup> (E > 1.0 MeV) at 550°F caused less than a 3 ksi increase in the 0.2 percent offset yield strength and less than a 3 ksi increase in the ultimate tensile strength when compared to unirradiated data<sup>[1]</sup> (Figure 5-9).

The results of the tension tests performed on the lower shell plate B8628-1 (transverse orientation) indicated that irradiation to  $4.44 \times 10^{18}$  n/cm<sup>2</sup> (E > 1.0 MeV) at 550°F caused less than a 3 ksi increase in the 0.2 percent offset yield strength and less than a 2 ksi increase in the ultimate tensile strength when compared to unirradiated data<sup>[1]</sup> (Figure 5-10).

The results of the tension tests performed on the reactor vessel core region weld metal indicated that irradiation to  $4.44 \times 10^{18}$  n/cm<sup>2</sup> (E > 1.0 MeV) at 550°F caused less than a 5 ksi increase in the 0.2 percent offset yield strength and less than a 4 ksi increase in the ultimate tensile strength when compared to unirradiated data<sup>[1]</sup> (Figure 5-11).

The small increases in 0.2% yield strength and tensile strength exhibited by the lower shell plate B8628-1 and the weld metal indicate that this material is not highly sensitive to irradiation to  $4.44 \times 10^{18}$  n/cm<sup>2</sup> (E > 1.0 MeV), as is also indicated by the Charpy impact test results.

The fractured tension specimens for the lower shell plate B8628-1 material are shown in Figures 5-12 and 5-13, while the fractured specimens for the weld metal are shown in Figure 5-14.

The engineering stress-strain curves for the tension tests are shown in Figures 5-15 through 5-19.

#### 5.4 Compact Tension Tests

Per the surveillance capsule testing program with Georgia Power Company, 1/2 T-compact tension fracture mechanics specimens will not be tested and will be stored at the Westinghouse Science and Technology Center.

TABLE 5-1

CHARPY V-NOTCH IMPACT DATA FOR THE VOGTLE ELECTRIC GENERATING  
PLANT UNIT 2 LOWER SHELL PLATE B8628-1 IRRADIATED  
AT 550°F, FLUENCE  $4.44 \times 10^{18}$  n/cm<sup>2</sup> (E > 1.0 MeV)

Sample No.	Temperature		Impact Energy		Lateral Expansion		Shear (%)
	(°F)	(°C)	(ft-lb)	(J)	(mils)	(mm)	
<u>Longitudinal Orientation</u>							
BL9	-75	(-59)	5.0	( 7.0)	5.0	(0.13)	5
BL10	-45	(-43)	14.0	( 19.0)	10.0	(0.25)	10
BL12	-15	(-26)	12.0	( 16.5)	9.0	(0.23)	10
BL1	0	(-18)	36.0	( 49.0)	27.0	(0.69)	25
BL6	15	( -9)	36.0	( 49.0)	27.0	(0.69)	25
BL2	25	( -4)	49.0	( 66.5)	34.0	(0.86)	40
BL15	40	( 4)	48.0	( 65.0)	40.0	(0.86)	40
BL8	50	( 10)	31.0	( 42.0)	32.0	(0.81)	40
BL5	65	( 18)	51.0	( 69.0)	36.0	(0.91)	50
BL7	80	( 27)	54.0	( 73.0)	44.0	(1.12)	55
BL4	100	( 38)	74.0	(100.5)	49.0	(1.24)	70
BL11	125	( 52)	73.0	( 99.0)	50.0	(1.27)	70
BL14	150	( 66)	102.0	(138.5)	74.0	(1.88)	100
BL13	200	( 93)	97.0	(131.5)	68.0	(1.73)	100
BL3	250	(121)	99.0	(134.)	65.0	(1.65)	100
<u>Transverse Orientation</u>							
BT5	-75	(-59)	6.0	( 8.0)	4.0	(0.10)	5
BT1	-50	(-46)	12.0	( 16.5)	10.0	(0.25)	10
BT12	-25	(-32)	17.0	( 23.0)	12.0	(0.30)	10
BT13	0	(-18)	23.0	( 31.0)	22.0	(0.56)	15
BT3	25	( -4)	36.0	( 49.0)	30.0	(0.76)	30
BT7	35	( 2)	38.0	( 51.5)	29.0	(0.74)	35
BT14	50	( 10)	40.0	( 54.0)	34.0	(0.86)	40
BT8	65	( 18)	45.0	( 61.0)	38.0	(0.97)	45
BT10	80	( 27)	43.0	( 58.5)	38.0	(0.97)	60
BT6	100	( 38)	50.0	( 68.0)	42.0	(1.07)	65
BT2	120	( 49)	66.0	( 89.5)	55.0	(1.40)	80
BT9	150	( 66)	65.0	( 88.0)	52.0	(1.32)	95
BT11	200	( 93)	74.0	(100.5)	61.0	(1.55)	100
BT4	275	(135)	82.0	(111.0)	55.0	(1.40)	100
BT15	375	(191)	81.0	(110.0)	54.0	(1.37)	100

TABLE 5-2

CHARPY V-NOTCH IMPACT DATA FOR THE VOGTLE ELECTRIC GENERATING  
PLANT UNIT 2 REACTOR VESSEL WELD METAL AND HAZ METAL IRRADIATED  
AT 550°F, FLUENCE  $4.44 \times 10^{18}$  n/cm<sup>2</sup> (E > 1.0 MeV)

<u>Temperature</u> <u>Sample No. (°F)</u>	<u>Impact Energy</u> <u>(°C)(ft-lb)</u>	<u>Lateral Expansion</u> <u>(J) (mils)</u>	<u>Shear</u> <u>(mm)</u>	<u>(%)</u>
<u>Weld Metal</u>				
BW2	-75 (-59)	7.0 (9.5)	3.0	(0.08) 5
BW14	-50 (-48)	14.0 (19.0)	9.0	(0.23) 10
BW11	-25 (-32)	20.0 (27.0)	19.0	(0.48) 15
BW9	-20 (-29)	58.0 (78.5)	38.0	(0.97) 55
BW12	-10 (-23)	54.0 (73.0)	38.0	(0.97) 55
BW8	0 (-18)	55.0 (74.5)	39.0	(0.99) 55
BW3	10 (-12)	63.0 (85.5)	40.0	(1.02) 65
BW15	25 (-4)	57.0 (77.5)	39.0	(0.99) 60
BW7	40 (4)	64.0 (87.0)	48.0	(1.22) 85
BW1	60 (16)	82.0 (111.0)	62.0	(1.57) 90
BW5	80 (27)	84.0 (114.0)	61.0	(1.55) 90
BW4	100 (38)	83.0 (112.5)	61.0	(1.55) 90
BW10	150 (66)	96.0 (130.0)	73.0	(1.85) 100
BW13	200 (93)	95.0 (129.0)	71.0	(1.80) 100
BW6	275 (135)	104.0 (141.0)	76.0	(1.93) 100
<u>HAZ Metal</u>				
BH9	-150 (-101)	17.0 (23.0)	7.0	(0.18) 10
BH3	-125 (-87)	22.0 (30.0)	11.0	(0.28) 15
BH5	-110 (-79)	32.0 (43.5)	17.0	(0.43) 25
BH15	-100 (-73)	51.0 (69.0)	25.0	(0.64) 45
BH1	-80 (-62)	40.0 (54.0)	19.0	(0.48) 40
BH6	-75 (-56)	39.0 (53.0)	23.0	(0.58) 40
BH2	-50 (-46)	52.0 (70.5)	35.0	(0.89) 50
BH13	-40 (-40)	99.0 (134.0)	67.0	(1.70) 90
BH10	-25 (-32)	112.0 (152.0)	60.0	(1.52) 95
BH12	-25 (-32)	112.0 (152.0)	60.0	(1.52) 90
BH11	0 (-18)	83.0 (112.5)	49.0	(1.24) 80
BH4	25 (-4)	108.0 (146.5)	62.0	(1.57) 100
BH7	75 (24)	125.0 (169.5)	70.0	(1.78) 100
BH14	110 (43)	128.0 (173.5)	69.0	(1.75) 100
BH8	150 (66)	126.0 (171.0)	60.0	(1.52) 100

TABLE 5-3

INSTRUMENTED CHARPY IMPACT TEST RESULTS FOR THE VOGTLE ELECTRIC GENERATING PLANT UNIT 2 LOWER SHELL  
 PLATE B8628-1 IRRADIATED AT 550°F, FLUENCE  $4.44 \times 10^{18}$  n/cm<sup>2</sup> (E > 1.0 MeV)

Sample Number	Test Temp (°F)	Charpy Energy (ft-lb)	Normalized Energies			Time to Yield (μsec)	Maximum Load (kips)	Time to Maximum (μsec)	Fracture Load (kips)	Arrest Load (kips)	Yield Stress (ksi)	Flow Stress (ksi)
			Charpy Ed/A (ft-lb/in <sup>2</sup> )	Maximum Ep/A	Prop Yield Load (kips)							
BL9	-75	5.0	40	26	14	3.50	85	95	3.70	0.01	116	121
BL10	-45	14.0	113	83	30	3.85	85	195	4.10	0.01	127	132
BL12	-15	12.0	97	46	51	3.45	85	130	3.90	0.01	115	122
BL1	0	36.0	290	264	26	3.50	80	505	5.15	0.01	119	147
BL8	15	36.0	290	256	34	3.80	85	500	4.85	0.01	125	145
BL2	25	49.0	395	235	160	3.55	80	498	4.40	0.01	117	137
BL15	40	48.0	387	COMPUTER MALFUNCTION**								
BL8	50	31.0	250	96	153	3.85	85	230	4.20	1.15	128	134
BL5	65	51.0	411	264	147	2.70	65	610	4.30	1.40	89	115
BL7	80	54.0	435	266	168	3.10	90	595	4.15	1.15	103	124
BL4	100	74.0	596	275	321	3.25	95	625	3.95	2.35	108	129
BL11	125	73.0	588	241	348	2.70	70	575	3.80	1.95	88	115
BL14	150	102.0	821	285	537	2.75	55	610	---	---	92	120
BL13	200	97.0	781	314	487	3.20	90	650	---	---	106	131
BL3	250	99.0	797	240	557	2.45	70	595	---	---	81	110
Longitudinal Orientation												
BT5	-75	6.0	48	43	6	3.70	95	130	3.90	0.01	122	125
BT1	-50	12.0	97	87	9	3.95	90	205	4.25	0.01	130	136
BT12	-25	17.0	137	86	52	3.85	85	200	4.10	0.01	127	132
BT13	0	23.0	185	135	50	3.55	85	330	4.50	0.15	118	133
BT3	25	36.0	290	176	114	4.15	90	355	4.95	0.75	137	150
BT7	35	38.0	306	201	105	2.85	75	455	4.35	0.55	95	120
BT14	50	40.0	322	156	166	3.65	80	335	4.55	1.60	120	140
BT8	65	45.0	352	251	111	3.35	75	505	4.75	1.85	110	137
BT10	80	43.0	346	137	709	2.60	60	345	3.85	2.90	86	108
BT6	100	50.0	403	259	144	3.15	60	505	4.95	3.05	104	137
BT2	120	66.0	531	209	322	2.60	90	495	3.85	2.50	86	113
BT9	150	65.0	523	239	284	2.00	45	570	4.15	3.35	65	103
BT11	200	74.0	596	235	361	2.90	60	510	---	---	95	123
BT4	375	82.0	560	192	468	2.95	95	470	---	---	97	118
BT15	375	81.0	552	280	372	2.80	50	505	---	---	92	120
Transverse Orientation												

\*Fully ductile fracture; no arrest load

\*\*Caused by data memory drop-out

TABLE 5-4

INSTRUMENTED CHARPY IMPACT TEST RESULTS FOR THE VOGTLE ELECTRIC GENERATING PLANT UNIT 2 WELD METAL AND HEAT-AFFECTED-ZONE (HAZ) METAL, IRRADIATED AT 550°F, FLUENCE  $4.44 \times 10^{18}$  n/cm<sup>2</sup> (E > 1.0 MeV)

Sample Number	Test Temp (°F)	Charpy Energy (ft-lb)	Normalized Energies			Yield Load (kips)	Time to Yield (µsec)	Maximum Load (kips)	Time to Maximum (µsec)	Fracture Load (kips)	Arrest Load (kips)	Yield Stress (ksi)	Flow Stress (ksi)	
			Charpy Ed/A	Maximum Em/A (ft-lb/in <sup>2</sup> )	Prop Ep/A									
<u>Weld Metal</u>														
BW2	-75	7.0	58	29	27	2.75	80	3.85	100	3.55	0.01	91	108	
BW14	-50	14.0	113	82	31	3.80	85	4.15	195	4.05	0.01	125	131	
BW11	-25	20.0	161	150	11	3.85	85	4.40	330	4.40	0.01	120	133	
BW9	-20	58.0	487	262	205	4.00	85	5.10	500	4.80	0.90	132	151	
BW12	-10	54.0	435	324	111	3.55	85	4.85	670	4.50	0.20	117	135	
BW8	0	55.0	443	288	155	3.50	95	4.80	805	4.35	1.00	116	134	
BW3	10	63.0	507	314	193	3.70	80	4.80	810	4.50	1.10	123	141	
BW15	25	57.9	459	302	157	3.05	55	4.80	840	4.35	0.85	100	129	
BW7	40	64.0	515	327	188	3.25	75	4.85	865	4.65	1.50	107	133	
BW1	60	82.0	680	300	361	3.00	75	4.40	855	3.85	2.25	99	122	
BW5	80	84.0	678	269	408	2.85	75	4.35	905	3.70	1.75	94	120	
BW6	80	84.0	678	269	408	2.85	75	4.35	905	3.70	1.75	94	120	
BW4	100	83.0	688	308	380	3.10	80	4.65	865	3.75	2.85	103	129	
BW10	150	96.0	773	310	463	2.25	50	4.25	730	---	---	74	107	
BW13	200	25.0	765	288	477	2.55	55	4.40	650	---	---	83	115	
BW8	275	104.0	837	340	497	2.80	50	4.60	725	---	---	93	123	
<u>HAZ Metal</u>														
BH9	-150	17.0	137	83	54	4.85	180	4.90	195	4.70	0.01	154	158	
BH3	-125	22.0	177	153	25	3.25	60	5.65	295	5.60	0.01	107	147	
BH5	-110	32.0	258	181	78	4.65	90	5.60	335	5.60	0.25	155	170	
BH15	-100	51.0	411	COMPUTER MALFUNCTION				---	---	---	---	---	---	---
BH1	-80	40.0	322	151	172	4.45	85	5.30	275	5.20	0.70	147	162	
BH6	-75	39.0	314	217	97	4.00	90	4.80	435	4.70	0.80	132	145	
BH2	-50	52.0	419	251	188	3.75	90	4.80	530	4.55	1.25	123	138	
BH13	-40	99.0	797	282	515	4.20	85	5.60	500	1.40	0.90	139	162	
BH12	-25	112.0	902	301	601	3.90	90	5.15	575	5.15	0.01	128	149	
BH10	-25	112.0	902	289	633	4.10	85	5.20	500	2.10	1.00	136	154	
BH11	0	83.0	668	289	380	3.80	80	4.75	575	3.35	1.95	120	138	
BH4	25	108.0	870	285	585	2.90	60	4.95	575	---	---	98	130	
BH7	75	125.0	1007	292	715	3.50	80	4.95	600	---	---	115	139	
BH14	110	128.0	1031	283	788	2.50	75	4.50	605	---	---	83	116	
BH8	150	126.0	1015	328	687	3.10	60	4.80	655	---	---	103	131	

\*Fully ductile fracture; no arrest load  
 \*\*Caused by data memory drop-out

TABLE 5-5

EFFECT OF 550°F IRRADIATION TO  $4.44 \times 10^{18}$  n/cm<sup>2</sup> (E > 1.0 MeV)

ON THE NOTCH TOUGHNESS PROPERTIES OF THE VOGTLE ELECTRIC GENERATING PLANT UNIT 2 REACTOR VESSEL SURVEILLANCE MATERIALS

Material	Average 30 ft-lb <sup>(1)</sup>			Average 35 mil <sup>(1)</sup>			Average 50 ft-lb <sup>(1)</sup>			Average Energy <sup>(1)</sup>		
	Transition			Lateral Expansion			Transition			Absorption at		
	Temperature (°F)			Temperature (°F)			Temperature (°F)			Full Shear (ft-lb)		
	Unirradiated	Irradiated	ΔT	Unirradiated	Irradiated	ΔT	Unirradiated	Irradiated	ΔT	Unirradiated	Irradiated	Δ(ft-lb)
Plate 88628-1 (Longitudinal)	10	10	0	35	40	5	45	50	5	89	99	+ 10
Plate 88628-1 (Transverse)	30	30	0	40	45	5	75	80	5	70	79	+ 9
Weld Metal	- 15	- 15	0	- 5	- 5	0	5	5	0	92	98	+ 6
HAZ Metal	- 80	- 80	0	- 50	- 50	0	- 45	- 45	0	106	122	+ 16

(1) "AVERAGE" is defined as the value read from the curve fitted through the data points of the Charpy tests (Figures 5-1 through 5-4).

TABLE 5-6

COMPARISON OF THE VOGTLE ELECTRIC GENERATING PLANT UNIT 2 SURVEILLANCE MATERIAL 30 FT-LB TRANSITION TEMPERATURE SHIFTS AND UPPER SHELF ENERGY DECREASES WITH REGULATORY GUIDE 1.99 REVISION 2 PREDICTIONS

Material	Capsule	Fluence $10^{19}$ n/cm <sup>2</sup>	30 ft-lb Transition Temp. Shift		Upper Shelf Energy Decrease	
			R.G. 1.99 Rev. 2 (Predicted) <sup>(a)</sup> (°F)	Measured (°F)	R.G. 1.99 Rev. 2 (Predicted) (%)	Measured (%)
Plate B8628-1 (Longitudinal)	U	0.444	24	0	16	0
Plate B8628-1 (Transverse)	U	0.444	24	0	16	0
Weld Metal	U	0.444	28	0	16	0
HAZ Metal	U	0.444	--	0	--	0

a) Mean wt. % values of Cu and Ni were used to calculate the chemistry factors for the surveillance material.

TABLE 5-7

TENSILE PROPERTIES FOR THE WOGTLE ELECTRIC GENERATING PLANT UNIT 2 REACTOR VESSEL SURVEILLANCE  
 MATERIALS IRRADIATED AT 550°F TO  $4.44 \times 10^{19}$  n/cm<sup>2</sup> (E > 1.0 MeV)

<u>Material</u>	<u>Sample Number</u>	<u>Test Temp. (°F)</u>	<u>0.2% Yield Strength (ksi)</u>	<u>Ultimate Strength (ksi)</u>	<u>Fracture Load (kip)</u>	<u>Fracture Stress (ksi)</u>	<u>Fracture Strength (ksi)</u>	<u>Uniform Elongation (%)</u>	<u>Total Elongation (%)</u>	<u>Reduction in Area (%)</u>
Plate B8628-1 (Longitudinal)	BL1	70	71.8	93.7	3.06	168.1	82.1	12.0	24.0	63
	BL2	150	68.8	88.0	2.80	139.3	67.0	9.9	22.7	59
	BL3	550	63.2	89.6	3.20	141.0	65.2	9.5	21.6	54
Plate B8628-1 (Transverse)	BT1	50	72.3	93.7	3.30	156.2	67.2	12.0	23.1	57
	BT2	150	68.2	87.6	3.00	142.0	61.1	11.4	22.1	57
	BT3	550	62.6	87.6	3.40	192.4	69.3	9.6	13.4	64
Weld	BW1	50	72.2	88.6	2.95	191.6	60.1	12.0	23.1	69
	BW2	150	67.2	83.5	2.70	170.5	55.0	12.0	24.5	68
	BW3	550	63.2	83.5	3.00	157.0	61.1	9.9	18.9	61

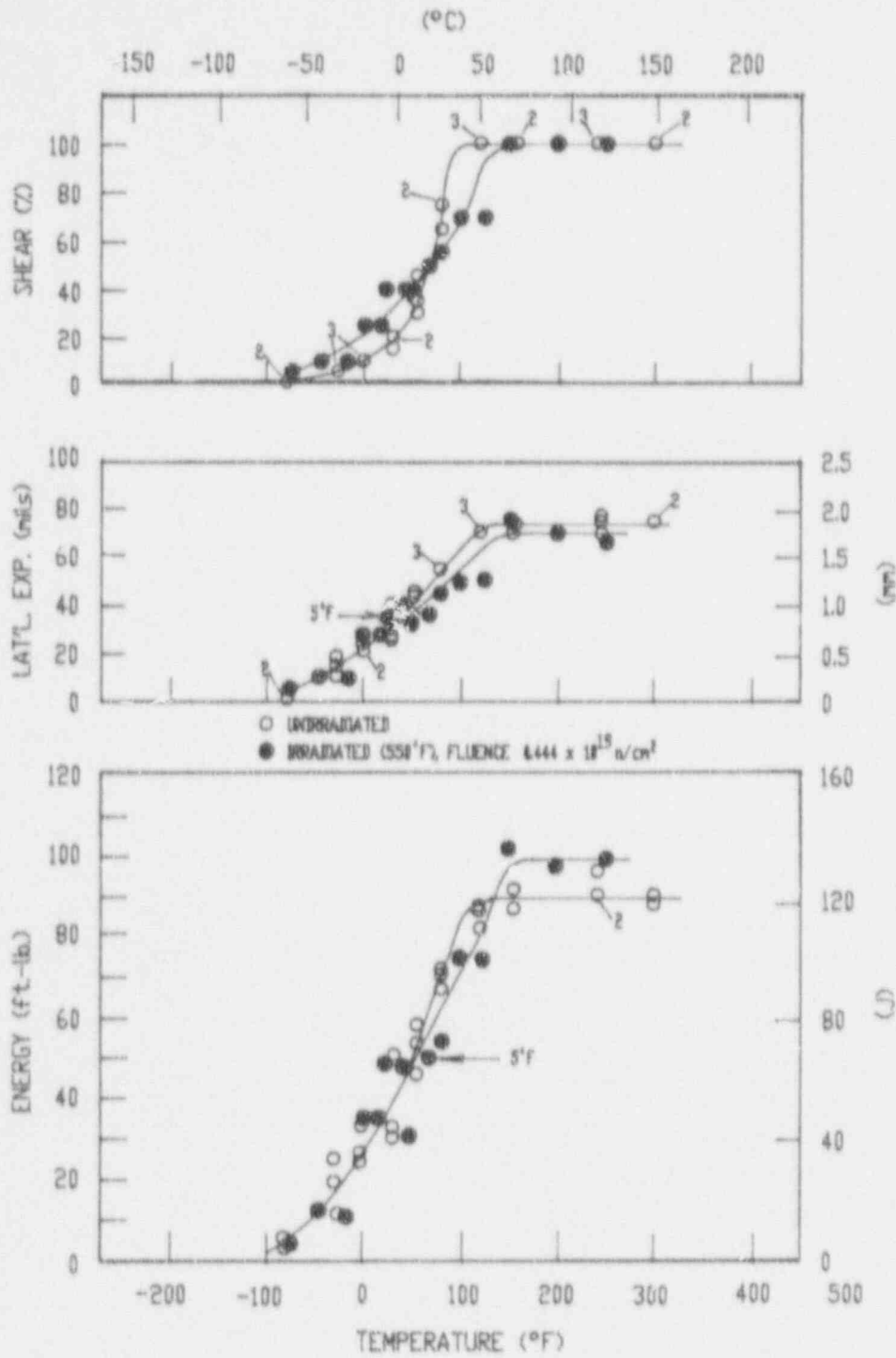


Figure 5-1. Charpy V-Notch Impact Properties for Vogtle Electric Generating Plant Unit 2 Reactor Vessel Lower Shell Plate B8528-1 (Longitudinal orientation)

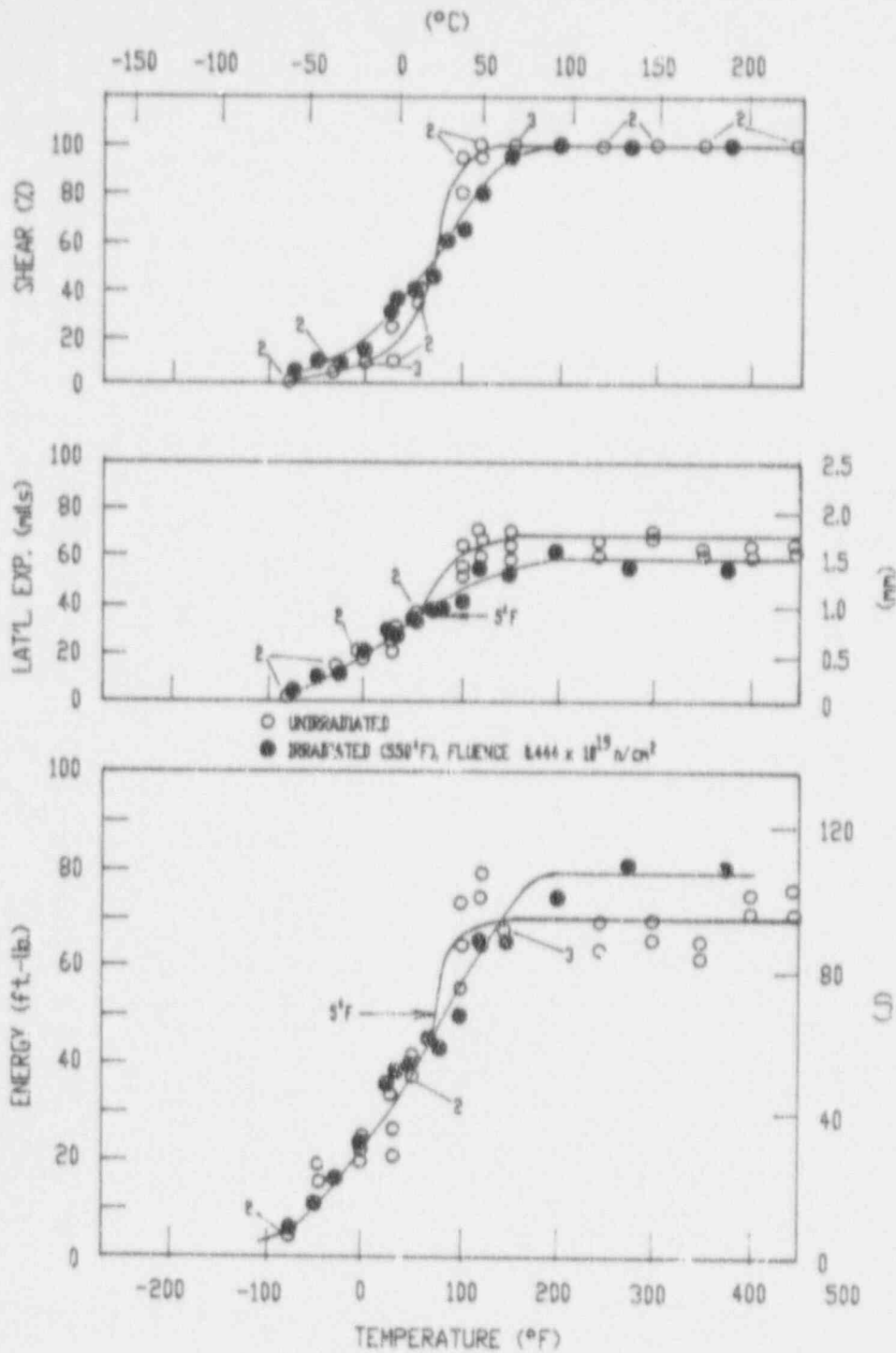


Figure 5-2. Charpy V-Notch Impact Properties for Vogtle Electric Generating Plant Unit 2 Reactor Vessel Lower Shell Plate B8628-1 (Transverse Orientation)

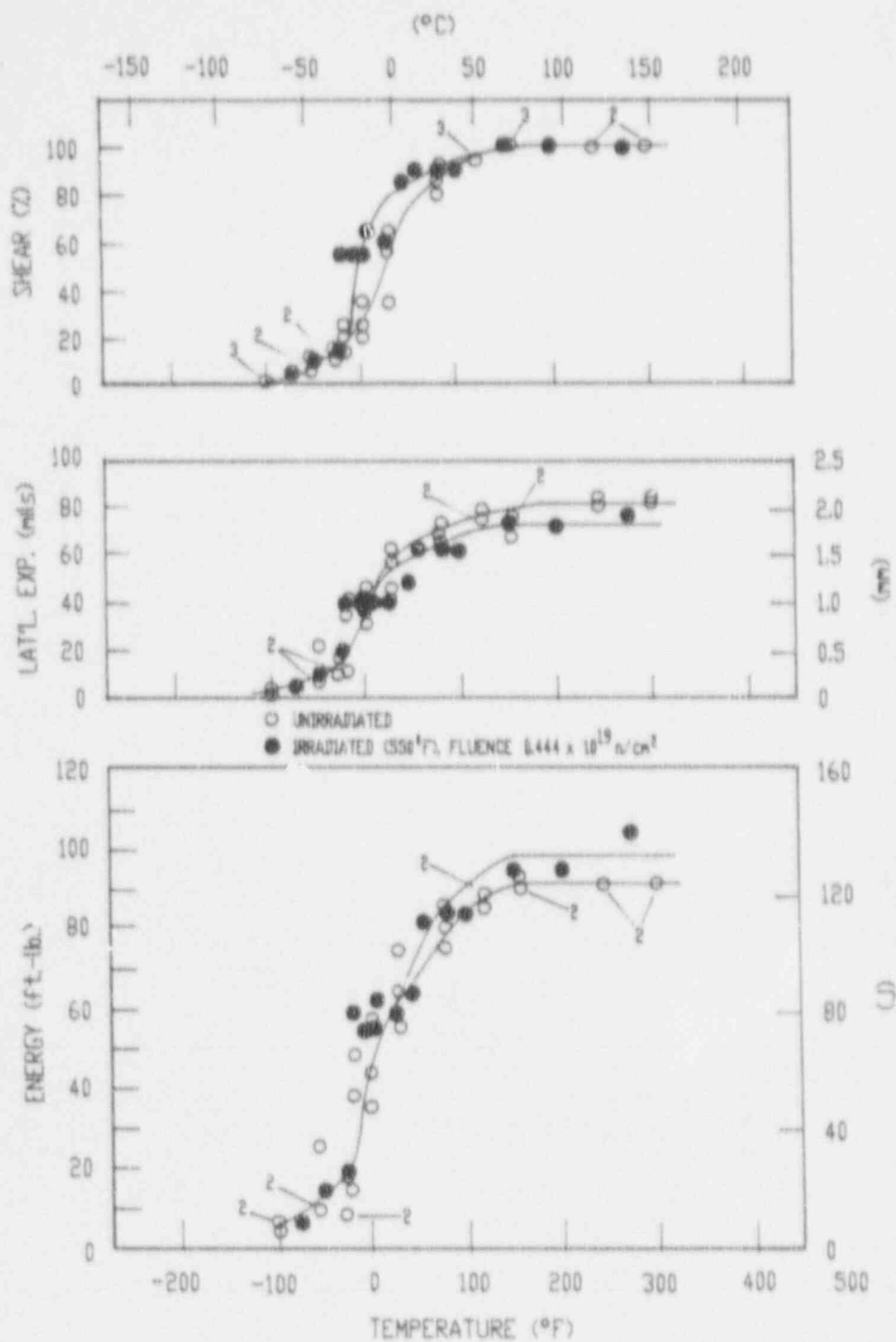


Figure 5-3. Charpy V-Notch Impact Properties for Vogtle Electric Generating Plant Unit 2 Reactor Vessel Surveillance Weld Metal

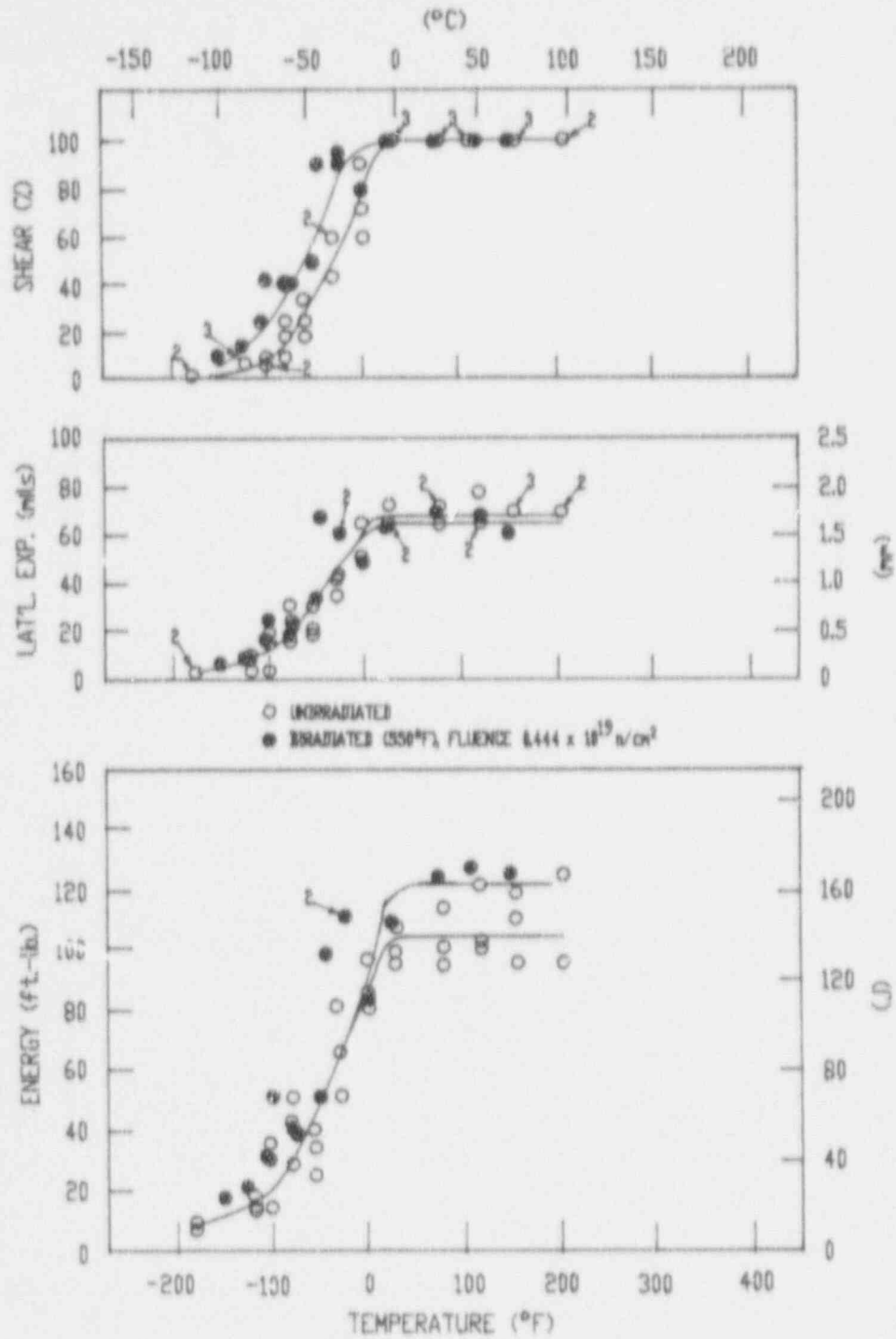


Figure 5-4. Charpy V-Notch Impact Properties for Vogtle Electric Generating Plant Unit 2 Reactor Vessel Weld Heat-Affected-Zone Metal

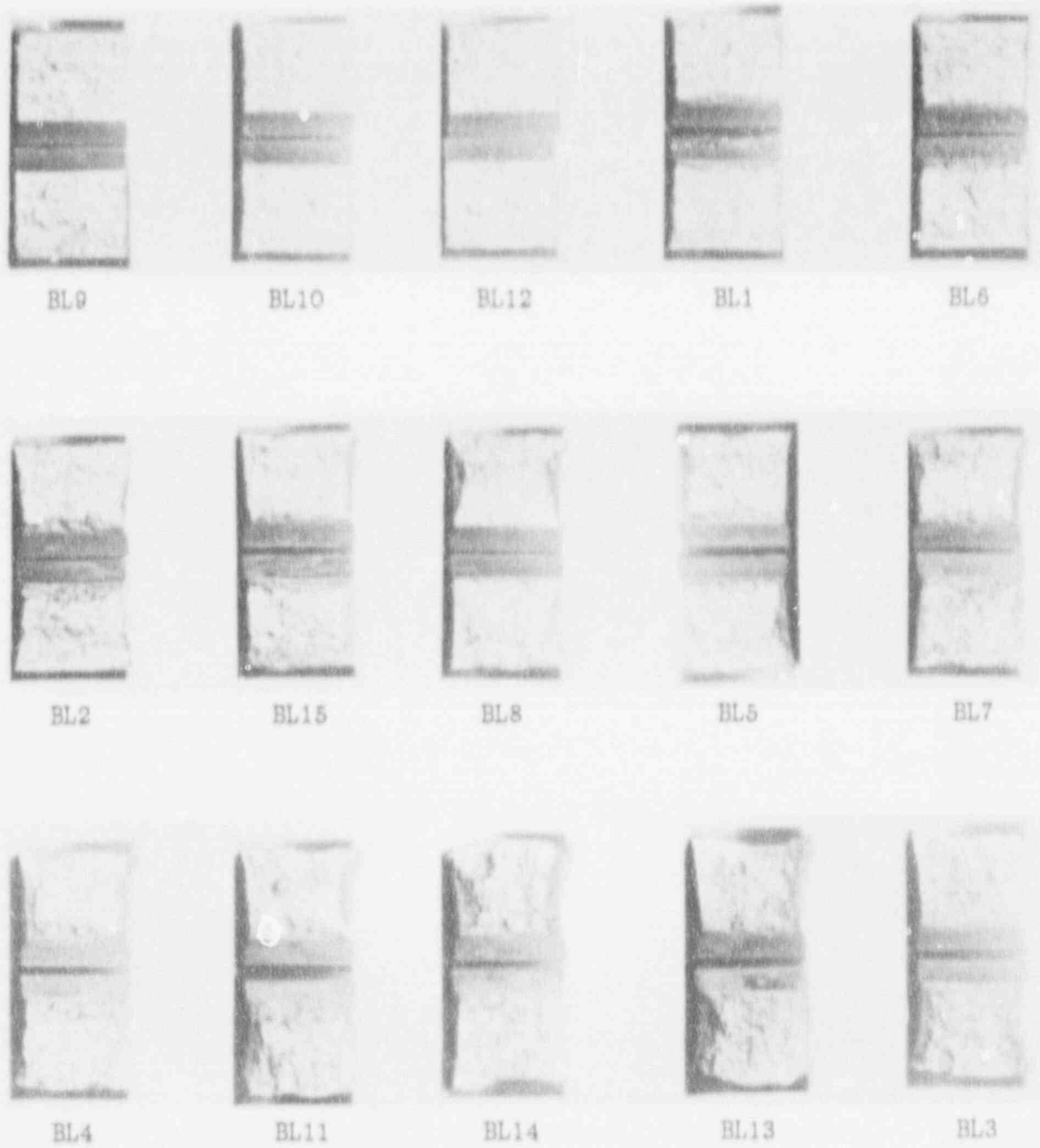


Figure 5-5. Charpy Impact Specimen Fracture Surfaces for Vogtle Electric Generating Plant Unit 2 Reactor Vessel Lower Shell Plate BB628-1 (Longitudinal Orientation)

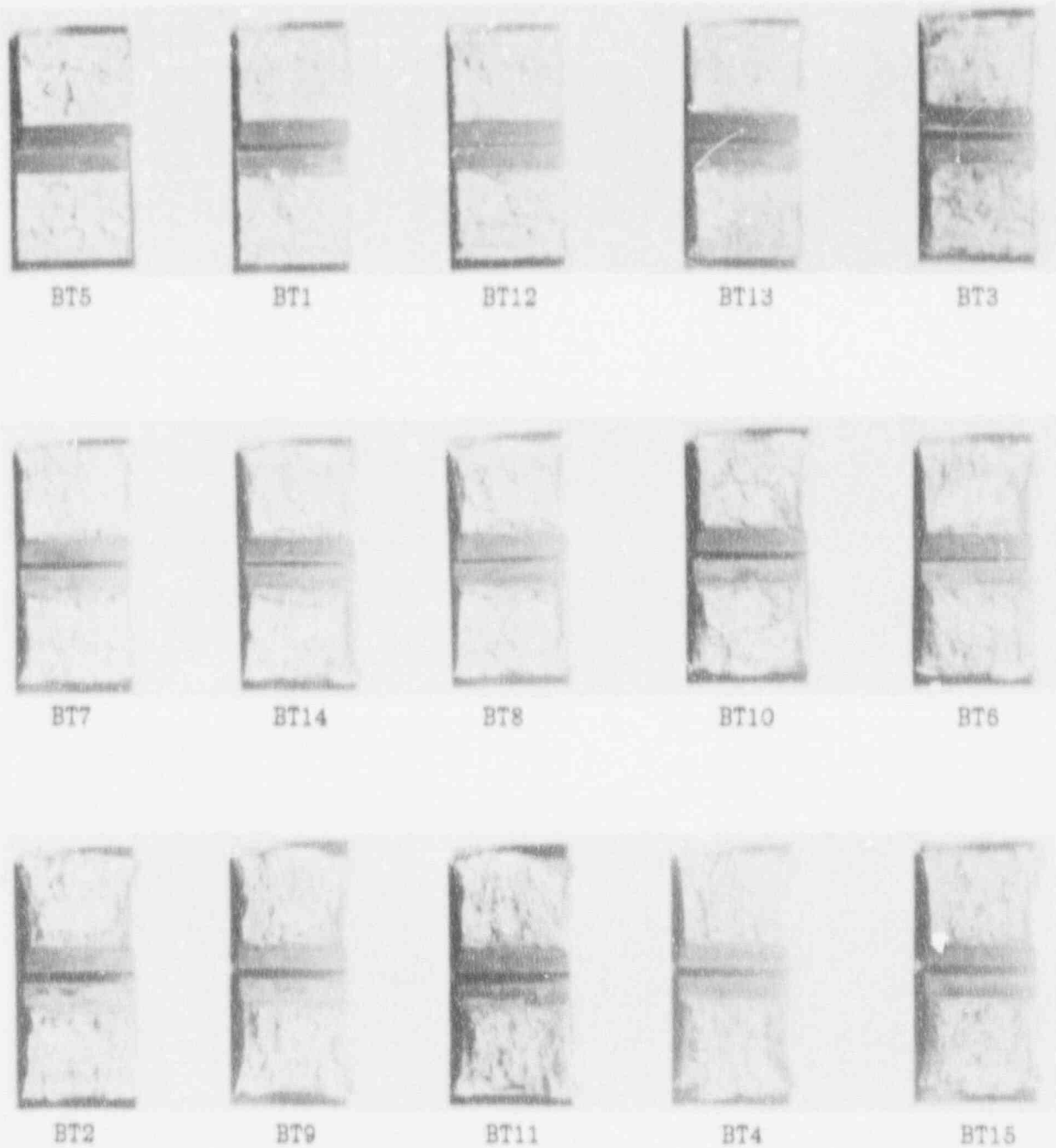


Figure 5-6. Charpy Impact Specimen Fracture Surfaces for Vogtle Electric Generating Plant Unit 2 Reactor Vessel Lower Shell Plate 88628-1 (Transverse Orientation)

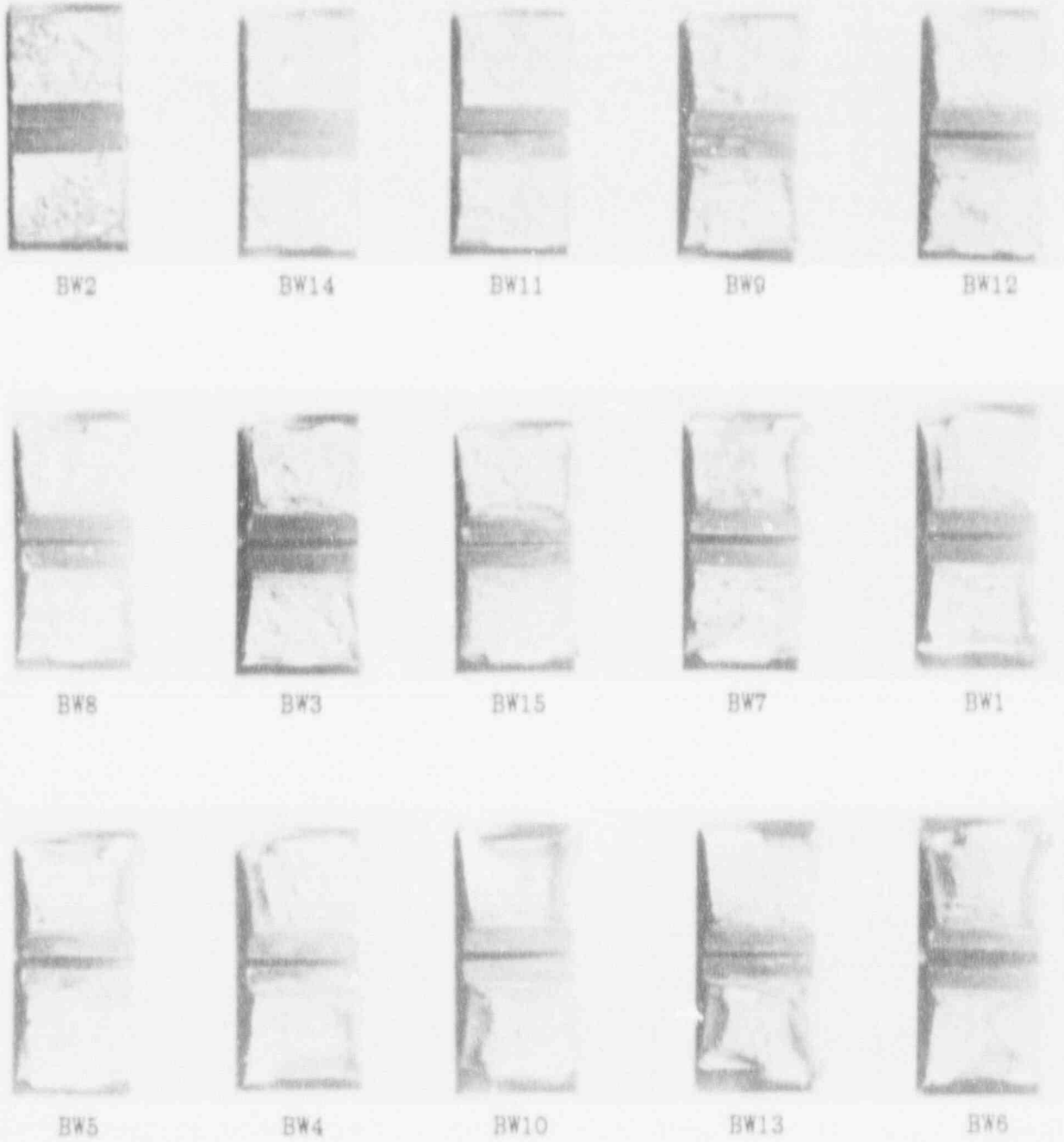


Figure 5-7. Charpy Impact Specimen Fracture Surfaces for Vogtle Electric Generating Plant Unit 2 Reactor Vessel Surveillance Weld Metal

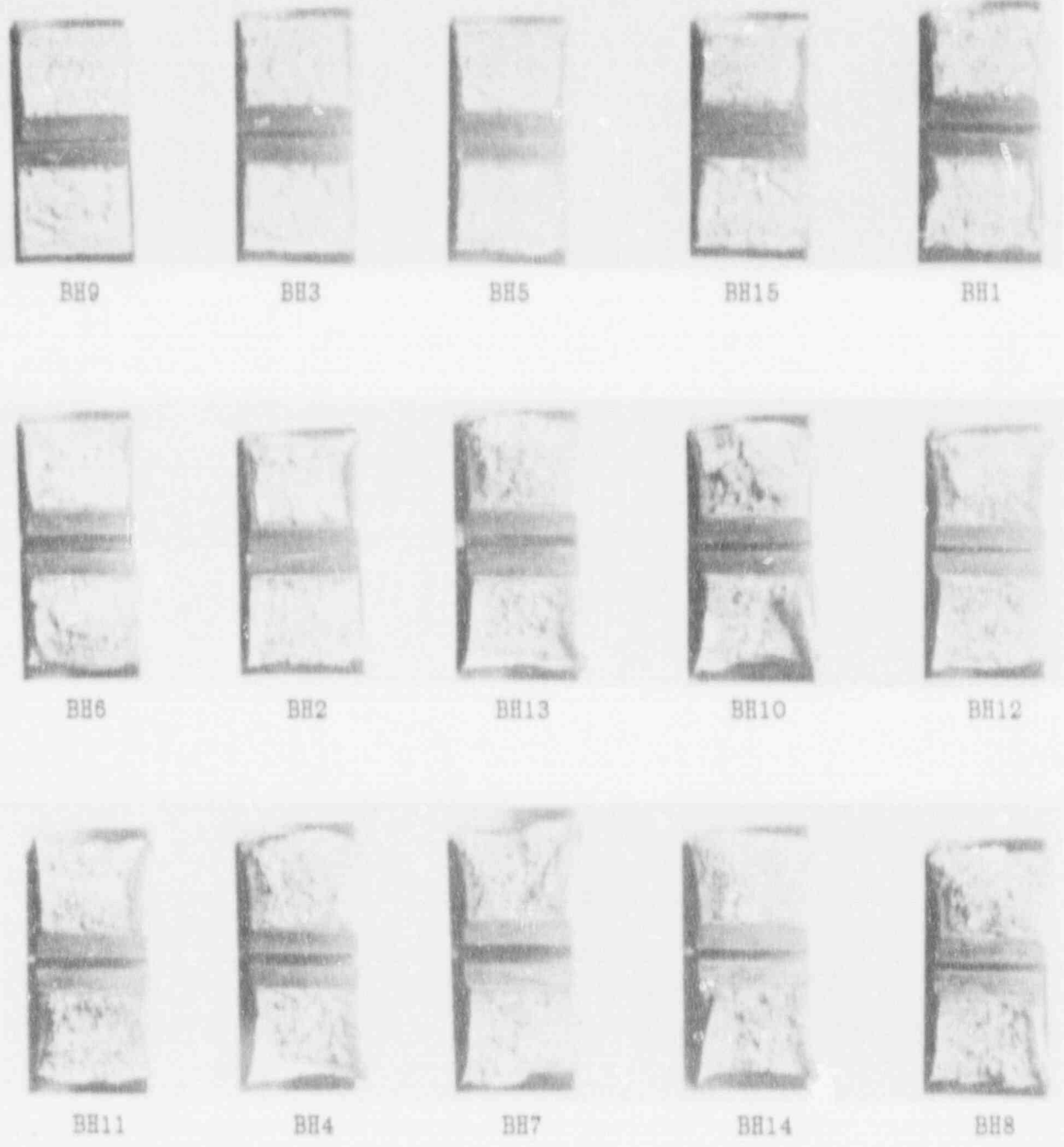


Figure 5-8. Charpy Impact Specimen Fracture Surfaces for Vogtle Electric Generating Plant Unit 2 Reactor Vessel Weld Heat-Affected-Zone Metal

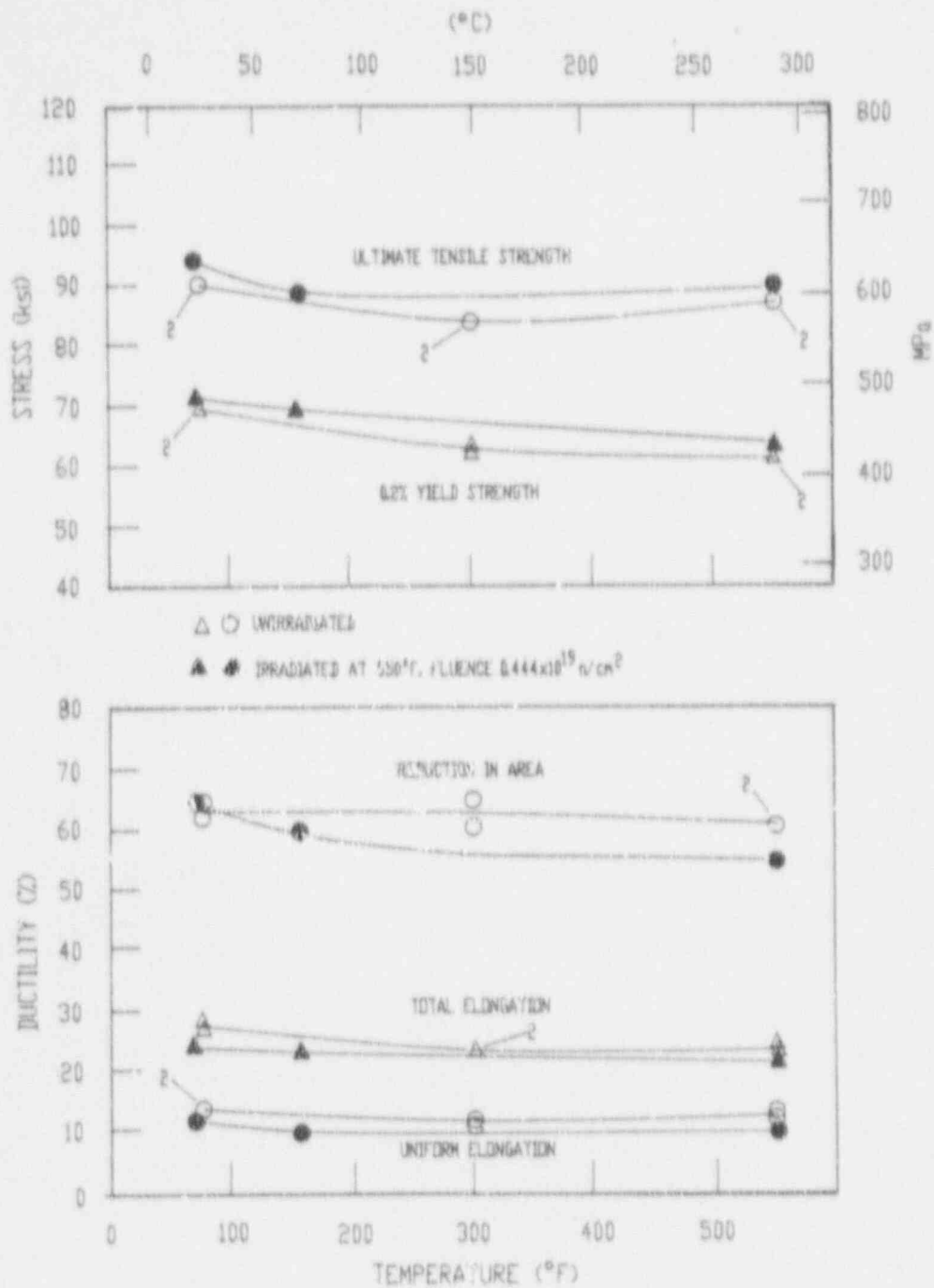


Figure 5-9. Tensile Properties for Vogtle Electric Generating Plant Unit 2 Reactor Vessel Lower Shell Plate B8628-1 (Longitudinal Orientation)

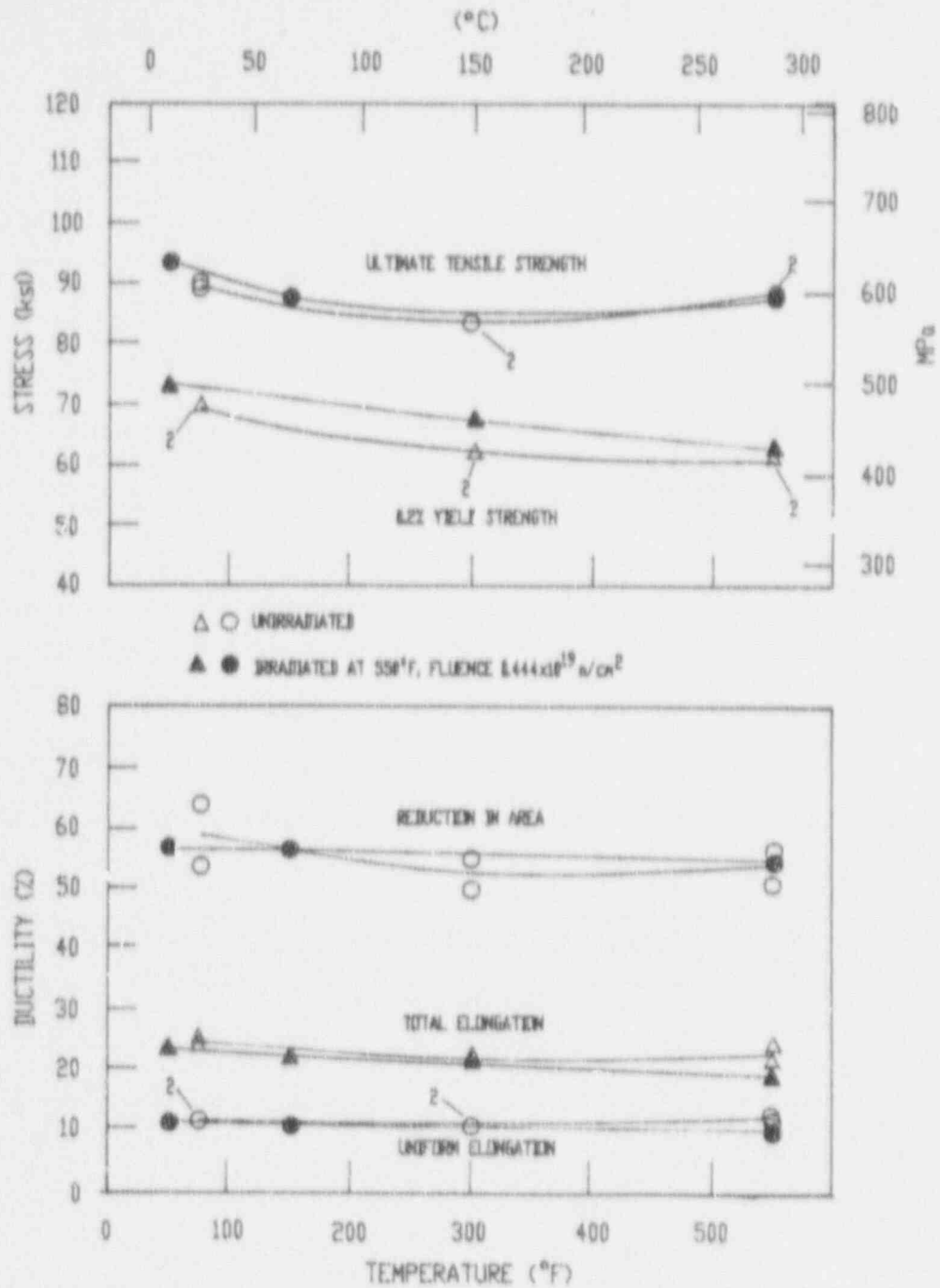


Figure 5-10. Tensile Properties for Vugtle Electric Generating Plant Unit 2 Reactor Vessel Lower Shell Plate B8328-1 (Transverse Orientation)

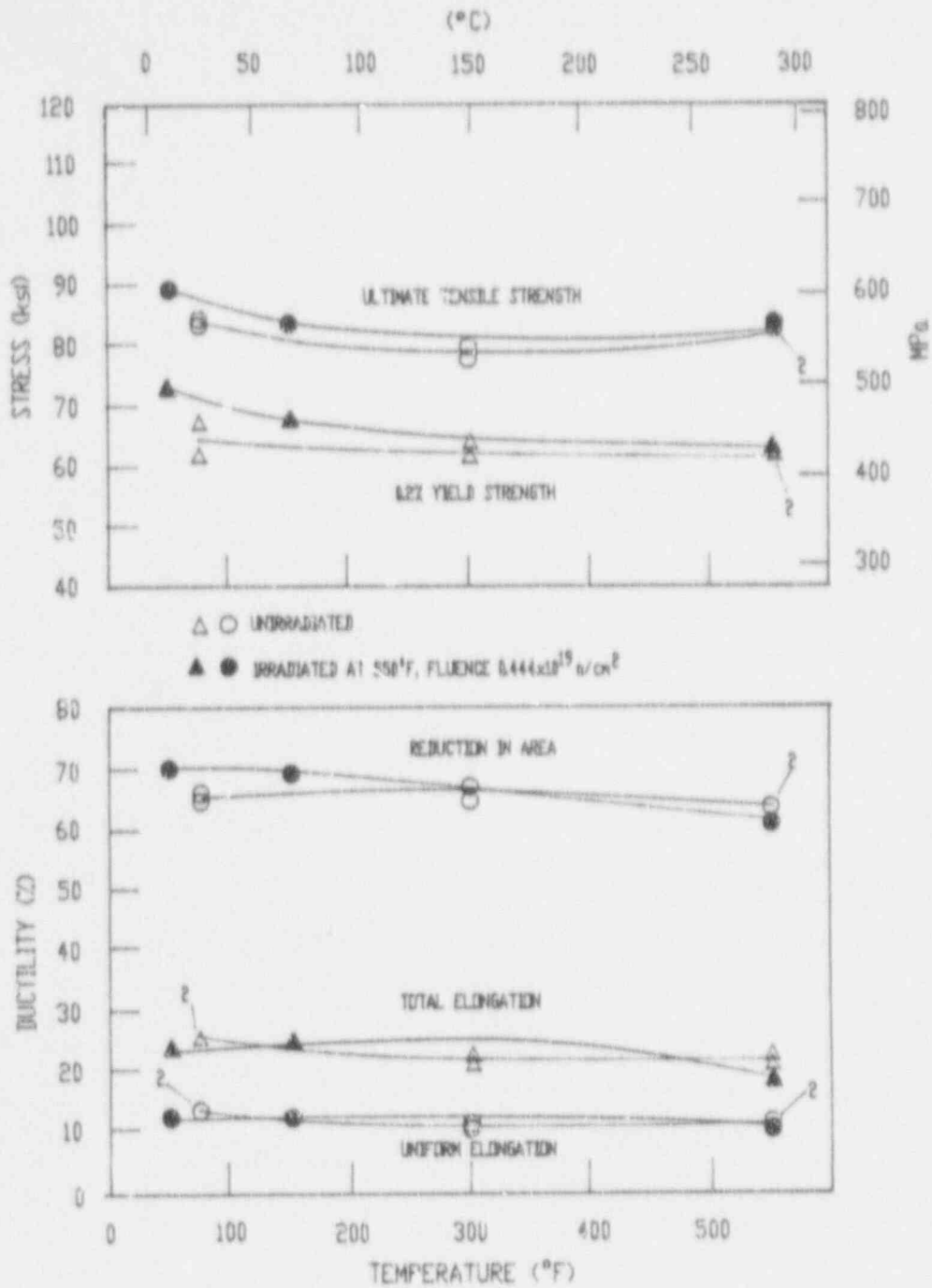
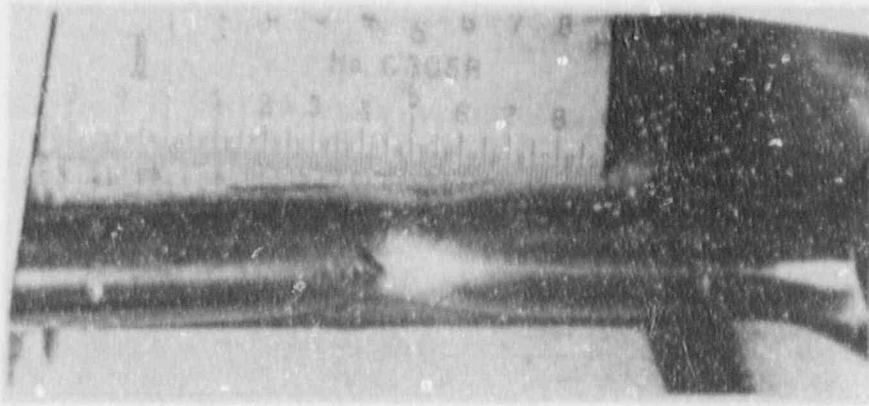
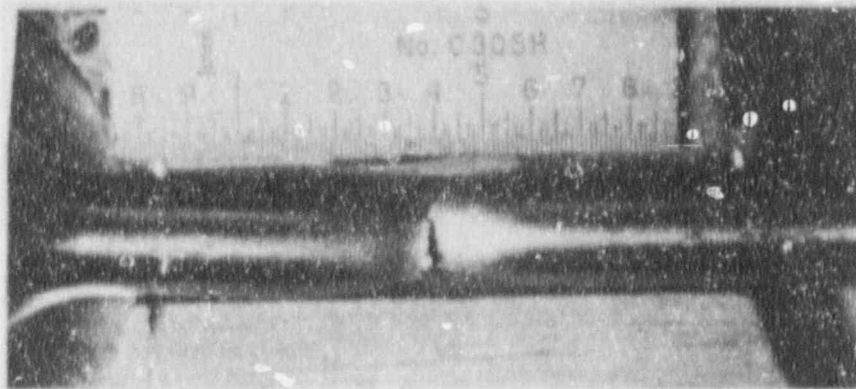


Figure 5-11. Tensile Properties for Vogtle Electric Generating Plant Unit 2 Reactor Vessel Surveillance Weld Metal



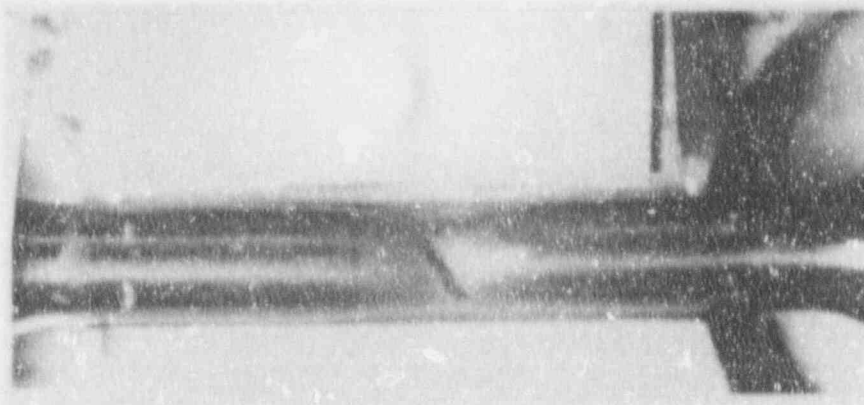
Specimen BL1

70°F



Specimen BL2

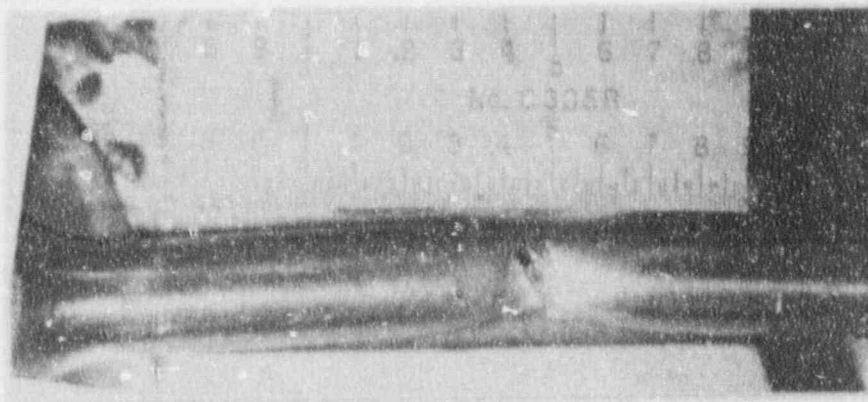
160°F



Specimen BL3

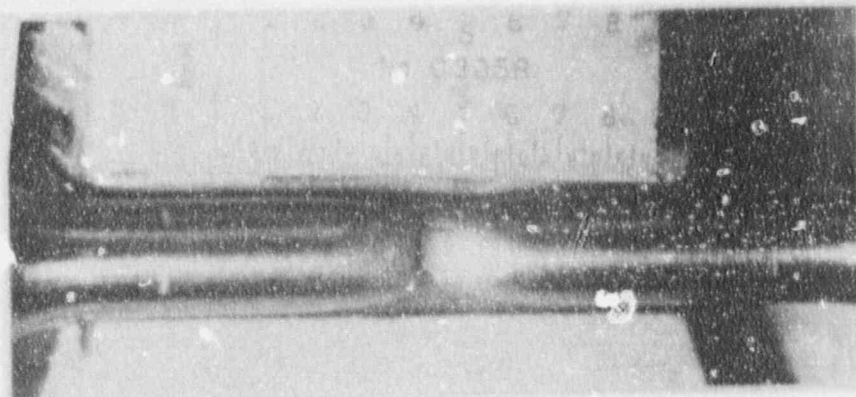
550°F

Figure 5-12. Fractured Tensile Specimens from Vogtle Electric Generating Plant Unit 2 Reactor Vessel Lower Shell Plate B8628-1 (Longitudinal Orientation)



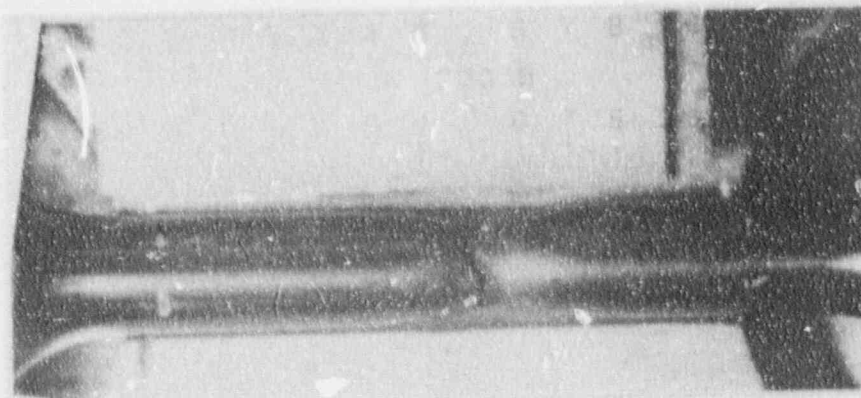
Specimen BT1

50°F



Specimen BT2

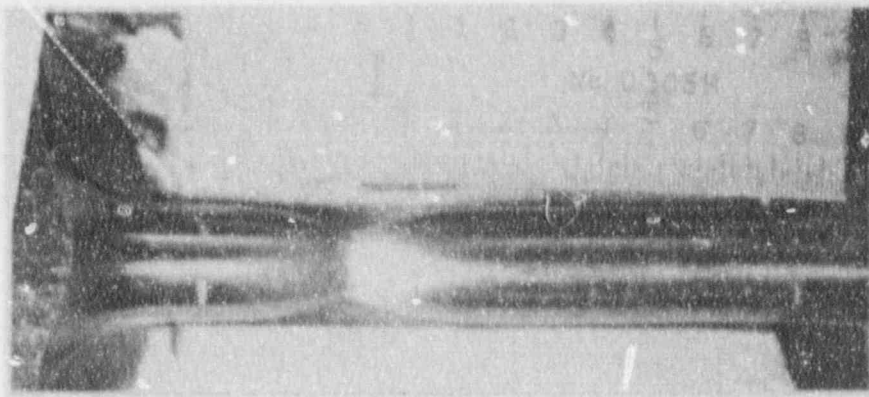
150°F



Specimen BT3

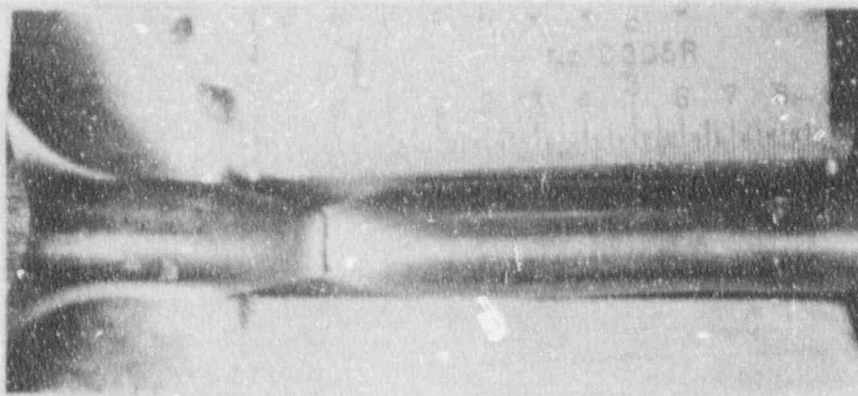
550°F

Figure 5-13. Fractured Tensile Specimens from Vogtle Electric Generating Plant Unit 2 Reactor Vessel Lower Shell Plate B8628-1 (Transverse Orientation)



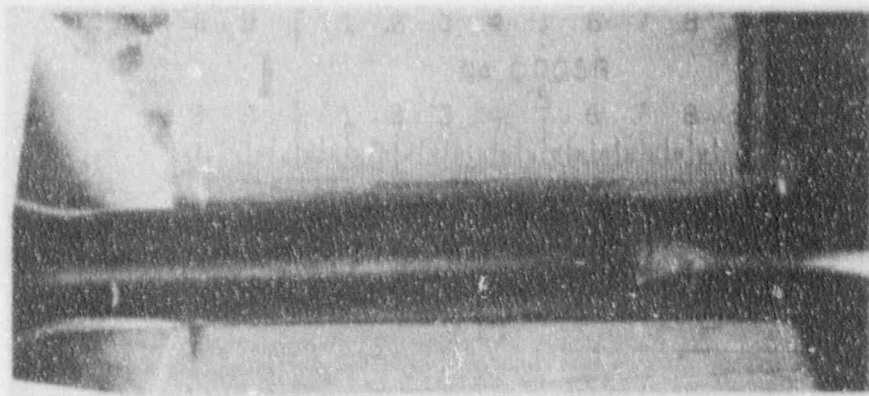
Specimen BW1

50°F



Specimen BW2

150°F



Specimen BW3

550°F

Figure 5-14. Fractured Tensile Specimens from Vogtle Electric Generating Plant Unit 2 Reactor Vessel Surveillance Weld Metal

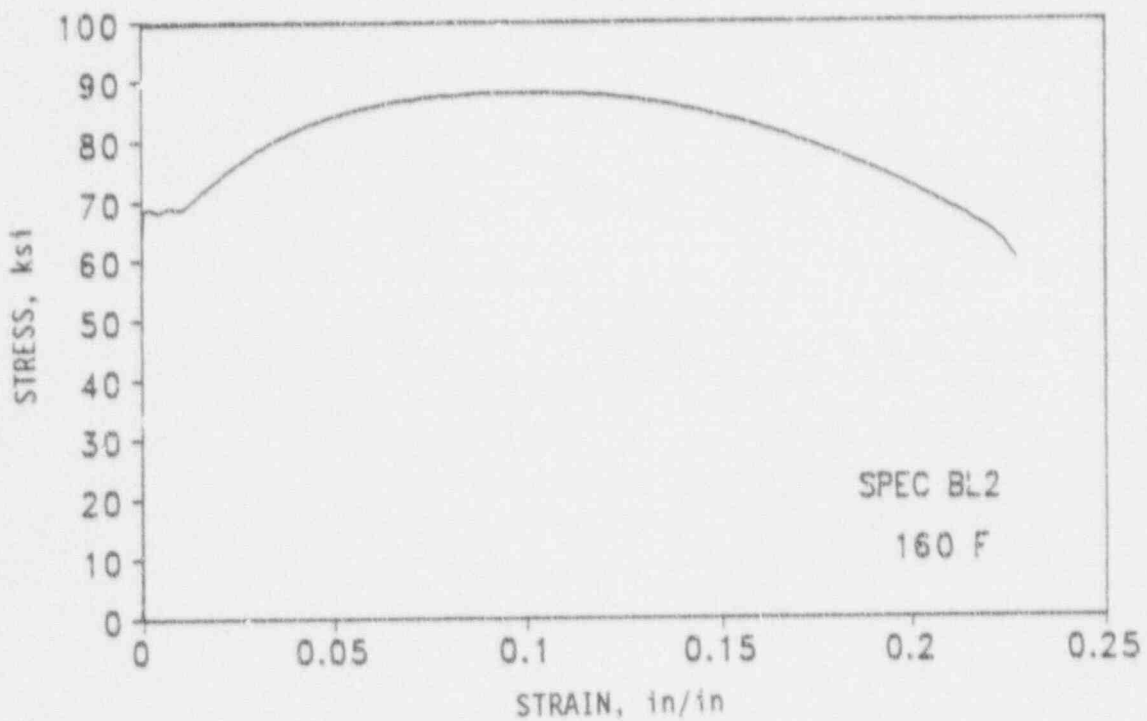
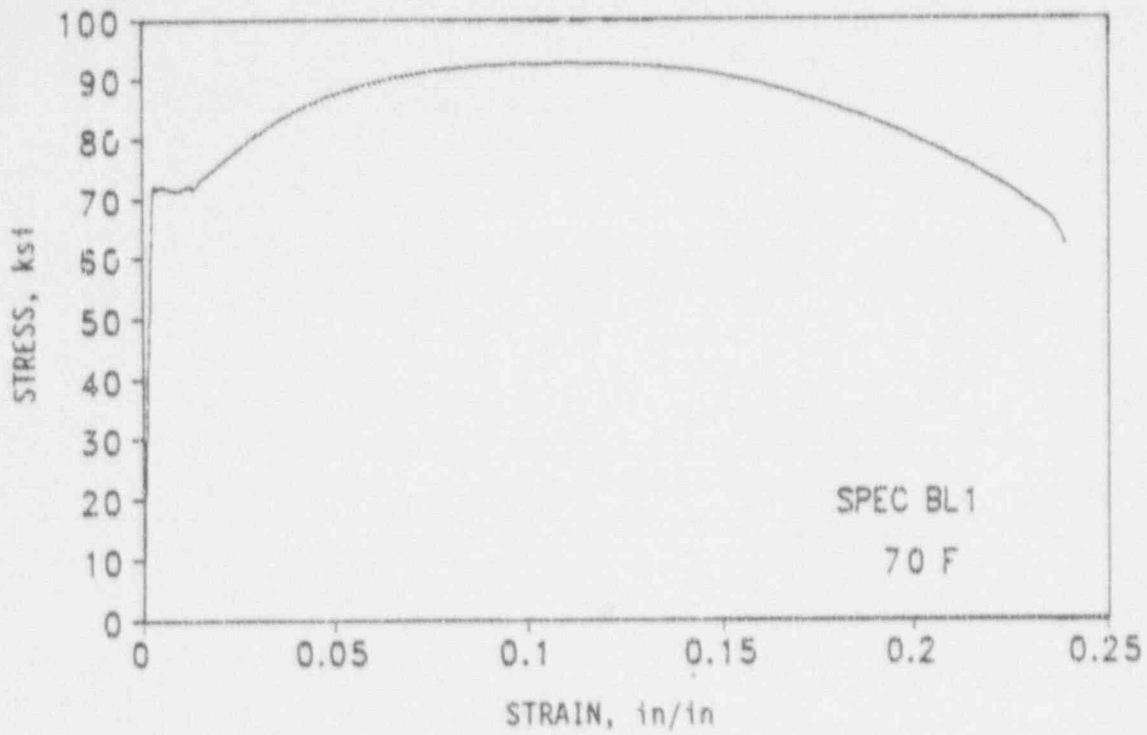


Figure 5-15. Engineering Stress-Strain Curves for Plate B8628-1 Tensile Specimens BL1 and BL2 (Longitudinal Orientation)

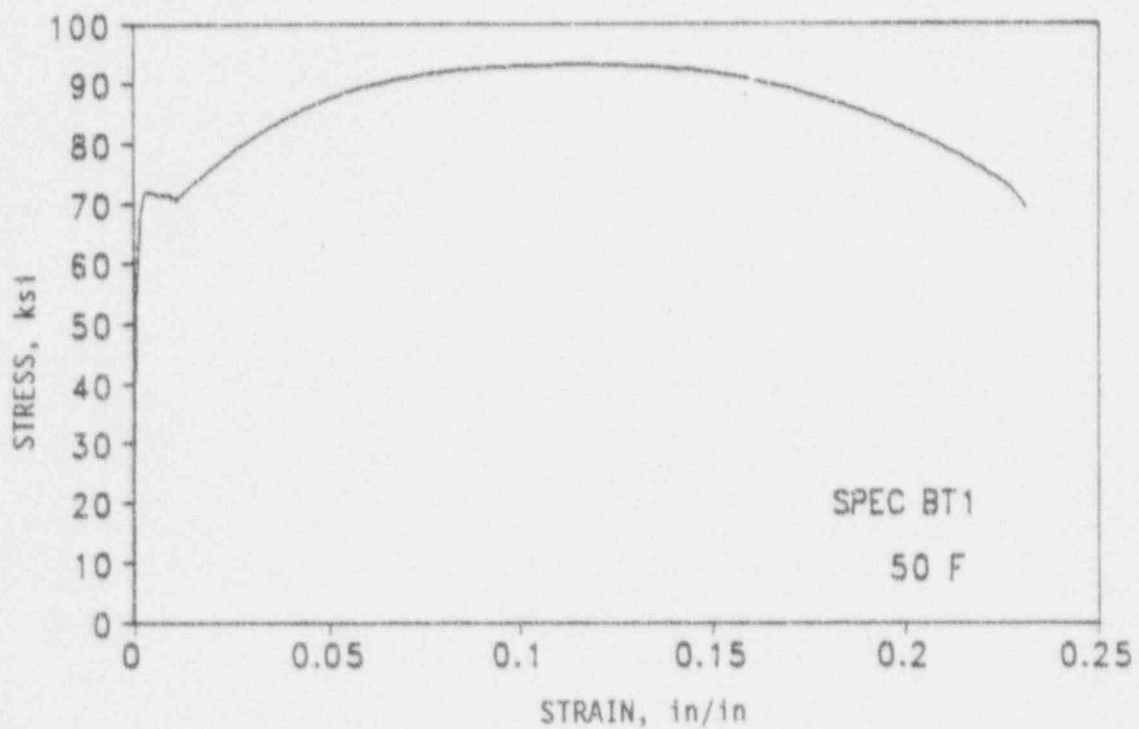
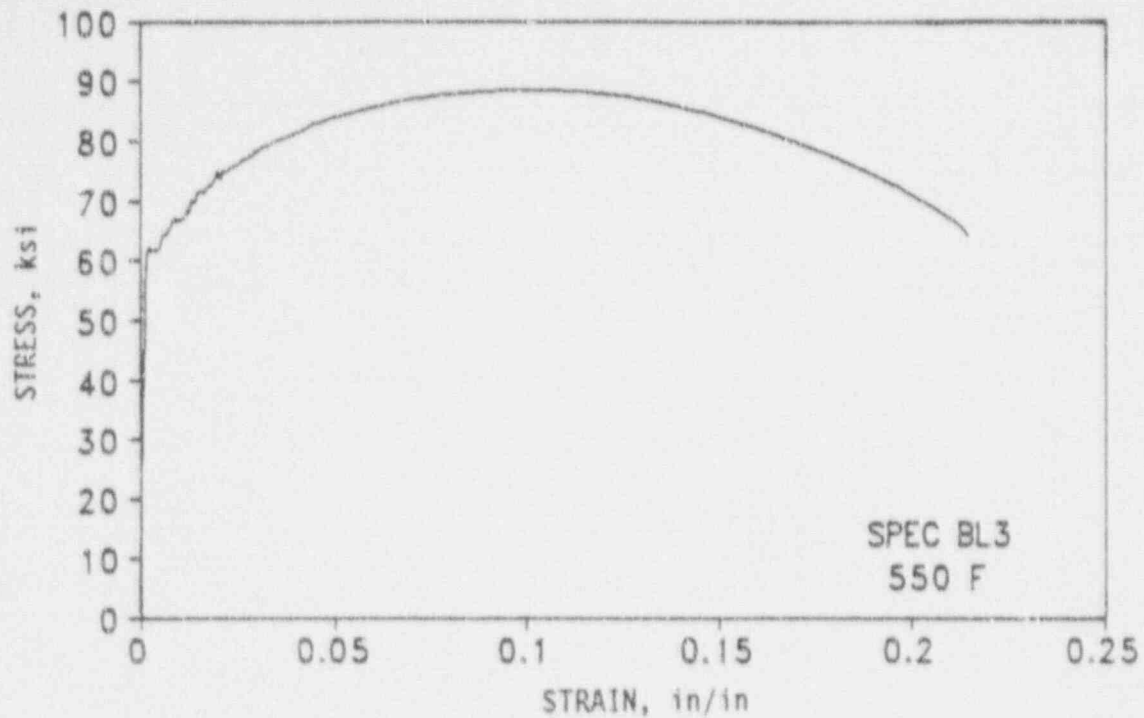


Figure 5-16. Engineering Stress-Strain Curve for Plate B8628-1 Tensile Specimens BL3 (Longitudinal Orientation) and BT1 (Transverse Orientation)

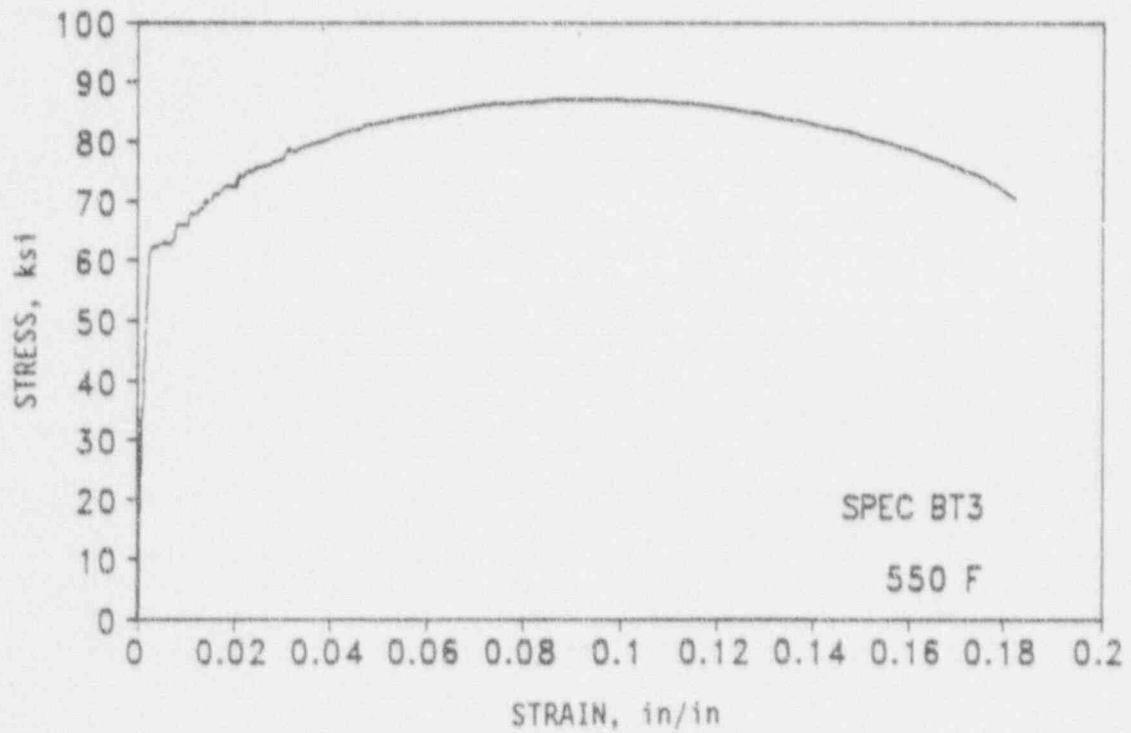
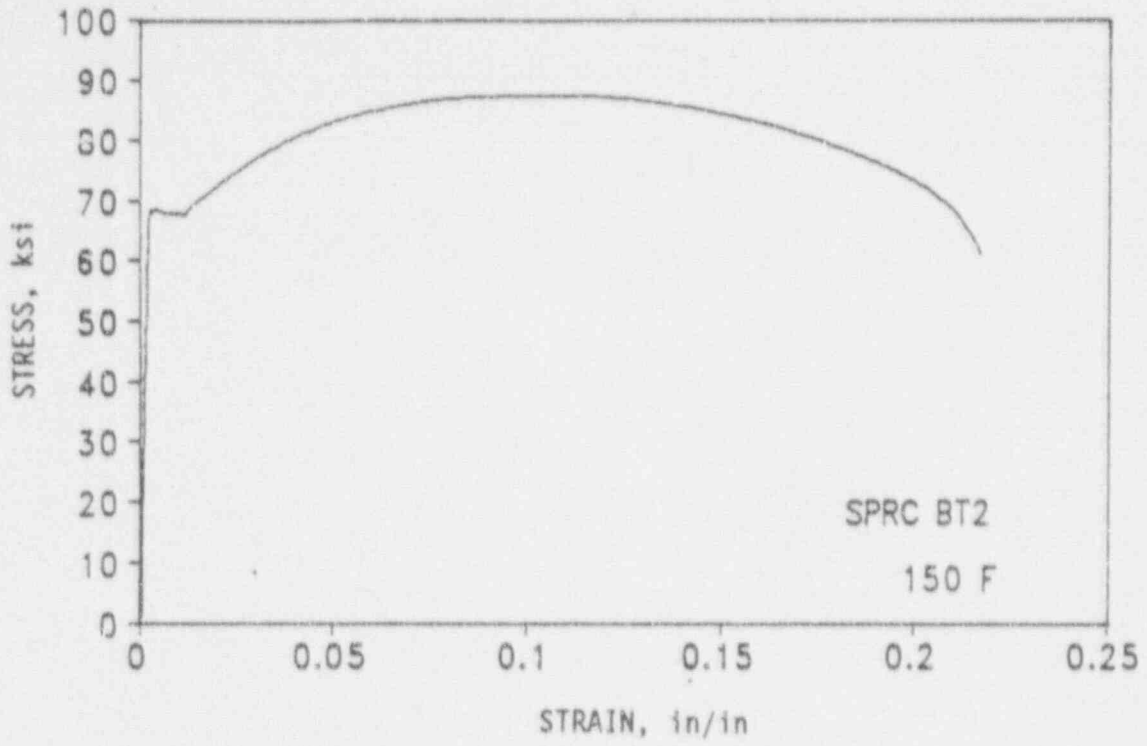


Figure 5-17. Engineering Stress-Strain Curves for Plate B8628-1 Tensile Specimens BT2 and BT3 (Transverse Orientation)

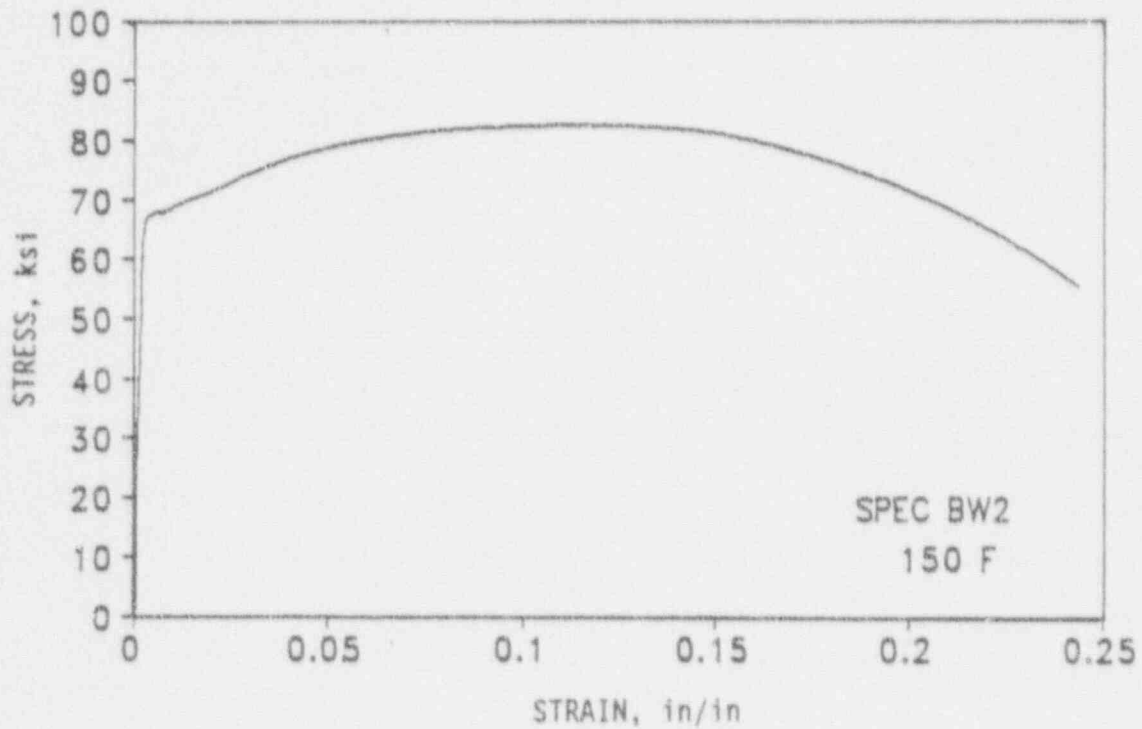
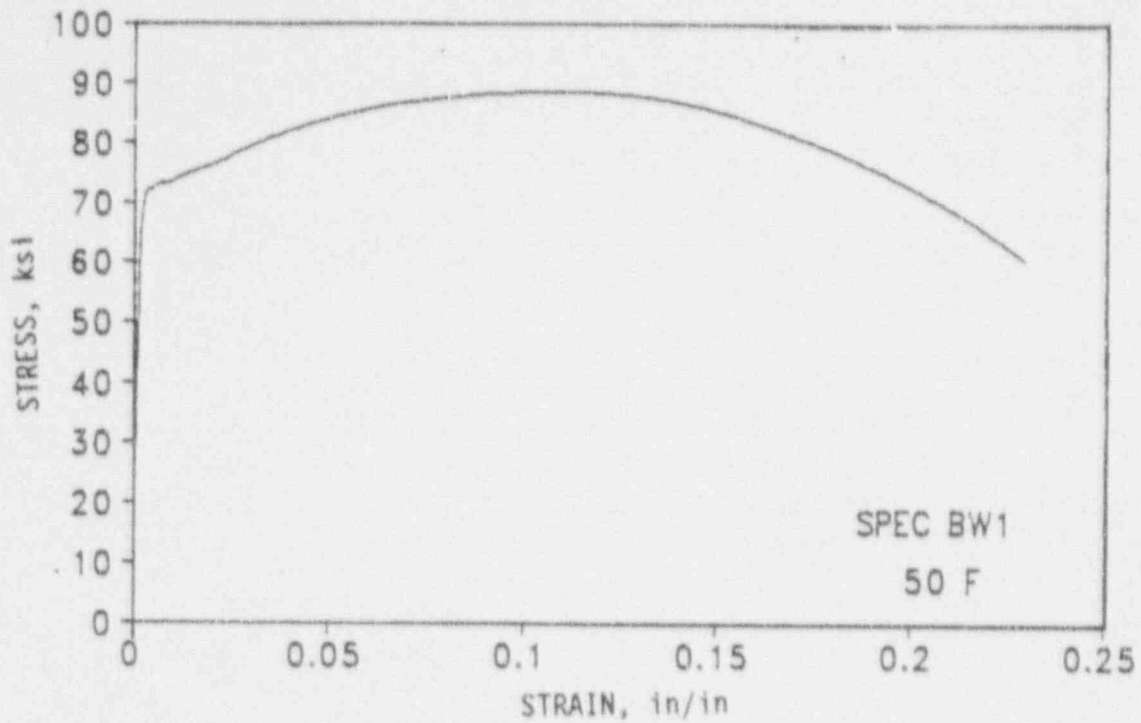


Figure 5-18. Engineering Stress-Strain Curve for Weld Metal Tensile Specimens BW1 and BW2

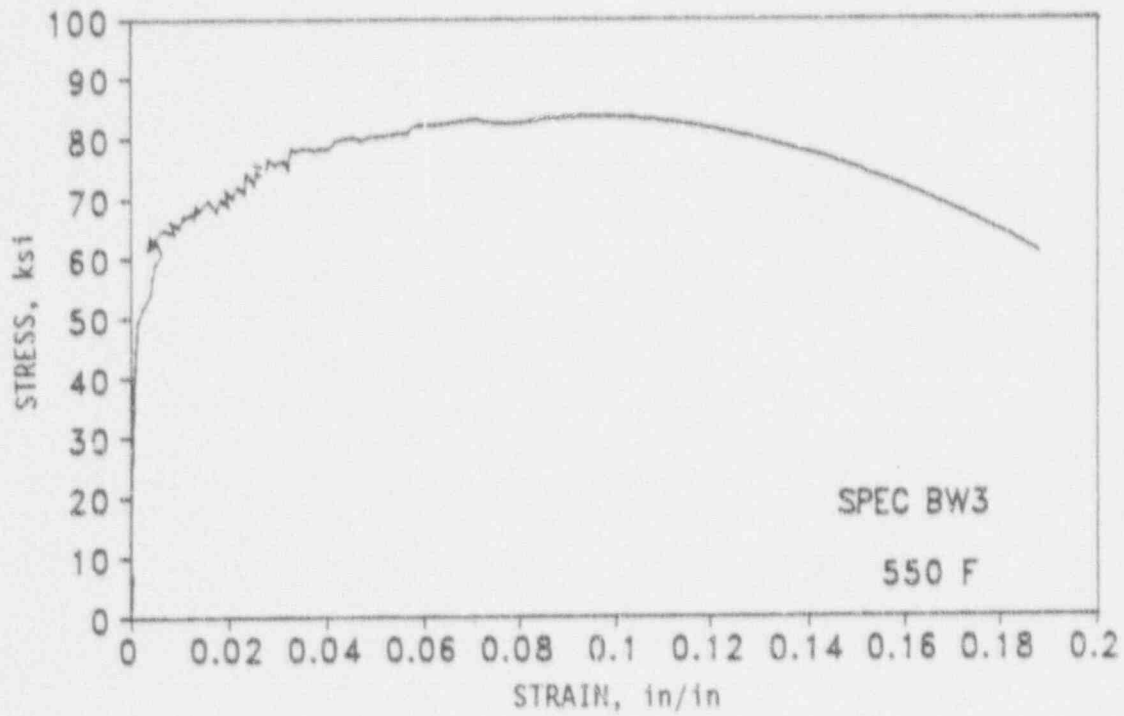


Figure 5-19. Engineering Stress-Strain Curve for Weld Metal Tensile Specimen BW3

SECTION 6.0  
RADIATION ANALYSIS AND NEUTRON DOSIMETRY

6.1 Introduction

Knowledge of the neutron environment within the reactor pressure vessel and surveillance capsule geometry is required as an integral part of LWR reactor pressure vessel surveillance programs for two reasons. First, in order to interpret the neutron radiation-induced material property changes observed in the test specimens, the neutron environment (energy spectrum, flux, fluence) to which the test specimens were exposed must be known. Second, in order to relate the changes observed in the test specimens to the present and future condition of the reactor vessel, a relationship must be established between the neutron environment at various positions within the reactor vessel and that experienced by the test specimens. The former requirement is normally met by employing a combination of rigorous analytical techniques and measurements obtained with passive neutron flux monitors contained in each of the surveillance capsules. The latter information is derived solely from analysis.

The use of fast neutron fluence ( $E > 1.0$  MeV) to correlate measured materials properties changes to the neutron exposure of the material for light water reactor applications has traditionally been accepted for development of damage trend curves as well as for the implementation of trend curve data to assess vessel condition. In recent years, however, it has been suggested that an exposure model that accounts for differences in neutron energy spectra between surveillance capsule locations and positions within the vessel wall could lead to an improvement in the uncertainties associated with damage trend curves as well as to a more accurate evaluation of damage gradients through the pressure vessel wall.

Because of this potential shift away from a threshold fluence toward an energy dependent damage function for data correlation, ASTM Standard Practice E853, "Analysis and Interpretation of Light Water Reactor

Surveillance Results," recommends reporting displacements per iron atom (dpa) along with fluence ( $E > 1.0$  MeV) to provide a data base for future reference. The energy dependent dpa function to be used for this evaluation is specified in ASTM Standard Practice E693, "Characterizing Neutron Exposures in Ferritic Steels in Terms of Displacements per Atom." The application of the dpa parameter to the assessment of embrittlement gradients through the thickness of the pressure vessel wall has already been promulgated in Revision 2 to the Regulatory Guide 1.99, "Radiation Damage to Reactor Vessel Materials."

This section provides the results of the neutron dosimetry evaluations performed in conjunction with the analysis of test specimens contained in surveillance Capsule U. Fast neutron exposure parameters in terms of fast neutron fluence ( $E > 1.0$  MeV), fast neutron fluence ( $E > 0.1$  MeV), and iron atom displacements (dpa) are established for the capsule irradiation history. The analytical formalism relating the measured capsule exposure to the exposure of the vessel wall is described and used to project the integrated exposure of the vessel itself. Also uncertainties associated with the derived exposure parameters at the surveillance capsule and with the projected exposure of the pressure vessel are provided.

## 6.2 Discrete Ordinates Analysis

A plan view of the reactor geometry at the core midplane is shown in Figure 4-1. Six irradiation capsules attached to the neutron pads are included in the reactor design to constitute the reactor vessel surveillance program. The capsules are located at azimuthal angles of  $58.5^\circ$ ,  $61.0^\circ$ ,  $121.5^\circ$ ,  $238.5^\circ$ ,  $241.0^\circ$ , and  $301.5^\circ$  relative to the core cardinal axes as shown in Figure 4-1.

A plan view of a dual surveillance capsule holder attached to the neutron pad is shown in Figure 6-1. The stainless steel specimen containers are 1.182 by 1-inch and approximately 56 inches in height. The containers are positioned axially such that the specimens are centered on the core midplane, thus spanning the central 5 feet of the 12-foot high reactor core.

From a neutron transport standpoint, the surveillance capsule structures are significant. They have a marked effect on both the distribution of neutron flux and the neutron energy spectrum in the water annulus between the neutron pad and the reactor vessel. In order to properly determine the neutron environment at the test specimen locations, the capsules themselves must be included in the analytical model.

In performing the fast neutron exposure evaluations for the surveillance capsules and reactor vessel, two distinct sets of transport calculations were carried out. The first, a single computation in the conventional forward mode, was used primarily to obtain relative neutron energy distributions throughout the reactor geometry as well as to establish relative radial distributions of exposure parameters ( $\phi(E > 1.0 \text{ MeV})$ ,  $\phi(E > 0.1 \text{ MeV})$ , and dpa) through the vessel wall. The neutron spectral information was required for the interpretation of neutron dosimetry withdrawn from the surveillance capsule as well as for the determination of exposure parameter ratios; i.e.,  $\text{dpa}/\phi(E > 1.0 \text{ MeV})$ , within the pressure vessel geometry. The relative radial gradient information was required to permit the projection of measured exposure parameters to locations interior to the pressure vessel wall; i.e., the 1/4T, 1/2T, and 3/4T locations.

The second set of calculations consisted of a series of adjoint analyses relating the fast neutron flux ( $E > 1.0 \text{ MeV}$ ) at surveillance capsule positions, and several azimuthal locations on the pressure vessel inner radius to neutron source distributions within the reactor core. The importance functions generated from these adjoint analyses provided the basis for all absolute exposure projections and comparison with measurement. These importance functions, when combined with cycle specific neutron source distributions, yielded absolute predictions of neutron exposure at the locations of interest for each cycle of irradiation; and established the means to perform similar predictions and dosimetry evaluations for all subsequent fuel cycles. It is important to note that the cycle specific neutron source distributions utilized in these analyses included not only spatial variations of fission rates within the reactor core; but, also accounted for the effects of varying neutron yield

per fission and fission spectrum introduced by the build-in of plutonium as the burnup of individual fuel assemblies increased.

The absolute cycle specific data from the adjoint evaluations together with relative neutron energy spectra and radial distribution information from the forward calculation provided the means to:

1. Evaluate neutron dosimetry obtained from surveillance capsule locations.
2. Extrapolate dosimetry results to key locations at the inner radius and through the thickness of the pressure vessel wall.
3. Enable a direct comparison of analytical prediction with measurement.
4. Establish a mechanism for projection of pressure vessel exposure as the design of each new fuel cycle evolves.

The forward transport calculation for the reactor model summarized in Figures 4-1 and 6-1 was carried out in R,  $\theta$  geometry using the DOT two-dimensional discrete ordinates code<sup>[12]</sup> and the SAILOR cross-section library<sup>[13]</sup>. The SAILOR library is a 47 group ENDFB-IV based data set produced specifically for light water reactor applications. In these analyses anisotropic scattering was treated with a  $P_3$  expansion of the cross-sections and the angular discretization was modeled with an  $S_8$  order of angular quadrature.

The reference core power distribution utilized in the forward analysis was derived from statistical studies of long-term operation of Westinghouse 4-loop plants. Inherent in the development of this reference core power distribution is the use of an out-in fuel management strategy; i.e., fresh fuel on the core periphery. Furthermore, for the peripheral fuel assemblies, a  $2\sigma$  uncertainty derived from the statistical evaluation of plant to plant and cycle to cycle variations in peripheral power was used. Since it is unlikely that a single reactor would have a power distribution at the nominal  $+2\sigma$

level for a large number of fuel cycles, the use of this reference distribution is expected to yield somewhat conservative results.

All adjoint analyses were also carried out using an  $S_8$  order of angular quadrature and the  $P_3$  cross-section approximation from the SAILOR library. Adjoint source locations were chosen at several azimuthal locations along the pressure vessel inner radius as well as the geometric center of each surveillance capsule. Again, these calculations were run in  $R, \theta$  geometry to provide neutron source distribution importance functions for the exposure parameter of interest; in this case,  $\phi (E > 1.0 \text{ MeV})$ . Having the importance functions and appropriate core source distributions, the response of interest could be calculated as:

$$R(r, \theta) = \int_r \int_{\theta} \int_E I(r, \theta, E) S(r, \theta, E) r dr d\theta dE$$

- where:  $R(r, \theta)$  =  $\phi (E > 1.0 \text{ MeV})$  at radius  $r$  and azimuthal angle  $\theta$
- $I(r, \theta, E)$  = Adjoint importance function at radius,  $r$ , azimuthal angle  $\theta$ , and neutron source energy  $E$ .
- $S(r, \theta, E)$  = Neutron source strength at core location  $r, \theta$  and energy  $E$ .

Although the adjoint importance functions used in the analysis were based on a response function defined by the threshold neutron flux ( $E > 1.0 \text{ MeV}$ ), prior calculations have shown that, while the implementation of low leakage loading patterns significantly impact the magnitude and the spatial distribution of the neutron field, changes in the relative neutron energy spectrum are of second order. Thus, for a given location the ratio of  $\text{dpa}/\phi (E > 1.0 \text{ MeV})$  is insensitive to changing core source distributions. In the application of these adjoint importance functions to the Vogtle Electric Generating Plant Unit 2 reactor, therefore, the iron displacement rates (dpa) and the neutron flux ( $E > 0.1 \text{ MeV}$ ) were computed on a cycle specific basis by using  $\text{dpa}/\phi (E > 1.0 \text{ MeV})$  and  $\phi (E > 0.1 \text{ MeV})/\phi (E > 1.0 \text{ MeV})$  ratios from the forward analysis in conjunction with the cycle specific  $\phi (E > 1.0 \text{ MeV})$  solutions from the individual adjoint evaluations.

The reactor core power distribution used in the plant specific adjoint calculations was taken from the fuel cycle design report for the first operating cycle of the Electric Generating Plant Unit 2<sup>[14]</sup>.

Selected results from the neutron transport analyses are provided in Tables 6-1 through 6-5. The data listed in these tables establish the means for absolute comparisons of analysis and measurement for the capsule irradiation period and provide the means to correlate dosimetry results with the corresponding neutron exposure of the pressure vessel wall.

In Table 6-1, the calculated exposure parameters [ $\phi$  ( $E > 1.0$  MeV),  $\phi$  ( $E > 0.1$  MeV), and dpa] are given at the geometric center of the two surveillance capsule positions for both the design basis and the plant specific core power distributions. The plant specific data, based on the adjoint transport analysis, are meant to establish the absolute comparison of measurement with analysis. The design basis data derived from the forward calculation are provided as a point of reference against which plant specific fluence evaluations can be compared. Similar data is given in Table 6-2 for the pressure vessel inner radius. Again, the three pertinent exposure parameters are listed for both the design basis and the cycle 1 plant specific power distribution. It is important to note that the data for the vessel inner radius were taken at the clad/base metal interface; and, thus, represent the maximum exposure levels of the vessel wall itself.

Radial gradient information for neutron flux ( $E > 1.0$  MeV), neutron flux ( $E > 0.1$  MeV), and iron atom displacement rate is given in Tables 6-3, 6-4, and 6-5, respectively. The data, obtained from the forward neutron transport calculation, are presented on a relative basis for each exposure parameter at several azimuthal locations. Exposure parameter distributions within the wall may be obtained by normalizing the calculated or projected exposure at the vessel inner radius to the gradient data given in Tables 6-3 through 6-5.

For example, the neutron flux ( $E > 1.0$  MeV) at the 1/4T position on the  $45^\circ$  azimuth is given by:

$$\phi_{1/4T}(45^\circ) = \phi(220.27, 45^\circ) F(225.75, 45^\circ)$$

where:  $\phi_{1/4T}(45^\circ)$  = Projected neutron flux at the 1/4T position on the  $45^\circ$  azimuth

$\phi(220.27, 45^\circ)$  = Projected or calculated neutron flux at the vessel inner radius on the  $45^\circ$  azimuth.

$F(225.75, 45^\circ)$  = Relative radial distribution function from Table 6-3.

Similar expressions apply for exposure parameters in terms of  $\phi$  ( $E > 0.1$  MeV) and dpa/sec.

The DOT calculations were carried out for a typical octant of the reactor. However, for the neutron pad arrangement in Vogtle Electric Generating Plant Unit 2, the pad extent for all octants is not the same. For the analysis of the flux to the pressure vessel, an octant was chosen with the neutron pad extending from  $32.5 - 45.0$  degrees which produces the maximum flux. Other octants have neutron pads spanning larger azimuthal sectors which provide more shielding. For the octant with  $12.5$  degree pad, the maximum flux to the vessel occurs near  $25$  degrees and the values in the tables for the  $25$  degree angle are vessel maximum values. Exposure values for  $0$ ,  $15$ , and  $45$  degrees can be used for all octants; values in the tables for  $25$  and  $35$  degrees are maximum values and only apply to octants with a  $12.5$  degree neutron pad.

### 6.3 Neutron Dosimetry

The passive neutron sensors included in the Vogtle Electric Generating Plant Unit 2 surveillance program are listed in Table 6-6. Also given in Table 6-6 are the primary nuclear reactions and associated nuclear constants that were used in the evaluation of the neutron energy spectrum within the capsule and the subsequent determination of the various exposure parameters of interest [ $\phi$  ( $E > 1.0$  MeV),  $\phi$  ( $E > 0.1$  MeV), dpa].

The relative locations of the neutron sensors within the capsules are shown in Figure 4-2. The iron, nickel, copper, and cobalt-aluminum monitors, in wire form, were placed in holes drilled in spacers at several axial levels within the capsules. The cadmium-shielded neptunium and uranium fission monitors were accommodated within the dosimeter block located near the center of the capsule.

The use of passive monitors such as those listed in Table 6-6 does not yield a direct measure of the energy dependent flux level at the point of interest. Rather, the activation or fission process is a measure of the integrated effect that the time- and energy-dependent neutron flux has on the target material over the course of the irradiation period. An accurate assessment of the average neutron flux level incident on the various monitors may be derived from the activation measurements only if the irradiation parameters are well known. In particular, the following variables are of interest:

- o The specific activity of each monitor.
- o The operating history of the reactor.
- o The energy response of the monitor.
- o The neutron energy spectrum at the monitor location.
- o The physical characteristics of the monitor.

The specific activity of each of the neutron monitors was determined using established ASTM procedures [15 through 28]. Following sample preparation and weighing, the activity of each monitor was determined by means of a lithium-drifted germanium, Ge(Li), gamma spectrometer. The irradiation history of the Vogtle Electric Generating Plant Unit 2 reactor during cycle 1 was obtained from NUREG-0020, "Licensed Operating Reactors Status Summary Report" and the Nucleonics Week Data Sheets for the applicable period.

The irradiation history applicable to Capsule U is given in Table 6-7. Measured and saturated reaction product specific activities as well as measured full power reaction rates are listed in Table 6-8. Reaction rate values were derived using the pertinent data from Tables 6-6 and 6-7.

Values of key fast neutron exposure parameters were derived from the measured reaction rates using the FERRET least squares adjustment code [29]. The

FERRET approach used the measured reaction rate data and the calculated neutron energy spectrum at the center of the surveillance capsule as input and proceeded to adjust a priori (calculated) group fluxes to produce a best fit (in a least squares sense) to the reaction rate data. The exposure parameters along with associated uncertainties were then obtained from the adjusted spectra.

In the FERRET evaluations, a log-normal least-squares algorithm weights both the a priori values and the measured data in accordance with the assigned uncertainties and correlations. In general, the measured values  $f$  are linearly related to the flux  $\phi$  by some response matrix  $A$ :

$$f^{(s, \alpha)} = \sum_g A_{ig}^{(s)} \phi_g^{(\alpha)}$$

where  $i$  indexes the measured values belonging to a single data set  $s$ ,  $g$  designates the energy group and  $\alpha$  delineates spectra that may be simultaneously adjusted. For example,

$$R_i = \sum_g \sigma_{ig} \phi_g$$

relates a set of measured reaction rates  $R_i$  to a single spectrum  $\phi_g$  by the multigroup cross section  $\sigma_{ig}$ . (In this case, FERRET also adjusts the cross-sections.) The log-normal approach automatically accounts for the physical constraint of positive fluxes, even with the large assigned uncertainties.

In the FERRET analysis of the dosimetry data, the continuous quantities (i.e., fluxes and cross-sections) were approximated in 53 groups. The calculated fluxes from the discrete ordinates analysis were expanded into the FERRET group structure using the SAND-II code [30]. This procedure was carried out by first expanding the a priori spectrum into the SAND-II 620 group structure using a SPLINE interpolation procedure for interpolation in regions where group boundaries do not coincide. The 620-point spectrum was then easily collapsed

to the group scheme used in FERRET.

The cross-sections were also collapsed into the 53 energy-group structure using SAND II with calculated spectra (as expanded to 620 groups) as weighting functions. The cross sections were taken from the ENDF/B-V dosimetry file. Uncertainty estimates and 53 x 53 covariance matrices were constructed for each cross section. Correlations between cross sections were neglected due to data and code limitations, but are expected to be unimportant.

For each set of data or a priori values, the inverse of the corresponding relative covariance matrix  $M$  is used as a statistical weight. In some cases, as for the cross sections, a multigroup covariance matrix is used. More often, a simple parameterized form is used:

$$M_{gg'} = R_N^2 + R_g R_{g'} P_{gg'}$$

where  $R_N$  specifies an overall fractional normalization uncertainty (i.e., complete correlation) for the corresponding set of values. The fractional uncertainties  $R_g$  specify additional random uncertainties for group  $g$  that are correlated with a correlation matrix:

$$P_{gg'} = (1 - \theta) \delta_{gg'} + \theta \exp \left[ \frac{-(g-g')^2}{2\theta^2} \right]$$

The first term specifies purely random uncertainties while the second term describes short-range correlations over a range  $\theta$  ( $\theta$  specifies the strength of the latter term).

For the a priori calculated fluxes, a short-range correlation of  $\theta = 6$  groups was used. This choice implies that neighboring groups are strongly correlated when  $\theta$  is close to 1. Strong long-range correlations (or anticorrelations) were justified based on information presented by R.E. Maerker<sup>[31]</sup>. Maerker's results are closely duplicated when  $\theta = 6$ . For the integral reaction rate covariances, simple normalization and random uncertainties were combined as deduced from experimental uncertainties.

integrated exposure of  $4.44 \times 10^{-10}$  n/cm ( $E > 1.0$  MeV) with an associated uncertainty of  $\pm 8\%$ . Also reported are capsule exposures in terms of fluence ( $E > 0.1$  MeV) and iron atom displacements (dpa). Summaries of the fit of the adjusted spectrum are provided in Table 6-10. In general, excellent results were achieved in the fits of the adjusted spectrum to the individual experimental reaction rates. The adjusted spectrum itself is tabulated in Table 6-11 for the FERRET 53 energy group structure.

A summary of the measured and calculated neutron exposure of Capsule U is presented in Table 6-12. The agreement between calculation and measurement falls within  $\pm 24\%$  for all fast neutron exposure parameters listed. The thermal neutron exposure calculated for the exposure period underpredicted the measured value by 61 percent.

Neutron exposure projections at key locations on the pressure vessel inner radius are given in Table 6-13. Along with the current (1.18 EFPY) exposure derived from the Capsule U measurements, projections are also provided for an exposure period of 16 EFPY and to end of vessel design life (32 EFPY).

In the evaluation of the future exposure of the reactor pressure vessel the design basis exposure rates from Table 6-2 were employed. Since the Vogtle Electric Generating Plant Unit 2 reactor has operated for only one fuel cycle and equilibrium fuel management has not been fully established, the use of these design basis values is still appropriate. The use of the design basis values should result in conservative predictions of future vessel exposure that can be refined as additional dosimetry becomes available.

In the calculation of exposure gradients for use in the development of heatup and cooldown curves for the Vogtle Electric Generating Plant Unit 2 reactor coolant system, exposure projections to 16 EFPY and 32 EFPY were also employed. Data based on both a fluence ( $E > 1.0$  MeV) slope and a plant specific dpa slope through the vessel wall are provided in Table 6-14.

In order to access  $RT_{NDI}$  vs. fluence trend curves, dpa equivalent fast neutron fluence levels for the 1/4T and 3/4T positions were defined by the relations

$$\phi' (1/4T) = \phi (\text{Surface}) \left\{ \frac{\text{dpa} (1/4T)}{\text{dpa} (\text{Surface})} \right\}$$

$$\phi' (3/4T) = \phi (\text{Surface}) \left\{ \frac{\text{dpa} (3/4T)}{\text{dpa} (\text{Surface})} \right\}$$

Using this approach results in the dpa equivalent fluence values listed in Table 6-14.

In Table 6-15 updated lead factors are listed for each of the Vogtle Electric Generating Plant Unit 2 surveillance capsules. These data may be used as a guide in establishing future withdrawal schedules for the remaining capsules.

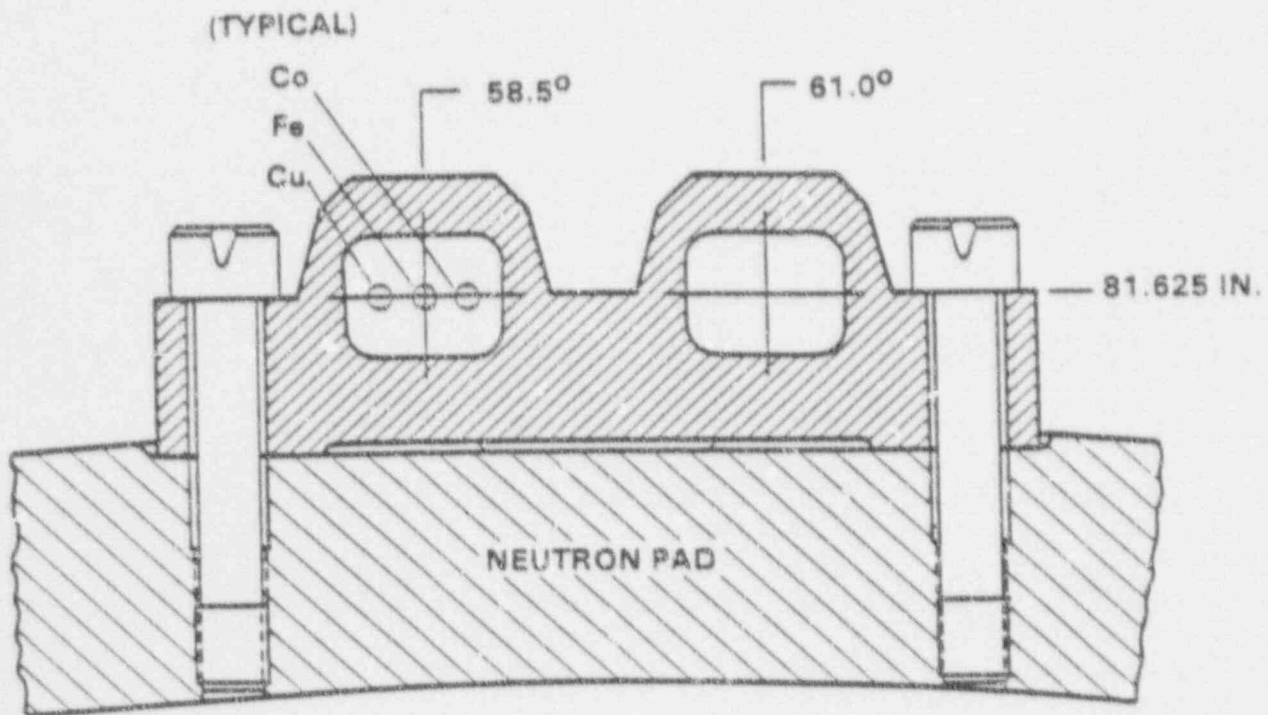


Figure 6-1. Plan View of a Dual Reactor Vessel Surveillance Capsule

TABLE 6-1

CALCULATED FAST NEUTRON EXPOSURE PARAMETERS  
AT THE SURVEILLANCE CAPSULE CENTER

	$\phi(E > 1.0\text{MeV})$ [n/cm <sup>2</sup> -sec]		$\phi(E > 0.1\text{MeV})$ [n/cm <sup>2</sup> -sec]		Iron Displacement Rate [dpa/sec]	
	<u>29.0°</u>	<u>31.5°</u>	<u>29.0°</u>	<u>31.5°</u>	<u>29.0°</u>	<u>31.5°</u>
DESIGN BASIS	$1.13 \times 10^{11}$	$1.21 \times 10^{11}$	$5.08 \times 10^{11}$	$5.44 \times 10^{11}$	$2.21 \times 10^{-10}$	$2.37 \times 10^{-10}$
CYCLE 1	$8.47 \times 10^{10}$	$9.03 \times 10^{10}$	$3.81 \times 10^{11}$	$4.06 \times 10^{11}$	$1.66 \times 10^{-10}$	$1.77 \times 10^{-10}$

TABLE 6-2

CALCULATED FAST NEUTRON EXPOSURE RATES AT  
THE PRESSURE VESSEL CLAD/BASE METAL INTERFACE

$\phi(E > 1.0\text{MeV})$  [n/cm<sup>2</sup>-sec]

	<u>0.0°</u>	<u>15.0°</u>	<u>25.0°</u>	<u>35.0°</u>	<u>45.0°</u>
DESIGN BASIS	1.78 X 10 <sup>10</sup>	2.66 X 10 <sup>10</sup>	3.01 X 10 <sup>10</sup>	2.45 X 10 <sup>10</sup>	2.81 X 10 <sup>10</sup>
CYCLE 1	1.36 X 10 <sup>10</sup>	2.00 X 10 <sup>10</sup>	2.29 X 10 <sup>10</sup>	1.86 X 10 <sup>10</sup>	2.13 X 10 <sup>10</sup>

$\phi(E > 0.1\text{MeV})$  [n/cm<sup>2</sup>-sec]

	<u>0.0°</u>	<u>15.0°</u>	<u>25.0°</u>	<u>35.0°</u>	<u>45.0°</u>
DESIGN BASIS	3.70 X 10 <sup>10</sup>	5.60 X 10 <sup>10</sup>	8.22 X 10 <sup>10</sup>	6.96 X 10 <sup>10</sup>	7.04 X 10 <sup>10</sup>
CYCLE 1	2.83 X 10 <sup>10</sup>	4.21 X 10 <sup>10</sup>	6.25 X 10 <sup>10</sup>	5.28 X 10 <sup>10</sup>	5.34 X 10 <sup>10</sup>

Iron Atom Displacement Rate [dpa/sec]

	<u>0.0°</u>	<u>15.0°</u>	<u>25.0°</u>	<u>35.0°</u>	<u>45.0°</u>
DESIGN BASIS	2.77 X 10 <sup>-11</sup>	4.12 X 10 <sup>-11</sup>	5.04 X 10 <sup>-11</sup>	4.15 X 10 <sup>-11</sup>	4.48 X 10 <sup>-11</sup>
CYCLE 1	2.12 X 10 <sup>-11</sup>	3.10 X 10 <sup>-11</sup>	3.83 X 10 <sup>-11</sup>	3.15 X 10 <sup>-11</sup>	3.40 X 10 <sup>-11</sup>

TABLE 6-3

RELATIVE RADIAL DISTRIBUTIONS OF NEUTRON FLUX ( $E > 1.0$  MeV)  
WITHIN THE PRESSURE VESSEL WALL

Radius (cm)	0°	15°	25°	35°	45°
220.27 <sup>(1)</sup>	1.00	1.00	1.00	1.00	1.00
220.64	0.976	0.979	0.980	0.977	0.979
221.66	0.888	0.891	0.893	0.891	0.889
222.99	0.768	0.770	0.772	0.770	0.766
224.31	0.653	0.653	0.657	0.655	0.648
225.63	0.551	0.550	0.554	0.552	0.543
226.95	0.462	0.460	0.465	0.463	0.452
228.28	0.386	0.384	0.388	0.386	0.375
229.60	0.321	0.319	0.324	0.321	0.311
230.92	0.267	0.263	0.275	0.267	0.257
232.25	0.221	0.219	0.225	0.221	0.211
233.57	0.183	0.181	0.185	0.183	0.174
234.89	0.151	0.149	0.153	0.151	0.142
236.22	0.124	0.122	0.126	0.124	0.116
237.54	0.102	0.100	0.104	0.102	0.0945
238.86	0.0828	0.0817	0.0846	0.0835	0.0762
240.19	0.0671	0.0660	0.0689	0.0679	0.0608
241.51	0.0538	0.0522	0.0550	0.0545	0.0471
242.17 <sup>(2)</sup>	0.0506	0.0488	0.0518	0.0521	0.0438

NOTES: 1) Base Metal Inner Radius  
2) Base Metal Outer Radius

TABLE 6-4

RELATIVE RADIAL DISTRIBUTIONS OF NEUTRON FLUX ( $E > 0.1$  MeV)  
WITHIN THE PRESSURE VESSEL WALL

Radius (cm)	0°	15°	25°	35°	45°
220.27 <sup>(1)</sup>	1.00	1.00	1.00	1.00	1.00
220.64	1.00	1.00	1.00	1.00	1.00
221.66	1.00	1.00	1.00	0.999	0.995
222.99	0.974	0.969	0.974	0.959	0.956
224.31	0.927	0.920	0.927	0.907	0.901
225.63	0.874	0.865	0.874	0.850	0.842
226.95	0.818	0.808	0.818	0.792	0.782
228.28	0.761	0.750	0.716	0.734	0.721
229.60	0.705	0.693	0.704	0.677	0.662
230.92	0.649	0.637	0.649	0.621	0.605
232.25	0.594	0.582	0.594	0.567	0.549
233.57	0.540	0.529	0.542	0.515	0.495
234.89	0.487	0.478	0.490	0.465	0.443
236.22	0.436	0.428	0.440	0.416	0.392
237.54	0.386	0.380	0.392	0.369	0.343
238.86	0.337	0.333	0.344	0.324	0.295
240.19	0.289	0.287	0.298	0.279	0.248
241.51	0.244	0.238	0.249	0.233	0.201
242.17 <sup>(2)</sup>	0.233	0.226	0.237	0.223	0.188

NOTES: 1) Base Metal Inner Radius

2) Base Metal Outer Radius

TABLE 6-5

RELATIVE RADIAL DISTRIBUTIONS OF IRON DISPLACEMENT RATE (dpa)  
WITHIN THE PRESSURE VESSEL WALL

Radius (cm)	0°	15°	25°	35°	45°
220.27 <sup>(1)</sup>	1.00	1.00	1.00	1.00	1.00
220.64	0.984	0.981	0.984	0.983	0.984
221.66	0.912	0.909	0.917	0.921	0.915
222.99	0.815	0.812	0.826	0.833	0.821
224.31	0.722	0.719	0.737	0.747	0.730
225.63	0.638	0.634	0.656	0.668	0.647
226.95	0.563	0.559	0.584	0.597	0.572
228.28	0.497	0.493	0.519	0.533	0.506
229.60	0.439	0.435	0.462	0.475	0.447
230.92	0.387	0.383	0.410	0.423	0.394
232.25	0.341	0.338	0.364	0.376	0.347
233.57	0.300	0.297	0.322	0.334	0.305
234.89	0.263	0.261	0.285	0.295	0.266
236.22	0.230	0.228	0.250	0.260	0.231
237.54	0.199	0.198	0.218	0.227	0.199
238.86	0.171	0.170	0.189	0.196	0.169
240.19	0.145	0.144	0.161	0.167	0.140
241.51	0.121	0.119	0.135	0.139	0.113
242.17 <sup>(2)</sup>	0.116	0.113	0.128	0.134	0.106

---

NOTES: 1) Base Metal Inner Radius

2) Base Metal Outer Radius

TABLE 6-6

## NUCLEAR PARAMETERS FOR NEUTRON FLUX MONITORS

<u>Monitor Material</u>	<u>Reaction of Interest</u>	<u>Target Weight Fraction</u>	<u>Response Range</u>	<u>Product Half-Life</u>	<u>Fission Yield (%)</u>
Copper	$\text{Cu}^{63}(n,\alpha)\text{Co}^{60}$	0.6917	$E > 4.7 \text{ MeV}$	5.272 yrs	
Iron	$\text{Fe}^{54}(n,p)\text{Mn}^{54}$	0.0582	$E > 1.0 \text{ MeV}$	312.2 days	
Nickel	$\text{Ni}^{58}(n,p)\text{Co}^{58}$	0.6830	$E > 1.0 \text{ MeV}$	70.90 days	
Uranium-238*	$\text{U}^{238}(n,f)\text{Cs}^{137}$	1.0	$E > 0.4 \text{ MeV}$	30.12 yrs	5.99
Neptunium-237*	$\text{Np}^{237}(n,f)\text{Cs}^{137}$	1.0	$E > 0.08 \text{ MeV}$	30.12 yrs	6.50
Cobalt-Aluminum*	$\text{Co}^{59}(n,\beta)\text{Co}^{60}$	0.0015	$0.4\text{eV} > E > 0.015 \text{ MeV}$	5.272 yrs	
Cobalt-Aluminum	$\text{Co}^{59}(n,\beta)\text{Co}^{60}$	0.0015	$E > 0.015 \text{ MeV}$	5.272 yrs	

\*Denotes that monitor is cadmium shielded.

TABLE 6-7

MONTHLY THERMAL GENERATION DURING THE FIRST FUEL CYCLE  
OF THE VOGTLE ELECTRIC GENERATING PLANT UNIT 2 REACTOR

<u>MONTH</u>	<u>THERMAL GENERATION (MW-hr)</u>
4/89	475504
5/89	617966
6/89	2450888
7/89	2452023
8/89	2526703
9/89	2439109
10/89	2034639
11/89	2350213
12/89	2335572
1/90	2503482
2/90	2289775
3/90	2332504
4/90	2367059
5/90	2394293
6/90	2119961
7/90	1730098
8/90	1413553
9/90	524543

TABLE 6-8  
MEASURED SENSOR ACTIVITIES AND REACTION RATES

Monitor and Axial Location	Measured Activity (dis/sec-gm)	Saturated Activity (dis/sec-gm)	Reaction Rate (RPS/NUCLEUS)
<hr/> Cu-63 (n,α) Co-60			
Top	$5.51 \times 10^4$	$4.01 \times 10^5$	
Middle	$4.96 \times 10^4$	$3.61 \times 10^5$	
Bottom	$4.86 \times 10^4$	$3.53 \times 10^5$	
Average	$5.11 \times 10^4$	$3.71 \times 10^5$	$5.67 \times 10^{-17}$
<hr/> Fe-54(n,p) Mn-54			
Top	$1.88 \times 10^6$	$4.05 \times 10^6$	
Middle	$1.65 \times 10^6$	$3.55 \times 10^6$	
Bottom	$1.67 \times 10^6$	$3.59 \times 10^6$	
Average	$1.73 \times 10^6$	$3.73 \times 10^6$	$5.94 \times 10^{-15}$
<hr/> Ni-58 (n,p) Co-58			
Top	$1.86 \times 10^7$	$6.04 \times 10^7$	
Middle	$1.70 \times 10^7$	$5.52 \times 10^7$	
Bottom	$1.65 \times 10^7$	$5.36 \times 10^7$	
Average	$1.74 \times 10^7$	$5.64 \times 10^7$	$8.05 \times 10^{-15}$
<hr/> U-238 (n,f) Cs-137 (Cd)			
Middle	$1.59 \times 10^5$	$5.99 \times 10^6$	$3.95 \times 10^{-14}$

TABLE 6-8  
 MEASURED SENSOR ACTIVITIES AND REACTION RATES - cont'd

Monitor and Axial Location	Measured Activity (dis/sec-gm)	Saturated Activity (dis/sec-gm)	Reaction Rate (RPS/NUCLEUS)
<u>Np-237(n,f) Cs-137 (Cd)</u>			
Middle	$1.56 \times 10^6$	$5.86 \times 10^7$	$3.55 \times 10^{-13}$
<u>Co-59 (n,<math>\beta</math>) Co-60</u>			
Top	$1.13 \times 10^7$	$8.21 \times 10^7$	
Middle	$1.26 \times 10^7$	$9.16 \times 10^7$	
Bottom	$1.15 \times 10^7$	$8.36 \times 10^7$	
Average	$1.18 \times 10^7$	$8.58 \times 10^7$	$5.60 \times 10^{-12}$
<u>Co-59 (n,<math>\beta</math>) Co-60 (Cd)</u>			
Top	$5.99 \times 10^6$	$4.35 \times 10^7$	
Middle	$6.21 \times 10^6$	$4.51 \times 10^7$	
Bottom	$6.19 \times 10^6$	$4.50 \times 10^7$	
Average	$6.13 \times 10^6$	$4.46 \times 10^7$	$2.91 \times 10^{-12}$

TABLE 6-9

## SUMMARY OF NEUTRON DOSIMETRY RESULTS

<u>TIME AVERAGED EXPOSURE RATES</u>		
$\phi$ (E > 1.0 MeV) (n/cm <sup>2</sup> -sec)	$1.19 \times 10^{11}$	$\pm 8\%$
$\phi$ (E > 0.1 MeV) (n/cm <sup>2</sup> -sec)	$5.19 \times 10^{11}$	$\pm 15\%$
dpa/sec	$2.26 \times 10^{-10}$	$\pm 11\%$
$\phi$ (E < 0.414 eV) (n/cm <sup>2</sup> -sec)	$1.11 \times 10^{11}$	$\pm 21\%$
<u>INTEGRATED CAPSULE EXPOSURE</u>		
$\Phi$ (E > 1.0 MeV) (n/cm <sup>2</sup> )	$4.44 \times 10^{18}$	$\pm 8\%$
$\Phi$ (E > 0.1 MeV) (n/cm <sup>2</sup> )	$1.94 \times 10^{19}$	$\pm 15\%$
dpa	$8.43 \times 10^{-3}$	$\pm 11\%$
$\Phi$ (E < 0.414 eV) (n/cm <sup>2</sup> )	$4.14 \times 10^{18}$	$\pm 21\%$

NOTE: Total Irradiation Time = 1.18 [FPY

TABLE 6-10

COMPARISON OF MEASURED AND FERRET CALCULATED  
REACTION RATES AT THE SURVEILLANCE CAPSULE CENTER

<u>Reaction</u>	<u>Measured</u>	<u>Adjusted Calculation</u>	<u>C/M</u>
Cu-63 (n, $\alpha$ ) Co-60	$5.67 \times 10^{-17}$	$5.77 \times 10^{-17}$	1.02
Fe-54 (n,p) Mn-54	$5.94 \times 10^{-15}$	$5.92 \times 10^{-15}$	1.00
Ni-58 (n,p) Co-58	$8.05 \times 10^{-15}$	$8.09 \times 10^{-15}$	1.00
U-238 (n,f) Cs-137 (Cd)	$3.95 \times 10^{-14}$	$3.60 \times 10^{-14}$	0.91
Np-237 (n,f) Cs-137 (Cd)	$3.55 \times 10^{-13}$	$3.67 \times 10^{-13}$	1.03
Co-59 (n, $\beta$ ) Co-60 (Cd)	$5.60 \times 10^{-12}$	$5.56 \times 10^{-12}$	0.99
Co-59 (n, $\beta$ ) Co-60	$2.91 \times 10^{-12}$	$2.92 \times 10^{-12}$	1.00

TABLE 6-11  
 ADJUSTED NEUTRON ENERGY SPECTRUM AT  
 THE SURVEILLANCE CAPSULE CENTER

Group	Energy (Mev)	Adjusted Flux (n/cm <sup>2</sup> -sec)	Group	Energy (Mev)	Adjusted Flux (n/cm <sup>2</sup> -sec)
1	1.73x10 <sup>1</sup>	8.10x10 <sup>6</sup>	28	9.12x10 <sup>-3</sup>	2.23x10 <sup>10</sup>
2	1.49x10 <sup>1</sup>	1.82x10 <sup>7</sup>	29	5.53x10 <sup>-3</sup>	2.89x10 <sup>10</sup>
3	1.35x10 <sup>1</sup>	7.01x10 <sup>7</sup>	30	3.36x10 <sup>-3</sup>	9.00x10 <sup>9</sup>
4	1.16x10 <sup>1</sup>	1.57x10 <sup>8</sup>	31	2.84x10 <sup>-3</sup>	8.59x10 <sup>9</sup>
5	1.00x10 <sup>1</sup>	3.47x10 <sup>8</sup>	32	2.40x10 <sup>-3</sup>	8.28x10 <sup>9</sup>
6	8.61x10 <sup>0</sup>	5.98x10 <sup>8</sup>	33	2.04x10 <sup>-3</sup>	2.33x10 <sup>10</sup>
7	7.41x10 <sup>0</sup>	1.39x10 <sup>9</sup>	34	1.23x10 <sup>-3</sup>	2.14x10 <sup>10</sup>
8	6.07x10 <sup>0</sup>	2.03x10 <sup>9</sup>	35	7.49x10 <sup>-4</sup>	1.99x10 <sup>10</sup>
9	4.97x10 <sup>0</sup>	4.37x10 <sup>9</sup>	36	4.54x10 <sup>-4</sup>	1.89x10 <sup>10</sup>
10	3.68x10 <sup>0</sup>	5.94x10 <sup>9</sup>	37	2.75x10 <sup>-4</sup>	2.03x10 <sup>10</sup>
11	2.87x10 <sup>0</sup>	1.28x10 <sup>10</sup>	38	1.67x10 <sup>-4</sup>	2.17x10 <sup>10</sup>
12	2.23x10 <sup>0</sup>	1.81x10 <sup>10</sup>	39	1.01x10 <sup>-4</sup>	2.19x10 <sup>10</sup>
13	1.74x10 <sup>0</sup>	2.59x10 <sup>10</sup>	40	6.14x10 <sup>-5</sup>	2.18x10 <sup>10</sup>
14	1.35x10 <sup>0</sup>	2.89x10 <sup>10</sup>	41	3.73x10 <sup>-5</sup>	2.13x10 <sup>10</sup>
15	1.11x10 <sup>0</sup>	5.30x10 <sup>10</sup>	42	2.26x10 <sup>-5</sup>	2.07x10 <sup>10</sup>
16	8.21x10 <sup>-1</sup>	6.04x10 <sup>10</sup>	43	1.37x10 <sup>-5</sup>	2.02x10 <sup>10</sup>
17	6.39x10 <sup>-1</sup>	6.23x10 <sup>10</sup>	44	8.32x10 <sup>-6</sup>	1.92x10 <sup>10</sup>
18	4.98x10 <sup>-1</sup>	4.48x10 <sup>10</sup>	45	5.04x10 <sup>-6</sup>	1.77x10 <sup>10</sup>
19	3.88x10 <sup>-1</sup>	6.24x10 <sup>10</sup>	46	3.06x10 <sup>-6</sup>	1.66x10 <sup>10</sup>
20	3.02x10 <sup>-1</sup>	6.35x10 <sup>10</sup>	47	1.86x10 <sup>-6</sup>	1.53x10 <sup>10</sup>
21	1.83x10 <sup>-1</sup>	6.22x10 <sup>10</sup>	48	1.13x10 <sup>-6</sup>	1.13x10 <sup>10</sup>
22	1.11x10 <sup>-1</sup>	4.92x10 <sup>10</sup>	49	6.83x10 <sup>-7</sup>	1.45x10 <sup>10</sup>
23	6.74x10 <sup>-2</sup>	3.39x10 <sup>10</sup>	50	4.14x10 <sup>-7</sup>	1.93x10 <sup>10</sup>
24	4.09x10 <sup>-2</sup>	1.91x10 <sup>10</sup>	51	2.51x10 <sup>-7</sup>	1.92x10 <sup>10</sup>
25	2.55x10 <sup>-2</sup>	2.49x10 <sup>10</sup>	52	1.52x10 <sup>-7</sup>	1.83x10 <sup>10</sup>
26	1.99x10 <sup>-2</sup>	1.22x10 <sup>10</sup>	53	9.24x10 <sup>-8</sup>	5.45x10 <sup>10</sup>
27	1.50x10 <sup>-2</sup>	1.55x10 <sup>10</sup>			

NOTE: Tabulated energy levels represent the upper energy of each group.

TABLE 6-12

COMPARISON OF CALCULATED AND MEASURED  
EXPOSURE LEVELS FOR CAPSULE U

	<u>Calculated</u>	<u>Measured</u>	<u>C/M</u>
$\Phi(E > 1.0 \text{ MeV}) \text{ (n/cm}^2\text{)}$	$3.37 \times 10^{18}$	$4.44 \times 10^{18}$	0.76
$\Phi(E > 0.1 \text{ MeV}) \text{ (n/cm}^2\text{)}$	$1.52 \times 10^{19}$	$1.94 \times 10^{19}$	0.78
dpa	$6.60 \times 10^{-3}$	$8.43 \times 10^{-3}$	0.78
$\Phi(E < 0.414 \text{ eV}) \text{ (n/cm}^2\text{)}$	$1.61 \times 10^{18}$	$4.14 \times 10^{18}$	0.39

TABLE 6-13  
NEUTRON EXPOSURE PROJECTIONS AT KEY LOCATIONS  
ON THE PRESSURE VESSEL CLAD/BASE METAL INTERFACE

		<u>1.18 EFY</u>				
		$0^\circ$	$15^\circ$	$25^\circ$	$35^\circ$	$45^\circ$
$\phi$	(E > 1.0 Mev) [n/cm <sup>2</sup> ]	$6.68 \times 10^{17}$	$9.86 \times 10^{17}$	$1.13 \times 10^{18}$	$9.17 \times 10^{17}$	$1.05 \times 10^{18}$
$\phi$	(E > 0.1 MeV) [n/cm <sup>2</sup> ]	$1.34 \times 10^{18}$	$2.00 \times 10^{18}$	$2.98 \times 10^{18}$	$2.53 \times 10^{18}$	$2.54 \times 10^{18}$
	Iron Atom Displacements [dpa]	$1.01 \times 10^{-3}$	$1.48 \times 10^{-3}$	$1.83 \times 10^{-3}$	$1.51 \times 10^{-3}$	$1.62 \times 10^{-3}$
		<u>16.0 EFY</u>				
		$0^\circ$	$15^\circ$	$25^\circ$	$35^\circ$	$45^\circ$
$\phi$	(E > 1.0 Mev) [n/cm <sup>2</sup> ]	$8.99 \times 10^{18}$	$1.34 \times 10^{19}$	$1.52 \times 10^{19}$	$1.24 \times 10^{19}$	$1.42 \times 10^{19}$
$\phi$	(E > 0.1 MeV) [n/cm <sup>2</sup> ]	$1.86 \times 10^{19}$	$2.82 \times 10^{19}$	$4.14 \times 10^{19}$	$3.51 \times 10^{19}$	$3.55 \times 10^{19}$
	Iron Atom Displacements [dpa]	$1.40 \times 10^{-2}$	$2.07 \times 10^{-2}$	$2.54 \times 10^{-2}$	$2.09 \times 10^{-2}$	$2.26 \times 10^{-2}$
		<u>32.0 EFY</u>				
		$0^\circ$	$15^\circ$	$25^\circ$	$35^\circ$	$45^\circ$
$\phi$	(E > 1.0 Mev) [n/cm <sup>2</sup> ]	$1.80 \times 10^{19}$	$2.69 \times 10^{19}$	$3.04 \times 10^{19}$	$2.47 \times 10^{19}$	$2.84 \times 10^{19}$
$\phi$	(E > 0.1 MeV) [n/cm <sup>2</sup> ]	$3.73 \times 10^{19}$	$5.65 \times 10^{19}$	$8.29 \times 10^{19}$	$7.02 \times 10^{19}$	$7.10 \times 10^{19}$
	Iron Atom Displacements [dpa]	$2.80 \times 10^{-2}$	$4.16 \times 10^{-2}$	$5.08 \times 10^{-2}$	$4.19 \times 10^{-2}$	$4.52 \times 10^{-2}$

TABLE 6-14  
NEUTRON EXPOSURE VALUES FOR USE IN THE GENERATION OF HEATUP/COOLDOWN CURVES

16 EFPY

	<u>NEUTRON FLUENCE (E &gt; 1.0 MeV) SLOPE</u> (n/cm <sup>2</sup> )			<u>dpa SLOPE</u> (equivalent n/cm <sup>2</sup> )		
	<u>Surface</u>	<u>1/4 T</u>	<u>3/4 T</u>	<u>Surface</u>	<u>1/4 T</u>	<u>3/4 T</u>
0°	8.99 x 10 <sup>18</sup>	4.88 x 10 <sup>18</sup>	1.04 x 10 <sup>18</sup>	8.99 x 10 <sup>18</sup>	5.67 x 10 <sup>18</sup>	1.97 x 10 <sup>18</sup>
15°	1.34 x 10 <sup>19</sup>	7.28 x 10 <sup>18</sup>	1.53 x 10 <sup>18</sup>	1.34 x 10 <sup>19</sup>	8.42 x 10 <sup>18</sup>	2.91 x 10 <sup>18</sup>
25 (a)	1.52 x 10 <sup>19</sup>	8.30 x 10 <sup>18</sup>	1.79 x 10 <sup>18</sup>	1.52 x 10 <sup>19</sup>	9.87 x 10 <sup>18</sup>	3.62 x 10 <sup>18</sup>
35°	1.24 x 10 <sup>19</sup>	6.73 x 10 <sup>18</sup>	1.44 x 10 <sup>18</sup>	1.24 x 10 <sup>19</sup>	8.19 x 10 <sup>18</sup>	3.07 x 10 <sup>18</sup>
45°	1.42 x 10 <sup>19</sup>	7.59 x 10 <sup>18</sup>	1.53 x 10 <sup>18</sup>	1.42 x 10 <sup>19</sup>	9.08 x 10 <sup>18</sup>	3.11 x 10 <sup>18</sup>

32 EFPY

	<u>NEUTRON FLUENCE (E &gt; 1.0 MeV) SLOPE</u> (n/cm <sup>2</sup> )			<u>dpa SLOPE</u> (equivalent n/cm <sup>2</sup> )		
	<u>Surface</u>	<u>1/4 T</u>	<u>3/4 T</u>	<u>Surface</u>	<u>1/4 T</u>	<u>3/4 T</u>
0°	1.80 x 10 <sup>19</sup>	9.76 x 10 <sup>18</sup>	2.09 x 10 <sup>18</sup>	1.80 x 10 <sup>19</sup>	1.13 x 10 <sup>19</sup>	3.94 x 10 <sup>18</sup>
15°	2.69 x 10 <sup>19</sup>	1.46 x 10 <sup>19</sup>	3.06 x 10 <sup>18</sup>	2.69 x 10 <sup>19</sup>	1.68 x 10 <sup>19</sup>	5.83 x 10 <sup>18</sup>
25 (a)	3.04 x 10 <sup>19</sup>	1.66 x 10 <sup>19</sup>	3.59 x 10 <sup>18</sup>	3.04 x 10 <sup>19</sup>	1.97 x 10 <sup>19</sup>	7.24 x 10 <sup>18</sup>
35°	2.47 x 10 <sup>19</sup>	1.35 x 10 <sup>19</sup>	2.87 x 10 <sup>18</sup>	2.47 x 10 <sup>19</sup>	1.64 x 10 <sup>19</sup>	6.14 x 10 <sup>18</sup>
45°	2.84 x 10 <sup>19</sup>	1.52 x 10 <sup>19</sup>	3.07 x 10 <sup>18</sup>	2.84 x 10 <sup>19</sup>	1.82 x 10 <sup>19</sup>	6.22 x 10 <sup>18</sup>

(a) Maximum point on the pressure vessel

TABLE 6-15

UPDATED LEAD FACTORS FOR VOGTLE ELECTRIC GENERATING PLANT  
UNIT 2 SURVEILLANCE CAPSULES

<u>Capsule</u>	<u>Lead Factor</u>
U	3.94(a)
Y	3.75(b)
V	3.75(b)
W	4.02(b)
X	4.02(b)
Z	4.02(b)

- (a) Plant specific evaluation based on end of cycle 1 calculated fluence.  
(b) Projection based on design basis flux.

SECTION 7.0  
SURVEILLANCE CAPSULE REMOVAL SCHEDULE

The following removal schedule meets ASTM E185-82 and is recommended for future capsules to be removed from the Vogtle Electric Generating Plant Unit 2 reactor vessel:

Capsule	Location (deg.)	Capsule Lead Factor	Removal Time (b)	Estimated Fluence (n/cm <sup>2</sup> )
U	58.5	3.94	1.18 (Removed) <sup>(a)</sup>	4.44 x 10 <sup>18</sup> (Actual)
Y	241.0	3.75	5.0	1.78 x 10 <sup>19</sup> (c)
V	61.0	3.75	9.0	3.21 x 10 <sup>19</sup> (d)
X	238.5	4.02	15.0	5.74 x 10 <sup>19</sup>
W	121.5	4.02	Standby	---
	301.5	4.02	Standby	---

(a) Plant Specific Evaluation

(b) Effective Full Power Years (EFPY) from plant startup.

(c) Approximate fluence at 1/4 thickness of reactor vessel wall at end of life (32 EFPY).

(d) Approximate fluence at reactor vessel inner wall at end of life (32 EFPY).



SECTION 8.0  
REFERENCES

1. L.R. Singer, et. al., "Georgia Power Company Alvin W. Vogtle Unit No. 2, Reactor Vessel Radiation Surveillance Program," WCAP-11331, April 1986.
2. Code of Federal Regulations, 10CFR50, Appendix G, "Fracture Toughness Requirements", and Appendix H, "Reactor Vessel Material Surveillance Program Requirements," U.S. Nuclear Regulatory Commission, Washington, D.C.
3. Regulatory Guide 1.99, Revision 2, "Radiation Embrittlement of Reactor Vessel Materials", U.S. Nuclear Regulatory Commission, May, 1988.
4. Section III of the ASME Boiler and Pressure Vessel Code, Appendix G, "Protection Against Nonductile Failure."
5. ASTM E208, "Standard Test Method for Conducting Drop-Weight Test to Determine Nil-Ductility Transition Temperature of Ferritic Steels."
6. ASTM E185-82, "Standard Practice for Conducting Surveillance Tests for Light-Water Cooled Nuclear Power Reactor Vessels, E706 (IF)."
7. ASTM F23-88, "Standard Test Methods for Notched Bar Impact Testing of Metallic Materials."
8. ASTM A370-89, "Standard Test Methods and Definitions for Mechanical Testing of Steel Products."
9. ASTM E8-89b, "Standard Test Methods of Tension Testing of Metallic Materials."
10. ASTM E21-79 (1988), "Standard Practice for Elevated Temperature Tension Tests of Metallic Materials."

11. ASTM E83-85, "Standard Practice for Verification and Classification of Extensometers."
12. R. G. Soltesz, R. K. Disney, J. Jedruch, and S. L. Ziegler, "Nuclear Rocket Shielding Methods, Modification, Updating and Input Data Preparation. Vol. 5--Two-Dimensional Discrete Ordinates Transport Technique", WANL-PR(LL)-034, Vol. 5, August 1970.
13. "ORNL RSCI Data Library Collection DLC-76 SAILOR Coupled Self-Shielded, 47 Neutron, 20 Gamma-Ray, P3, Cross Section Library for Light Water Reactors".
14. K.W. Bonadio, et. al., "The Nuclear Design and Core Physics Characteristics of the Alvin W. Vogtle Unit 2 Nuclear Power Plant - Cycle 1", WCAP-12099, December 1988. (Proprietary)
15. ASTM Designation E482-82, "Standard Guide for Application of Neutron Transport Methods for Reactor Vessel Surveillance", in ASTM Standards, Section 12, American Society for Testing and Materials, Philadelphia, PA, 1984.
16. ASTM Designation E560-77, "Standard Recommended Practice for Extrapolating Reactor Vessel Surveillance Dosimetry Results", in ASTM Standards, Section 12, American Society for Testing and Materials, Philadelphia, PA, 1984.
17. ASTM Designation E693-79, "Standard Practice for Characterizing Neutron Exposures in Ferritic Steels in Terms of Displacements per Atom (dpa)", in ASTM Standards, Section 12, American Society for Testing and Materials, Philadelphia, PA, 1984.
18. ASTM Designation E706-81a, "Standard Master Matrix for Light-Water Reactor Pressure Vessel Surveillance Standard", in ASTM Standards, Section 12, American Society for Testing and Materials, Philadelphia, PA, 1984.

19. ASTM Designation E853-84, "Standard Practice for Analysis and Interpretation of Light-Water Reactor Surveillance Results", in ASTM Standards, Section 12, American Society for Testing and Materials, Philadelphia, PA, 1984.
20. ASTM Designation E261-77, "Standard Method for Determining Neutron Flux, Fluence, and Spectra by Radioactivation Techniques", in ASTM Standards, Section 12, American Society for Testing and Materials, Philadelphia, PA, 1984.
21. ASTM Designation E262-77, "Standard Method for Measuring Thermal Neutron Flux by Radioactivation Techniques", in ASTM Standards, Section 12, American Society for Testing and Materials, Philadelphia, PA, 1984.
22. ASTM Designation E263-82, "Standard Method for Determining Fast-Neutron Flux Density by Radioactivation of Iron", in ASTM Standards, Section 12, American Society for Testing and Materials, Philadelphia, PA, 1984.
23. ASTM Designation E264-82, "Standard Method for Determining Fast-Neutron Flux Density by Radioactivation of Nickel", in ASTM Standards, Section 12, American Society for Testing and Materials, Philadelphia, PA, 1984.
24. ASTM Designation E481-78, "Standard Method for Measuring Neutron-Flux Density by Radioactivation of Cobalt and Silver", in ASTM Standards, Section 12, American Society for Testing and Materials, Philadelphia, PA, 1984.
25. ASTM Designation E523-82, "Standard Method for Determining Fast-Neutron Flux Density by Radioactivation of Copper", in ASTM Standards, Section 12, American Society for Testing and Materials, Philadelphia, PA, 1984.
26. ASTM Designation E704-84, "Standard Method for Measuring Reaction Rates by Radioactivation of Uranium-238", in ASTM Standards, Section 12, American Society for Testing and Materials, Philadelphia, PA, 1984.

27. ASTM Designation E705-79, "Standard Method for Measuring Fast-Neutron Flux Density by Radioactivation of Neptunium-237", in ASTM Standards, Section 12, American Society for Testing and Materials, Philadelphia, PA, 1984.
28. ASTM Designation E1005-84, "Standard Method for Application and Analysis of Radiometric Monitors for Reactor Vessel Surveillance", in ASTM Standards, Section 12, American Society for Testing and Materials, Philadelphia, PA, 1984.
29. F. A. Schmittroth, FERRET Data Analysis Core, HEDL-TME 79-40. Hanford Engineering Development Laboratory, Richland, WA, September 1979.
30. W. N. McElroy, S. Berg and T. Crocket, A Computer-Automated Iterative Method of Neutron Flux Spectra Determined by Foil Activation, AFWL-TR-7-41, Vol. I-IV, Air Force Weapons Laboratory, Kirkland AFB, NM, July 1967.
31. EPRI-NP-2188, "Development and Demonstration of an Advanced Methodology for LWR Dosimetry Applications", R. E. Maerker, et al., 1981.

APPENDIX A

Load-Time Records for Charpy Specimen Tests

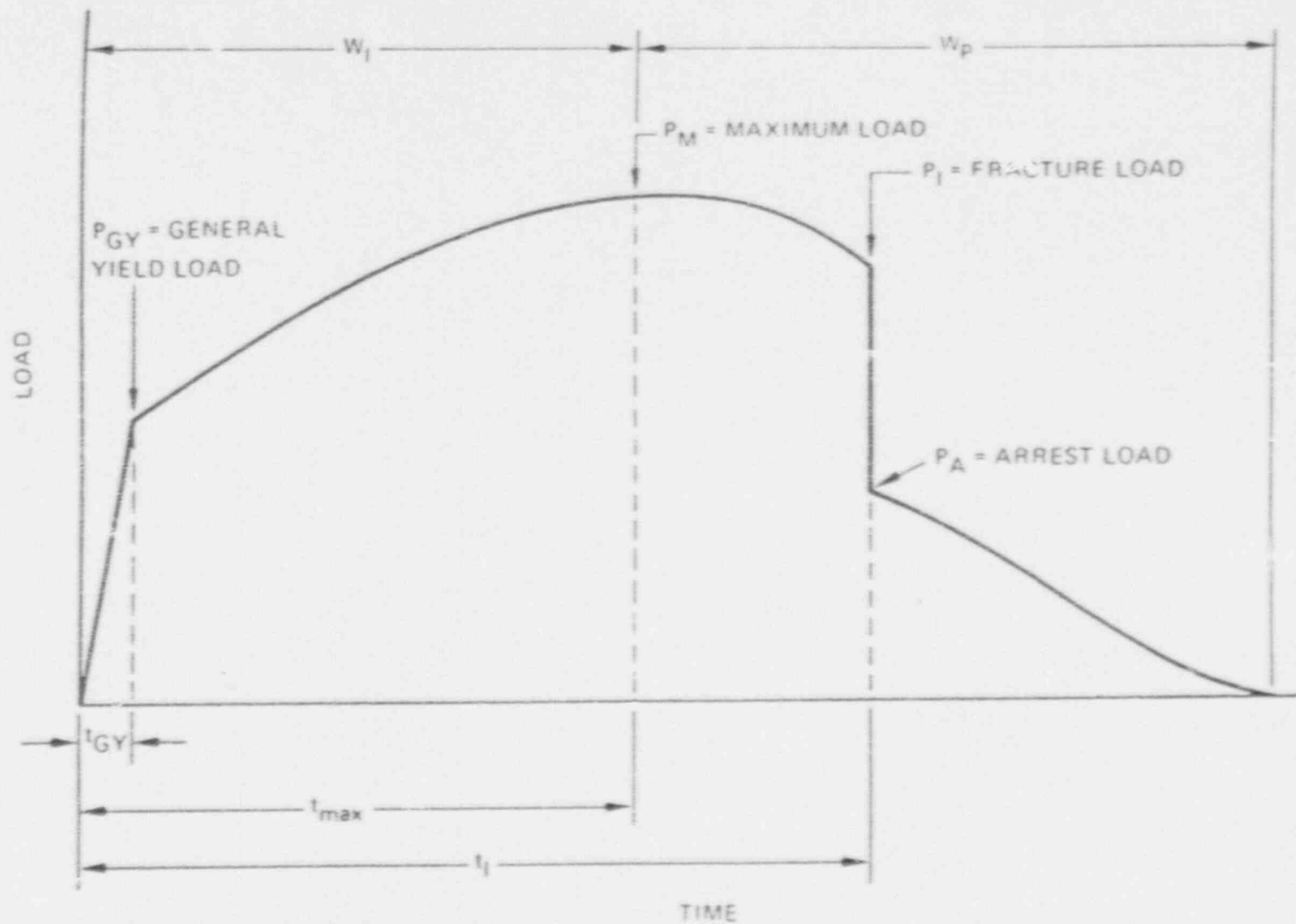


Figure A-1. Idealized load-time record for an instrumented Charpy impact test.

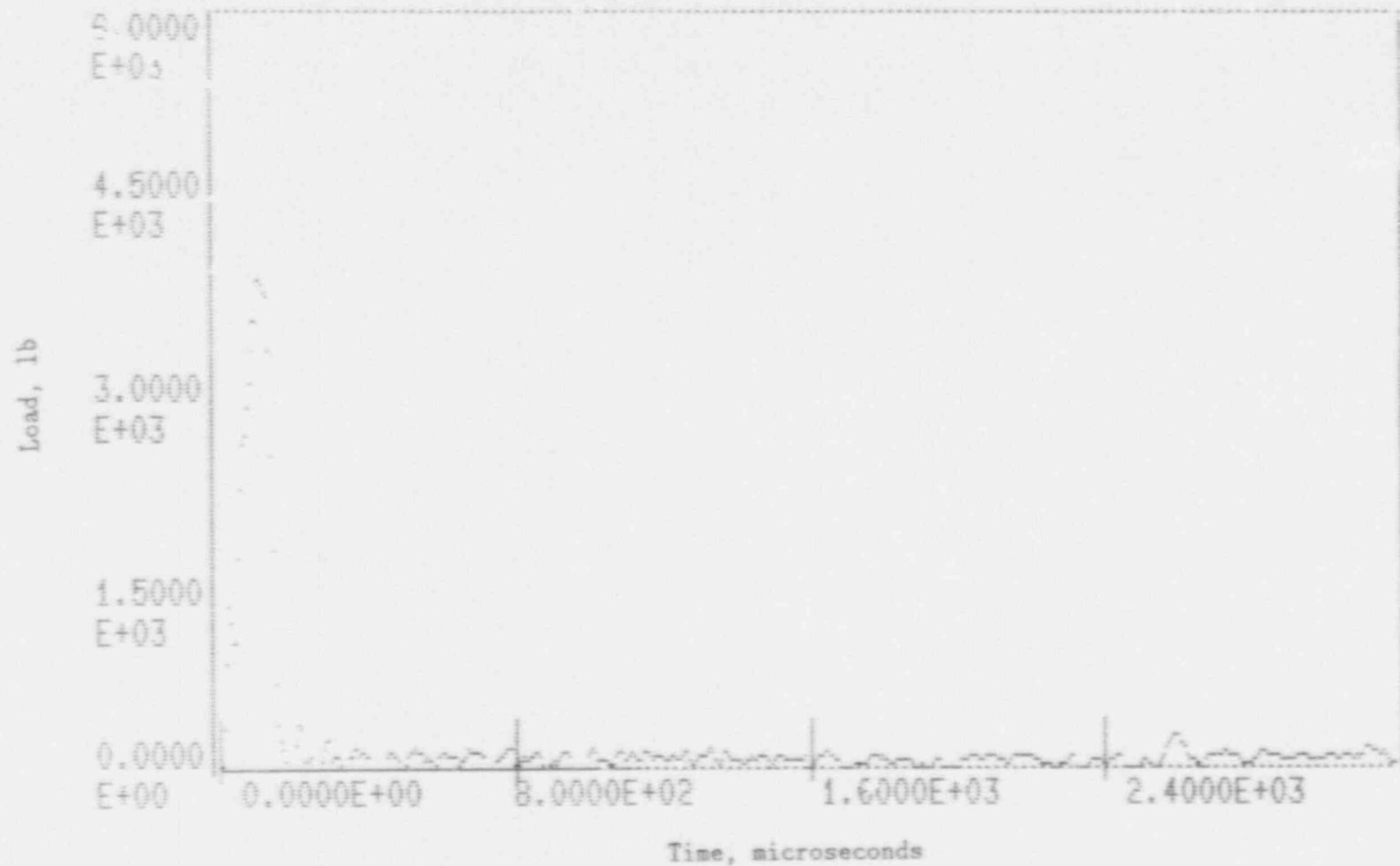


Figure A-2. Charpy impact test load-time record for Specimen BL9.

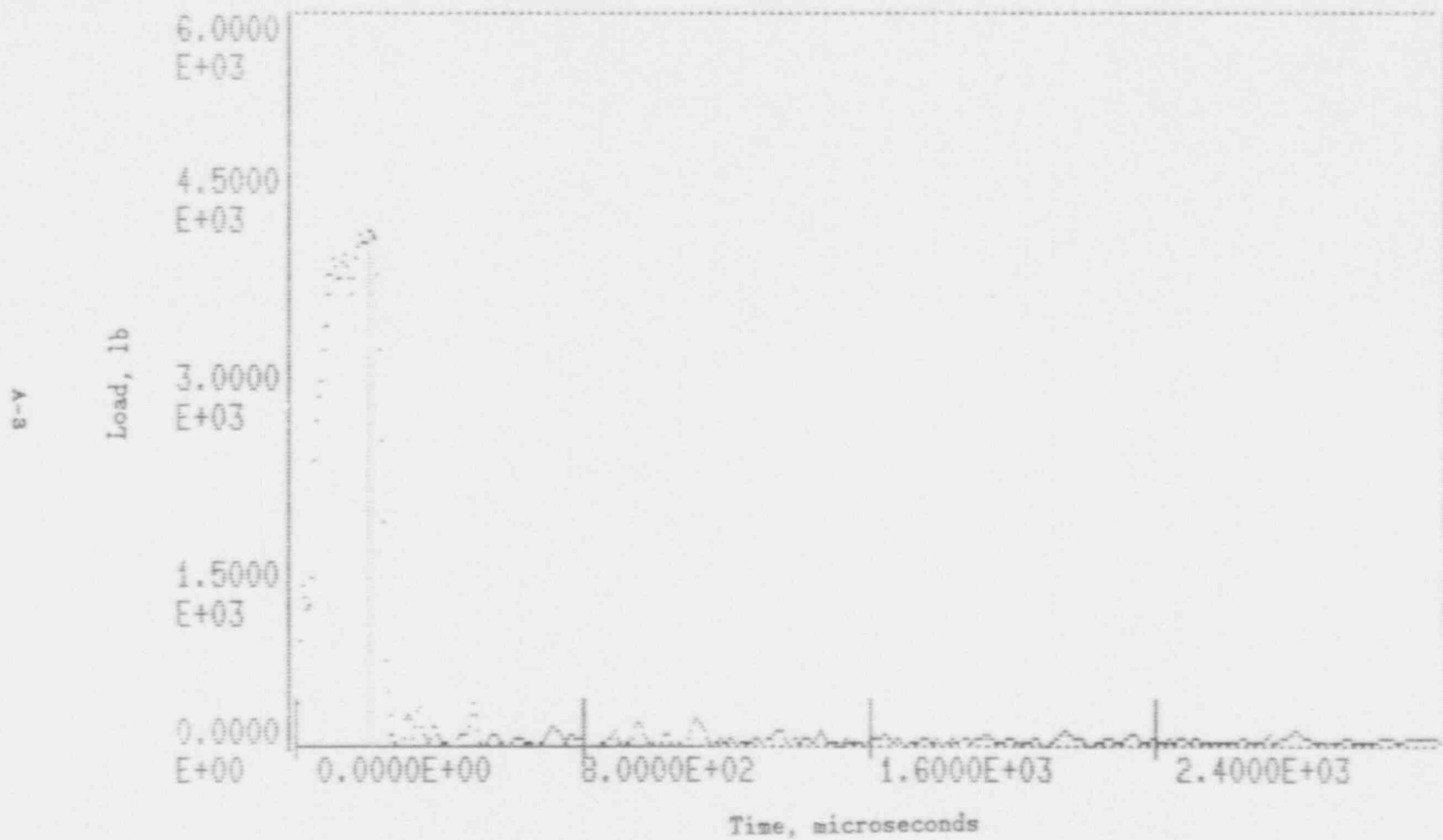


Figure A-3. Charpy impact test load-time record for Specimen BL10.

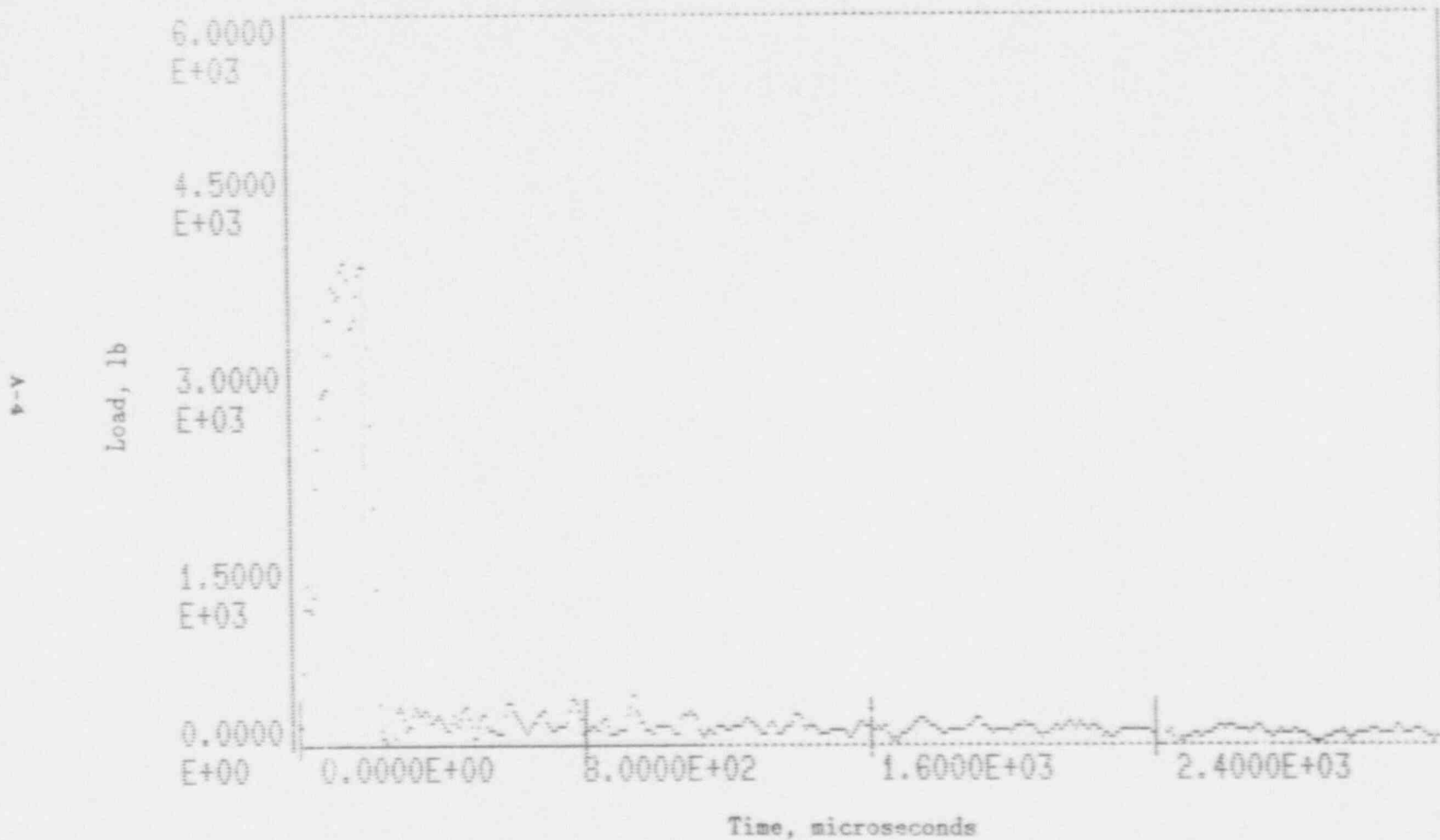


Figure A-4. Charpy impact test load-time record for Specimen BL12.

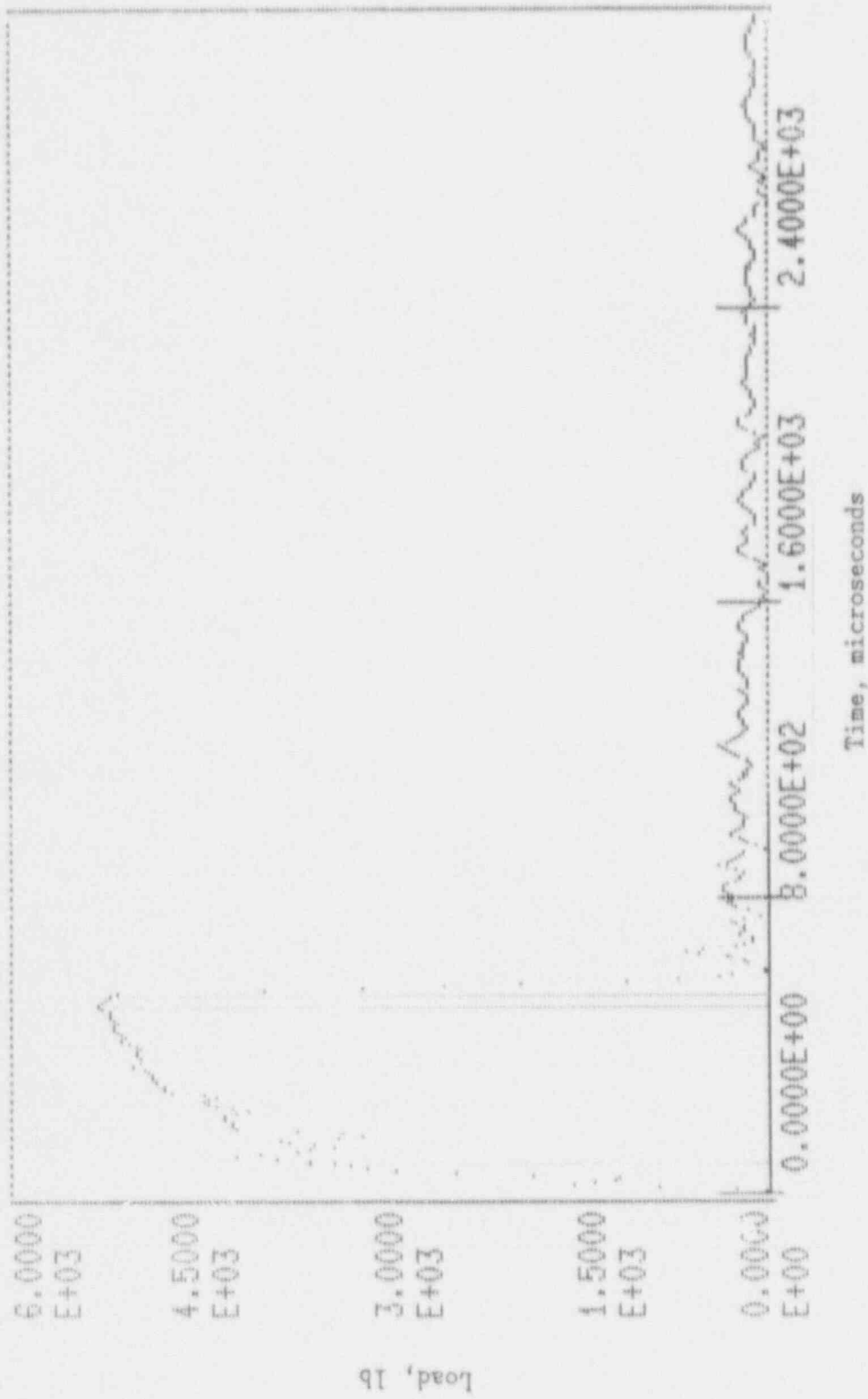


Figure A-5. Charpy impact test load-time record for Specimen BL1.

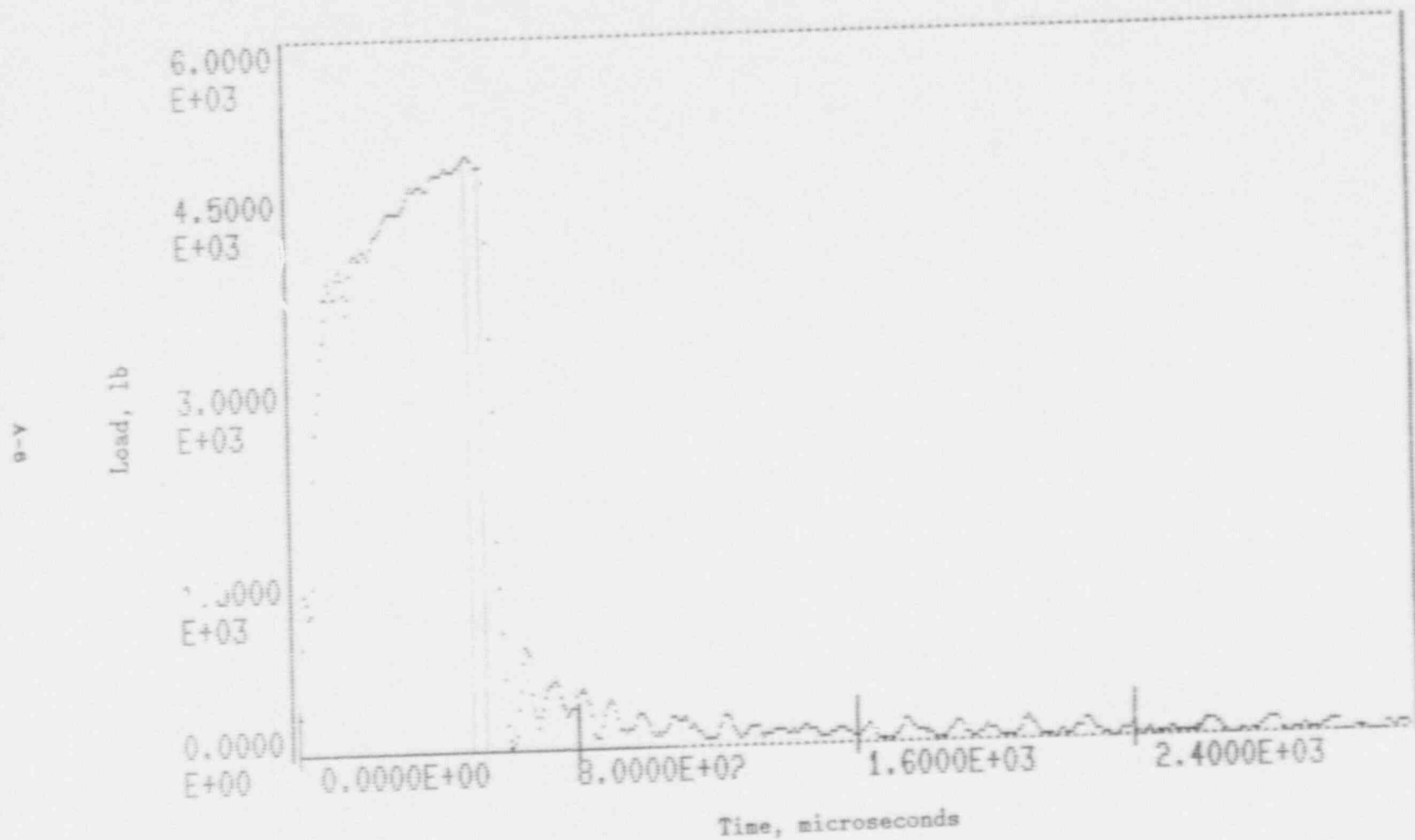


Figure A-6. Charpy impact test load-time record for Specimen BL6.

A-7

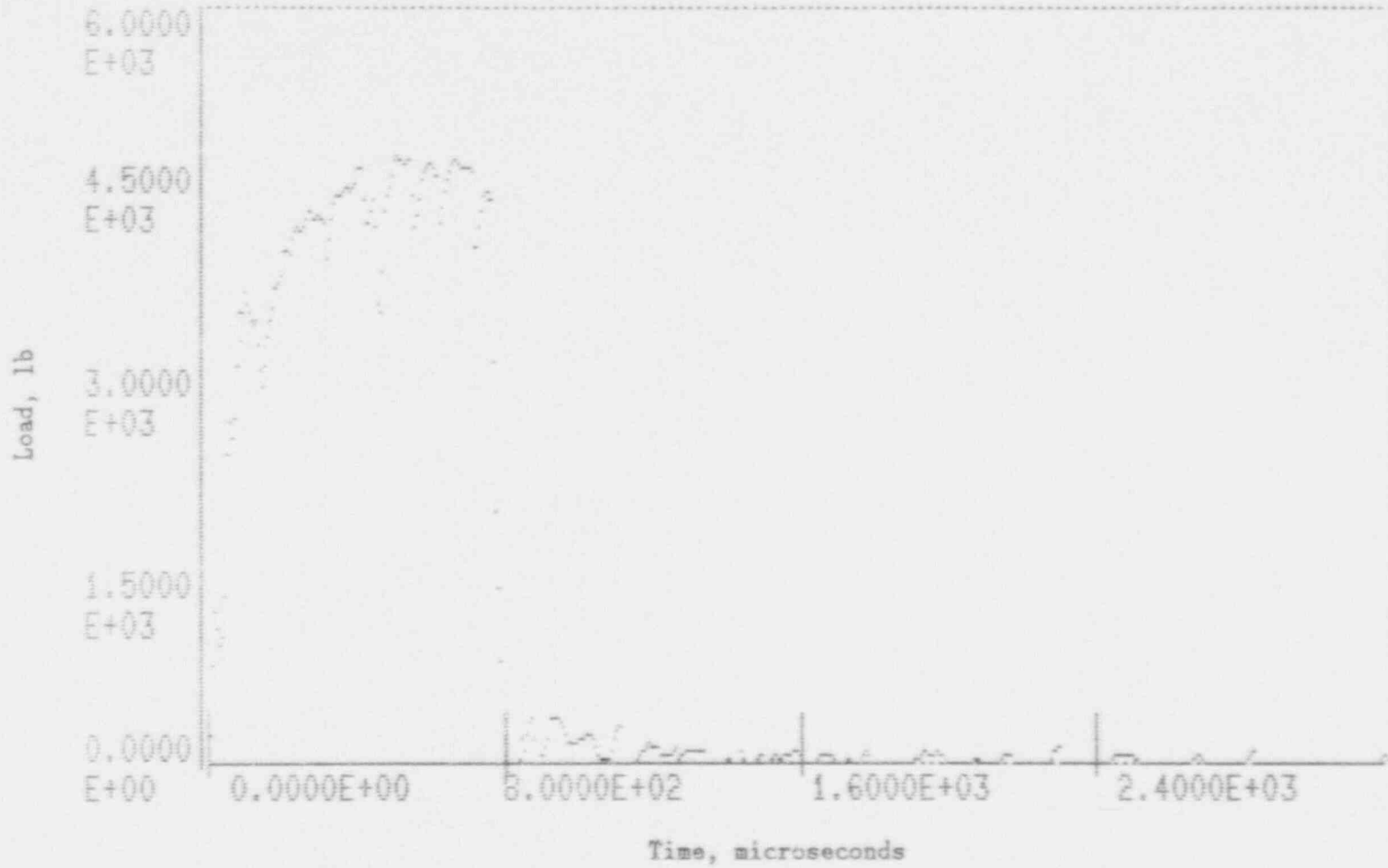


Figure A-7. Charpy impact test load-time record for Specimen BL2.

COMPUTER MALFUNCTION - NO LOAD TIME RECORD

(Data memory drop-out)

8-Y

Figure A-8. Charpy impact test load-time record for Specimen BL15.

6-V

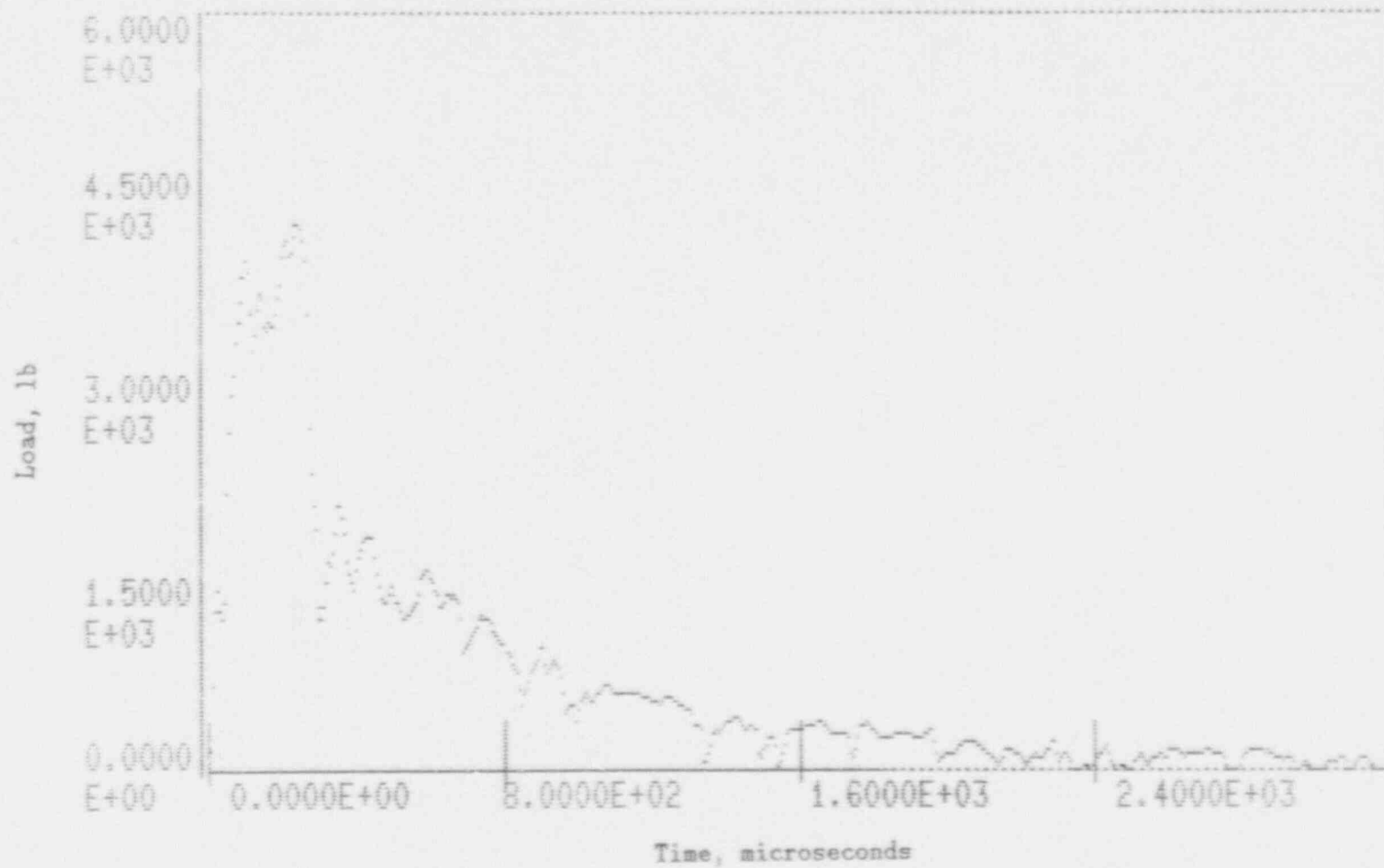


Figure A-9. Charpy impact test load-time record for Specimen BL8.

01-V

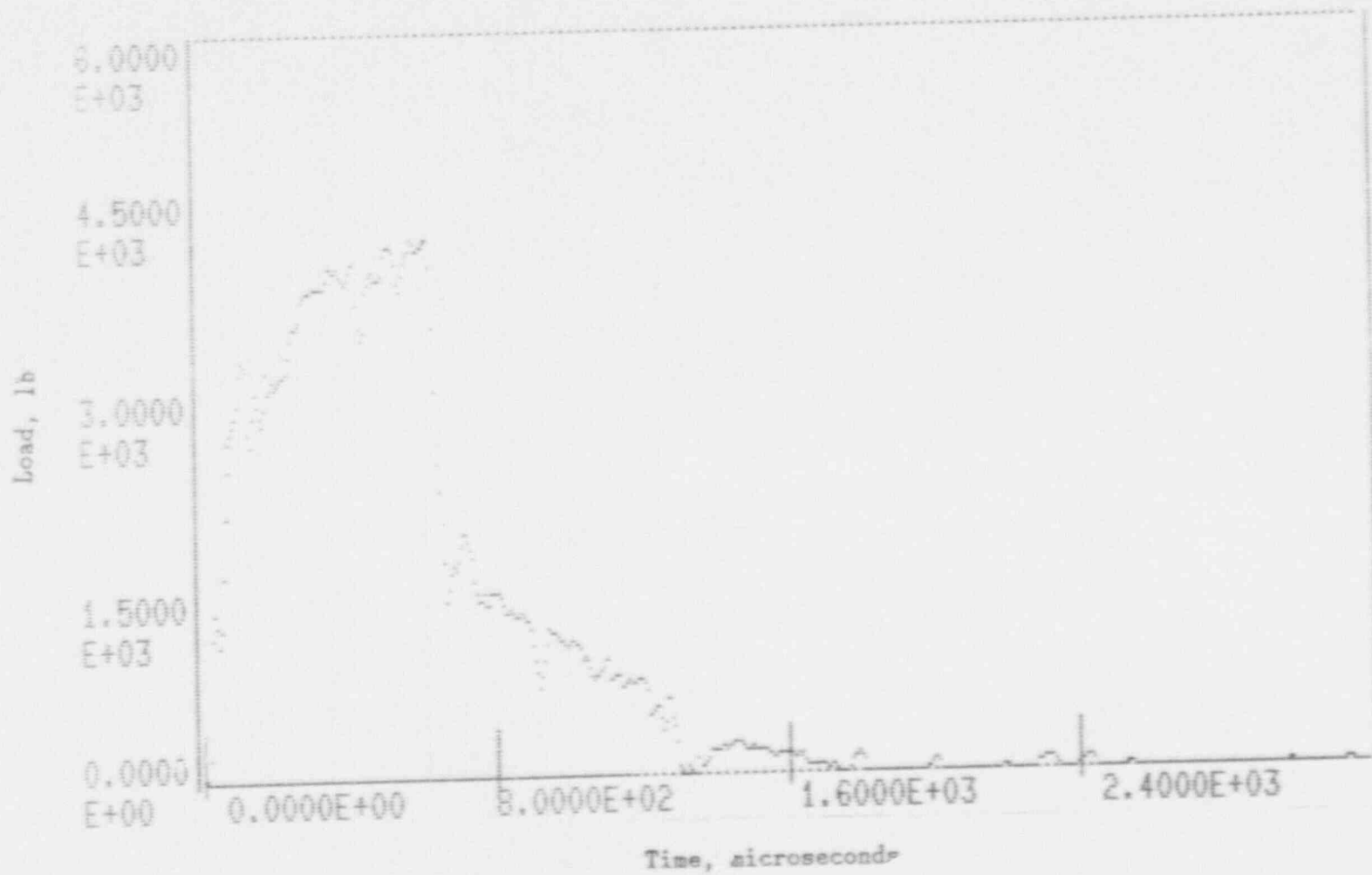


Figure A-10. Charpy impact test load-time record for Specimen BL5.

11-V

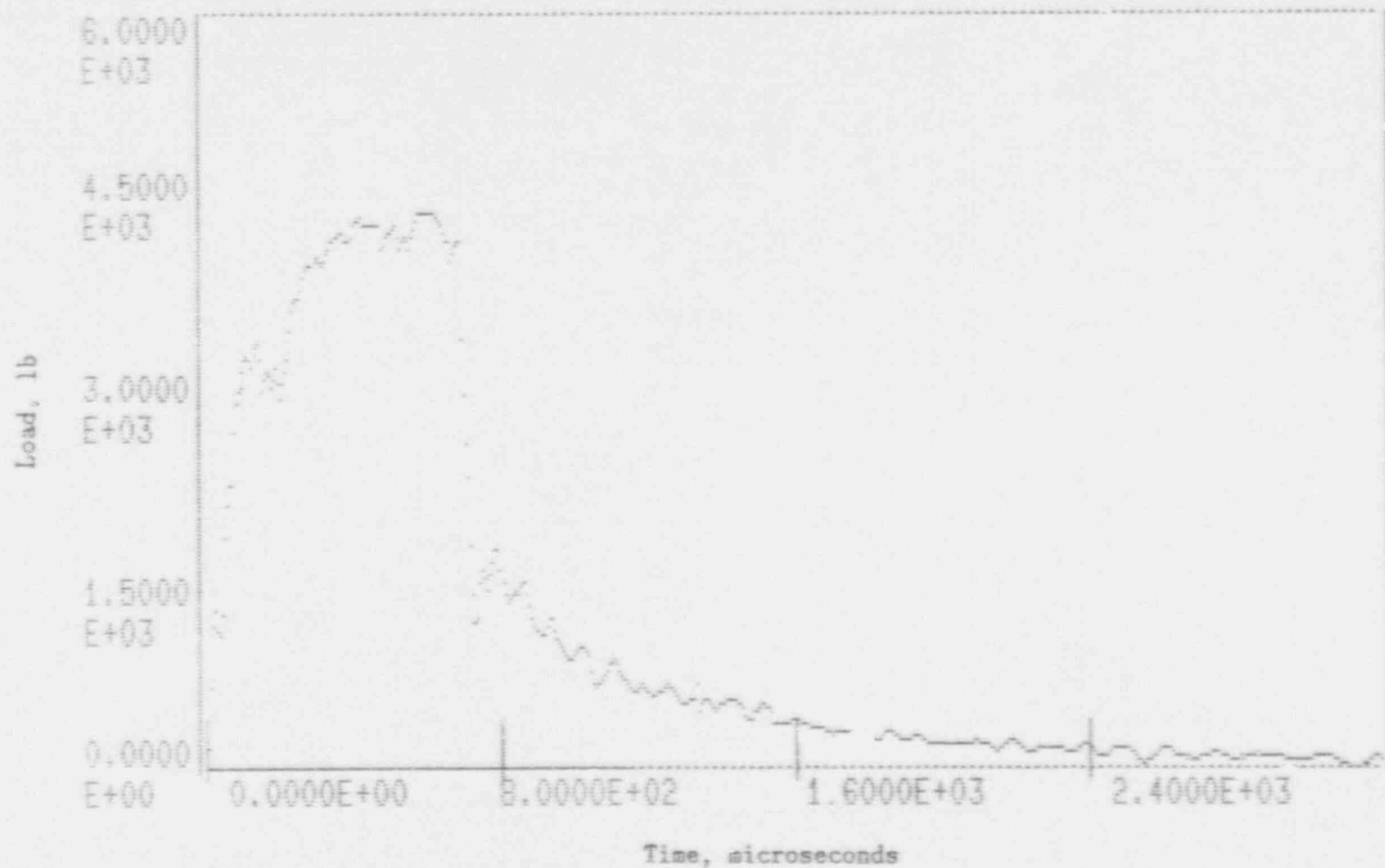


Figure A-11. Charpy impact test load-time record for Specimen BL7.

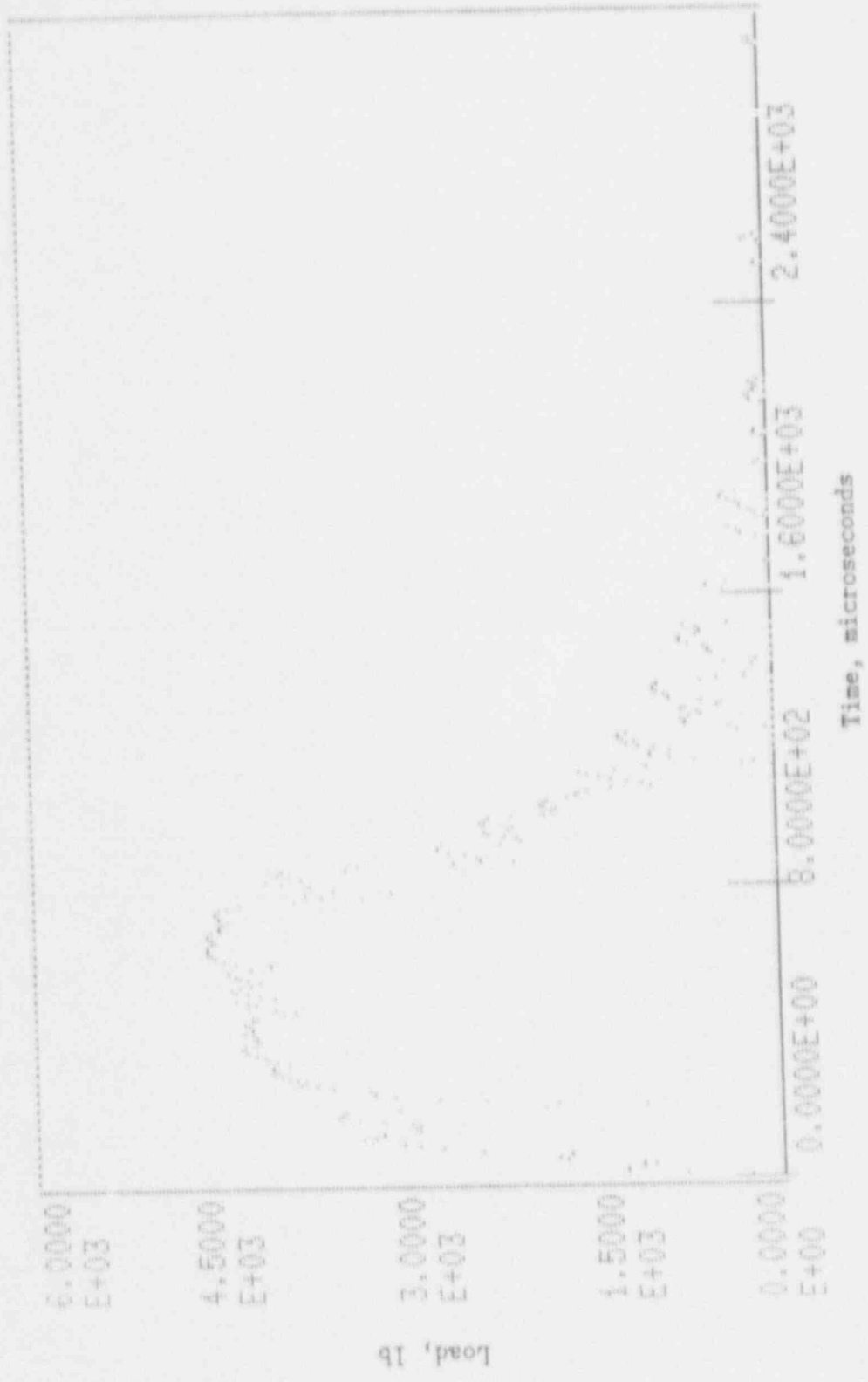


Figure A-12. Charpy impact test load-time record for Specimen BLA.

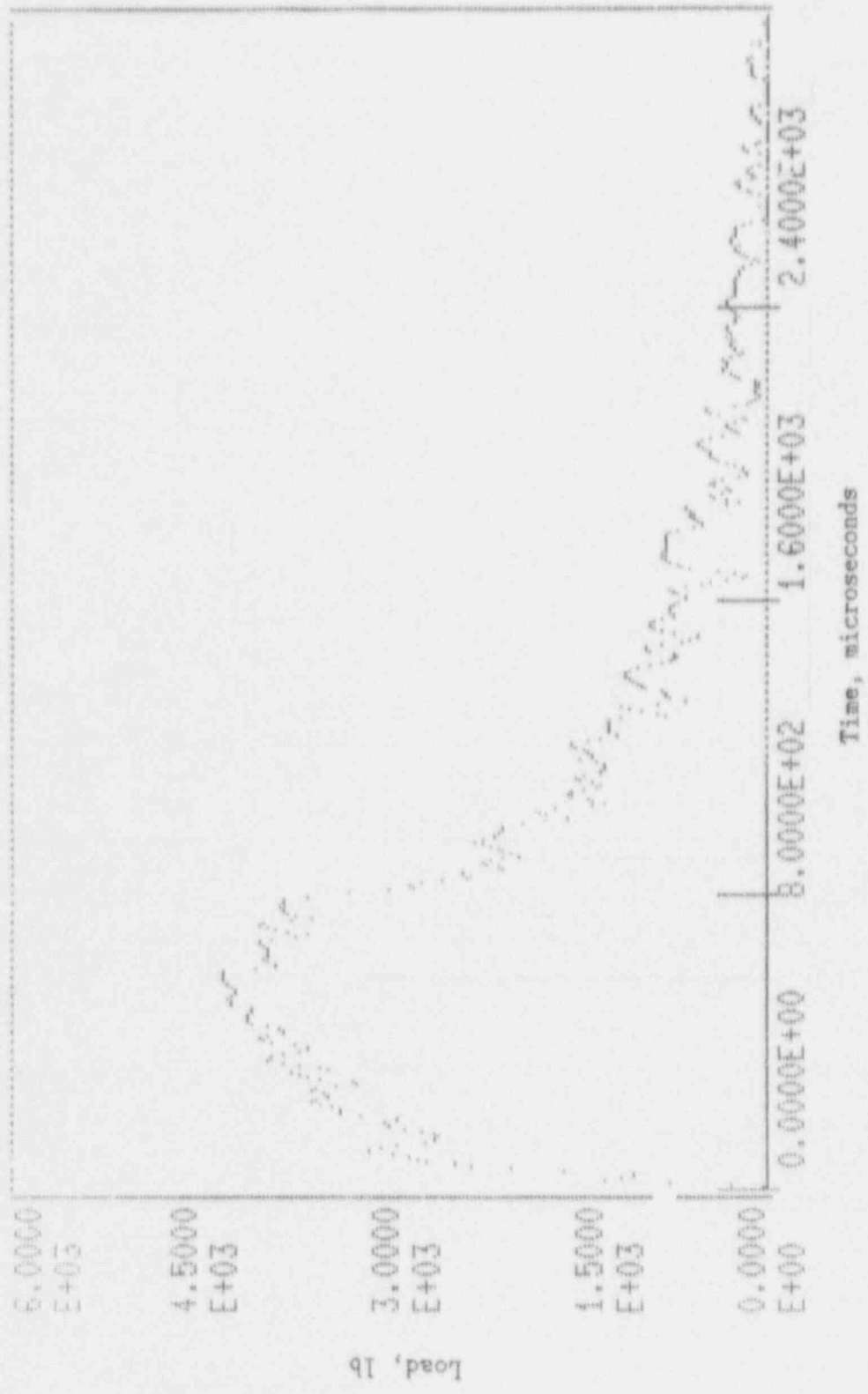


Figure A-13. Charpy impact test load-time record for Specimen BL11.

A-14

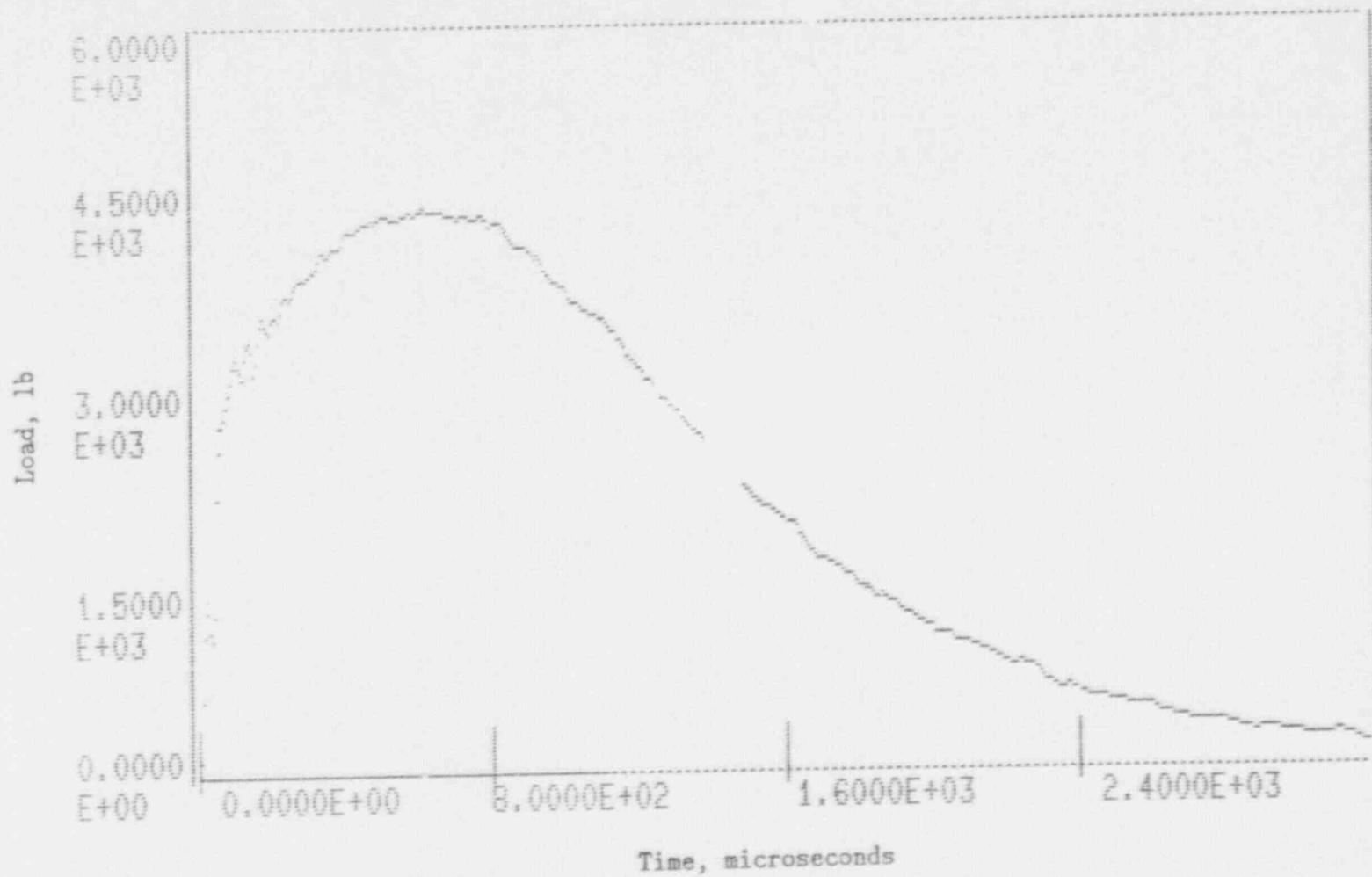


Figure A-14. Charpy impact test load-time record for Specimen BL14.

91-V

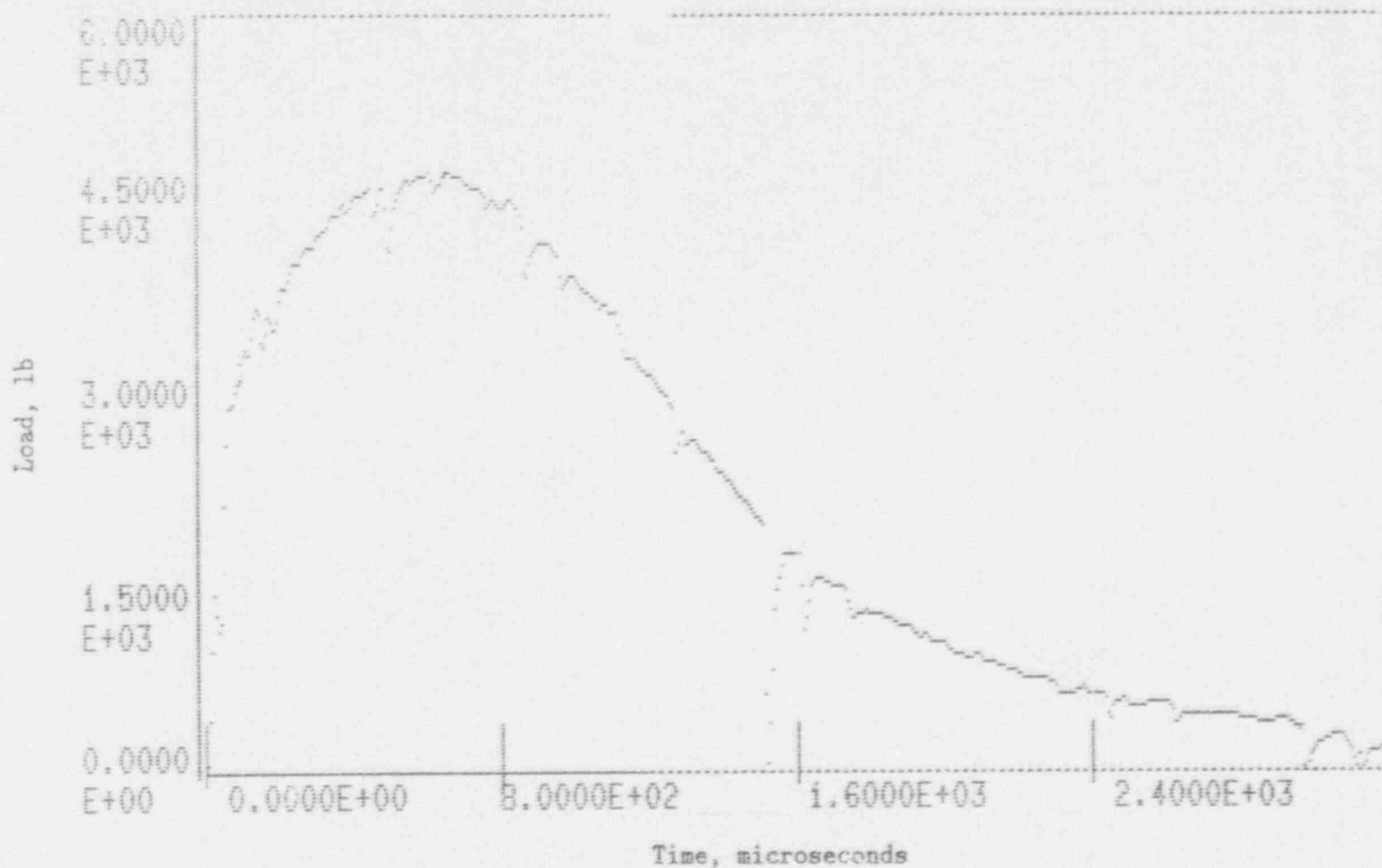


Figure A-15. Charpy impact test load-time record for Specimen BL13.

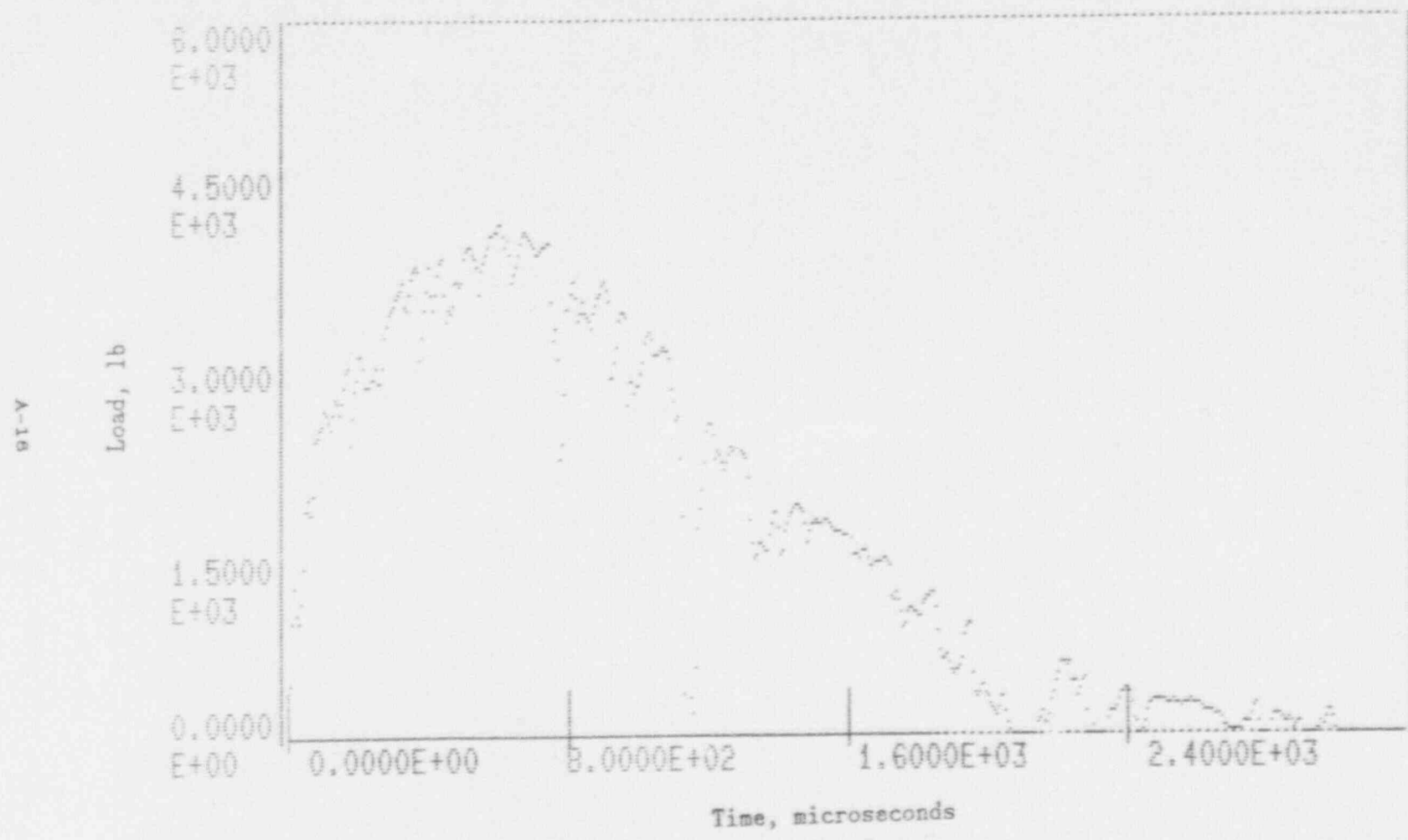


Figure A-16. Charpy impact test load-time record for Specimen BL3.

A-17

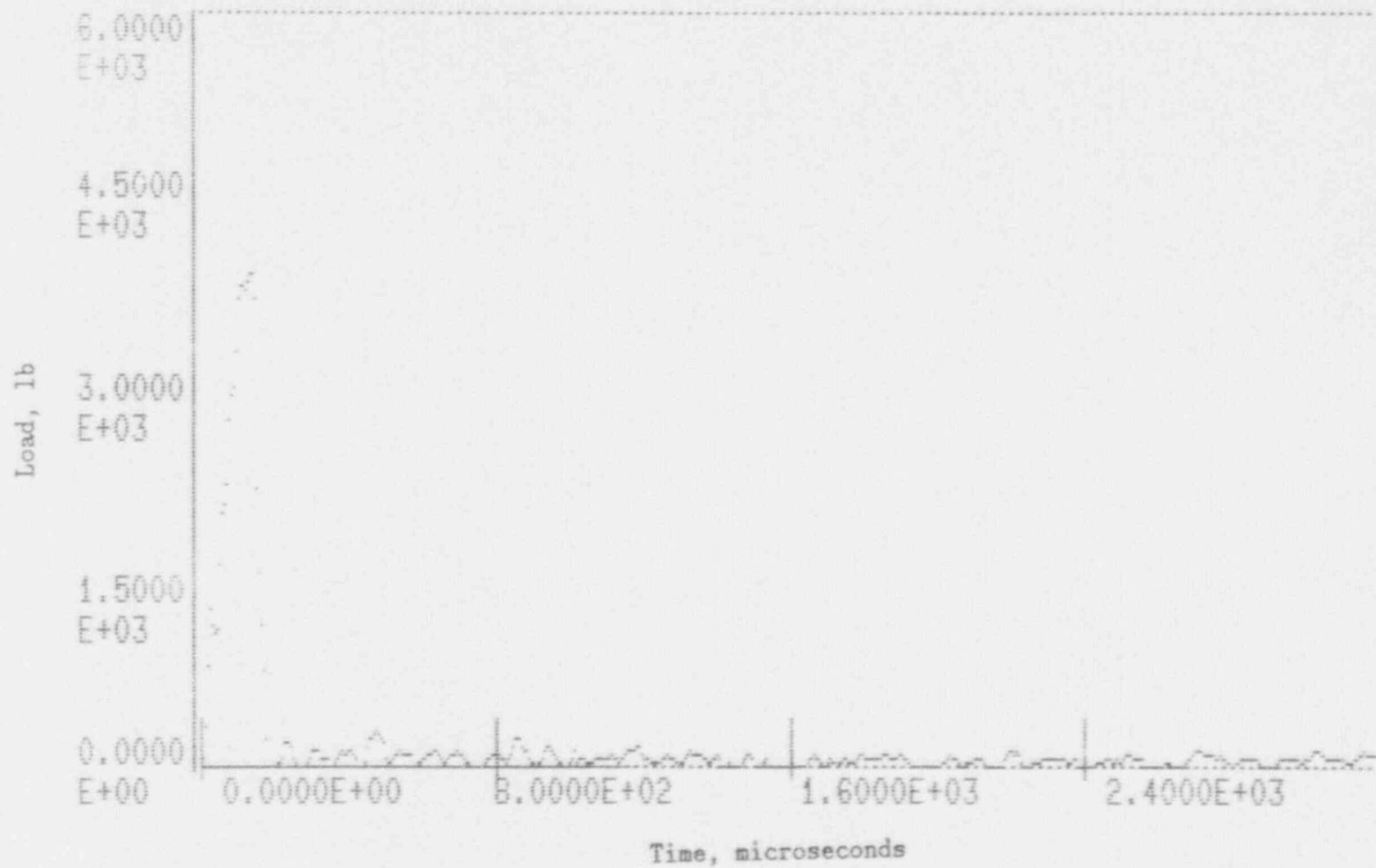


Figure A-17. Charpy impact test load-time record for Specimen BT5.

BT-1

Load, lb

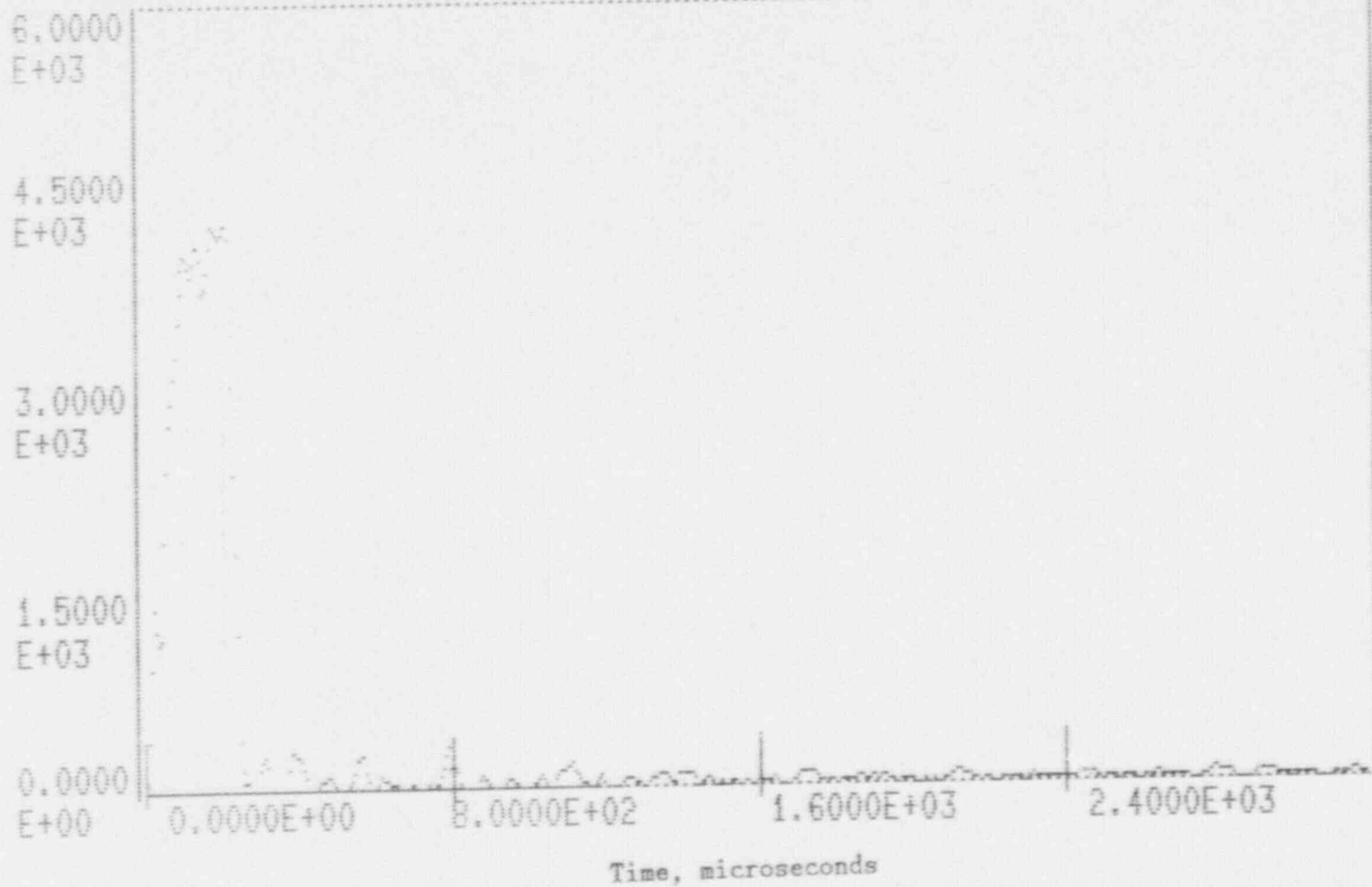


Figure A-18. Charpy impact test load-time record for Specimen BT1.

A-19

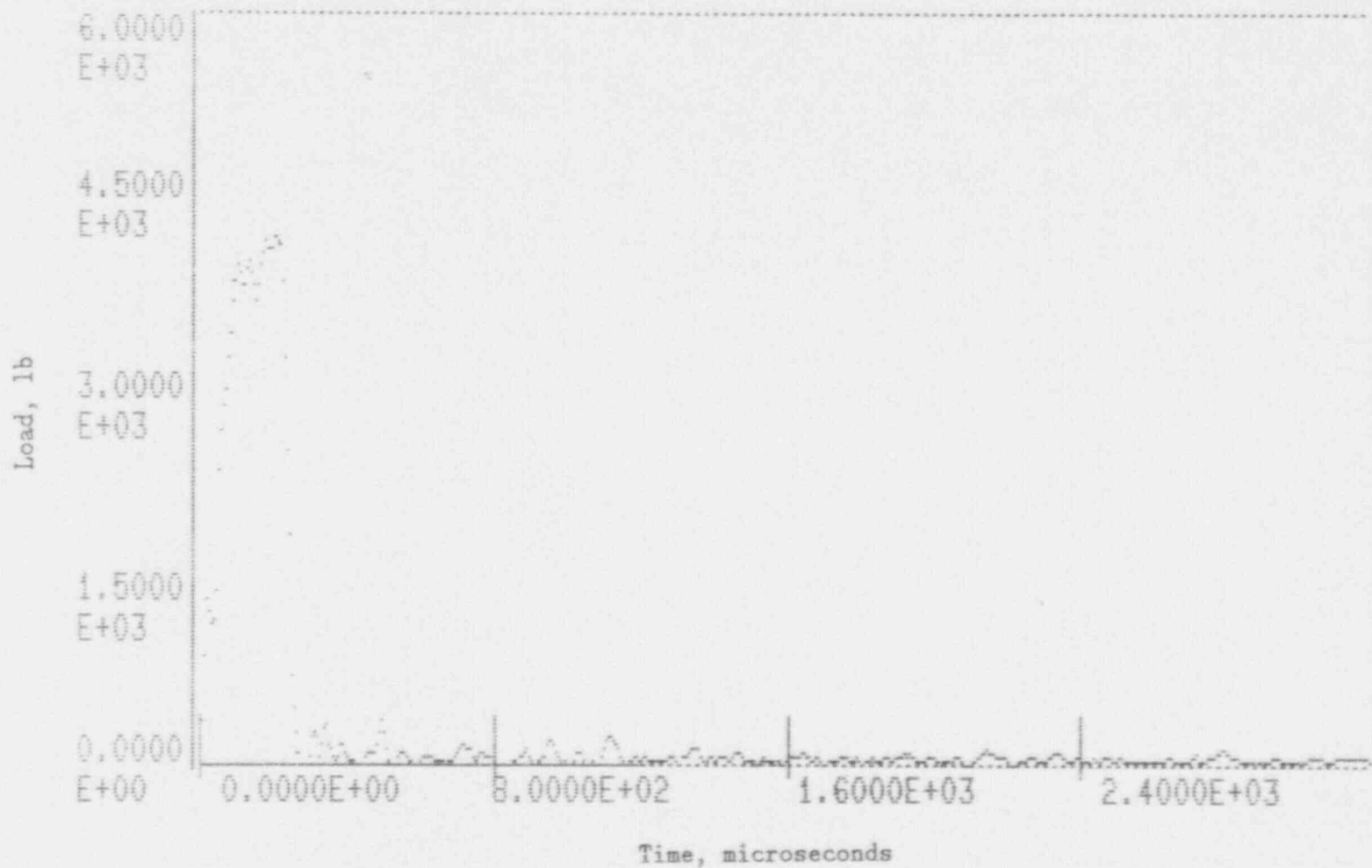


Figure A-19. Charpy impact test load-time record for Specimen BT12.

08-V

Load, lb

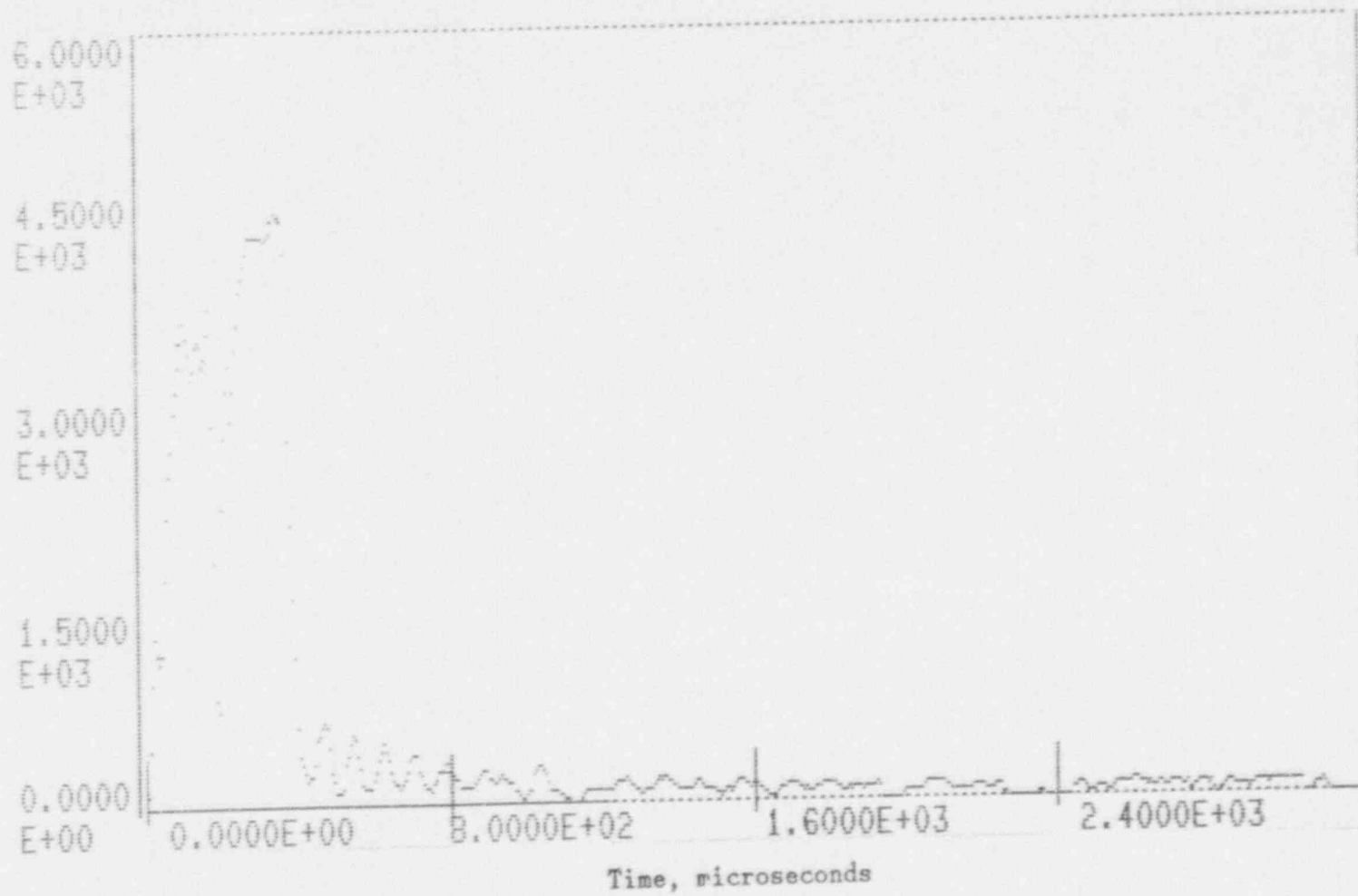


Figure A-20. Charpy impact test load-time record for Specimen BT13.

A-21

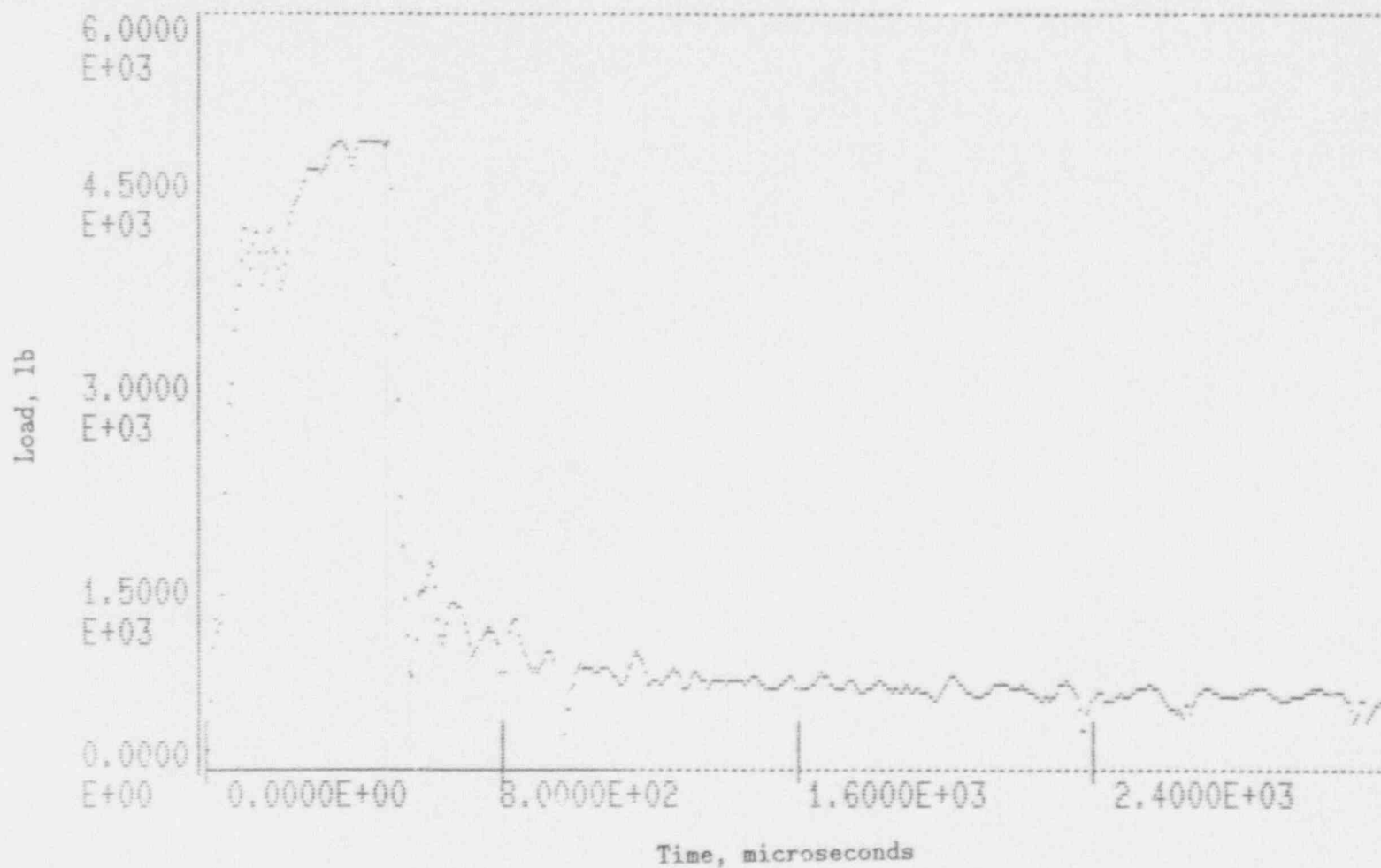


Figure A-21. Charpy impact test load-time record for Specimen BT3.

A-22

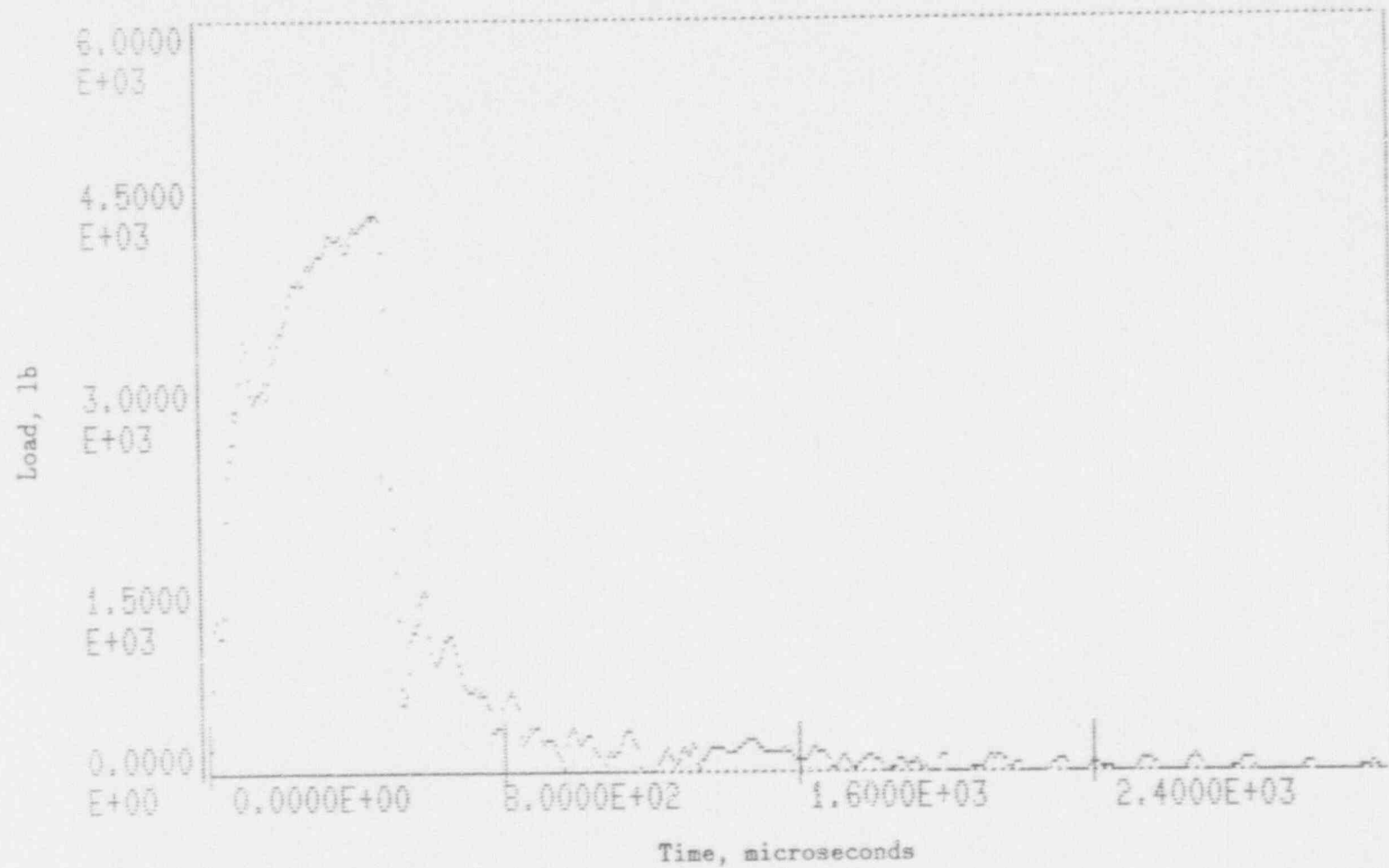


Figure A-22. Charpy impact test load-time record for Specimen BT7.

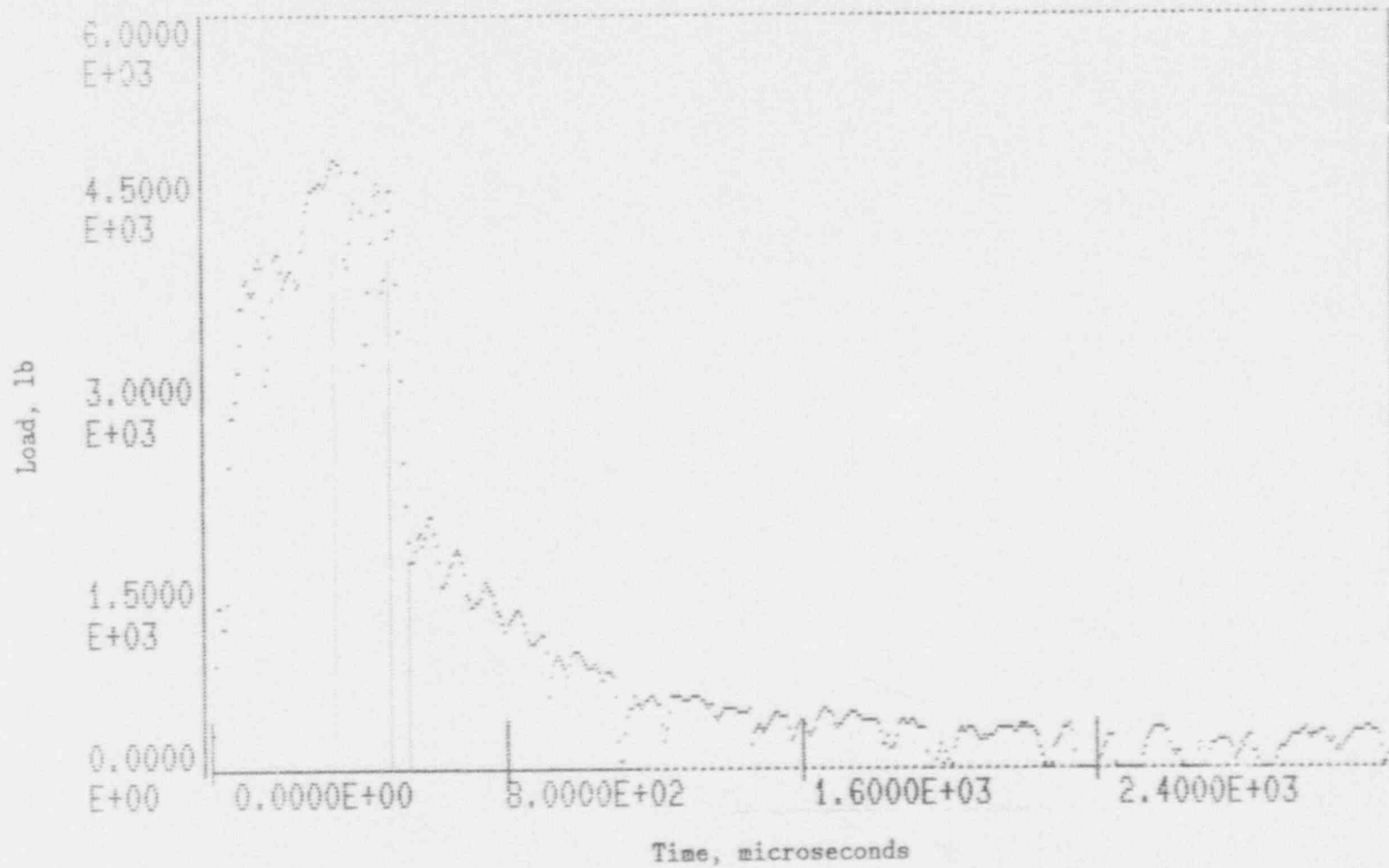


Figure A-23. Charpy impact test load-time record for Specimen BT14.

A-24

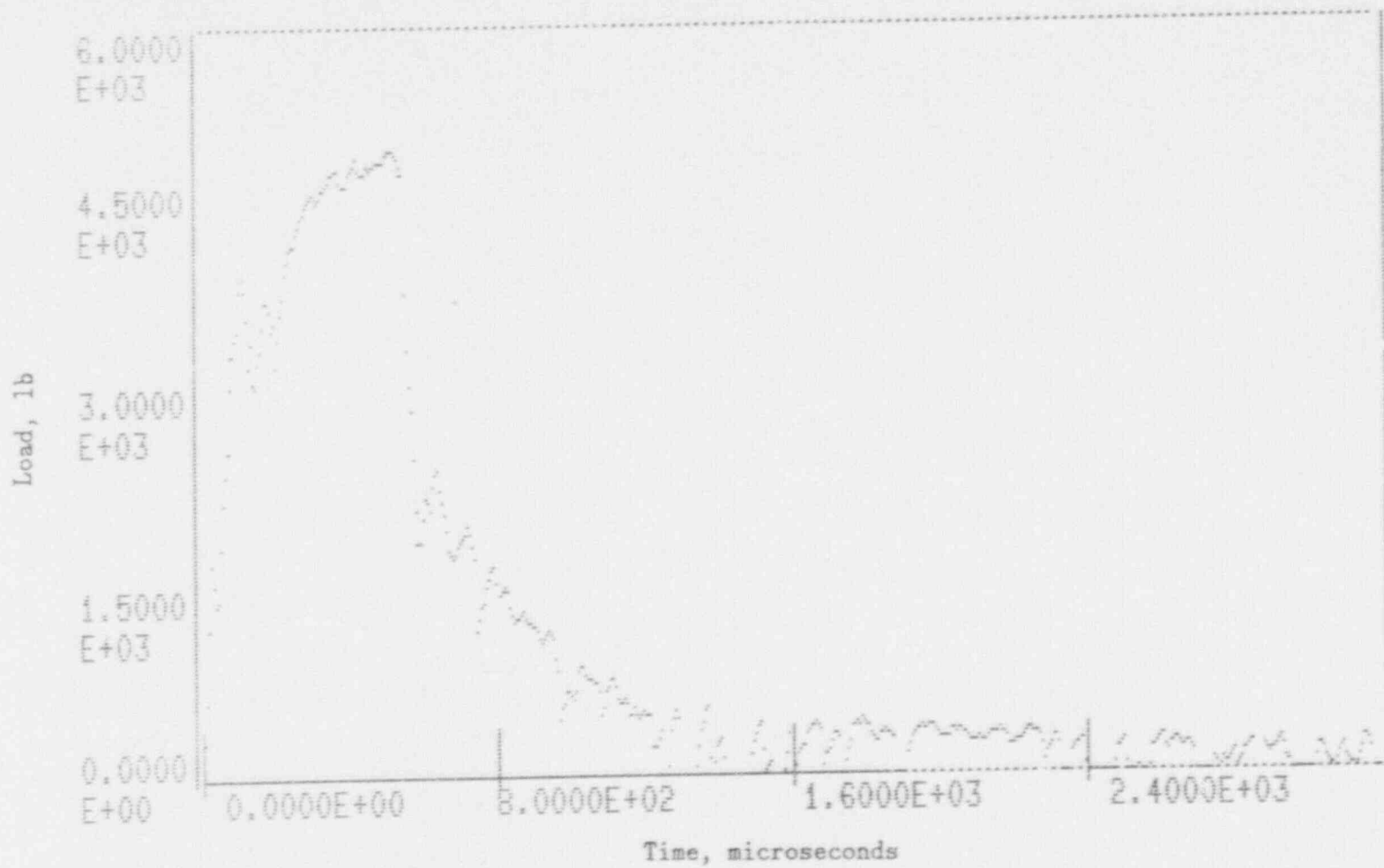


Figure A-24. Charpy impact test load-time record for Specimen BT8.

A-25

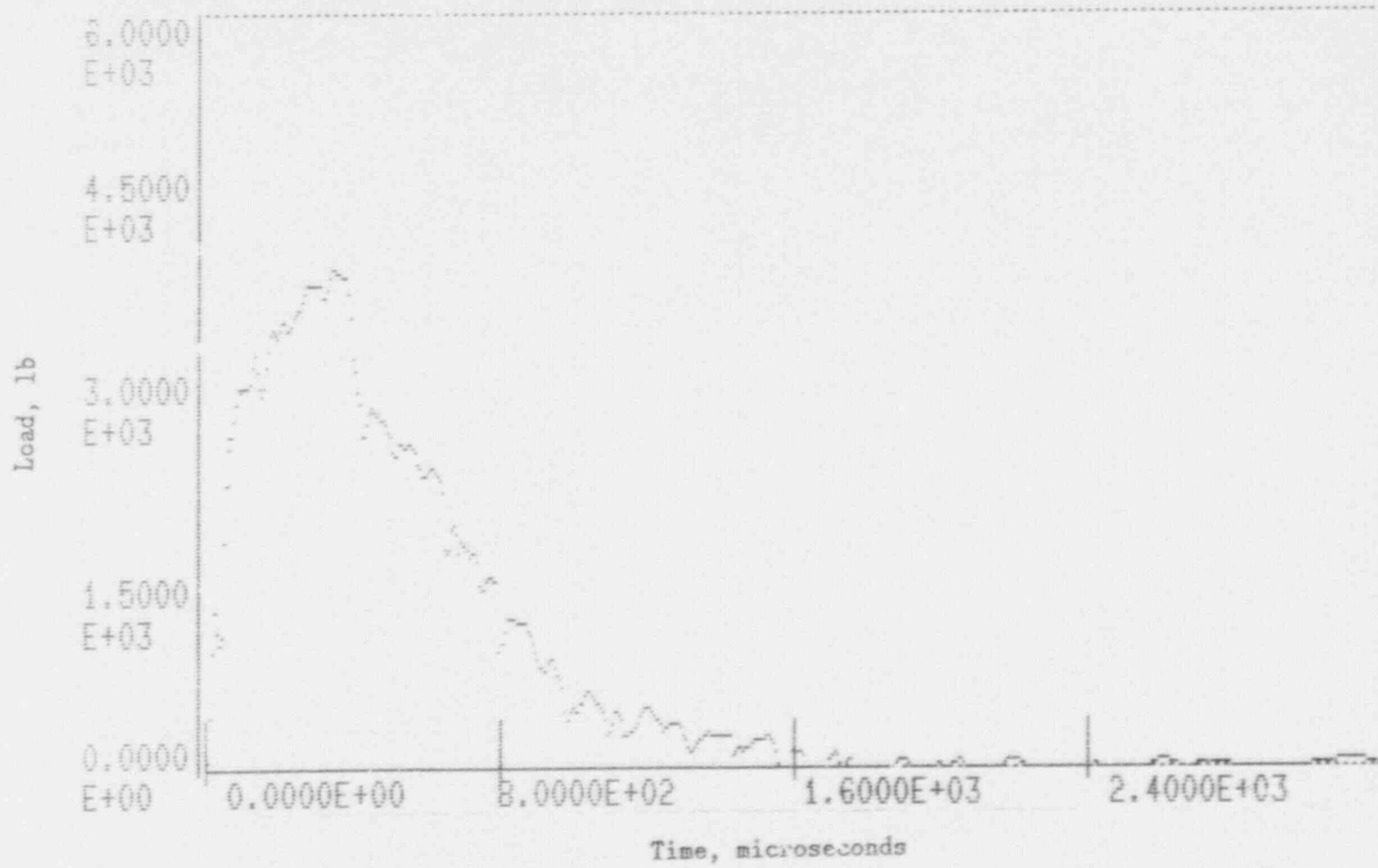


Figure A-25. Charpy impact test load-time record for Specimen BT10.

A-26

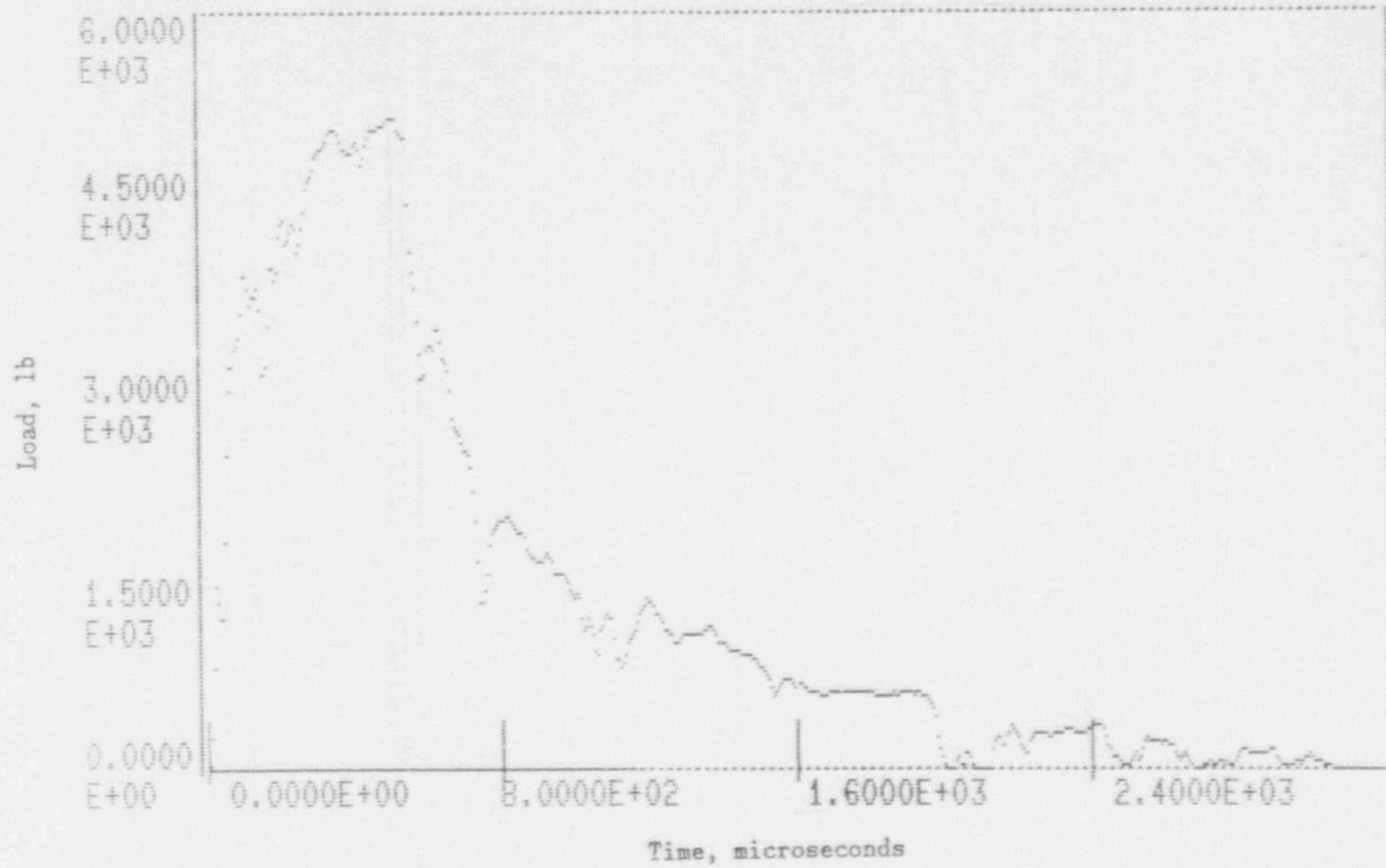


Figure A-26. Charpy impact test load-time record for Specimen BT6.

A-27

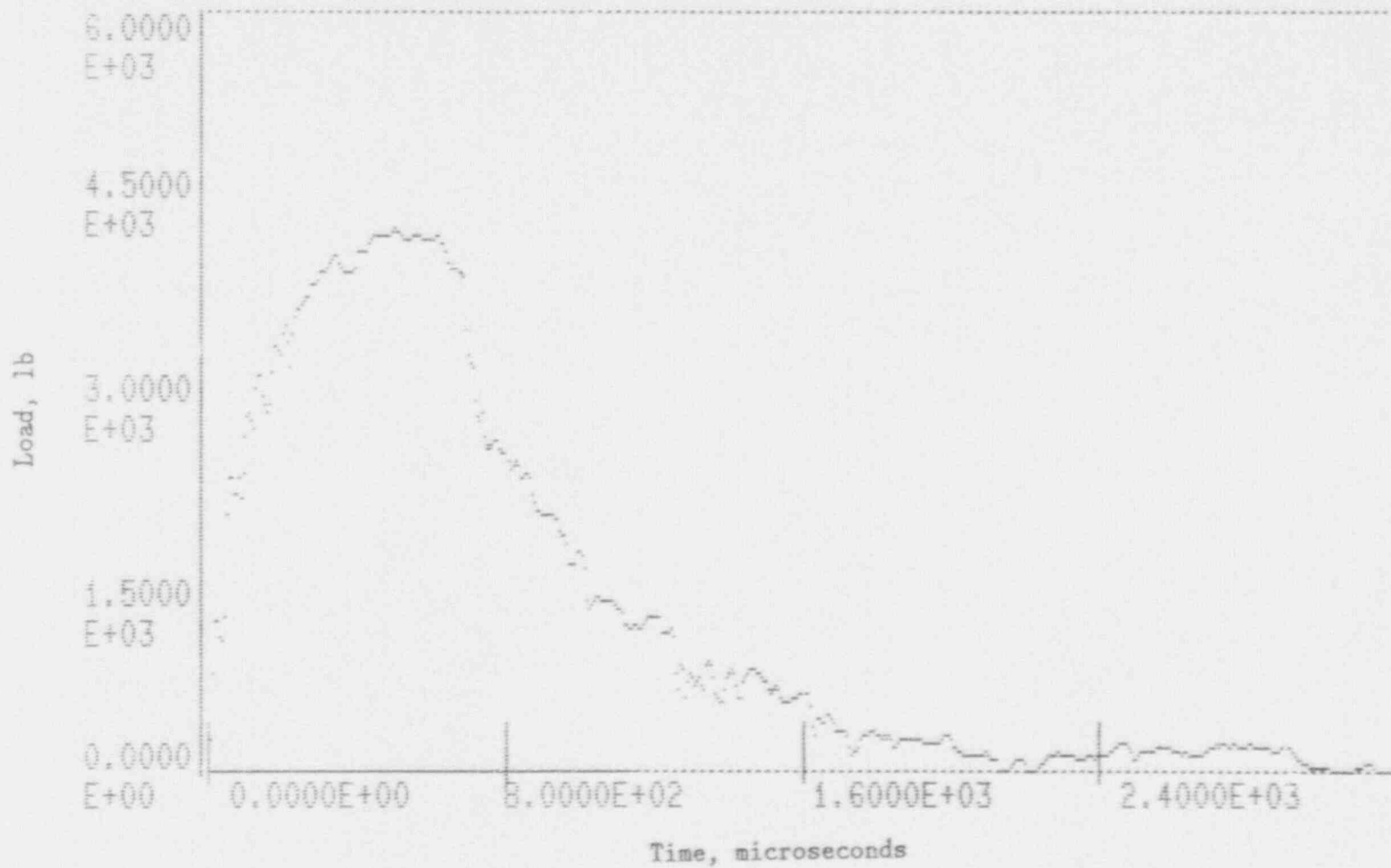


Figure A-27. Charpy impact test load-time record for Specimen 9T2.

A-28

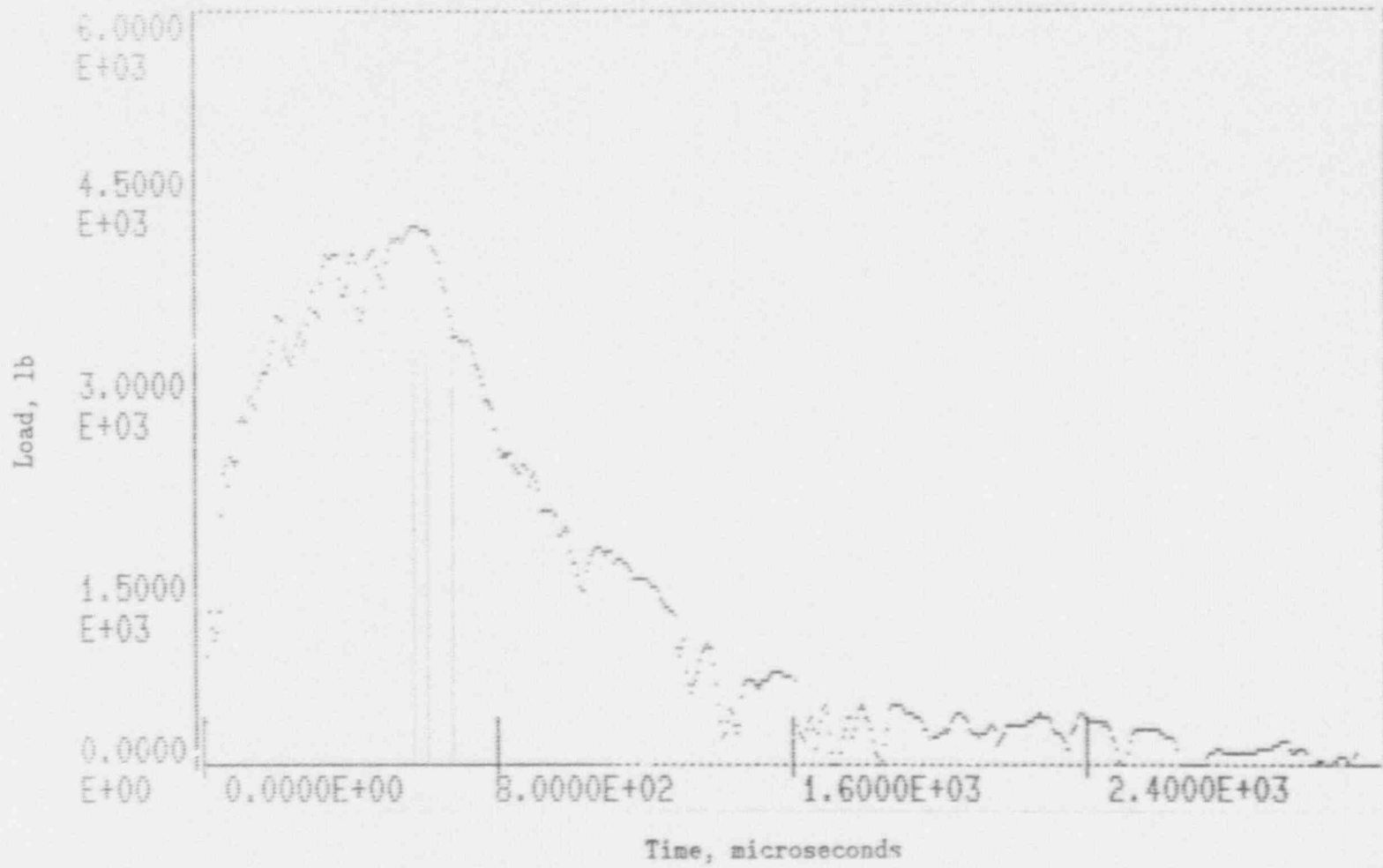


Figure A-28. Charpy impact test load-time record for Specimen BT9.

A-29

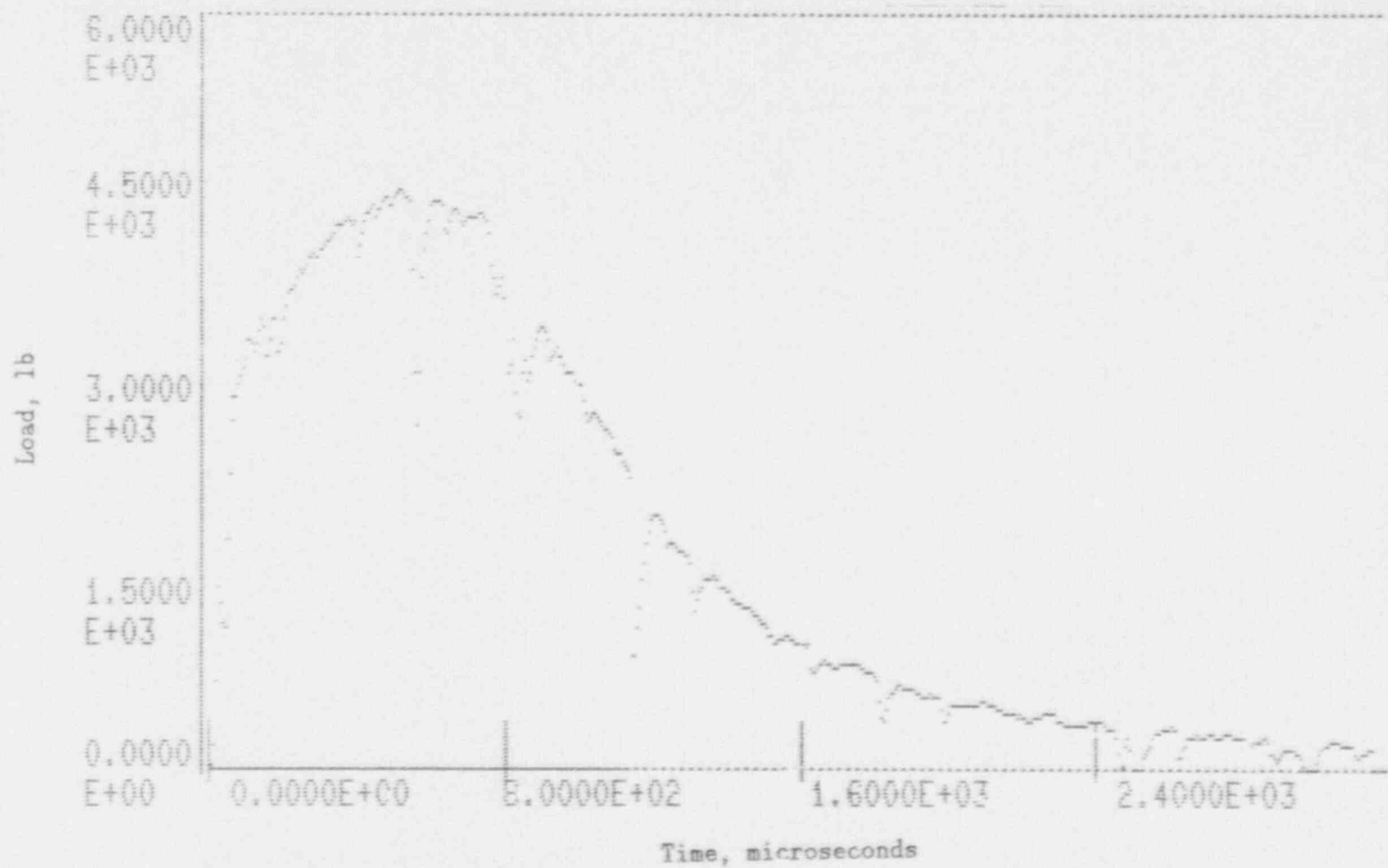


Figure A-29. Charpy impact test load-time record for Specimen BT11.

A-30

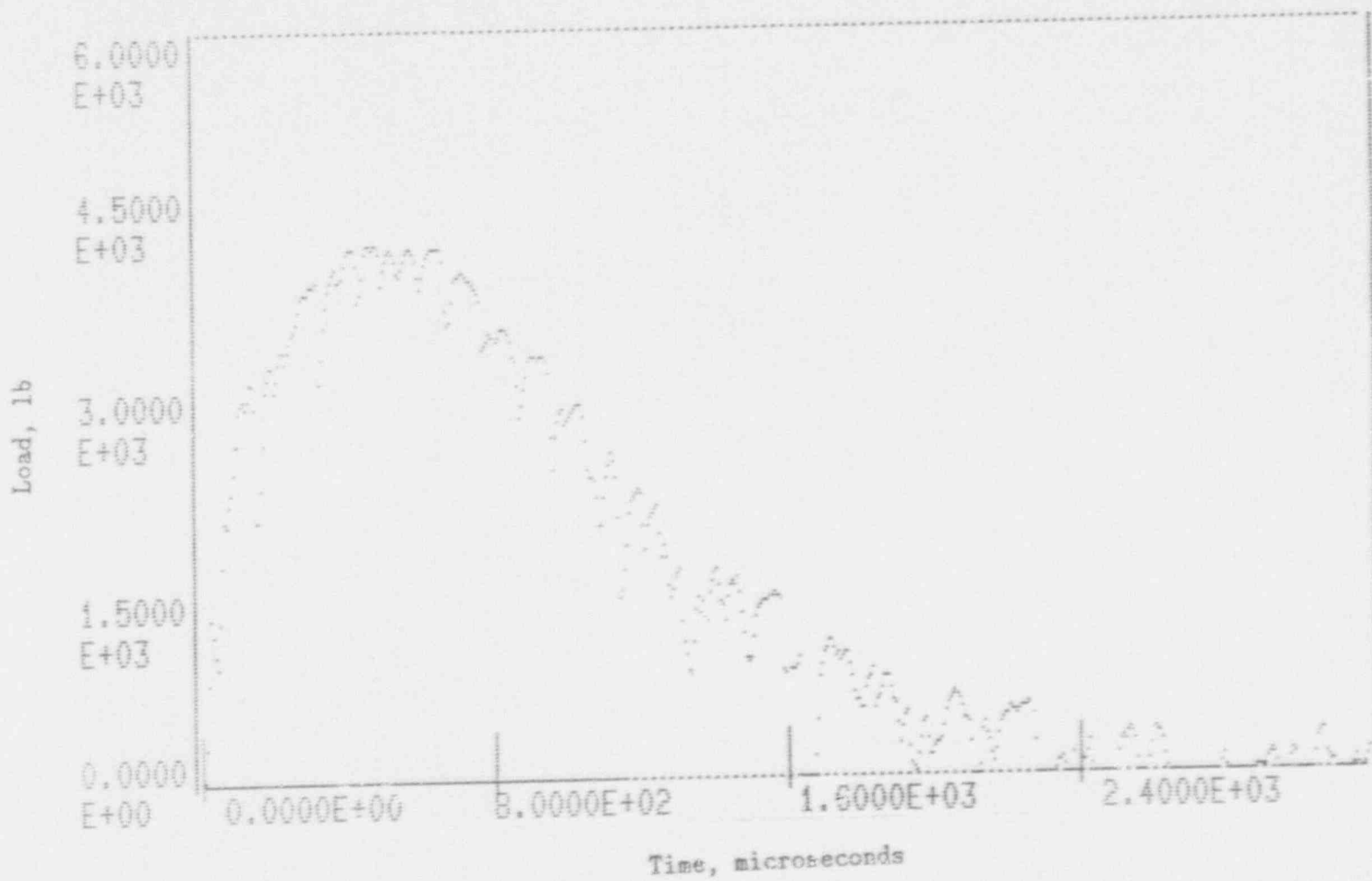


Figure A-30. Charpy impact test load-time record for Specimen BT4.

A-31

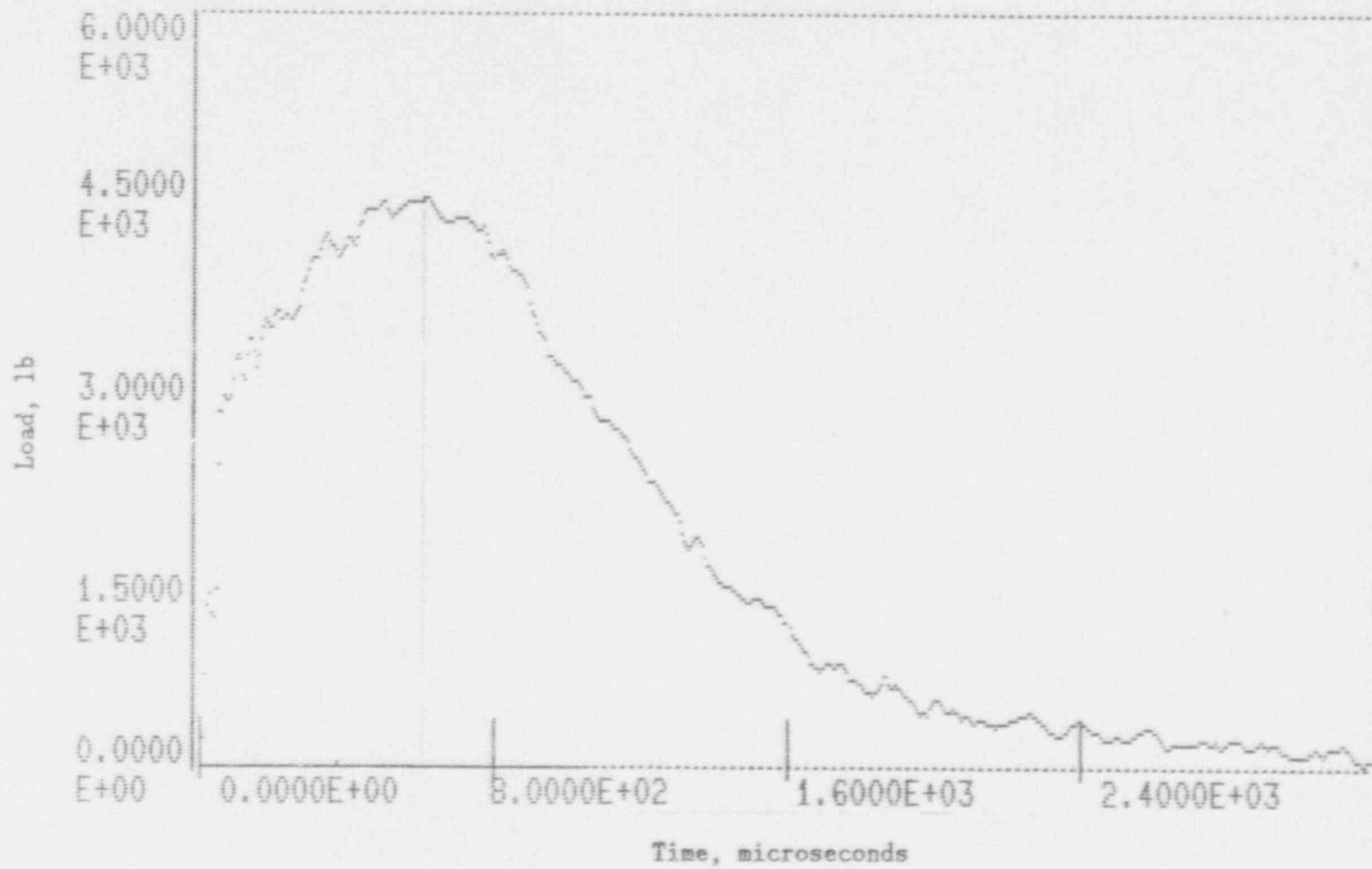


Figure A-31. Charpy impact test load-time record for Specimen BT15.

A-32

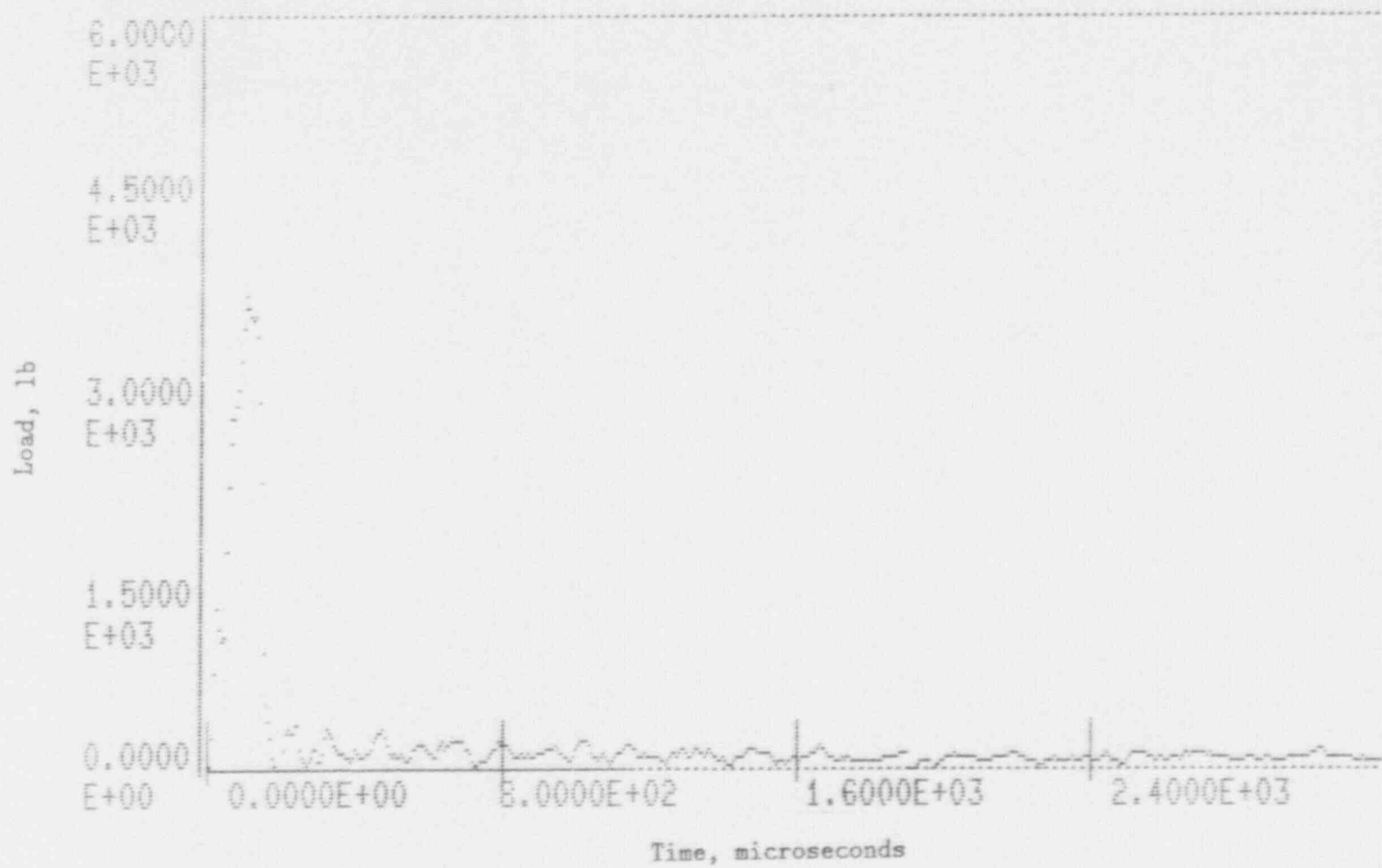


Figure A-32. Charpy impact test load-time record for Specimen BW2.

A-33

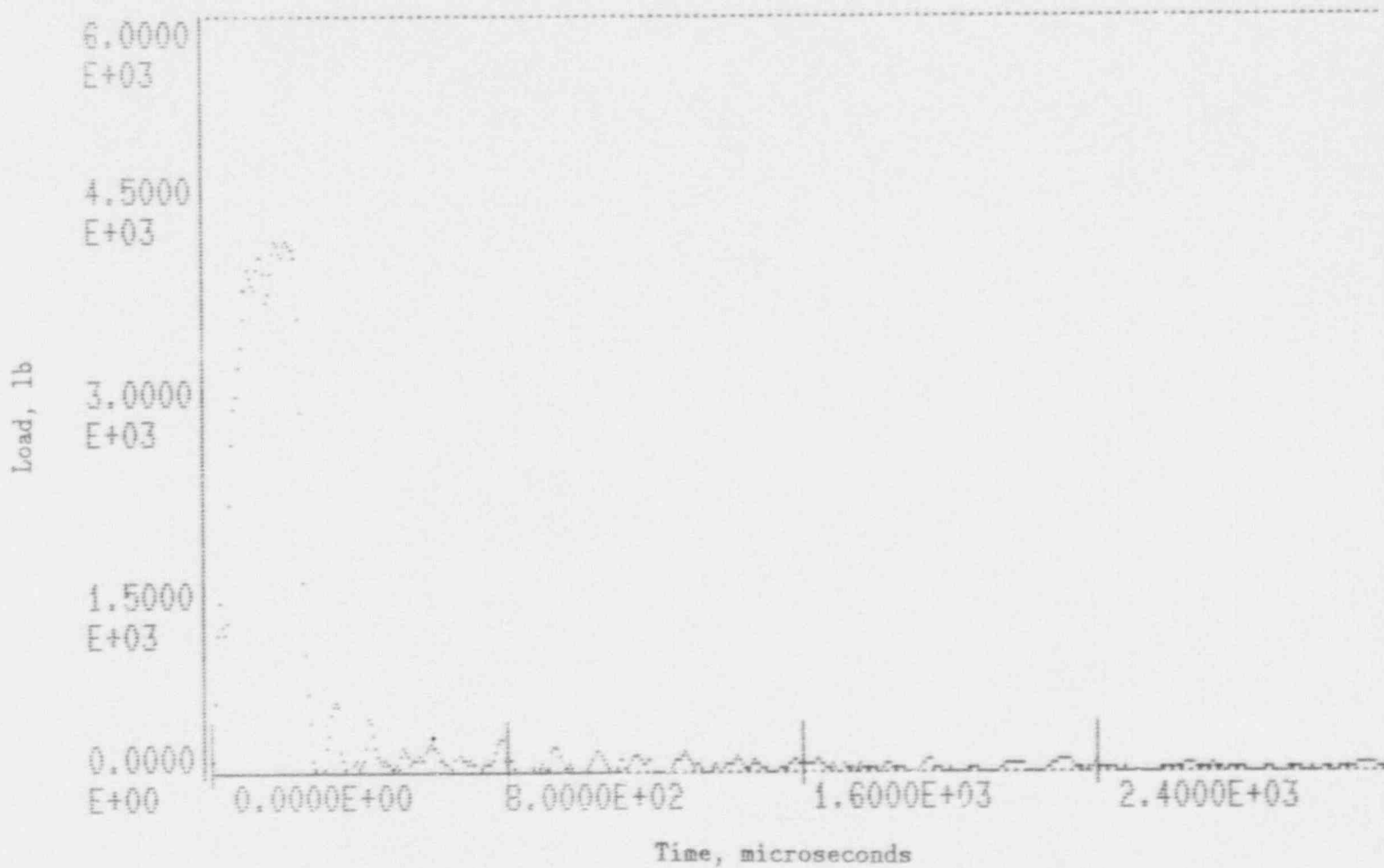


Figure A-33. Charpy impact test load-time record for Specimen BW1d.

A-34

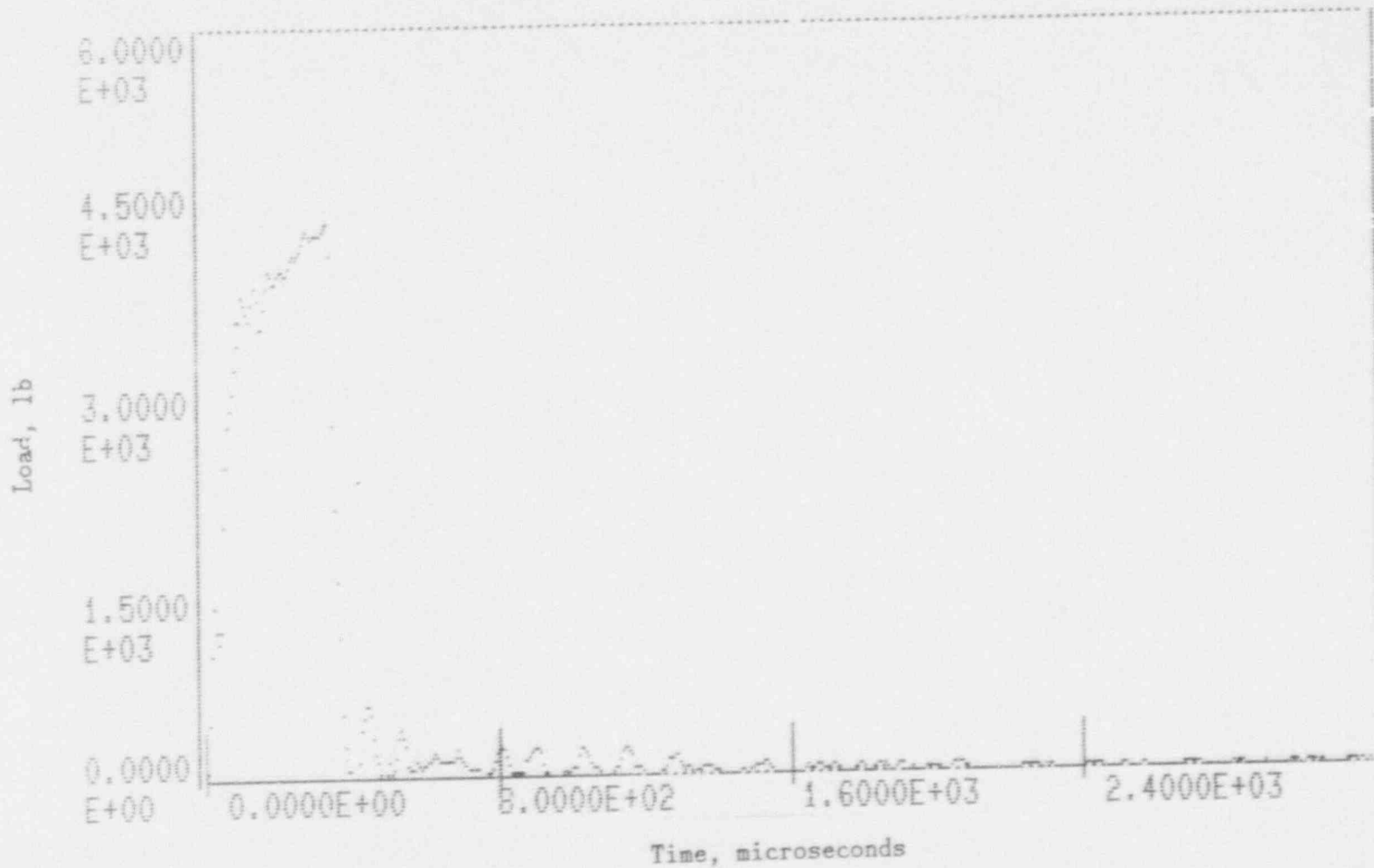


Figure A-34. Charpy impact test load-time record for Specimen BW11.

A-35

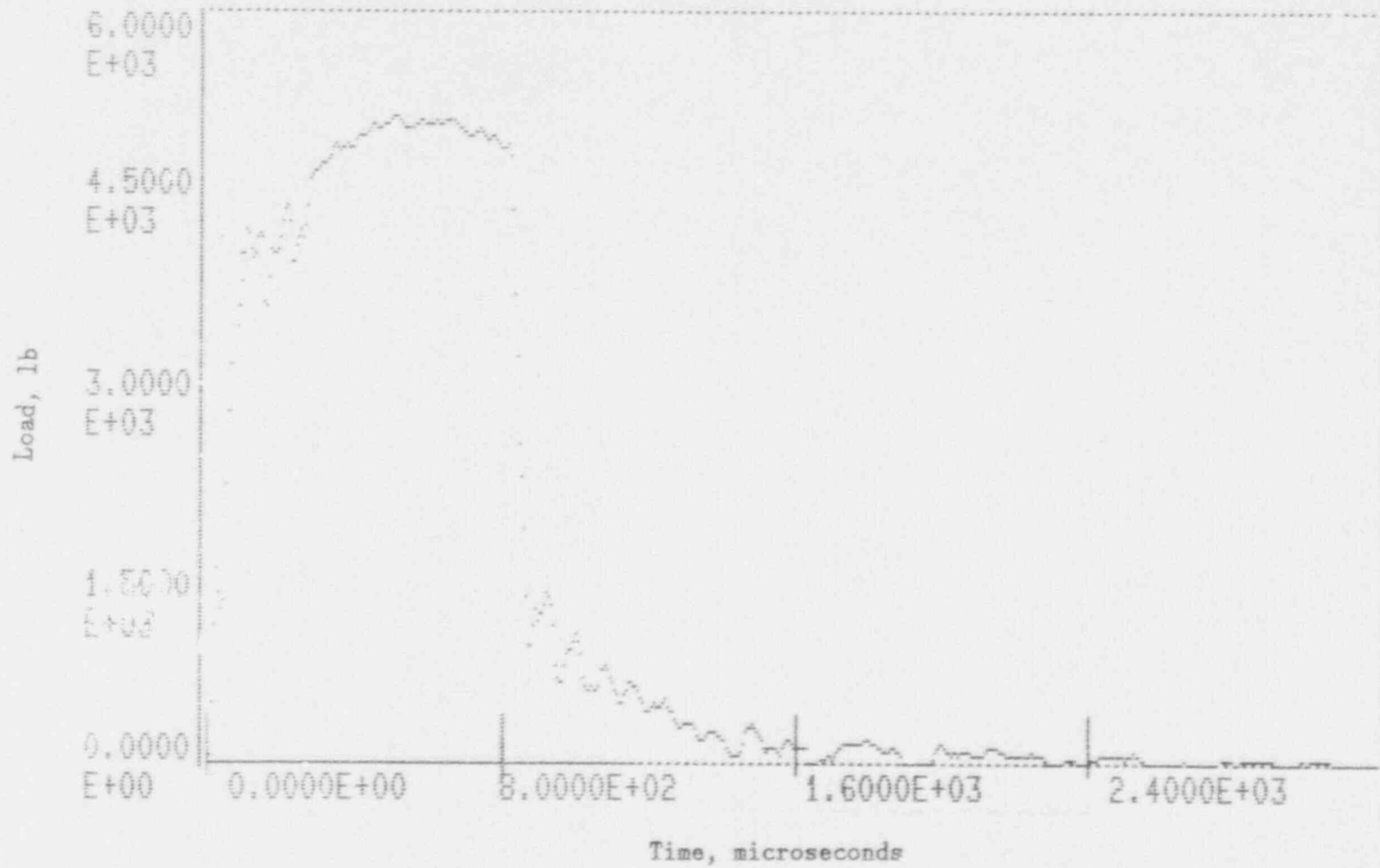


Figure A-35. Charpy impact test load-time record for Specimen BW9.

A-36

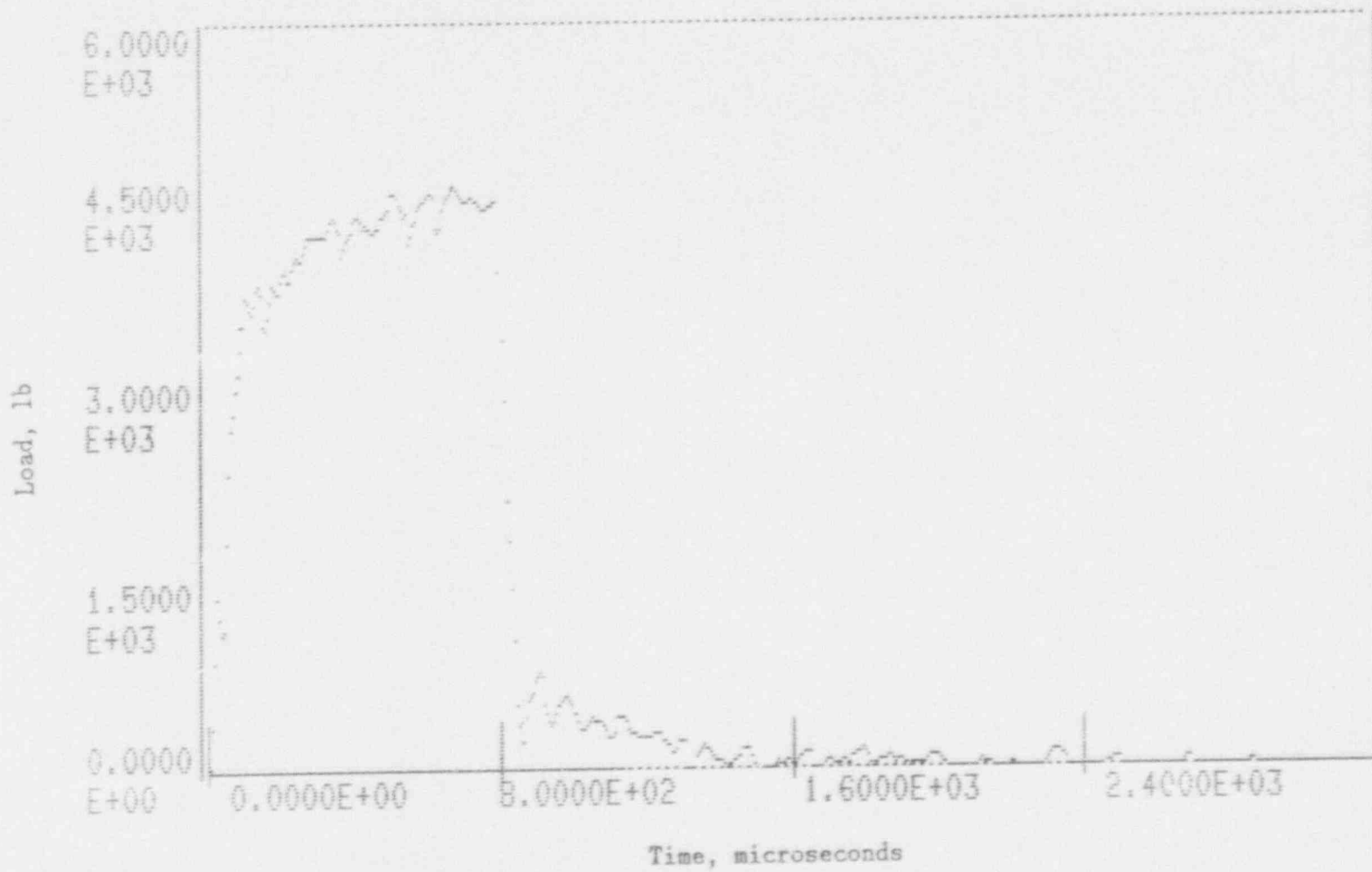


Figure A-36. Charpy impact test load-time record for Specimen BW12.

A-37

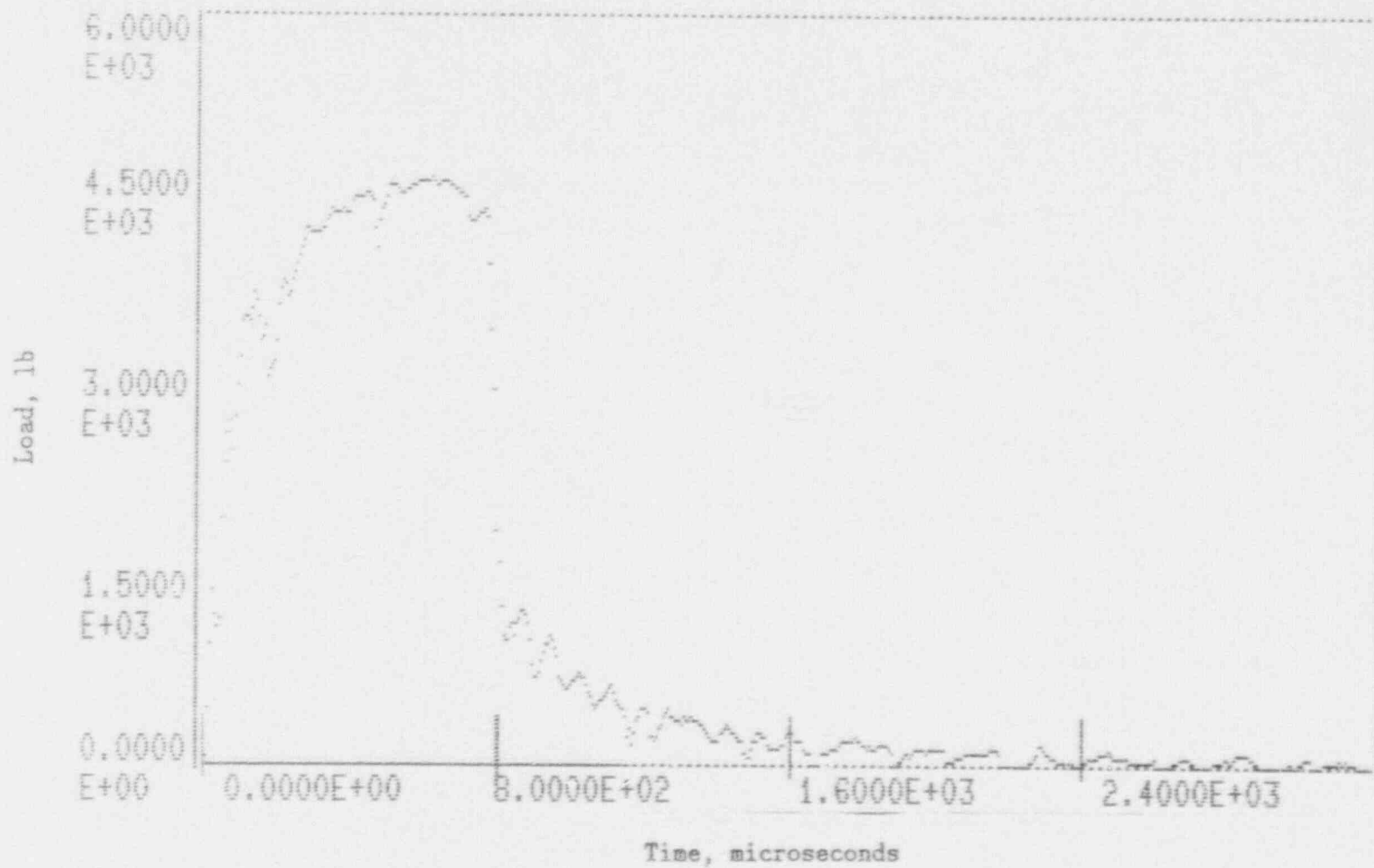


Figure A-37. Charpy impact test load-time record for Specimen BW8.

A-38

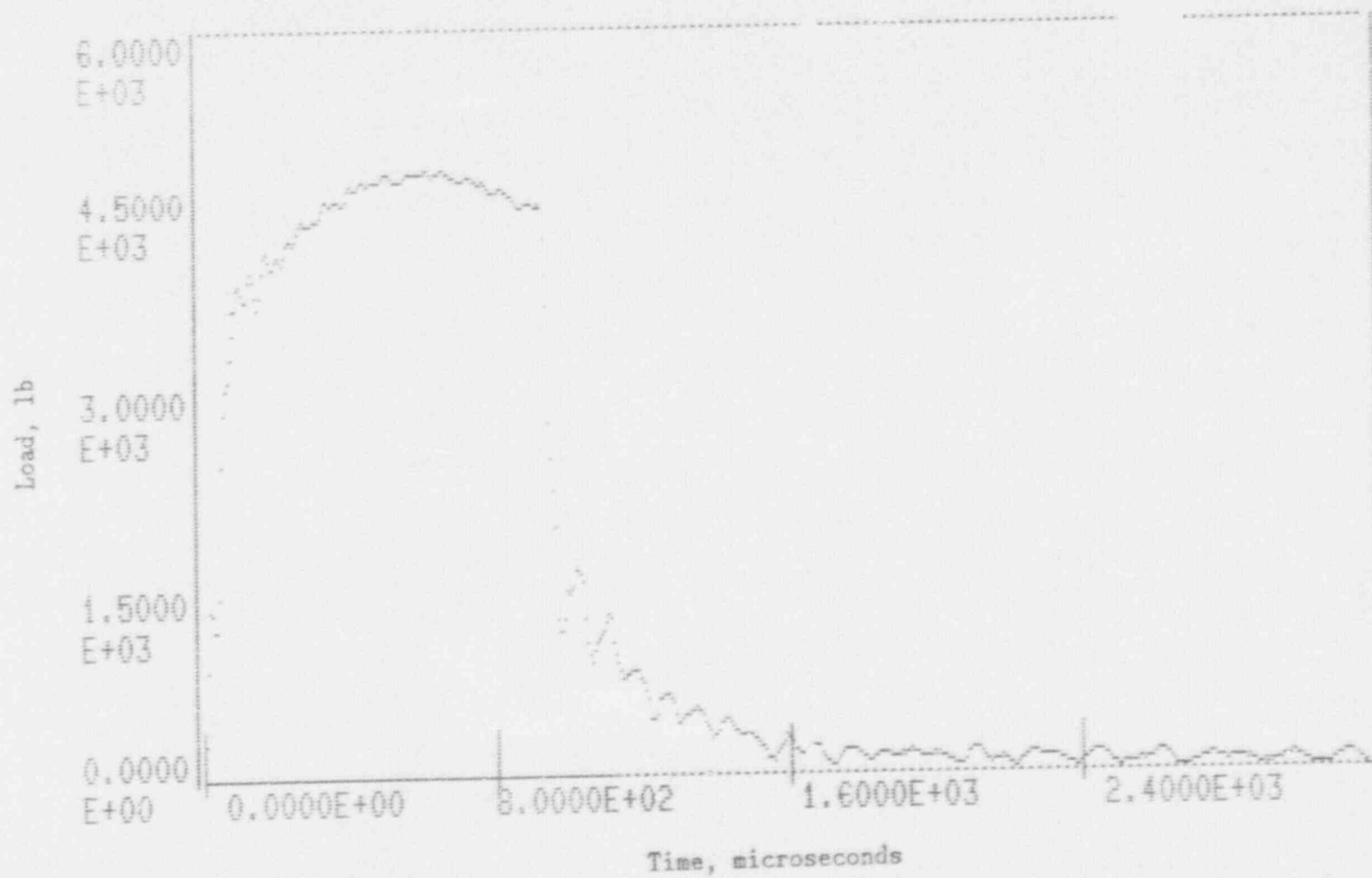


Figure A-38. Charpy impact test load-time record for Specimen BW3.

A-39

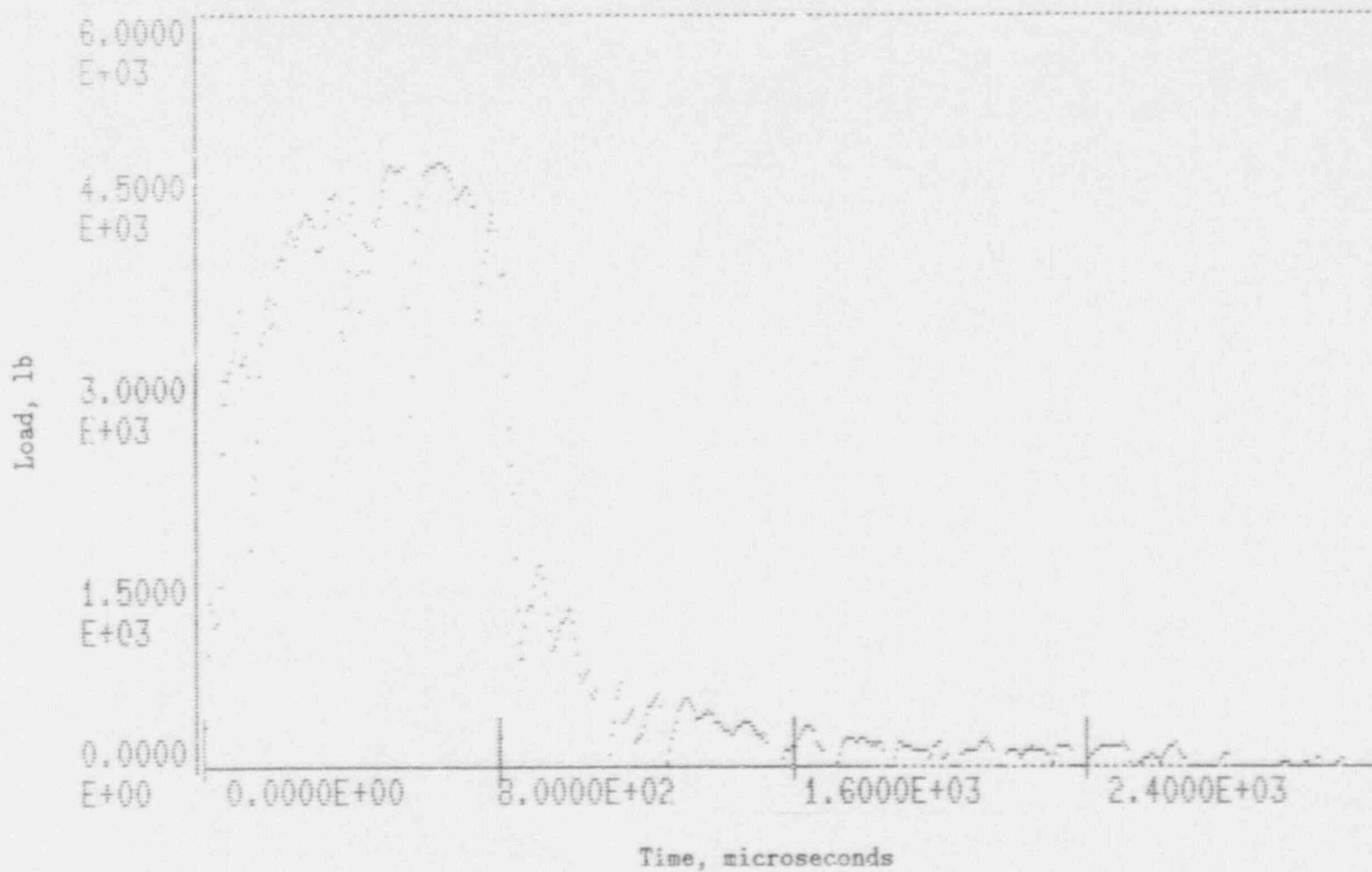


Figure A-39. Charpy impact test load-time record for Specimen BW15.

A-40

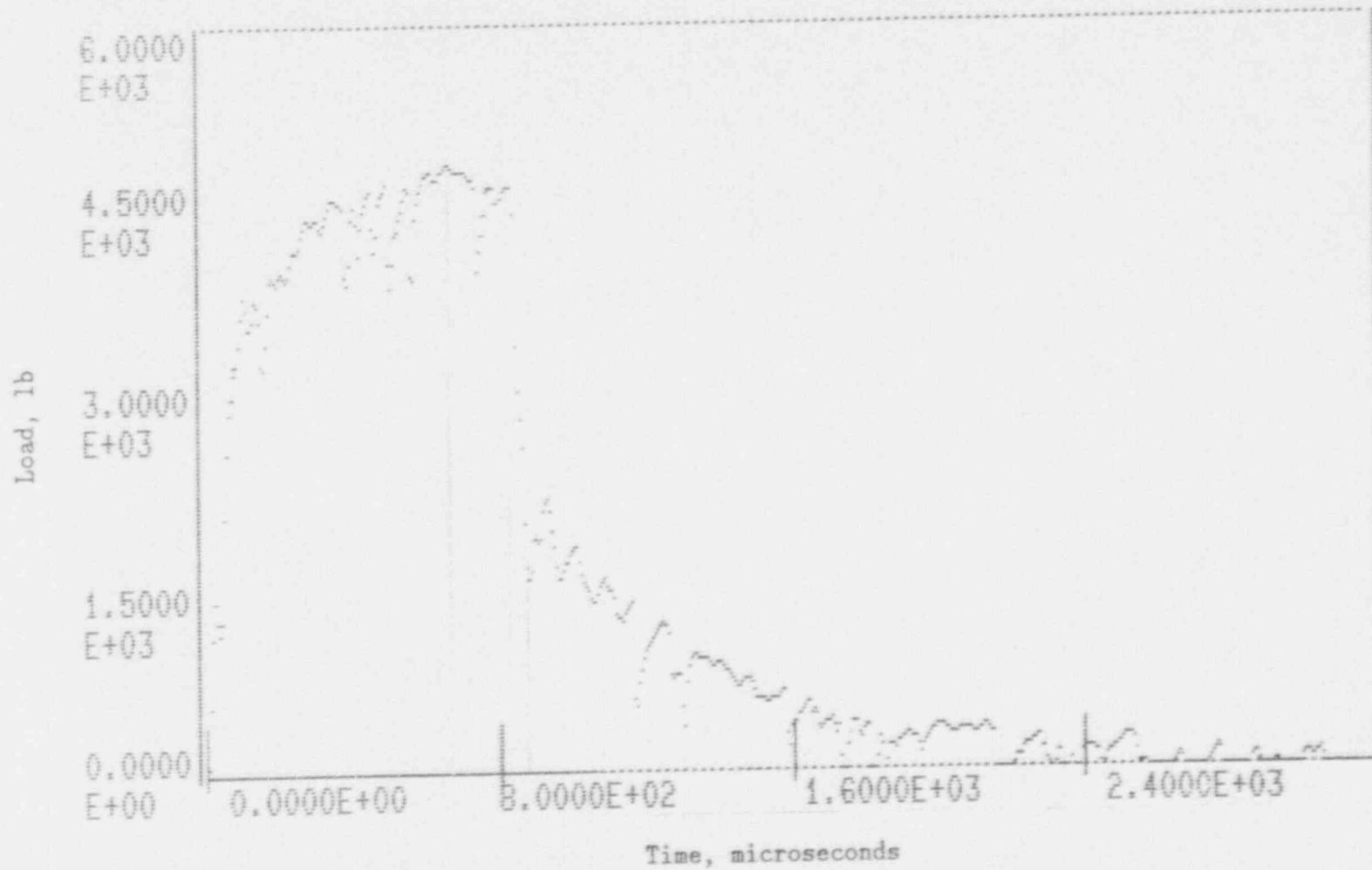


Figure A-40. Charpy impact test load-time record for Specimen BW7.

A-41

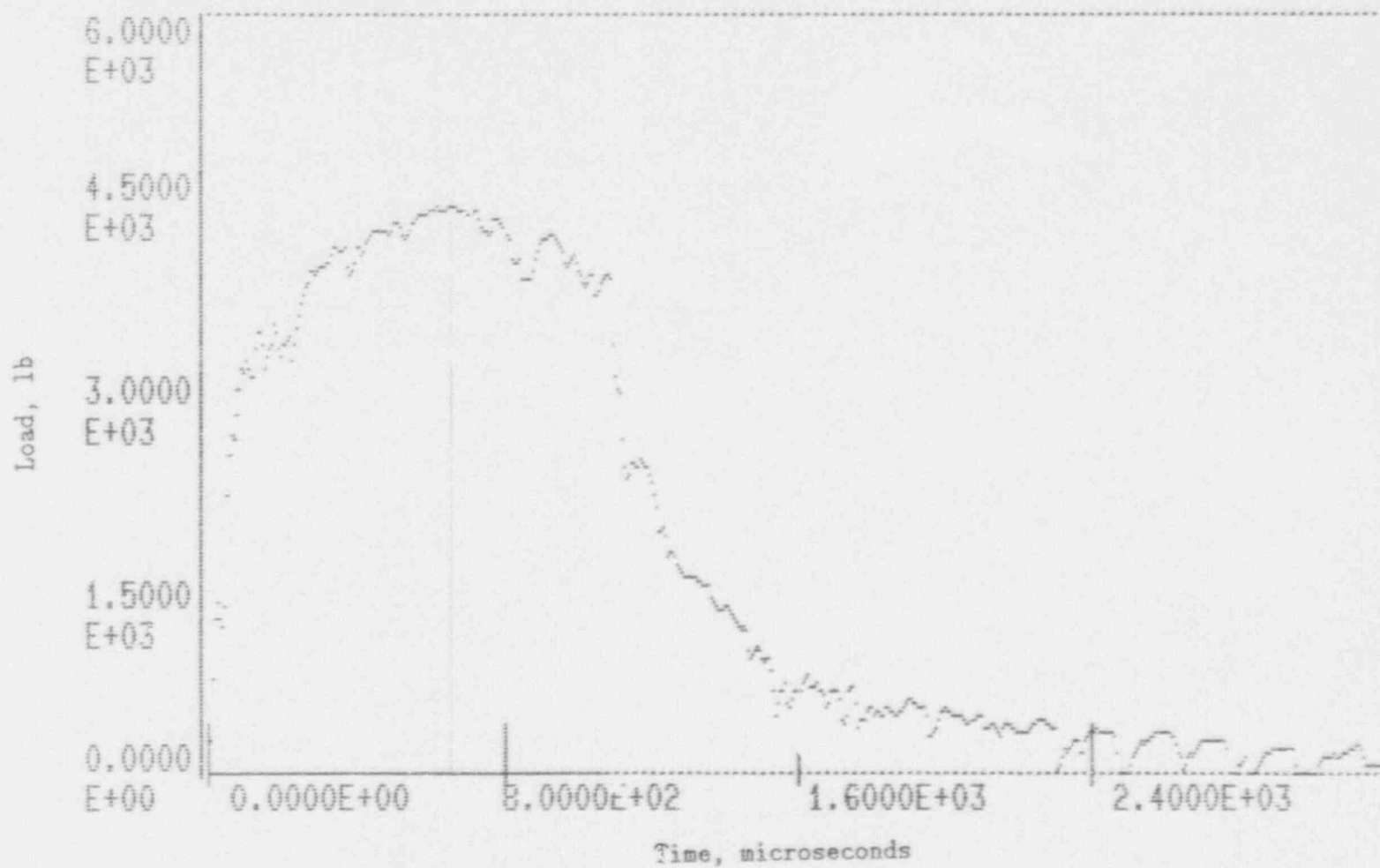


Figure A-41. Charpy impact test load-time record for Specimen BW1.

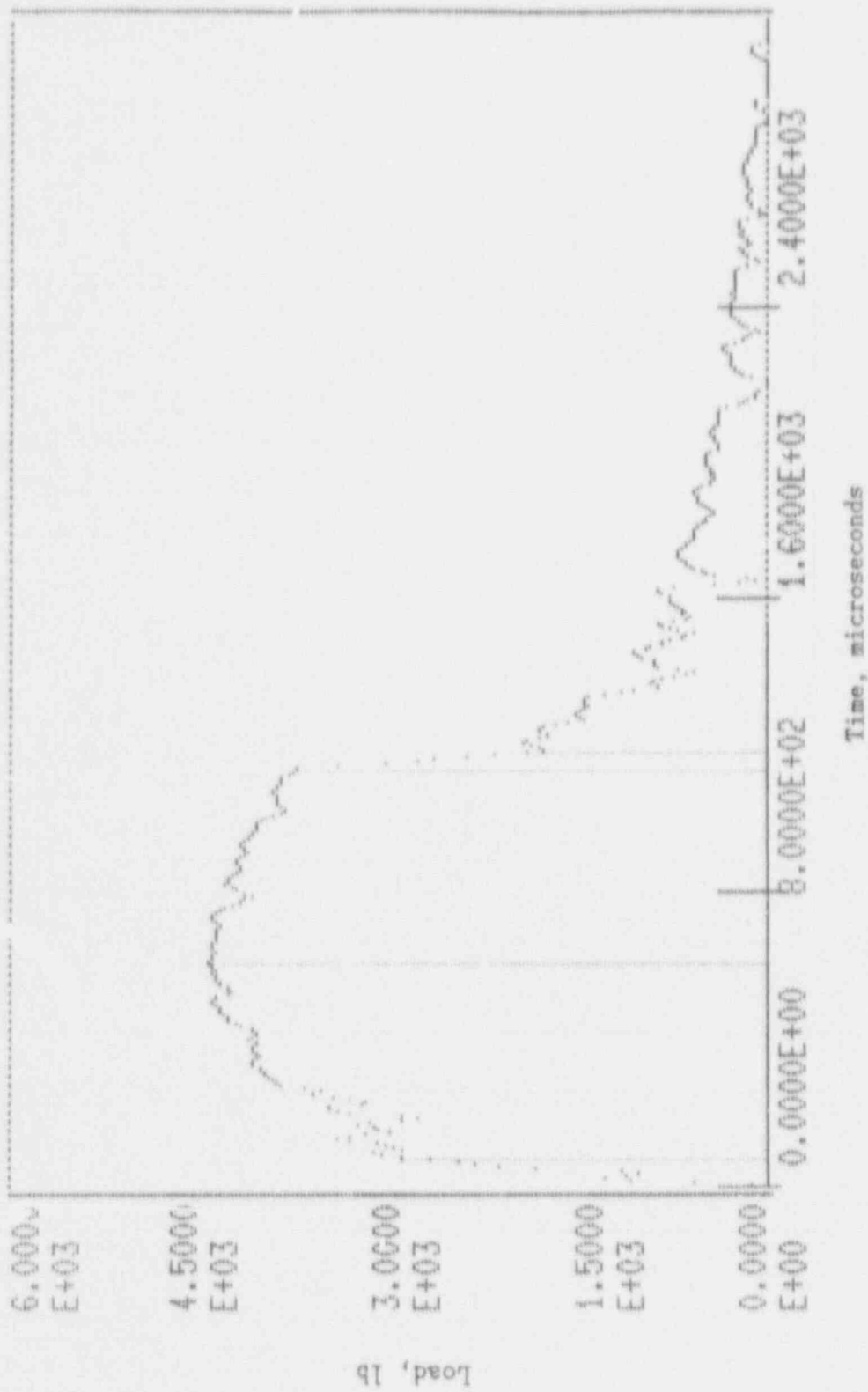


Figure A-41. Charpy impact test load-time record for Specimen BW5.

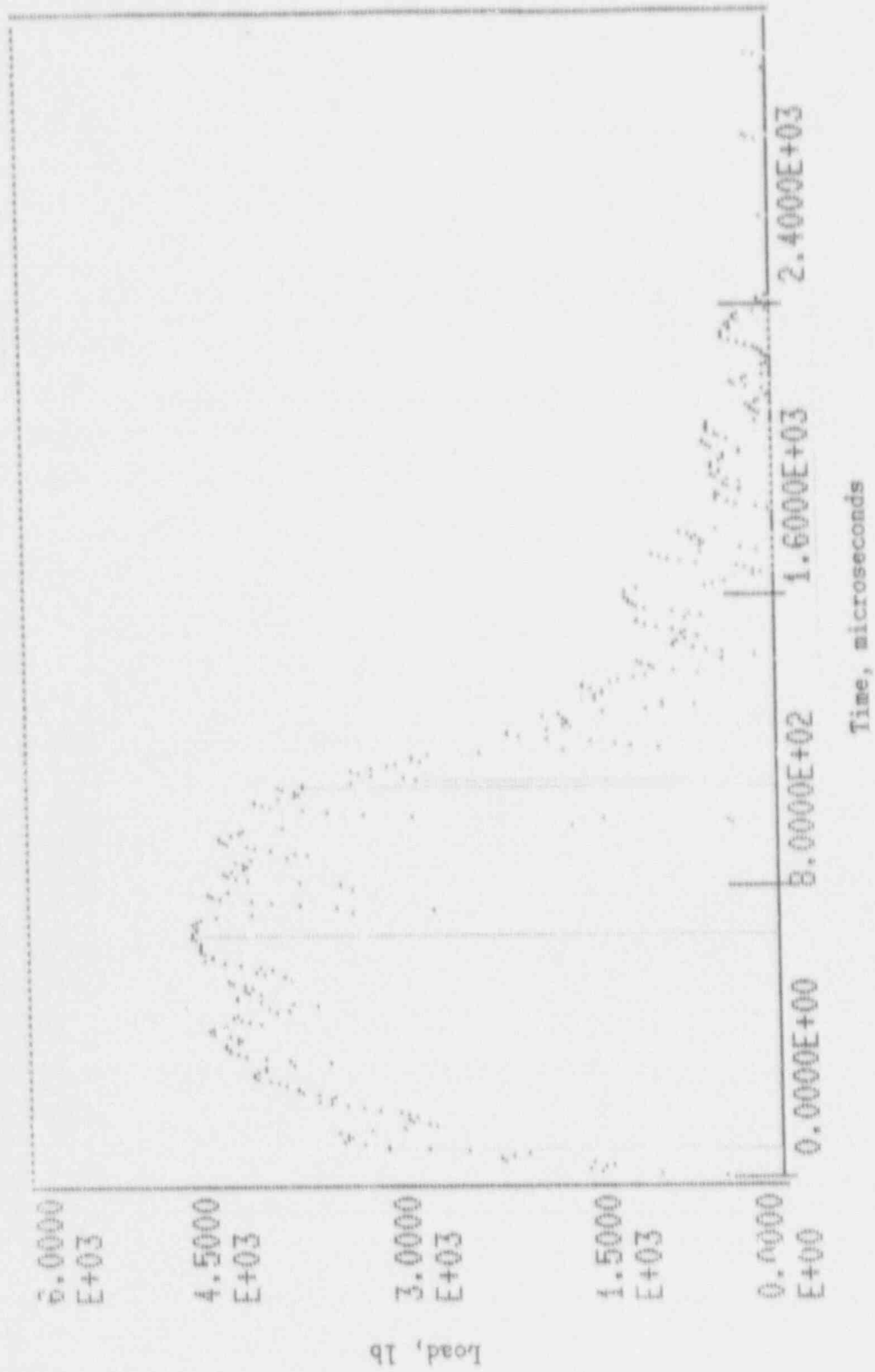


Figure A-43. Charpy impact test load-time record for Specimen BW4.

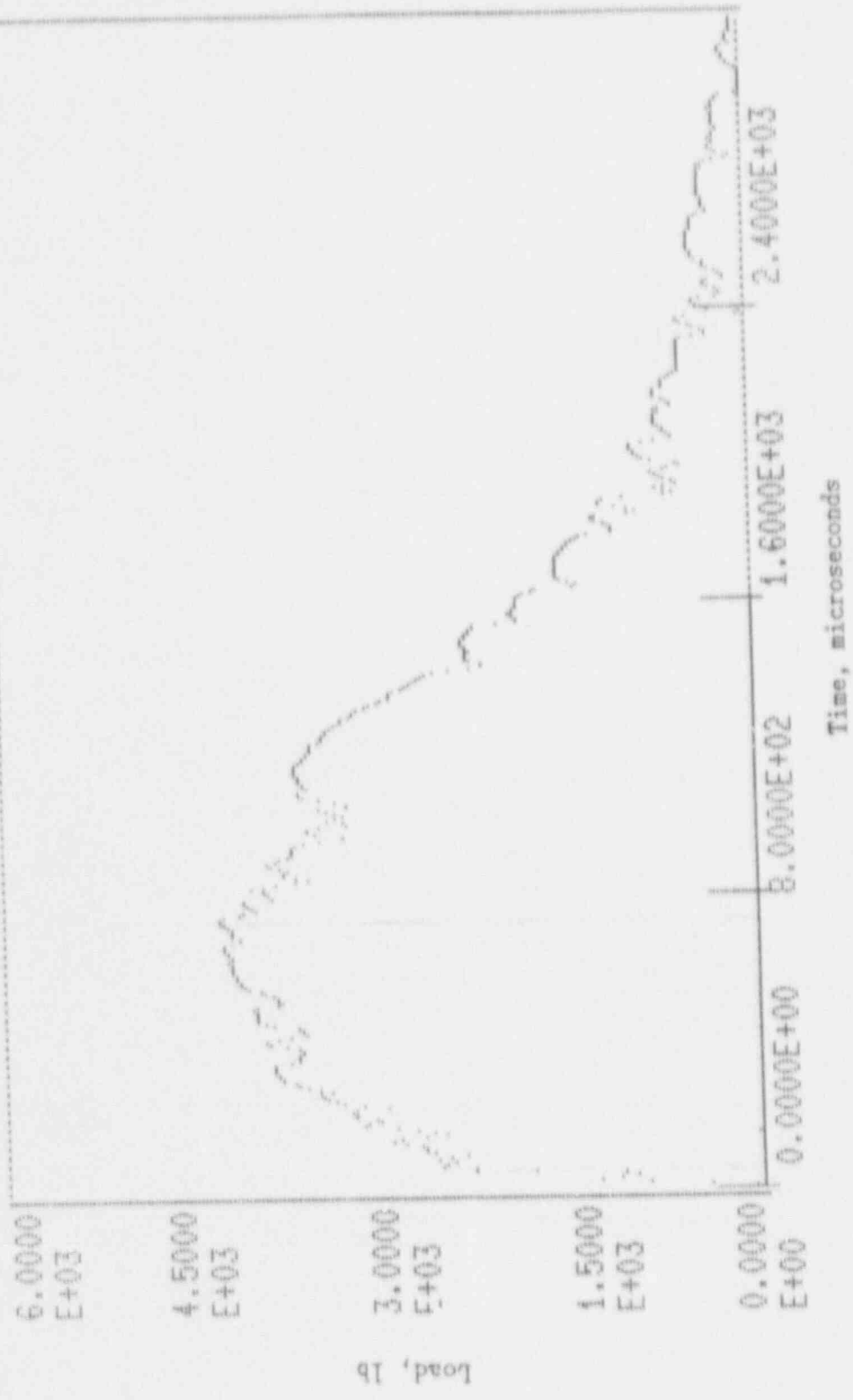


Figure A-44. Charpy impact test load-time record for Specimen EW10.

A-45

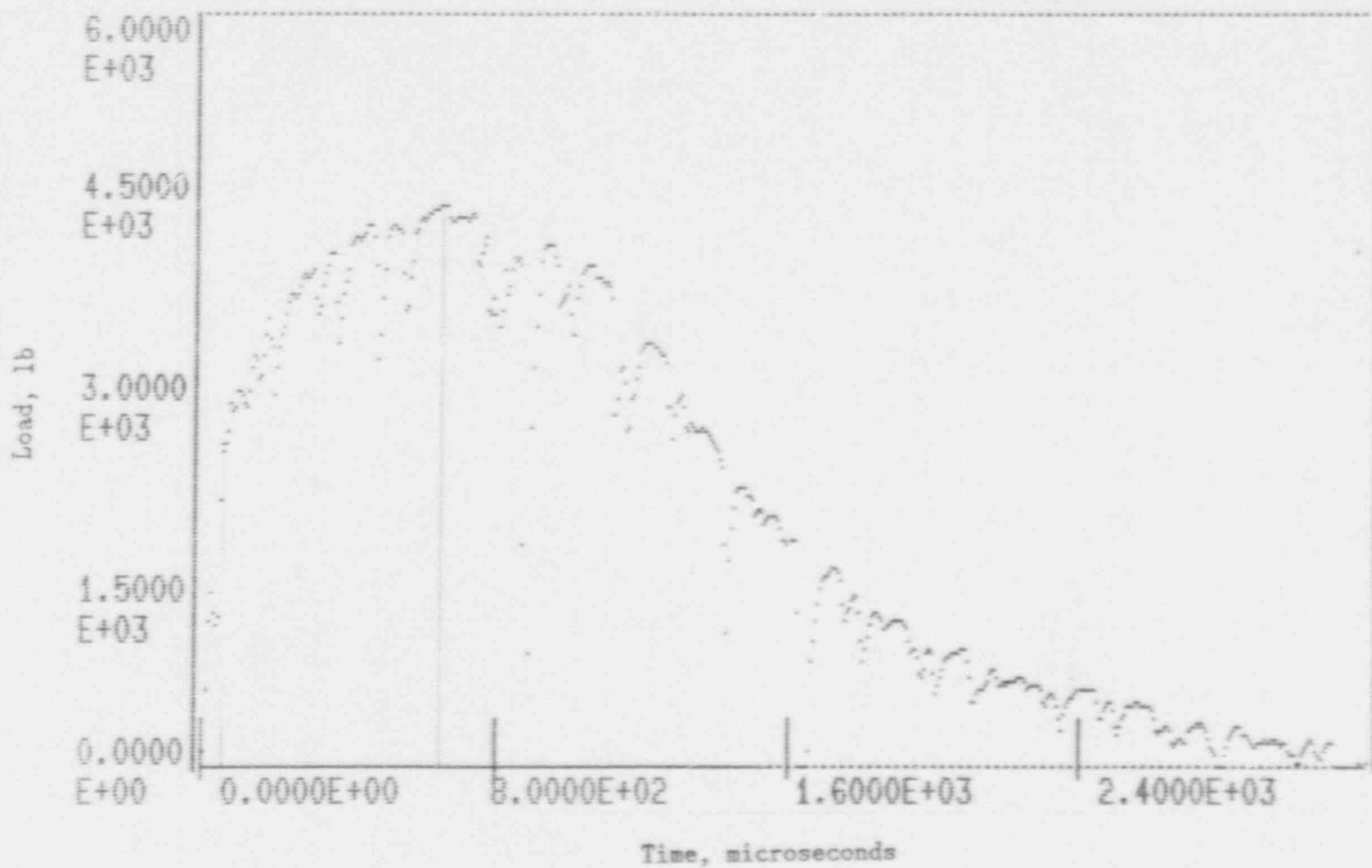


Figure A-45. Charpy impact test load-time record for Specimen BW13.

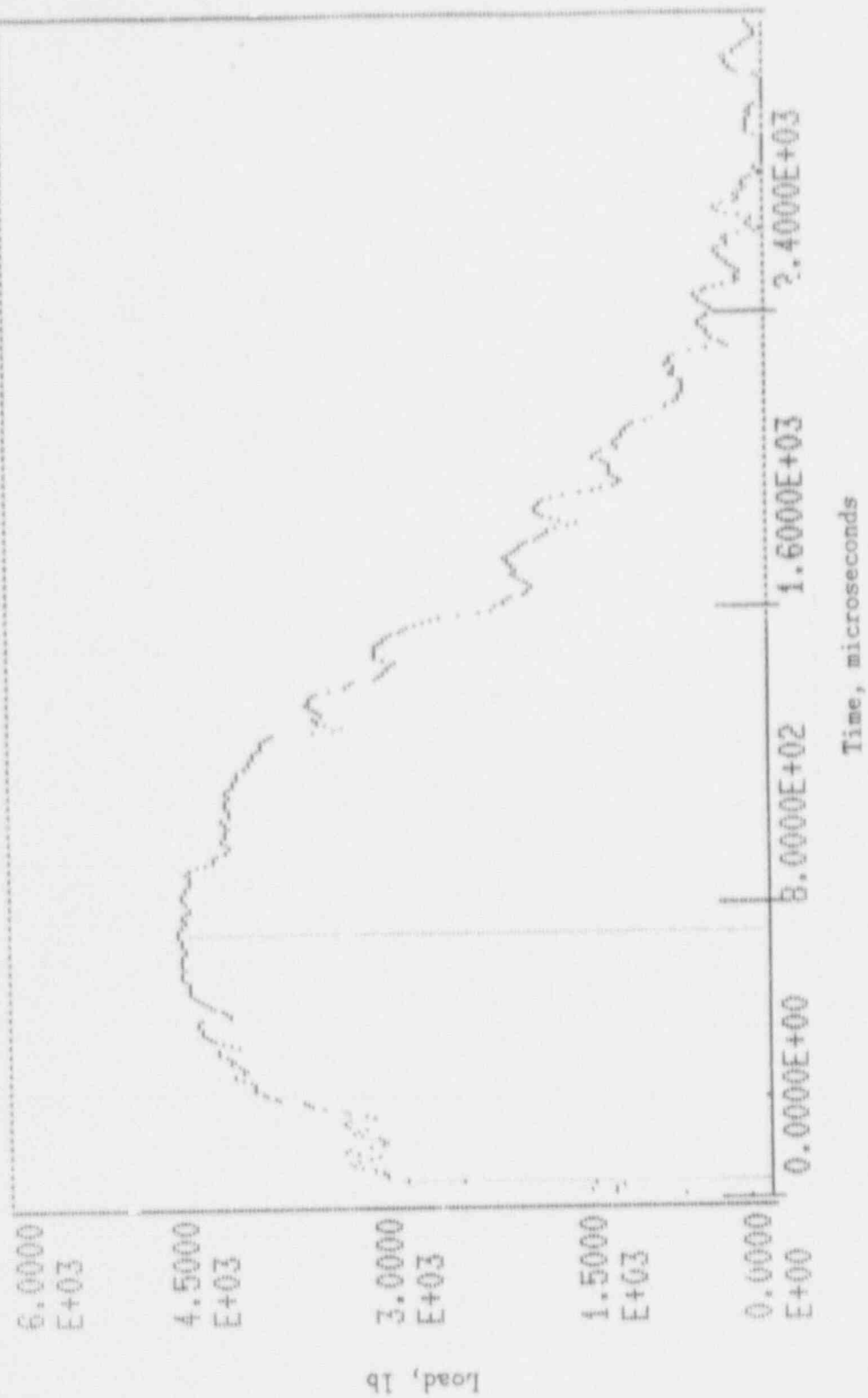


Figure A-46. Charpy impact test load-time record for Specimen BW6.

A-47

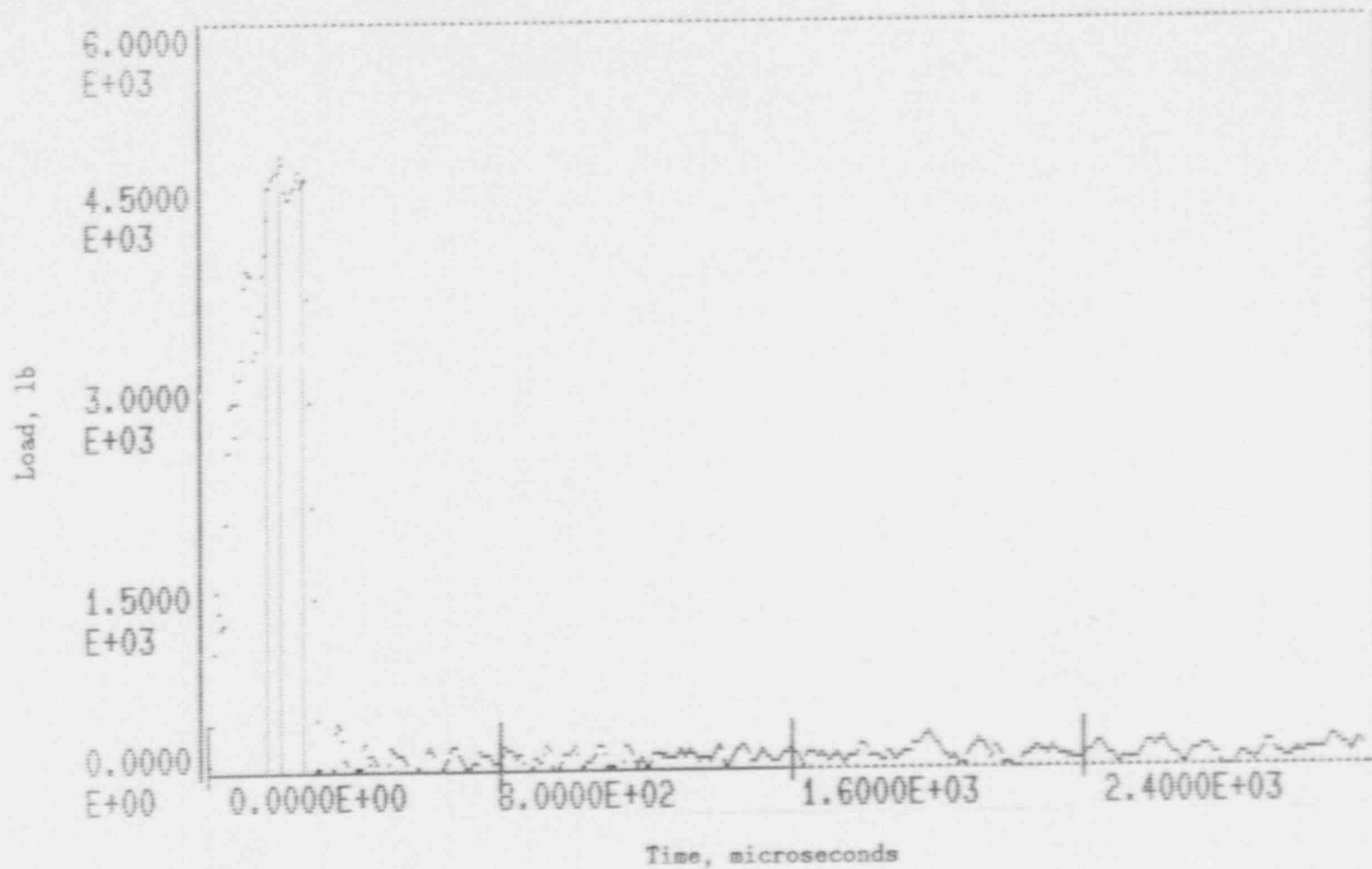


Figure A-47. Charpy impact test load-time record for Specimen BH9.

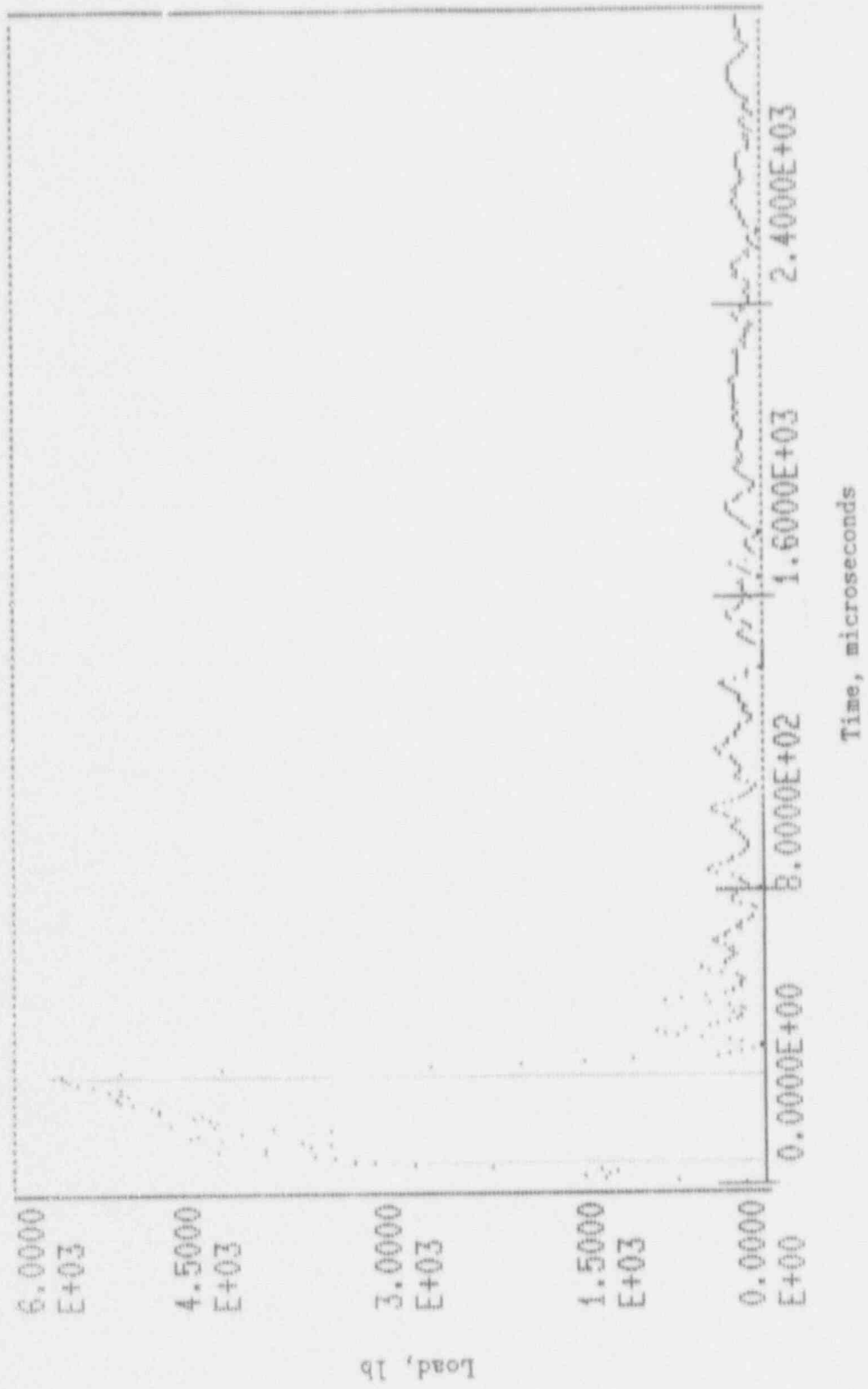


Figure A-48. Charpy impact test load-time record for Specimen BE3.

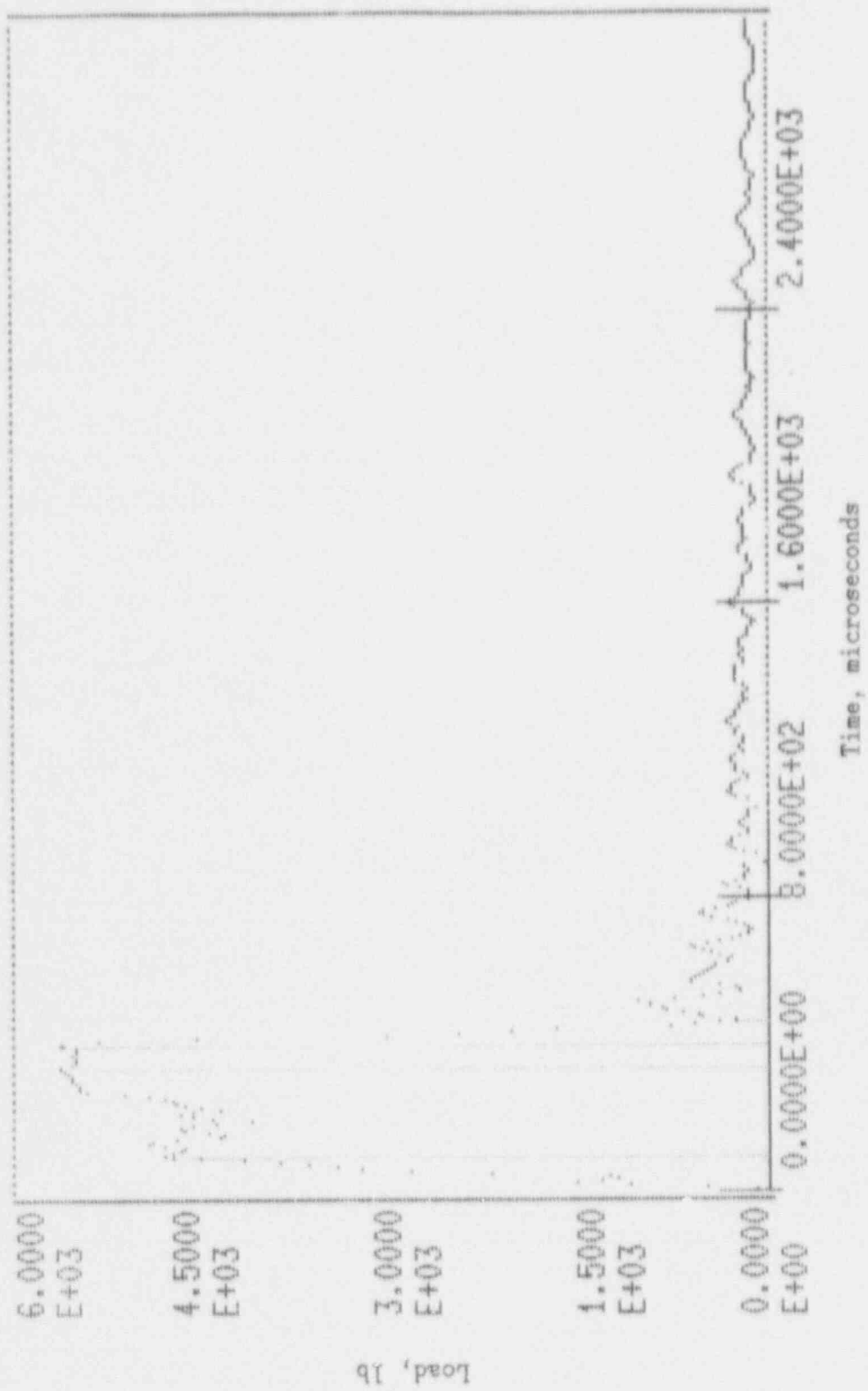


Figure A-49. Charpy impact test load-time record for Specimen BHS.

**COMPUTER MALFUNCTION - NO LOAD TIME RECORD**

**(Data memory drop-out)**

A-50

Figure A-50. Charpy impact test load-time record for Specimen BH15.

A-51

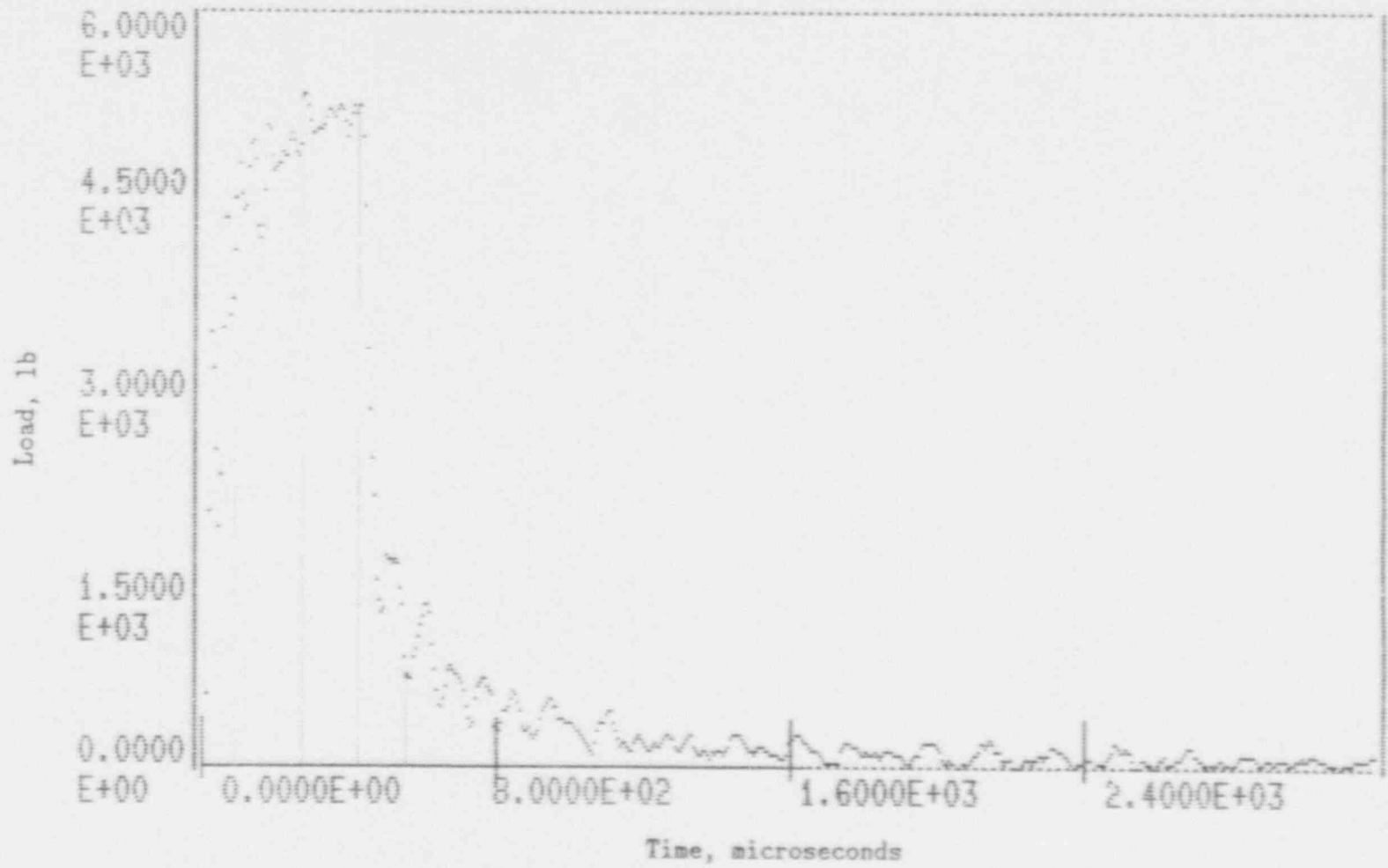


Figure A-51. Charpy impact test load-time record for Specimen BH1.

A-52

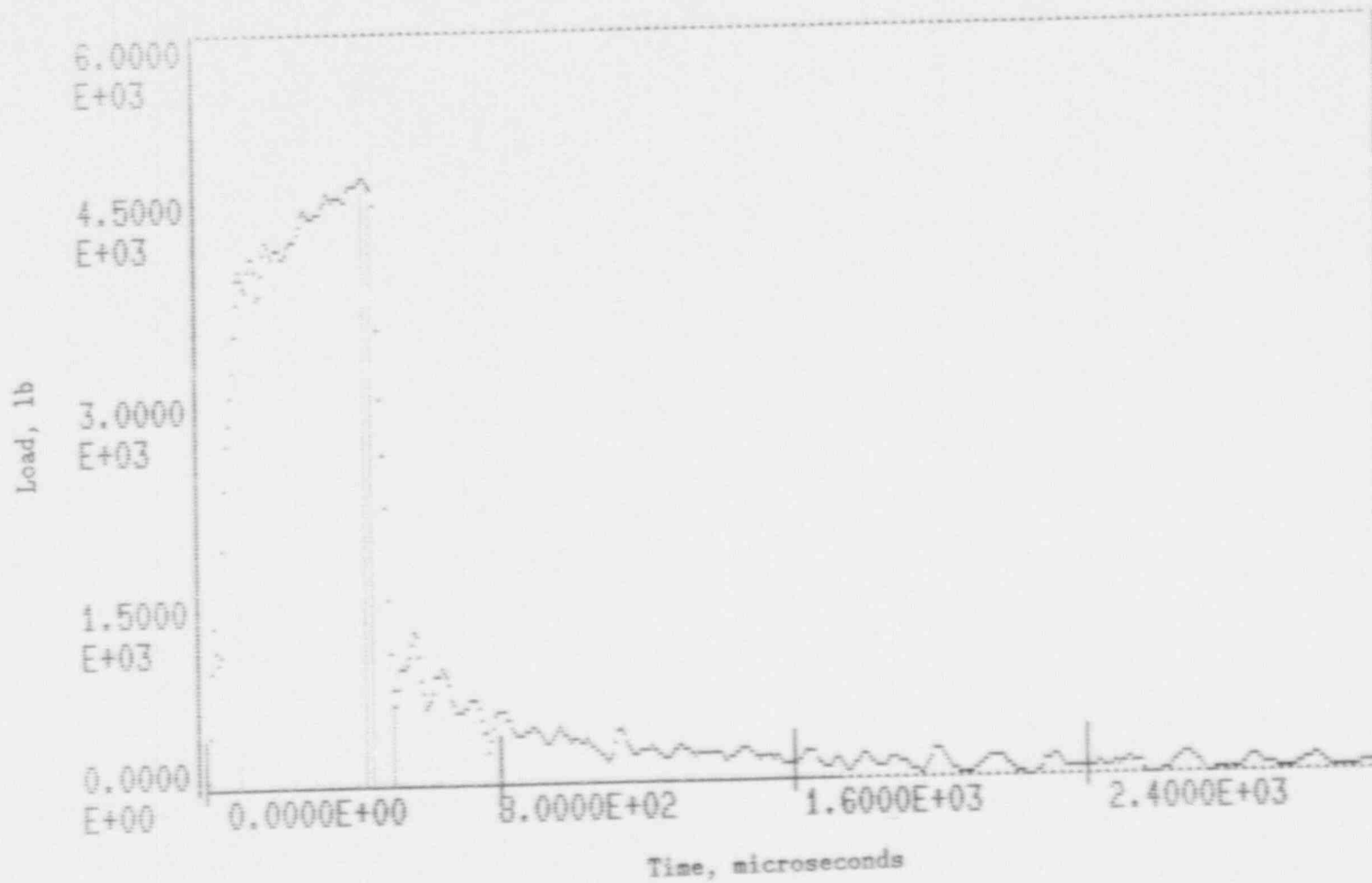


Figure A-52. Charpy impact test load-time record for Specimen BH6.

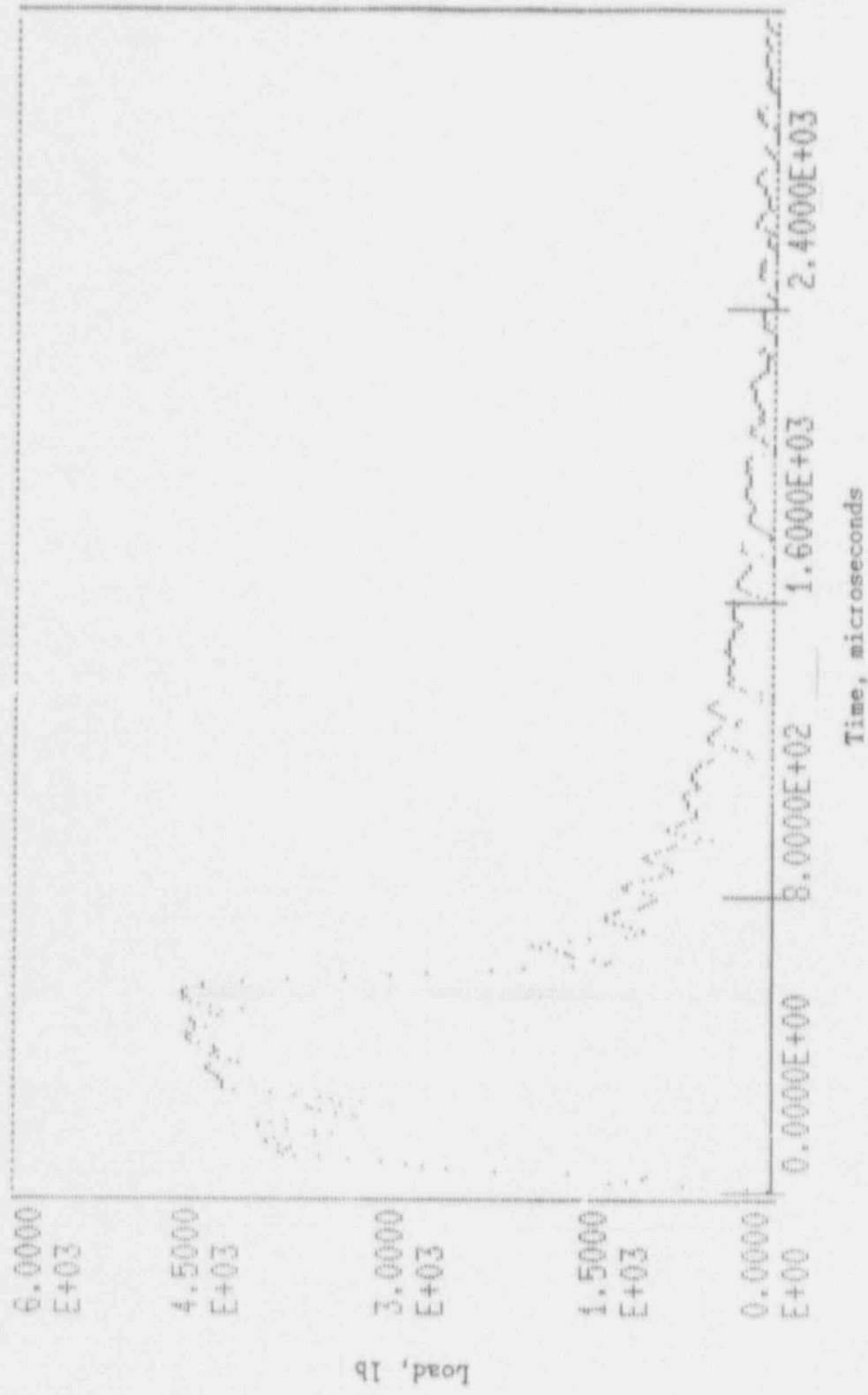


Figure A-53. Charpy impact test load-time record for Specimen BH2.

A-54

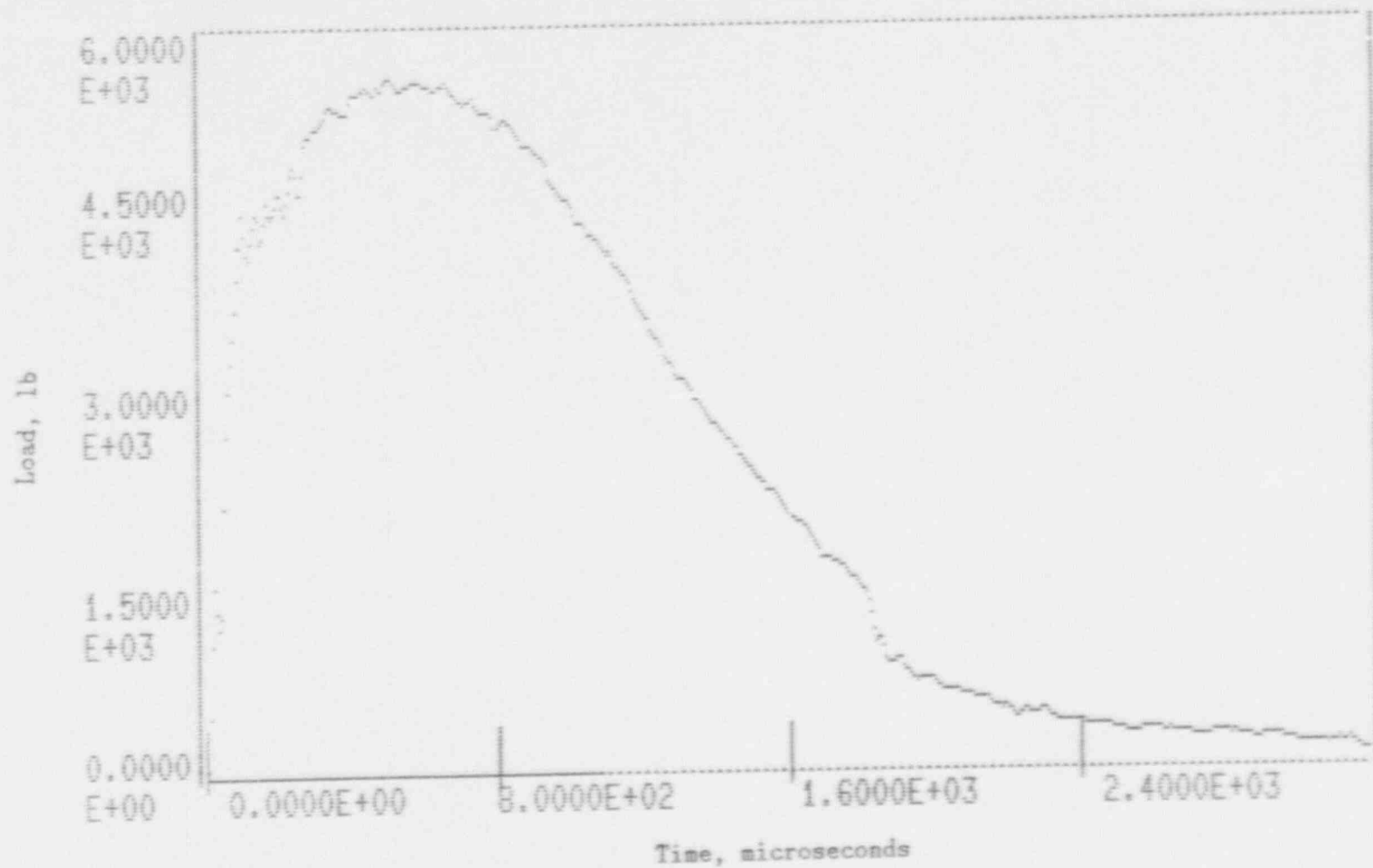


Figure A-54. Charpy impact test load-time record for Specimen BH13.

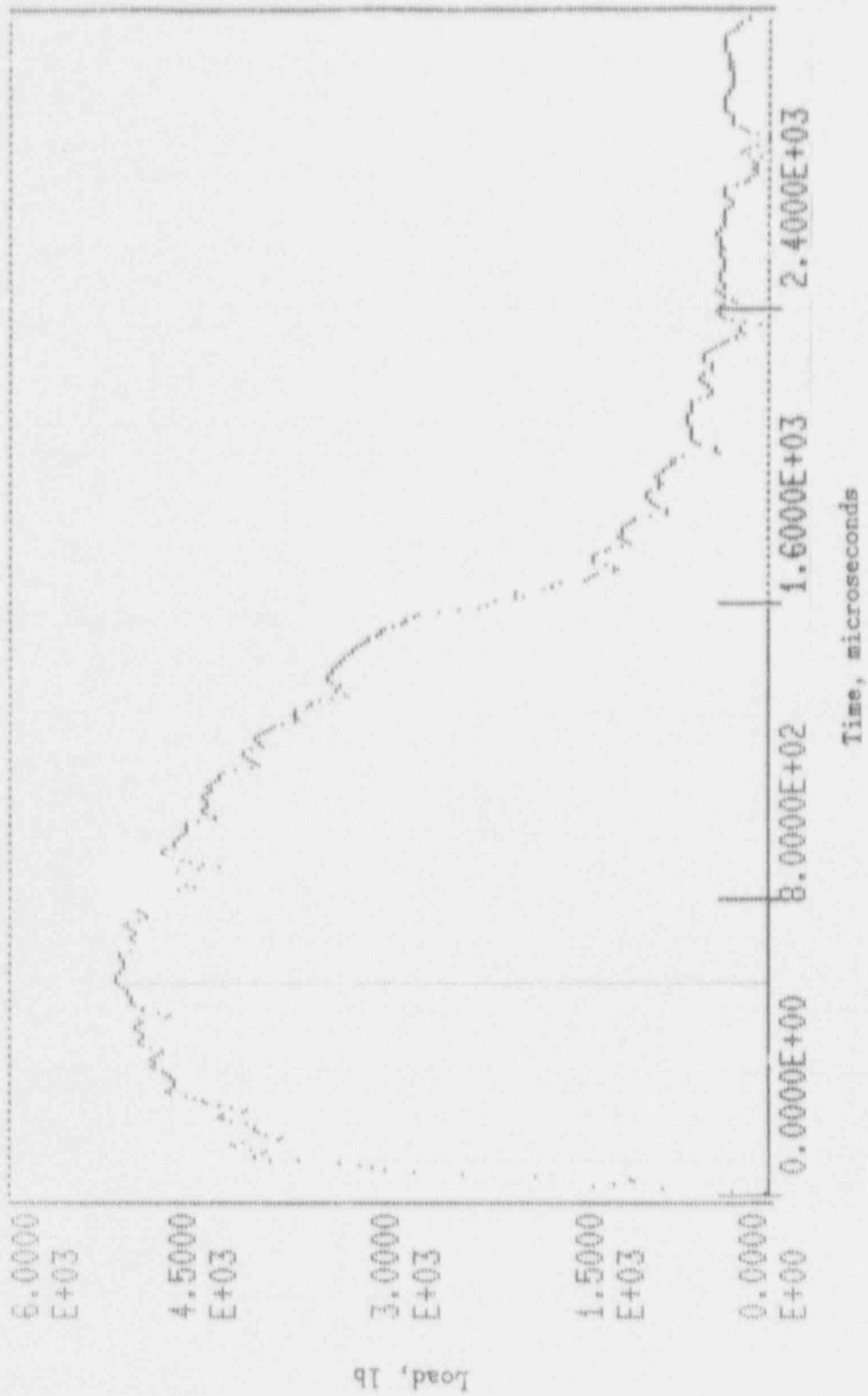


Figure A-55. Charpy impact test load-time record for Specimen BH12.

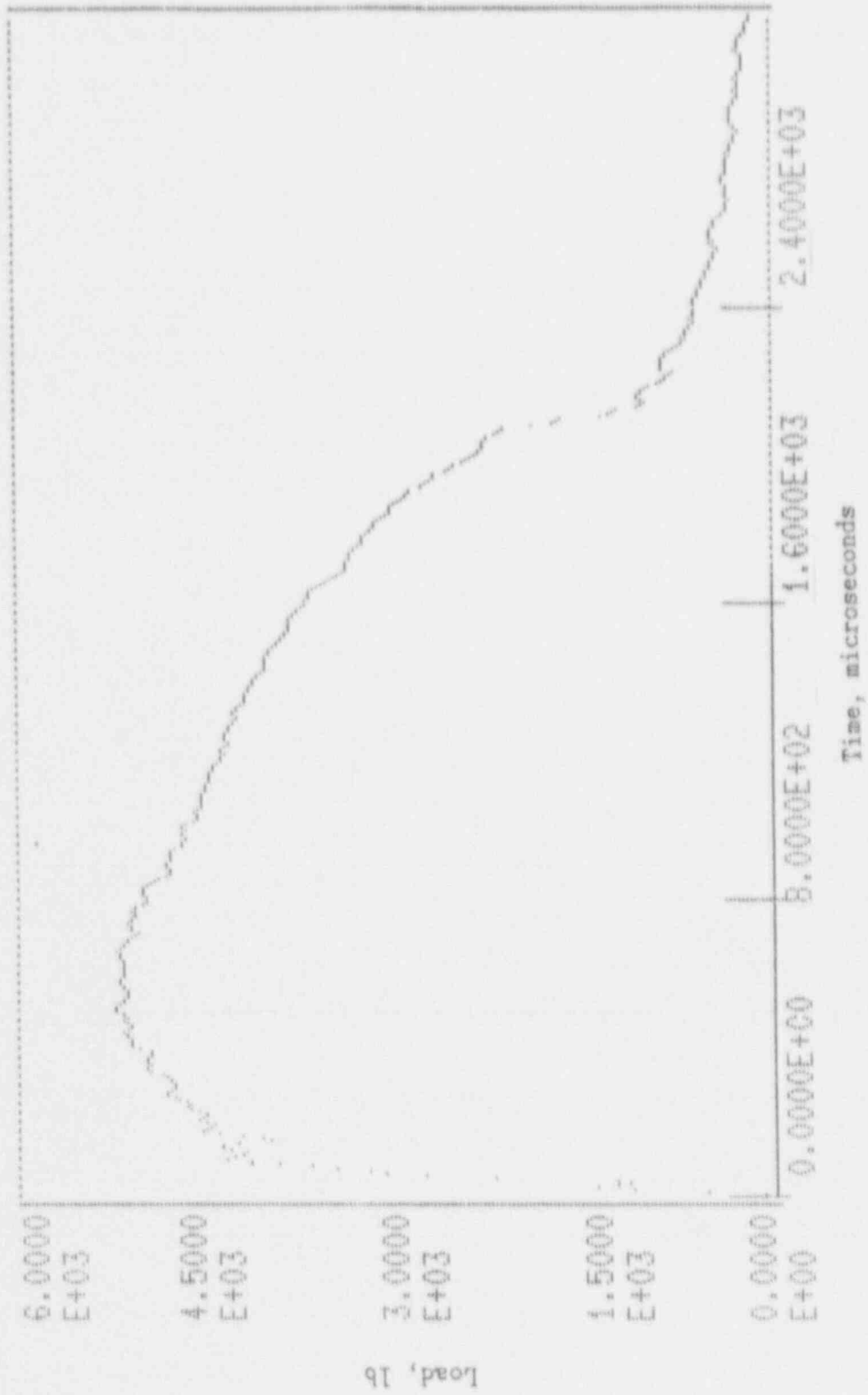


Figure A-56. Charpy impact test load-time record for Specimen BH10.

A-57

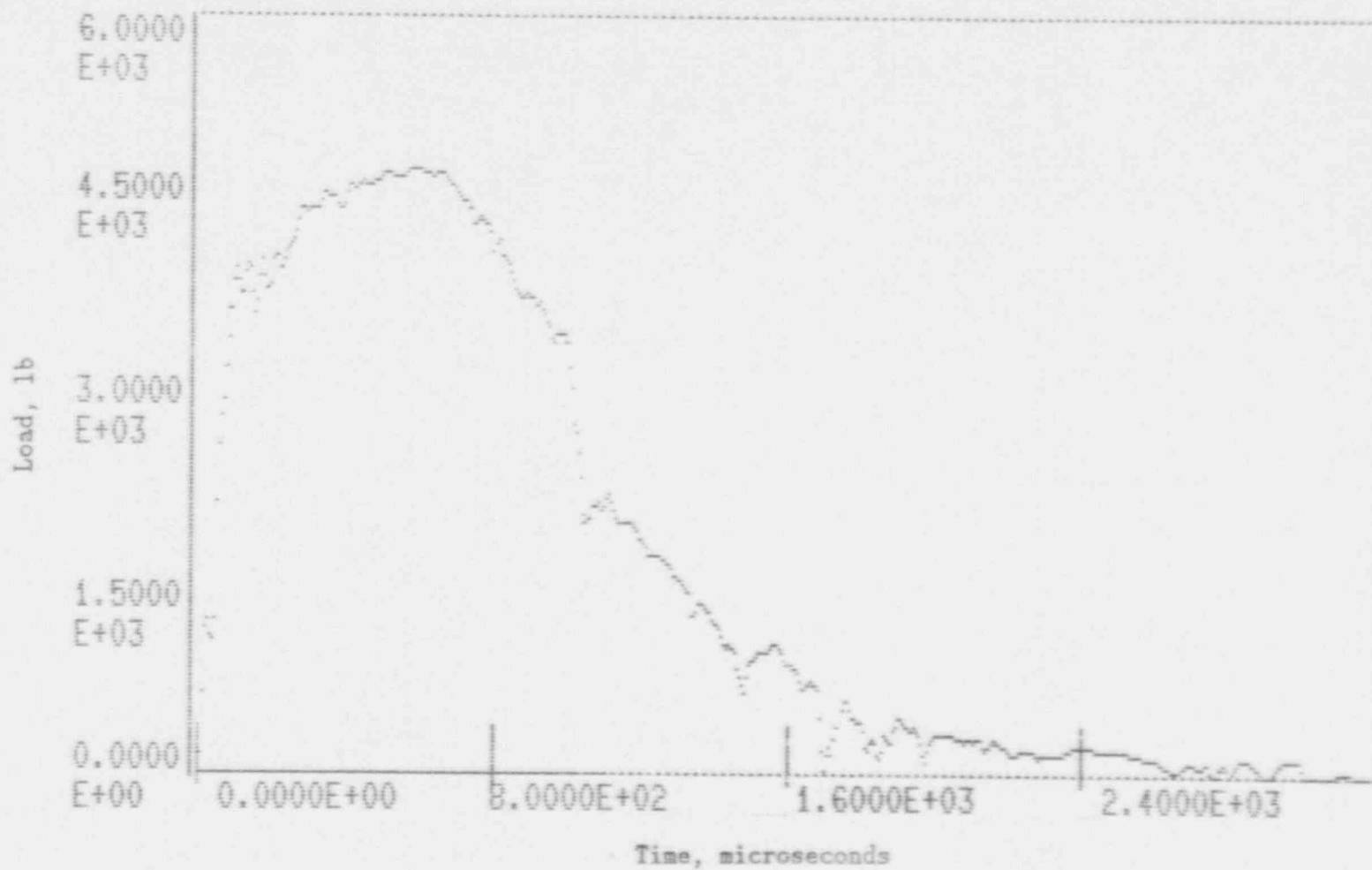


Figure A-57. Charpy impact test load-time record for Specimen BH11.

A-58

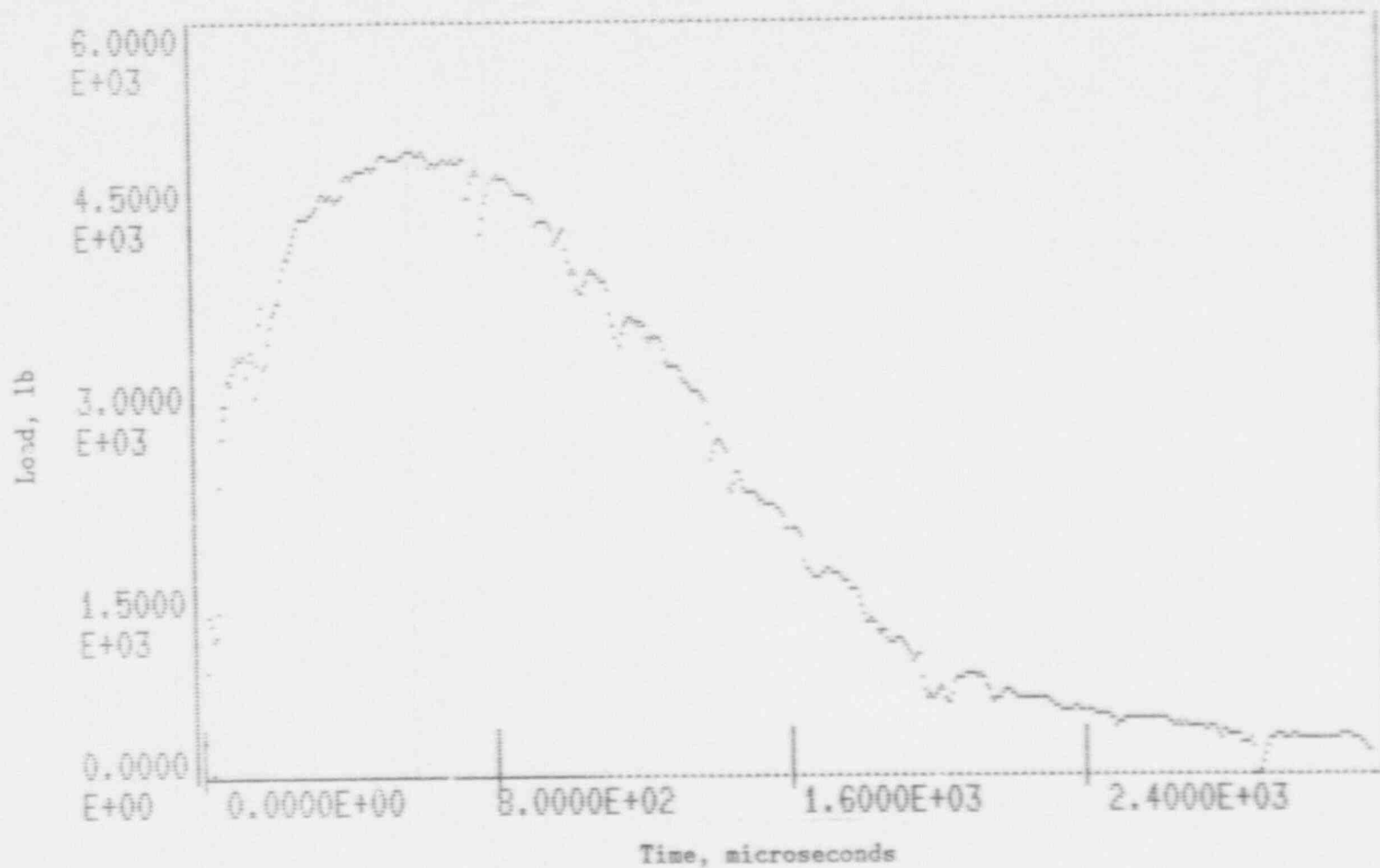


Figure A-58. Charpy impact test load-time record for Specimen BH4.

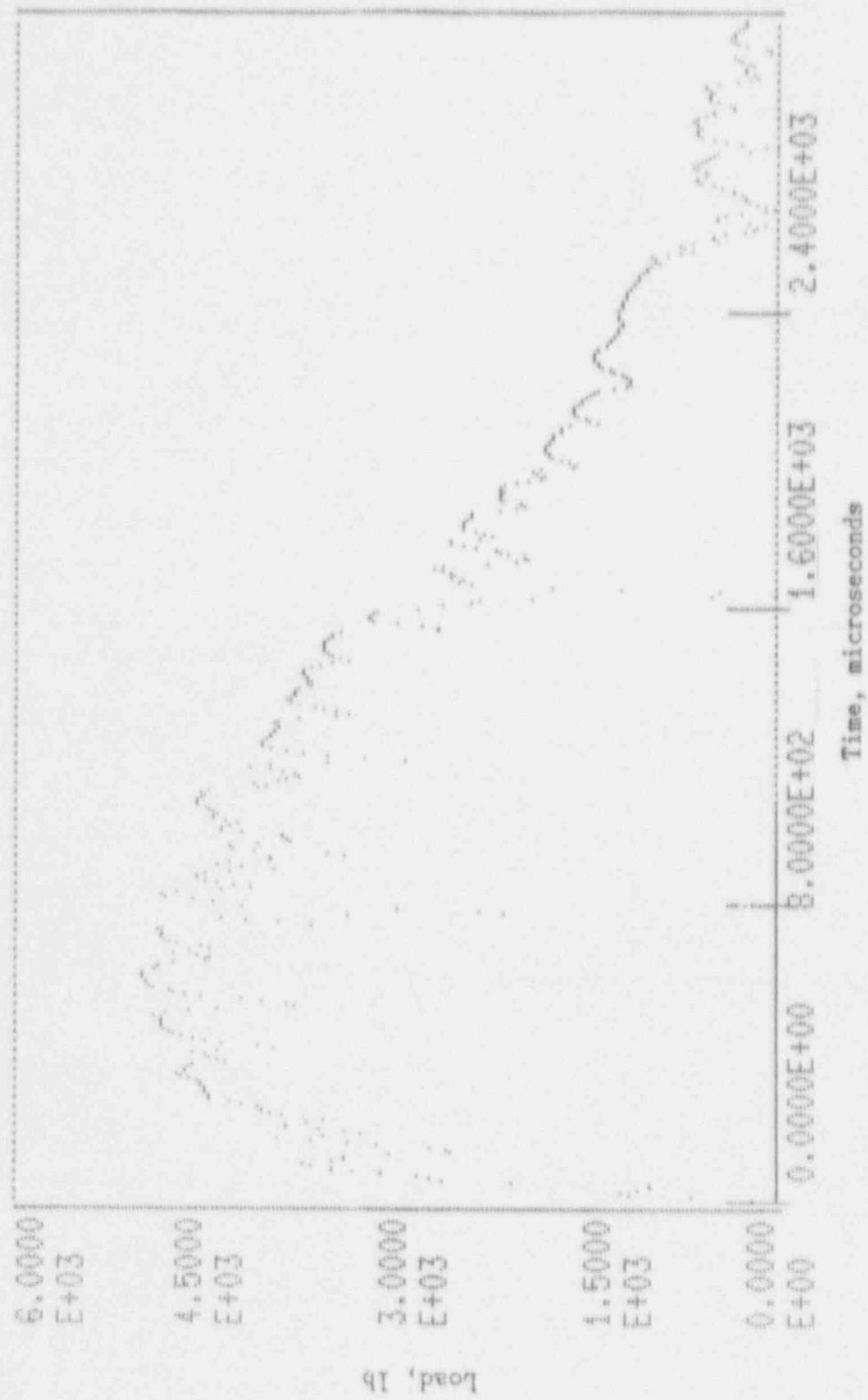


Figure A-59. Charpy impact test load-time record for Specimen BH7.

A-60

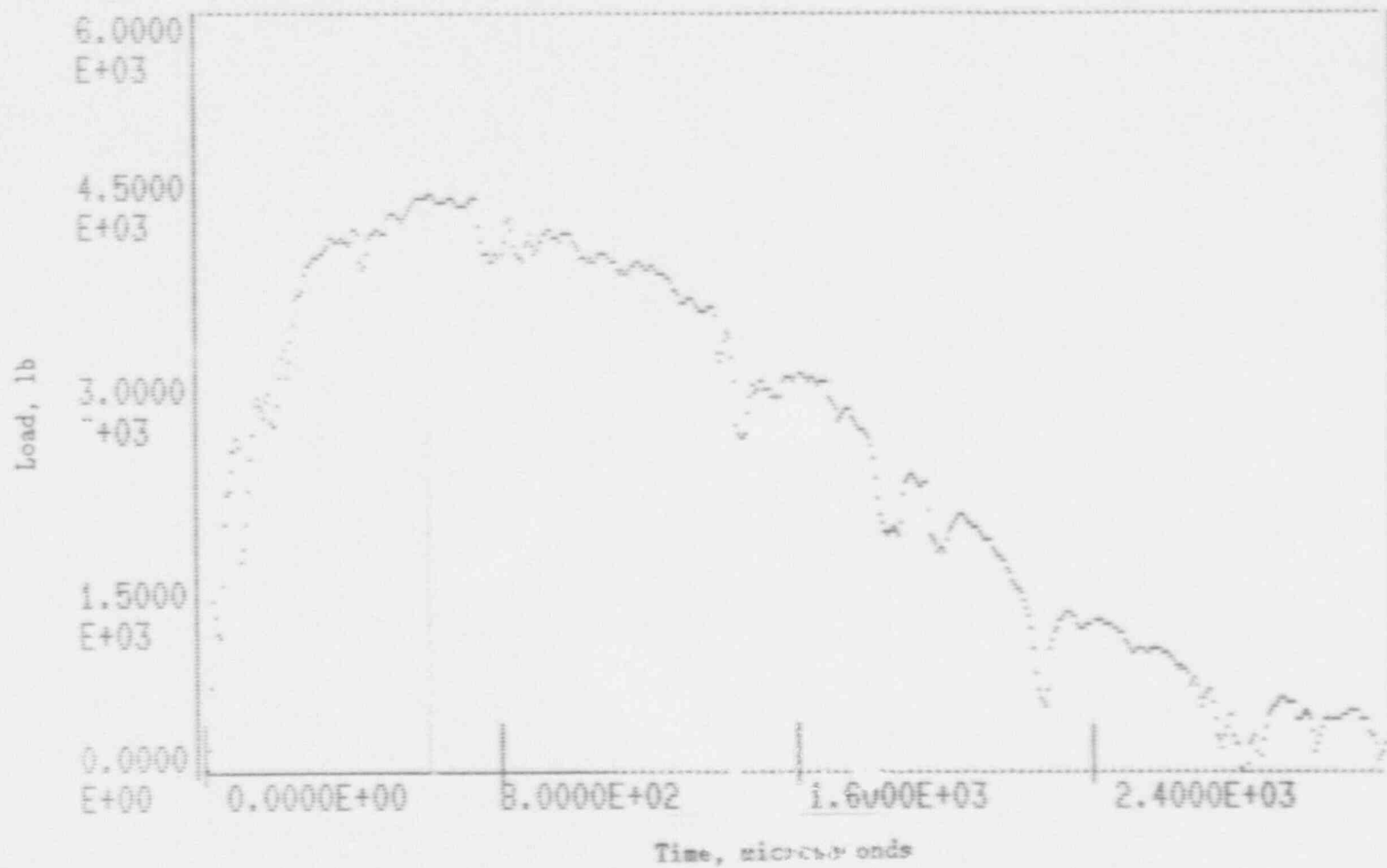


Figure A-60. Charpy impact test load-time record for Specimen BH14.

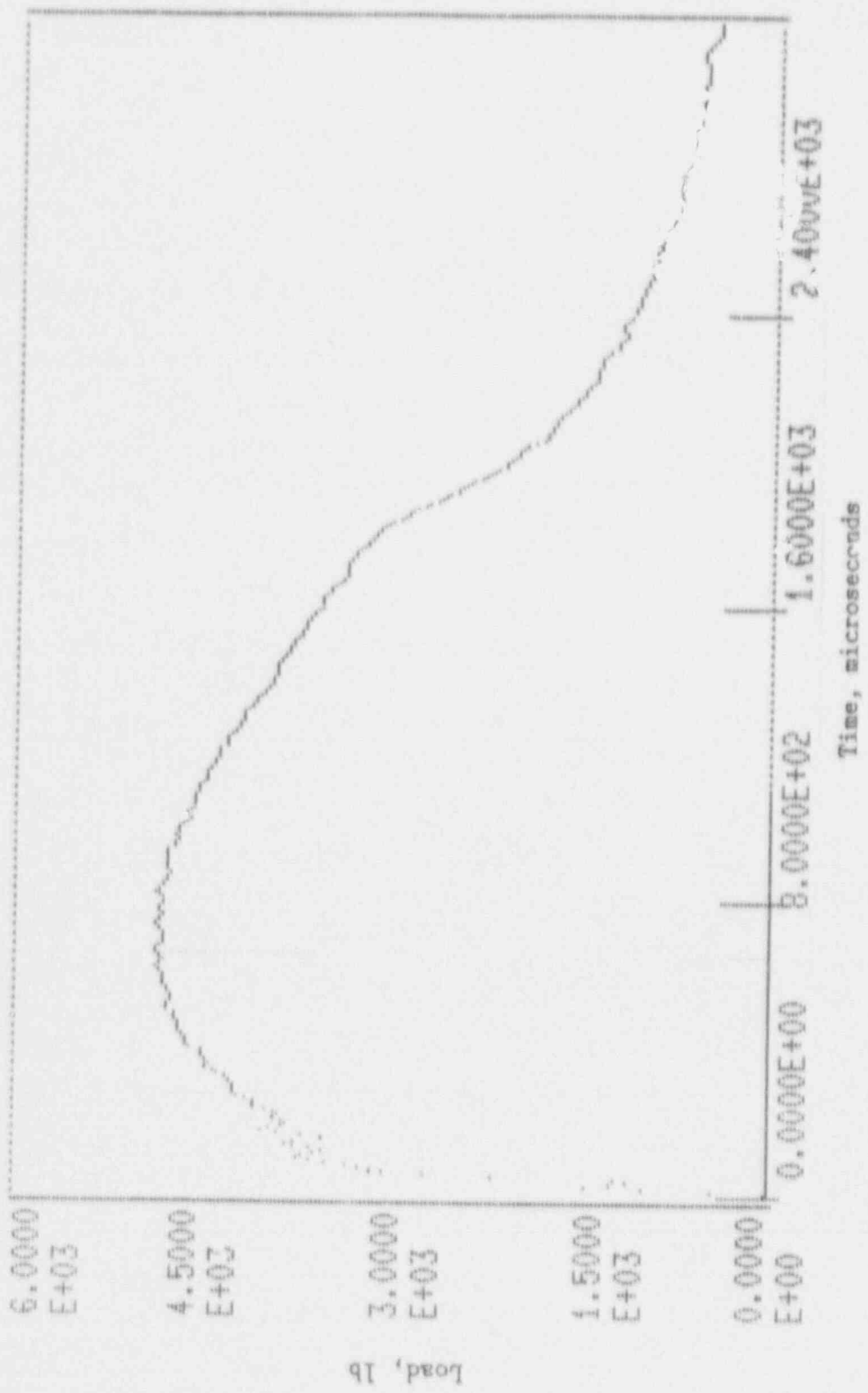


Figure A-61. Charpy impact test load-time record for Specimen B88.

APPENDIX B

EVALUATION OF PRESSURIZED THERMAL SHOCK  
FOR VOGTLE ELECTRIC GENERATING PLANT UNIT 2

## INTRODUCTION

A limiting condition on reactor vessel integrity known as pressurized thermal shock (PTS) may occur during a severe system transient such as a loss-of-coolant-accident (LOCA) or a steam line break. Such transients may challenge the integrity of a reactor vessel under the following conditions:

- severe overcooling of the inside surface of the vessel wall followed by high repressurization
- significant degradation of vessel material toughness caused by radiation embrittlement
- the presence of a critical-size defect in the vessel wall

Fracture mechanics analysis can be used to evaluate reactor vessel integrity under severe transient conditions.

In 1985 the Nuclear Regulatory Commission (NRC) issued a formal ruling on pressurized thermal shock. It established screening criterion on pressurized water reactor (PWR) vessel embrittlement as measured by the nil-ductility reference temperature, termed  $RT_{PTS}$ . The NRC guidelines for calculating the  $RT_{PTS}$  are defined in the PTS Rule<sup>[1]</sup>.  $RT_{PTS}$  screening values were set for beltline axial welds and plates and for beltline circumferential weld seams for end-of-life plant operation. The screening criteria were determined using conservative fracture mechanics analysis techniques. All PWR vessels in the United States have been required to evaluate vessel embrittlement in accordance with the criteria through end-of-life. The Nuclear Regulatory Commission has amended its regulations for light water nuclear power plants to change the procedure for calculating the radiation embrittlement. This revised PTS Rule was published in the Federal Register, May 15, 1991 with an effective date of June 14, 1991. This amendment makes the procedure for calculating  $RT_{PTS}$  values consistent with the one given in Regulatory Guide 1.99, Revision 2<sup>[2]</sup>.

The purpose of this report is to determine the reference temperature for

pressurized thermal shock ( $RT_{PTS}$ ) values for the Vogtle Electric Generating Plant Unit 2 reactor vessel to address the Pressurized Thermal Shock (PTS) Rule.

#### PRESSURIZED THERMAL SHOCK

The PTS Rule requires that the PTS submittal be updated whenever there are changes in core loadings, surveillance measurements or other information that indicates a significant change in projected values.

The Rule outlines regulations to address the potential for PTS events on pressurized water reactor (PWR) vessels in nuclear power plants that are operated with a license from the United States Nuclear Regulatory Commission (USNRC). PTS events have been shown from operating experience to be transients that result in a rapid and severe cooldown in the primary system coincident with a high or increasing primary system pressure. The PTS concern arises if one of these transients acts on the beltline region of a reactor vessel where a reduced fracture resistance exists because of neutron irradiation. Such an event may produce the propagation of flaws postulated to exist near the inner wall surface, thereby potentially affecting the integrity of the vessel.

The Rule establishes the following requirements for all domestic, operating PWRs:

- \* All plants must submit projected values of  $RT_{PTS}$  for reactor vessel beltline materials by giving values for time of submittal, the expiration date of the operating license, and the projected expiration date if a change in the operating license or renewal has been requested. This assessment must be submitted by six months after the effective date of this Rule if the value of  $RT_{PTS}$  for any material is projected to exceed the screening criteria. Otherwise, it should be submitted with the next update of the pressure-temperature limits, or the next reactor vessel surveillance report, or 5 years from the effective date of this Rule, whichever comes first. These values must be calculated based on the methodology specified in this rule. The submittal must include the following:
  - 1) the bases for the projection (including any assumptions regarding core loading patterns)
  - 2) copper and nickel content and fluence values used in the calculations for each beltline material. (If these values differ from those previously submitted to NRC, justification must be provided.)

- \* The  $RT_{PTS}$  (measure of fracture resistance) Screening Criteria for the reactor vessel beltline region is
  - 270°F for plates, forgings, axial welds
  - 300°F for circumferential weld materials
- \* The following equations should be used to calculate the  $RT_{PTS}$  values for each weld, plate or forging in the reactor vessel beltline.
  - Equation 1:  $RT_{PTS} = I + M + \Delta RT_{PTS}$
  - Equation 2:  $\Delta RT_{PTS} = (CF)f^{(0.28-0.10 \log f)}$
- \* All values of  $RT_{PTS}$  must be verified to be bounding values for the specific reactor vessel. In doing this each plant should consider plant-specific information that could affect the level of embrittlement.
- \* Plant-specific PTS safety analyses are required before a plant is within 3 years of reaching the Screening Criterion, including analyses of alternatives to minimize the PTS concern.
- \* NRC approval for operation beyond the Screening Criterion is required.

#### METHOD FOR CALCULATION OF $RT_{PTS}$

In the PTS Rule, the NRC Staff has selected a conservative and uniform method for determining plant-specific values of  $RT_{PTS}$  at a given time.

For the purpose of comparison with the Screening Criterion, the value of  $RT_{PTS}$  for the reactor vessel must be calculated for each weld and plate or forging in the beltline region as given below.

$$RT_{PTS} = I + M + \Delta RT_{PTS}, \text{ where } \Delta RT_{PTS} = (CF)f^{(0.28-0.10 \log f)}$$

I = Initial reference temperature ( $RT_{NDT}$ ) of the unirradiated material

M = Margin to be added to cover uncertainties in the values of initial  $RT_{NDT}$ , copper and nickel contents, fluence and calculational procedures. M = 66°F for welds and 48°F for base metal if generic values of I are used. M = 56°F for welds and 34°F for base metal if measured values of I are used.

- f = Neutron fluence,  $n/cm^2$  ( $E > 1MeV$  at the clad/base metal interface), divided by  $10^{19}$
- CF = Chemistry factor from tables<sup>[2]</sup> for welds and for base metals (plates and forgings)

## VERIFICATION OF PLANT-SPECIFIC MATERIAL PROPERTIES

Before performing the pressurized thermal shock evaluation, a review of the latest plant-specific material properties was performed.

The beltline region is defined by the PTS Rule<sup>[1]</sup> to be "the region of the reactor vessel (shell material including welds, heat affected zones and plates or forgings) that directly surrounds the effective height of the active core and adjacent regions of the reactor vessel that are predicted to experience sufficient neutron irradiation damage to be considered in the selection of the most limiting material with regard to radiation damage." Figure 1 identifies and indicates the location of all beltline region materials for the Vogtle Electric Generating Plant Unit 2 reactor vessel.

Material property values were derived from vessel fabrication test certificate results. Fast neutron irradiation-induced changes in the tension, fracture and impact properties of reactor vessel materials are largely dependent on chemical composition, particularly in the copper concentration. The variability in irradiation-induced property changes, which exists in general, is compounded by the variability of copper concentration with the weldments.

A summary of the pertinent chemical and mechanical properties of the beltline region plate and weld materials of the Vogtle Electric Generating Plant Unit 2 reactor vessel are given in Table 1. All of the initial  $RT_{NDT}$  values ( $I-RT_{NDT}$ ) are also presented in Table 1<sup>[3]</sup>.

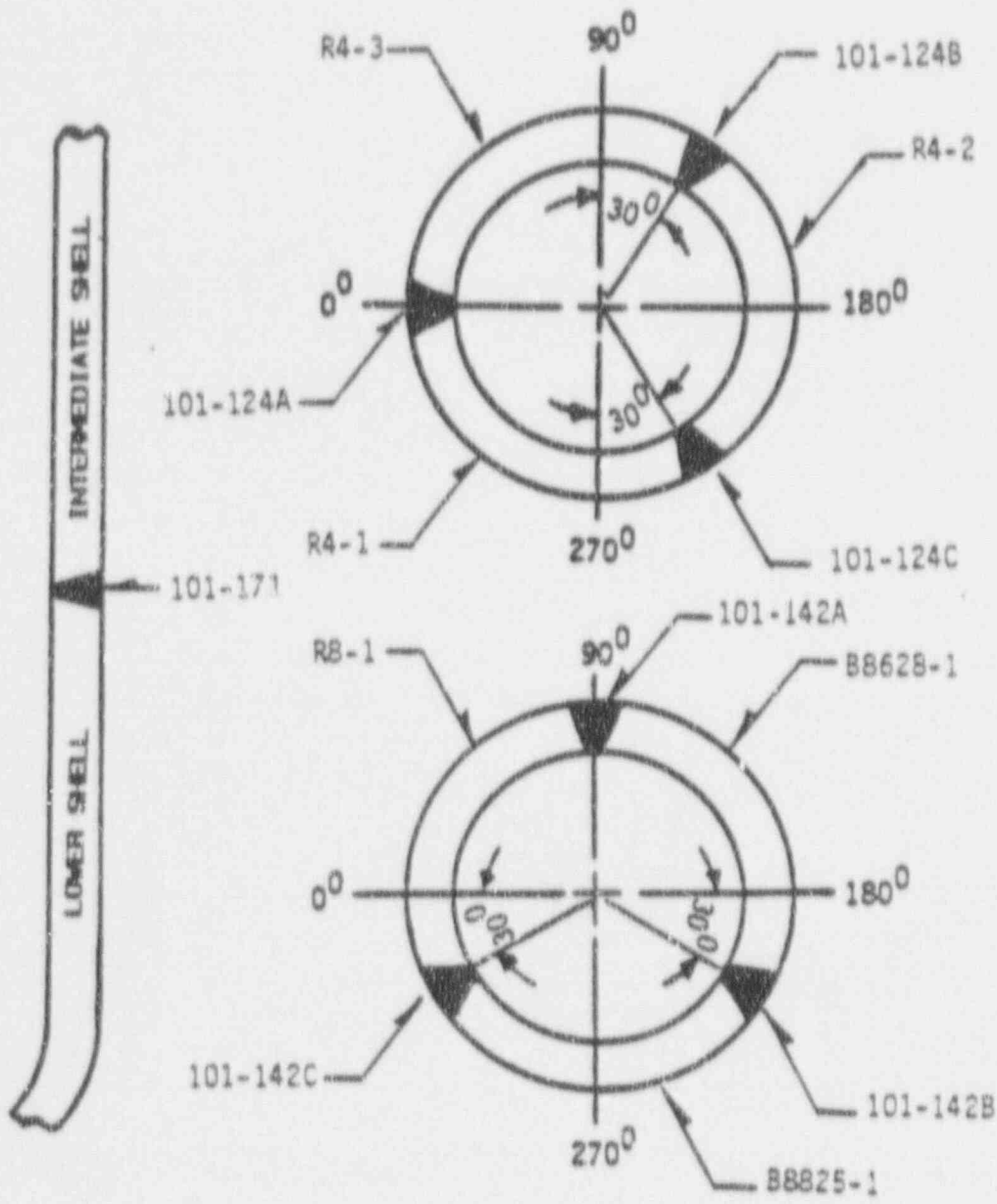


Figure 1. Identification and Location of Beltline Region Material for the Vogtle Electric Generating Plant Unit 2 Reactor Vessel

TABLE 1  
 VOGTLE ELECTRIC GENERATING PLANT UNIT 2  
 REACTOR VESSEL BELTLINE REGION MATERIAL PROPERTIES

Material Description	CU (%)	NI (%)	I-RTNDT (°F)
Intermediate Shell, R4-1	0.06	0.64	10
Intermediate Shell, R4-2	0.05	0.62	10
Intermediate Shell, R4-3	0.05	0.59	30
Lower Shell, B8825-1	0.05	0.59	40
Lower Shell, R8-1	0.06	0.62	40
Lower Shell, B8628-1	0.05	0.59	50
Longitudinal Welds	0.07	0.13	-10
Circumferential Weld	0.06	0.12	-30

#### NEUTRON FLUENCE VALUES

The calculated fast neutron fluence ( $E > 1$  MeV) at the inner surface of the Vogtle Electric Generating Plant Unit 2 reactor vessel is shown in Figure 2. These values were projected using the results of the Capsule U radiation surveillance program (See Section 6 of this report) and are presented in Table 2.

TABLE 2  
 NEUTRON EXPOSURE PROJECTIONS AT KEY LOCATIONS ON THE  
 VOGTLE ELECTRIC GENERATING PLANT UNIT 2 PRESSURE VESSEL  
 CLAD/BASE METAL INTERFACE FOR 32 EFPY

	0°	15°	25°	35°	45°
Fluence x $10^{19}$ n/cm <sup>2</sup> ( $E > 1$ MeV)	1.80	2.69	3.04	2.47	2.84

## DETERMINATION OF $RT_{PTS}$ VALUES FOR ALL BELTLINE REGION MATERIALS

Using the prescribed PTS Rule methodology,  $RT_{PTS}$  values were generated for all beltline region materials of the Vogtle Electric Generating Plant Unit 2 reactor vessel as a function of end-of-life (32 EFPY) and 48 EFPY fluence values. The fluence data were generated based on the most recent surveillance capsule program results.

Table 3 provides a summary of the  $RT_{PTS}$  values for all beltline region materials for the end-of-life (32 EFPY) and 48 EFPY using the PTS Rule. The PTS Rule requires that each plant assess the  $RT_{PTS}$  values based on plant specific surveillance capsule data under certain conditions. These conditions are:

- Plant specific surveillance data has been deemed credible as defined in Regulatory Guide 1.99, Revision 2, and
- $RT_{PTS}$  values change significantly. (Changes to  $RT_{PTS}$  values are considered significant if the value determined with  $RT_{PTS}$  equations (1) and (2), or that using capsule data, or both, exceed the screening criteria prior to the expiration of the operating license, including any renewed term, if applicable, for the plant.)

For Vogtle Electric Generating Plant Unit 2, the use of plant specific surveillance capsule data does not arise because of the following reasons:

- 1) Capsule U is the first capsule removed from the reactor vessel, hence the data is not credible per Reference 2.
- 2) Based on the material chemistry and projected fluence the  $RT_{PTS}$  values are not expected to exceed the  $RT_{PTS}$  screening criteria up to the end of license life.

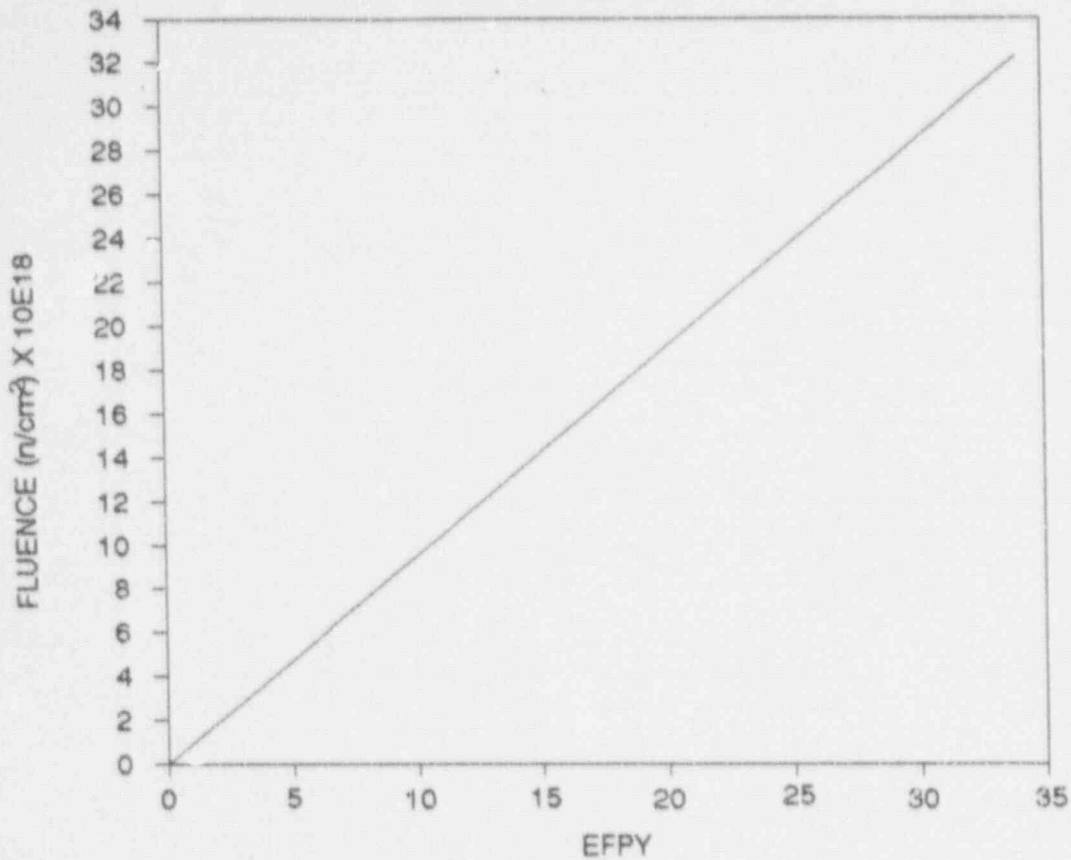


Figure 2. Fluence vs. Effective Full Power Years for Vogtle Electric Generating Plant Unit 2

TABLE 3  
RT<sub>PTS</sub> VALUES FOR VOGTLE ELECTRIC GENERATING PLANT UNIT 2

MATERIAL	32 EFPY	48 EFPY
Intermediate Shell Plate, R4-1	92	95
Intermediate Shell Plate, R4-2	84	87
Intermediate Shell Plate, R4-3	104	107
Lower Shell Plate, B8825-1	114	117
Lower Shell Plate, R8-1	122	125
Lower Shell Plate, B8628-1	124	127
Longitudinal Welds	107	111
Circumferential Weld	82	86

## CONCLUSIONS

As shown in Table 3, all the  $RT_{PTS}$  values remain below the NRC screening values for PTS using the projected fluence values for both the end-of-life (32 EFPY) and 48 EFPY. Using the PTS Rule, the highest  $RT_{PTS}$  values at 32 EFPY and 48 EFPY are at the lower shell plate, (B8628-1). These values are 124°F and 127°F, respectively. Plots of the  $RT_{PTS}$  values versus the fluence are shown in Figures 3 and 4. These plots indicate that none of the materials in the beltline region of the Vogtle Electric Generating Plant Unit 2 are expected to exceed the screening criteria based on the current fluence projections.

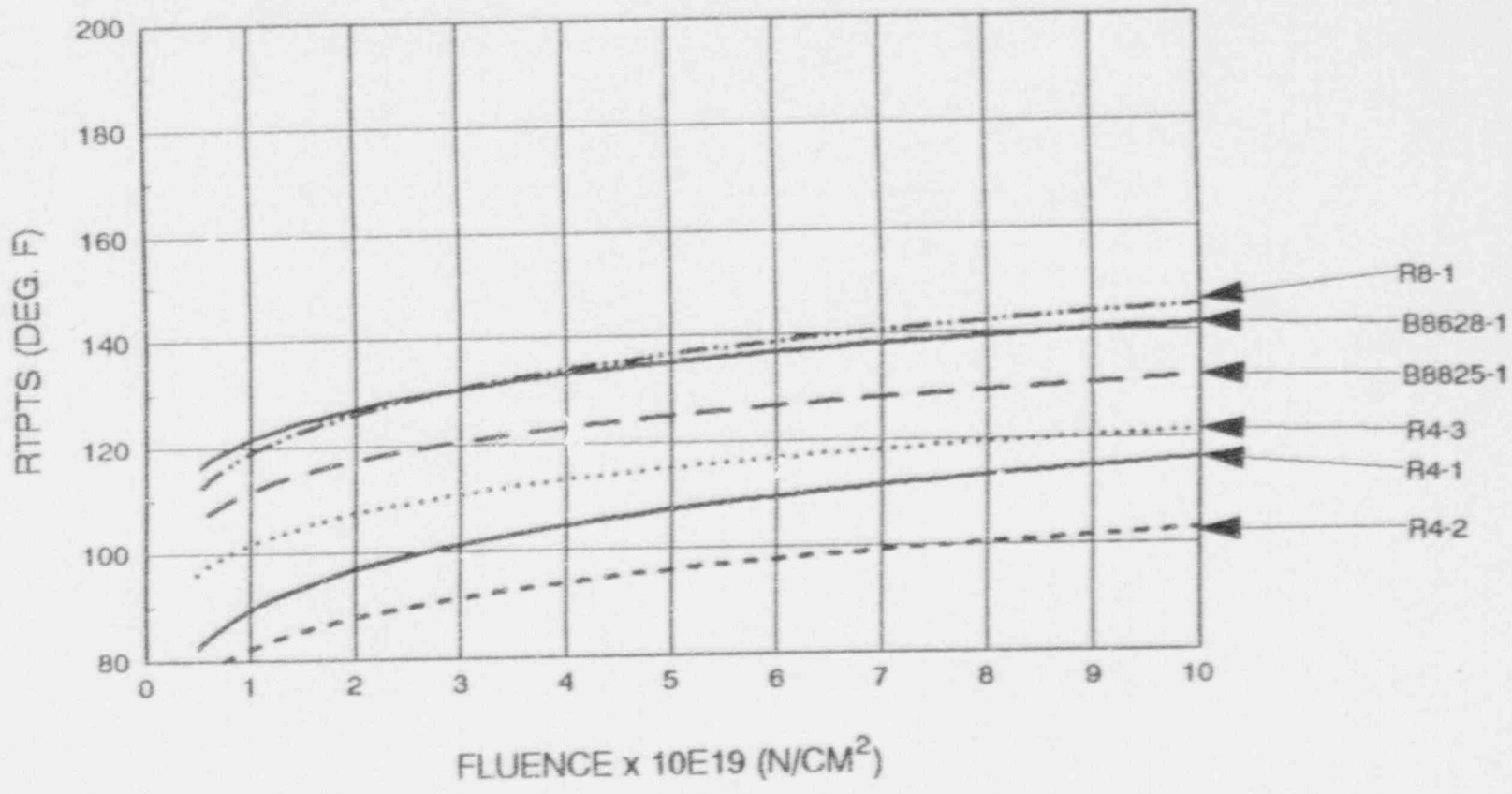


Figure 3. RTPTS versus Fluence Curves for Vogtle Electric Generating Plant Unit 2 - Base Plates

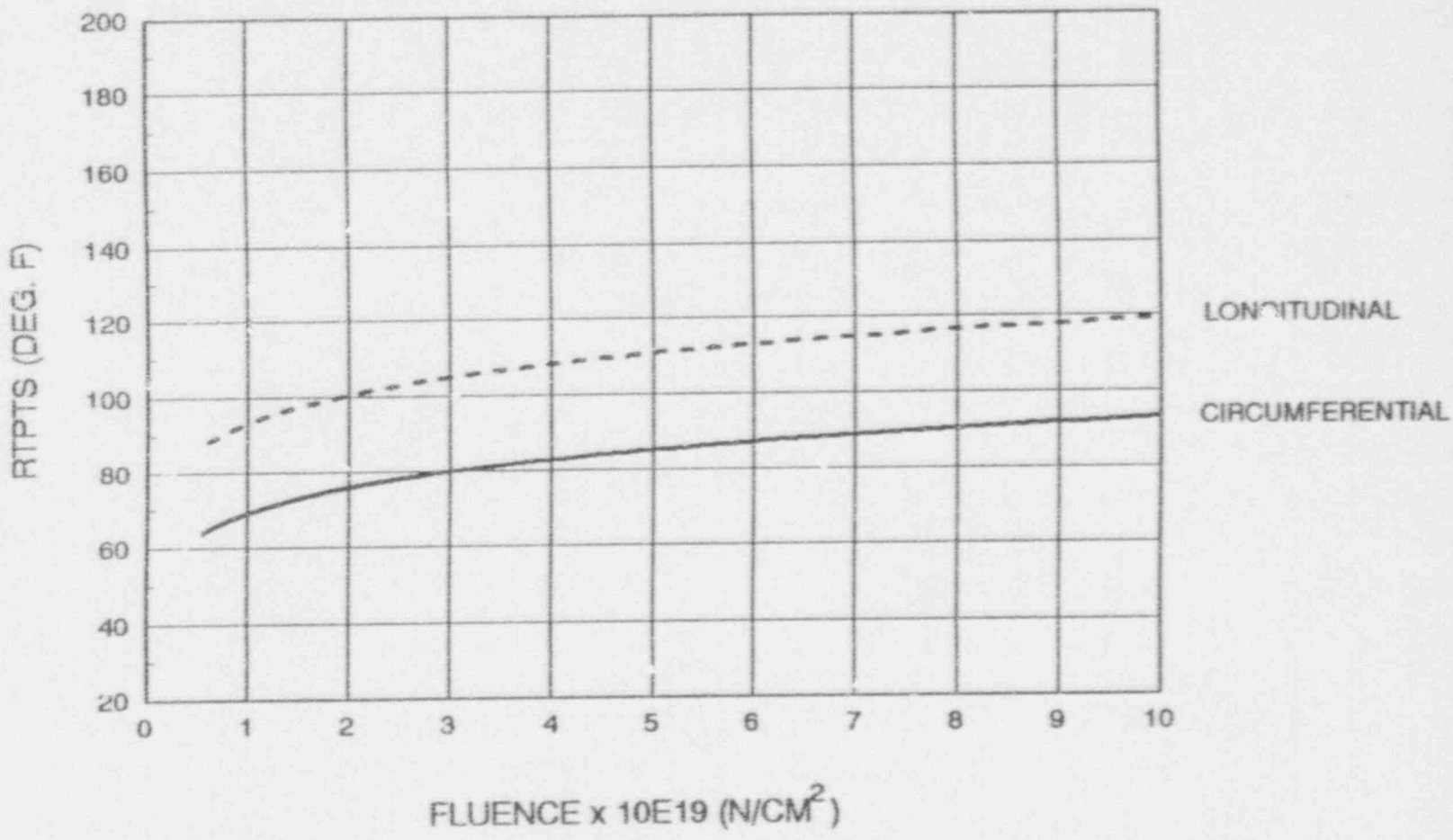


Figure 4. RTPTS versus Fluence Curves for Vogtle Electric Generating Plant Unit 2 - Welds

## REFERENCES

- [1] 10CFR Part 50, "Fracture Toughness Requirements for Protection Against Pressurized Thermal Shock Events", June 14, 1991.
- [2] Regulatory Guide 1.99, Revision 2, "Radiation Embrittlement of Reactor Vessel Materials," U.S. Nuclear Regulatory Commission, May 1989.
- [3] MT/SMART-213(88), "Vogtle Units 1 & 2 Reactor Vessel Heatup and Cooldown Limit Curves for Normal Operation", N. K. Ray, November, 1988.

